

THENE

LIBRARY Michigan State University

This is to certify that the

dissertation entitled

Study on Heme $\underline{\mathbf{d}}_1$ Of Cytochrome $\underline{\mathbf{cd}}_1$ Nitrite 1 Reductase

presented by

Weishih Wu

has been accepted towards fulfillment of the requirements for

Ph.D. degree in Chemistry

Date Feb 14, 1989

MSU is an Affirmative Action/Equal Opportunity Institution

0-12771

Click, Change Major professor



RETURNING MATERIALS:
Place in book drop to
remove this checkout from
your record. FINES will
be charged if book is
returned after the date
stamped below.

VAR + 5 1994

STUDY ON HEME \underline{d}_1 OF CYTOCHROME \underline{cd}_1 NITRITE REDUCTASE

Ву

Weishih Wu

A DISSERTATION

Submitted to
Michigan State University
in partial fulfillment of the requirements
for the degree of

DOCTOR OF PHILOSOPHY

Department of Chemistry

ABSTRACT

STUDY ON HEME \underline{d}_1 OF CYTOCHROME \underline{cd}_1 NITRITE REDUCTASE

By

Weishih Wu

Cytochrome \underline{cd}_1 nitrite reductase found in a large number of microbial denitrifiers, which play an important role in the biological nitrogen cycle, contains an extractable green heme prosthetic group. This so-called $\underline{\textbf{d}}_1$ heme has been assumed to be a chlorin since the late 1950's. Recently, a structure determination of isolated heme \underline{d}_1 by another laboratory also favored a chlorin structure. However, critical analysis of the available spectral data has led us to propose that heme \underline{d}_1 is not a chlorin but a novel porphyrindione The spectra of the model compounds derived from octaethylporphyrin and mesoporphyrin IX dimethyl ester provided solid evidence of the proposed structure. The methodologies developed in the synthesis of the 1,3-porphyrindione core structure and the acrylate side chain ultimately led to the total synthesis of heme \underline{d}_1 . By comparison with its stereo- and regioisomers, heme \underline{d}_1 has been shown to possess a 6-acrylic side chain and a cis arrangement of its two angular acetic side chains. Physicochemical studies have demonstrated that the most distinctive features of porphyrindione, as compared with porphyrin and isobacteriochlorin, are its electronegativity due to the two conjugated keto

groups on the macrocycle and its enlarged core size which is brought about by the saturation of the pyrrole rings. Reconstituted cytochrome \underline{cd}_1 nitrite reductase from <u>Pseudomonas stutzeri</u> with both native and synthetic heme \underline{d}_1 exhibit identical spectral properties and NO/N₂O producing activities. This proves that the porphyrindione structure is the true form of \underline{d}_1 and that the synthetic compound is completely bioactive. To explain the biosynthetic origin of this unprecedented \underline{d}_1 heme, two possible pathways, via protoporphyrin or sirohydrochlorin, have been proposed.

all friends of my generation, those who lost their lives during the Cultural Revolution (1966--1976, China); those who lost their opportunities to recieve education during Mao's era; those who have never lost their faith in building up a democratic, prosperous new China and those who are working hard for a world filled with freedom, equality and fraternity.

ACKNOWLEDGEMENTS

I would like to express my special thanks to Professor C. K. Chang, for his advice, friendship and guidance throughout the course of this work.

I would like to thank Professor E. LeGoff, for serving as the second reader and for always being ready to help. I would also like to thank Professor C. H. Brubaker and Professor A. Tulinsky for serving as members on my guidance committee.

Gratitude must be expressed to the National Institutes of Health for financial support in the form of research assistantship. In addition, I thank the Department of Chemistry at Michigan State University for providing support in the form of teaching assistantship and for rewarding of a one year SOHIO fellowship and a summer BASF fellowship.

Great thanks must be extended to the past and present members of Professor Chang's group — Dr. M. Kondylis, Dr. I. Abdalmuhdi, Dr. M. Koo, Dr. A. Salehi, Ms. G. Aviles and Mr. W. Lee for their encouragement and friendship. Particularly, I wish to thank Dr. C. Sotiriou, not only for her inseparable contribution to the "green heme" project, but also for being a good friend.

It has been my good fortune to be associated with a number of other research groups at MSU, especially professor J. Tiedje's and professor J. Babcock's groups. It was fun to do the enzyme purification and protein reconstitution experiment with Dr. E. Weeg-Aerssens in a 4 °C cold room and especially interesting to take Raman spectra with Dr. W. A. Otertling in the dark but colorful laser lab. I am also grateful to the NMR group of the Chemistry department for their prompt help, particularly to Dr. L. D. Le for

his demonstration of the NOE technique.

Thanks also go to my friends and colleagues at Chengdu Institute of Organic Chemistry Chinese Academy of Sciences. Especially, I wish to thank Professor G. N. Li, who was the director of the institute and my master thesis advisor, for his introducing me into the colorful porphyrin chemistry and his caring throughout my graduate career. I also extend my thanks to Mr. S. L. Pan for his helping me go through the Chinese red tapes otherwise my oversea study would not be so easy.

The deepest appreciation is due to my parents for their love, encouragement and faith in their youngest son, and above all, for always taking the education of the children as their first priority even during the most difficult time of their lives. Thanks also go to my brother, sister and my wife's family for their consistent support over the years.

Finally, I would like to thank my wife Xiaoming. I appreciate sincerely the support and love she has given me and looking forward a new life together with our two lovely children.

TABLE OF CONTENTS

	Page
LIST OF TABLE	SSx
LIST OF FIGUR	ESxii
CHAPTER 1	INTRODUCTION: THE GREEN HEME PROSTHETIC GROUP OF CYTOCHROME <u>cd</u> NITRITE REDUCTASE
I.	SIGNIFICANCE AND BACKGROUND
	A. NITROGEN CYCLE AND DENITRIFICATION
	B. CYTOCHROME <u>cd</u> ₁ NITRITE REDUCTASE
	C. ON THE MECHANISM OF NITRITE REDUCTION
	D. HEME <u>d</u> ₁
П.	OBJECTIVES OF THE PRESENT WORK
III.	RESULTS AND PRESENTATION
IV.	NOMENCLATURE OF HEME \underline{d}_1 AND RELATED COMPOUNDS
CHAPTER 2	FURTHER CHARACTERIZATION OF THE HEME \underline{d}_1 STRUCTURE 16
I.	EVIDENCE OF THE PORPHYRINDIONE STRUCTURE OF HEME $\underline{d}_1 \ldots 16$
II.	STUDY WITH MODEL COMPOUNDS
	A. FORMATION OF THE 1,3-PORPHYRINDIONE CORE STRUCTURE 22
	1. On the OsO ₄ Oxidation of Porphyrin Tetraacetate
	2. On the H ₂ O ₂ -H ₂ SO ₄ Oxidation of Mesoporphyrin IX
	3. On the Oxidation of Zn(II) Porphyrinone
	B. FORMATION OF THE ACRYLIC SIDE CHAIN
	C. SPECTROSCOPIC STUDIES OF MODEL COMPOUNDS
ш.	EXPERIMENTAL
CHAPTER 3	TOTAL SYNTHESIS OF HEME <u>d</u> ₁
I.	RATIONAL OF THE SYNTHETIC STRATEGY

П.	FROM 1,4-PORPHYRIN DIACETATE A TEST	61
Ш.	FROM PORPHYRINS WITH MASKED ACETIC SIDE CHAINS - A BYPASS	63
	A. 1,4-BIS-(2-CHLOROETHYL)-PORPHYRIN	63
	B. 1,3-BIS-(2-CHLOROETHYL)-PORPHYRIN	67
	C. OXIDATION OF 1,3-PORPHYRINDIONE SIDE CHAINS	7 0
IV.	FROM 2,4-PORPHYRIN DIACETATE - REACHING THE GOAL	72
V.	<u>d</u> ₁ ANALOGUES FROM COPROPORPHYRIN IV	81
VI.	EXPERIMENTAL	85
CHAPTER 4	ON THE STRUCTURE OF HEME d ₁	121
I.	THE STEREO- AND REGIOISOMERS	121
	A. Cis- AND trans-d ₁ STEREOCHEMISTRY DEDUCED FROM NMR SHIFT REAGENT	121
	B. Cis- AND tran-iso- \underline{d}_1 THE LOCATION OF ACRYLIC SIDE CHAIN	124
П.	THE NATIVE FORM OF HEME \underline{d}_1	124
III.	THE BIOSYNTHETIC ORIGINAL OF \underline{d}_1	128
CHAPTER 5	PHYSICOCHEMICAL PROPERTIES OF HEME \underline{d}_1 AND MODEL SYSTEMS	130
I.	GENERAL CONSIDERATION	130
II.	ABSOPTION SPECTRA	131
	A. SPECTRAL FEATURES OF PORPHYRINONES	131
	B. SPECTRAL FEATURES OF PORPHYRINDIONES	136
ш.	NUCLEAR MAGNETIC RESONANCE SPECTROSCOPY	142
	A. ¹ H-NMR SPECTRA	145
	B. ¹³ C-NMR SPECTRA	147
IV.	VIBRATIONAL SPECTROSCOPY	152
•	A. INFRARED SPECTRA	152

	B. RESONANCE RAMAN SPECTRA	161
V.	X-RAY DIFFRACTION ANALYSIS	165
VI.	REDOX POTENTIAL	168
VII.	BASICITY OF CENTRAL NITROGEN	170
VIII.	EXPERIMENTAL	171
CHAPTER 6	RECONSTITUTION OF CYTOCHROME $\underline{cd_1}$ NITRITE REDUCTASE WITH NATIVE AND SYNTHETIC HEME $\underline{d_1}$	173
L	PREVIOUS WORK	173
II.	EXPERIMENTAL	174
	A. PREPARATION OF APOPROTEIN	174
	B. PREPARATION OF HEME <u>d</u> ₁ SOLUTION	176
	C. RECONSTITUTION OF NITRITE REDUCTASE	176
	D. ESTIMATION OF PROTEIN	177
	E. ACTIVITY ASSAY	177
Ш.	SPECTRAL CHARACTERIZATION	178
IV.	RECOVERY OF ACTIVITY	183
IV.	DISCUSSION	188
CHAPTER 7	SUMMERY AND PROSPECTS	191
I.	EVALUATION OF THE PRESENT WORK	191
II.	FUTURE WORK	192
REFERENCES	•••••	194

LIST OF TABLES

Table	Pa	age
1	¹³ C-NMR chemical shifts of 1,3-porphyrindione 6, model compound	
	10 in comparison with that of natural heme \underline{d}_1	47
2	1 H-NMR chemical shifts of \underline{d}_{1} free base in comparison with its	
	stereo- and regioisomers	26
3	Meso proton chemical shifts differences between hemes and free base	27
4	UV-vis spectra of varies porphyrinones in comparison with chlorins	3 3
5	UV-vis spectra of Cu-metallated and protonated porphyrinones in	
	comparison with chlorins	35
6	UV-vis spectra of Cu-metallated and protonated porphyrindiones	39
7	UV-vis spectra of 1,3-porphyrindiones in comparison with	
	isobacteriochlorins	43
8	1 H-NMR chemical shifts of heme \underline{d}_{1} related porphyrin, porphyrinones	
	and porphyrindiones	46
9	¹ H-NMR chemical shifts of the meso protons of porphyrindiones in	
	comparison with their analogue bacteriochlorins and isobacteriochlorins 1	49
10	13 C-NMR chemical shifts of heme \underline{d}_1 related porphyrin, porphyrinone	
	and porphyrindione	.50
11	Infrared absorption bands of \underline{d}_1 and porphyrindiones in comparison with	
	sirohydrochlorin and isobacteriochlorin	.54
12	Infrared absorption bands of porphyrinones in comparison with chlorin	.59
13	Redox potentials of porphyrin, porphyrinones and porphyrindiones	69
14	The calculated energies for the HOMOs and LUMOs of porphyrin,	
	porphyrinone and porphyrindione zinc complexes	1 7 0

15	Recovery of nitrite reductase activity after reconstitution of the	
	apoprotein with native and synthetic heme $\underline{d}_1 \dots \dots$	39

LIST OF FIGURES

FIGURE	page
1	Examples of metalloporphyrinoids and their parent ring structures 2
2	The shape, dimension and symmetry of cytochrome $\underline{cd}_1 \dots 7$
3	UV-vis absorption spectra of heme \underline{d}_1 versus 1,3-OEPdione 8 in $CH_2Cl_2 \ldots 17$
4	UV-vis absorption spectrum changes of heme \underline{d}_1 during hydrogenation
	in formic acid
5	Natural abundance, broad-band proton-decoupled ¹³ C-NMR of the
	free base methyl ester of \underline{d}_1 in CDCl $_3$ at 32 ^oC
6	UV-vis absorption spectra of 1,3-dione 8, 53 and 10 in CH_2Cl_2 40
7	UV-vis absorption spectra of model compound 10 (A) in the form of
	$Cu(II)$ chelate in $CHCl_3$ and (B) in the protonated form in formic acid 42
8	UV-vis absorption spectra of 10, (A) ferriheme chloride in acetone with
	a trace amount of HCl; (B) alkaline ferriheme in CH ₂ Cl ₂ /acetone
	containing tetrabutylammonium hydroxide; (C) pyridine hemochrome in
	CH ₂ Cl ₂ /pyridine
9	250 MHz 1 H-NMR spectrum of model compound 10 in CDCl $_3$
10	Natural abundance, broad-band proton-decoupled ¹³ C-NMR of model
	compound 10
11	250 MHz 1 H-NMR spectra of cis- $\underline{\mathbf{d}}_1$ versus trans- $\underline{\mathbf{d}}_1$ in CDCl $_3$
12	The Eu(fod) ₃ induced chemical shift (in ppm) of meso protons of
	cis-dione 59a and trans-dione 59b
13	UV-vis absorption spectra of cis- \underline{d}_1 versus cis-iso- \underline{d}_1 in CH_2Cl_2
14	UV-vis absorption spectrum of porphyrinone 135 in CH ₂ Cl ₂
15	UV-vis absorption spectra of 2,3-dione 32, 1,3-dione 8 and
	1.A-dione 33 in CH ₂ Cl ₂

16	UV-vis absorption spectra of 1,5-dione 123 and 1,6-dione 124 in CH ₂ Cl ₂ 138
17	UV-vis absorption spectra of Cu (II) 2,3-dione 32 and 1,3-dione 8 in
	CH ₂ Cl ₂
18	UV-vis absorption spectra of 1,4-dione 33 and 1,3-dione 8 in CH ₂ Cl ₂
	with CF ₃ CO ₂ H (1%)
19	250 MHz ¹ H-NMR spectrum of porpnyrinone 111 in CDCl ₃
20	FT-IR spectra of \underline{d}_1 and Cu (II) \underline{d}_1 , samples are prepared as a thin films
	on NaCl pellets
21	FT-IR spectra of porphyrin 61 and acryloporphyrin 146, samples are
	prepared as a thin films on NaCl pellets
22	Resonance Raman spectra of (A) natural -d1 Cu (II) complex; (B) 1,3-dione
	6 Cu (II) complex and (C) acrylo-1,3-dione 10 Cu (II) complex at ~2 °C,
	sample A and B in CH2Cl2, and sample C as ~1 mg/100 mg KBr
23	Resonance Raman spectra of Cu (II) complexes of synthetic \underline{d}_1 and
	1,3-dione 59 in CH ₂ Cl ₂
24	(A) Molecular structure and atom names of Cu (II) 1,3-dione 8,
	(B) bond distance, (C) deviation from the plane of the four nitrogens.
	(D) Free base of 1,3-dione 8, (E) Another view of D
25	Geometric model of the ligand periphery of Ni (II) isobacteriochlorin
26	UV-vis spectra of Fe (III) \underline{d}_1 in acetone containing 0.024 N HCl and
	about 10% of water, (A) synthetic heme \underline{d}_1 ; (B) native heme \underline{d}_1 from
	<u>P. stutzeri</u>
27	UV-vis spectra of synthetic \underline{d}_1 in 0.25 M of phosphate buffer at PH 7.3 181
28	UV-vis spectra of pure preparation of nitrite reductase from P. stutzeri
	in 0.25 M phosphate buffer at PH 7.0
29	UV-vis spectra of apoprotein of nitrite reductase from P. stutzeri after
	removal of heme d1, the apoprotein was dissolved in 0.25 M of

	phosphate buffer at PH 7.0
30	UV-vis spectra of reconstituted nitrite reductase in 0.25 M of
	phosphate buffer at PH 7.0, (A) native \underline{d}_1 reconstituted and (B)
	synthetic \underline{d}_1 reconstituted
31	Progress curves of nitric oxide and nitrous oxide production from 1 mM of
	nitrite by intact nitrite reductase from <u>P. stutzeri</u>
32	Progress curves of nitric oxide and nitrous oxide production from 1 mM of
	nitrite by the reconstituted nitrite reductase, (A) reconstituted with
	synthetic heme \underline{d}_1 and (B) reconstituted with native heme $\underline{d}_1 \dots 187$

CHAPTER 1

INTRODUCTION: THE GREEN HEME PROSTHETIC GROUP OF CYTOCHROME cd₁ NITRITE REDUCTASE

I. SIGNIFICANCE AND BACKGROUND

Chemists interested in the bioorganic and bioinorganic fields are always fascinated by the rich and colorful chemistry of porphyrinoids. Varying a single structure theme, that of uroporphyrinogen, Nature has selected a rich variety of magnificent structures to take part in a diversity of fundamental biological functions in all kinds of organism ranging from bacteria to man. Examples shown in Figure 1 are the better known porphyrin family compounds; hemin (iron porphyrin), chlorophyll \underline{a} (magnesium chlorin), bacteriochlorophyll \underline{a} (magnesium bacteriochlorin), siroheme (iron isobacteriochlorin), vitamin \underline{B}_{12} (cobalt corrin) and coenzyme \underline{F}_{430} (nickel corphin). In fact, metalloporphyrinoids are of so much importance that they deserve the label as "the pigments of life".

This thesis concerns a new member of metalloporphyrinoids: heme \underline{d}_1 (1).³ This iron heme has an unprecedented 1,3-porphyrindione core structure with an arcylic side chain present, and has been found as the cofactor of cytochrome \underline{cd}_1 -type nitrite reductase in a large number of denitrifying bacteria.

The present work addresses various synthetic aspects of the unique structure of \underline{d}_1 heme, the physicochemical properties of its novel macrocyclic ligand and the biological significance of this prosthetic group in the

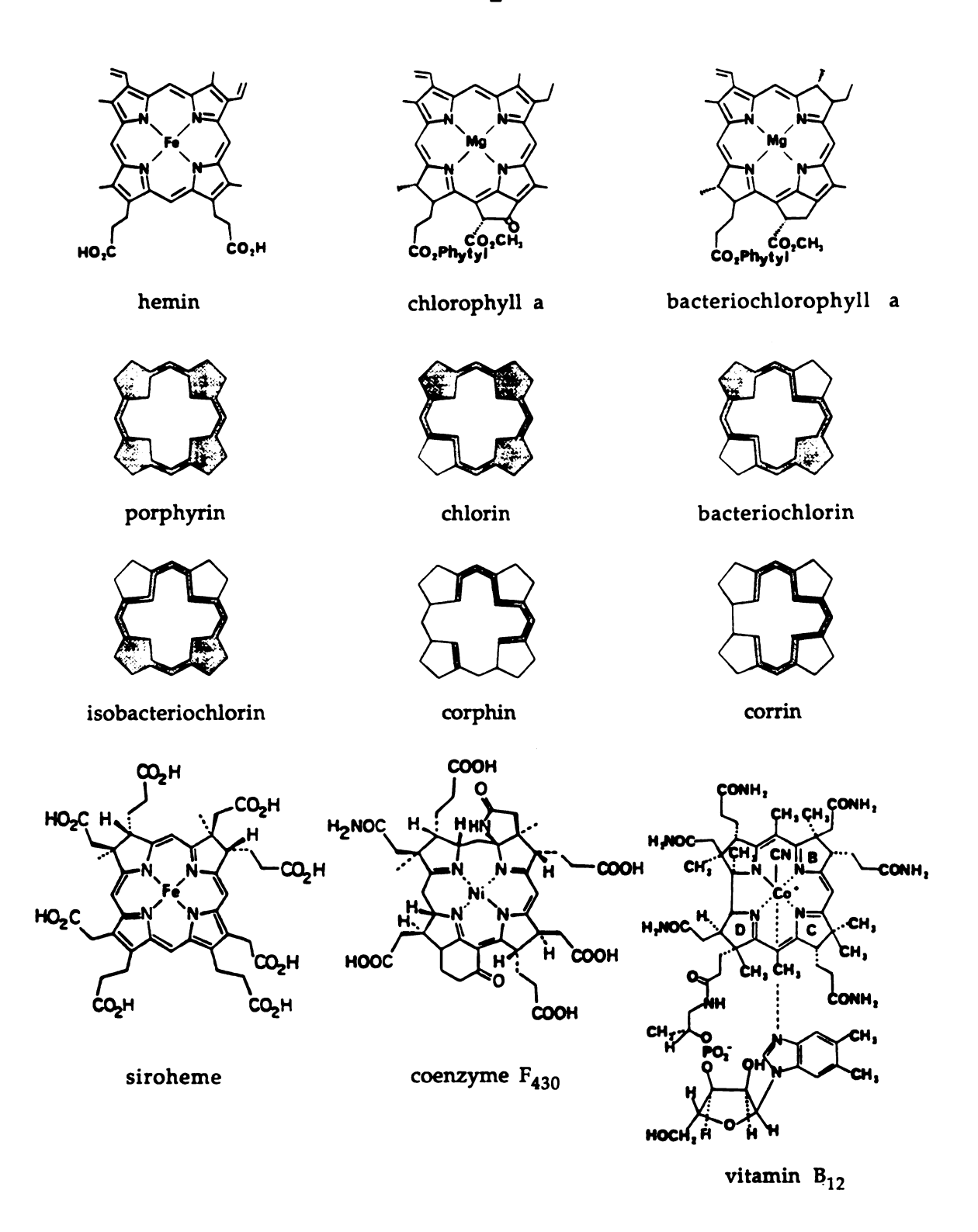


Figure 1 Examples of metalloporphyrinoids and their parent ring structures.

denitrification process.

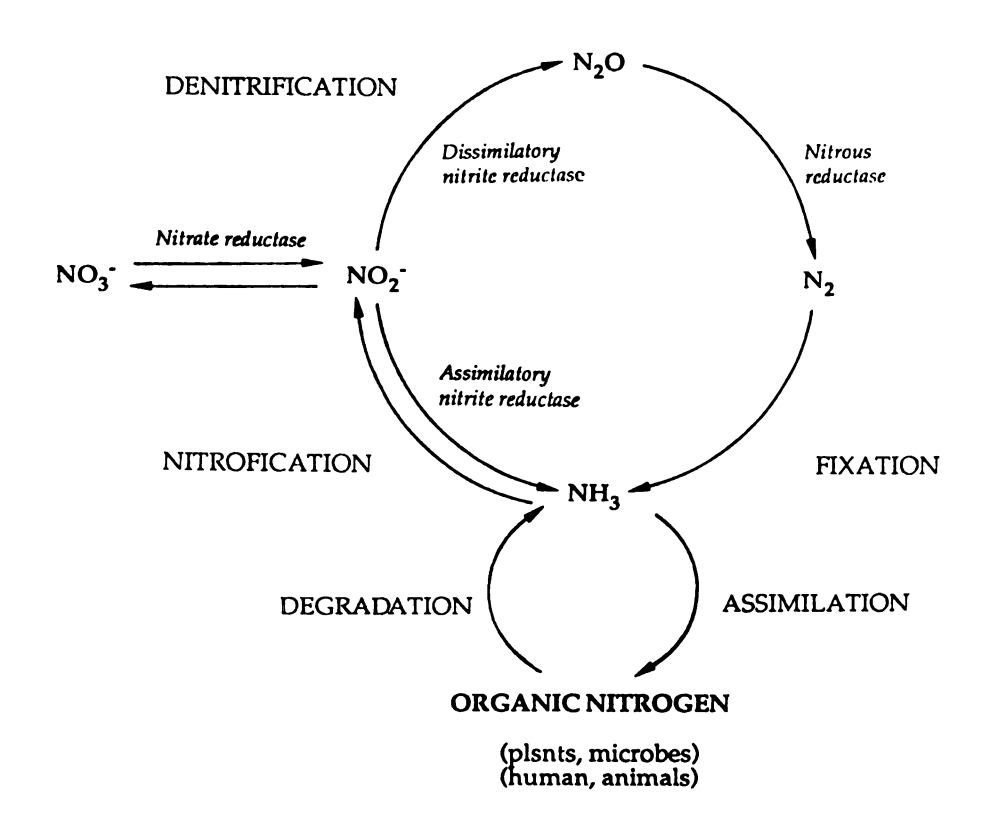
1. Heme <u>d</u>₁

A. Nitrogen Cycle and Denitrification⁴

Though the early history of the earth involved massive geochemical and geophysical changes, living things are today responsible for the major chemical transformations which take place on our planet. It is convenient to express these changes, on a gross scale, in the form of hypothetical cycles of the biologically active elements, such as nitrogen, sulfur and phosphorus. A simplified nitrogen cycle is shown in Scheme 1 to indicate the major biological processes involved.

The immediate product of biological dinitrogen fixation is ammonia, which is taken by plants and microbes to make their protein and other organic nitrogen matters, which then serves as the nutrients for human and animals. The degradation process brings organic nitrogen back to ammonia which is oxidized to nitrate. The reduction of nitrate and nitrite undergoes two different routes: the assimilatory nitrite-reducing process to generate ammonia; and the dissimilatory route producing nitrous oxide and dinitrogen gas. The balance between fixation-nitrification and denitrification

is fundamental to the persistence of life on this planet.



Scheme 1. The biological nitrogen cycle.

The important but often contradictory consequences of the denitrification process include that: (1) it generated in the past almost all of the gaseous nitrogen in the earth's atmosphere and now maintains the standing stock by continual production in an annual turnover of some 2 x 10⁸ tons of nitrogen; (2) it causes up to 30% loss of fertilizer-fixed nitrogen from agricultural soil, thus limiting plant productivity; (3) it emits free nitrous oxide which has been found to contribute to ozone destruction in the stratosphere and to the increased planet temperature through the so called "green house effect"; (4) it removes nitrate or nitrite from waste-water and finds important industrial uses in waste-water treatment plants; (5) finally, it

results in the temporary accumulation of toxic nitrite which is known to react with secondary amine to form carcinogenic nitrosamines in food, water or digestive system.

Man has dreamed of controlling and curtailing denitrification for decades. But without proper knowledge of the chemical mechanisms and its ecological impacts, there are enormous risks involved in tempering with a process of such global significance. The delineation of the general pathway of this process only occurred recently.

B. Cytochrome cd₁ Nitrite Reductase

It has been found that NO_3^- is first reduced by molybdenum-containing nitrate reductase to nitrite.^{5, 6} and the dissimilatory nitrite reductase reduce NO_2^- to nitrous oxide (N_2O) which is then converted to dinitrogen through a separate nitrous oxide reductase (a copper enzyme).^{7, 8} Clearly, it is nitrite reduction that defines denitrification.

There are two types of denitrifying nitrite reductases reported;⁴ one is a multiheme protein named cytochrome cd₁ and another is a Cu-containing enzyme. The cytochrome cd₁ enzyme appears to be more prevalent in nature and so far has been isolated from a large number of chemoautotrophic denitrifying bacteria, including Pseudomonas aeruginosa,⁹ Thiobacillus denitrificans, 10 Alcaligenes faecalis (formerly Pseudomonas denitrificans),¹¹ Paracoccus denitrificans (formerly Micrococcus denitrificans),¹² Paracoccus halodenitrificans and Pseudomonas stutzeri.¹⁴

In 1958, Horio extracted and partially purified four different kinds of soluble respiratory components from <u>Pseudomonas aeruginosa</u>. ^{15, 16} Among the purified components, there was a greenish-brown fraction which possessed a complex spectrum containing both a <u>c</u>-type cytochrome and a

so-called \underline{a}_2 cytochrome. This enzyme component exhibited general properties of a cytochrome oxidase: aerobically it oxidizes ascorbate, hydroquinone and reduced cytochrome c551. These reactions were found strongly inhibited in the presence of cyanide and carbon monoxide. During the early purification, this preparation was called cytochrome GB because of its greenish-brown color; later it was renamed pseudomonas cytochrome oxidase.¹⁷ The property of the same entity as a nitrite reductase was recognized by Yamanaka and Okunuki in the subsequent years. 18, 19 It was uncertain at that time whether this preparation is one enzyme, which itself has two activities, or the preparation contains two distinct enzymes. Yamanaka and Okunuki²⁰ in 1962 isolated the greenish-brown component in a pure crystalline state and proved it as a single enzyme. They further confirmed that the enzyme contains two different hemochromes and possess a dual enzymatic property, that is, it acts as both a nitrite reductase and a cytochrome oxidase. Thus the name "pseudomonas cytochrome \underline{c}_{551} : nitrite, O2 oxidoreductase" was once used by these workers to indicate the double function of the enzyme when cytochrome \underline{c}_{551} was involved in the redox reaction.²¹ Although the function initially attributed to this enzyme was that of cytochrome oxidase (or oxygen-reductase) and has been until recently the best known function, it is now considered as a secondary and nonphysiological function. The \underline{a}_2 heme has been renamed as \underline{d} , and later to \underline{d}_1 after 70's, thus this enzyme is most properly named as cytochrome \underline{cd}_1 nitrite reductase.

As shown in Figure 2, cytochrome cd_1 consists of two identical subunits and has a twofold axis. Both subunits have a oblong shape with a length of 90-100 A. The dimension of the enzyme is less than 73 A and the volume is around 145 nm³.²², ²³ Each subunit of molecular weight of 63,000 dalton

contains a red \underline{c} -type heme prosthetic group and a green colored heme \underline{d}_1

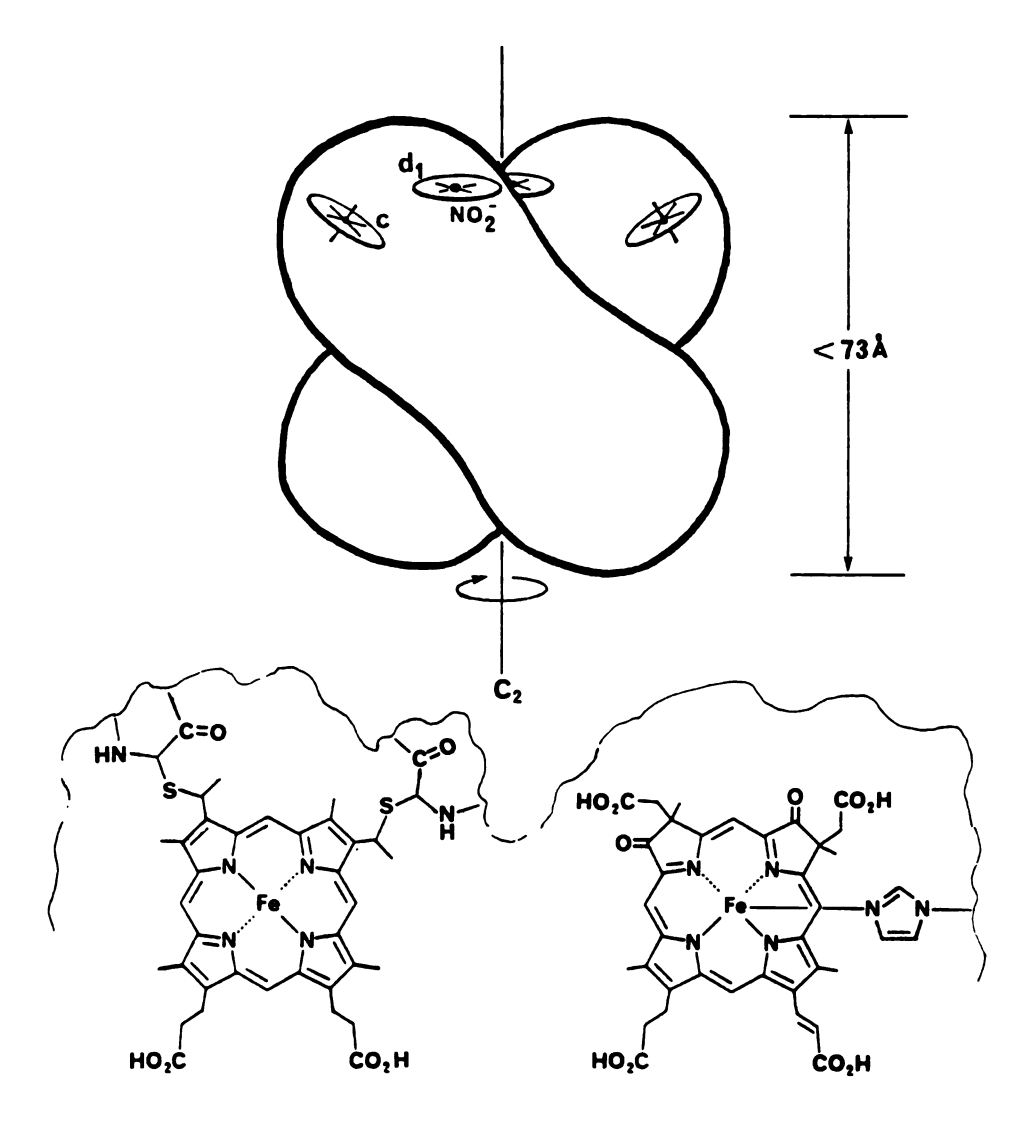


Figure 2. The shape, dimension and symmetry of cytochrome \underline{cd}_1 .

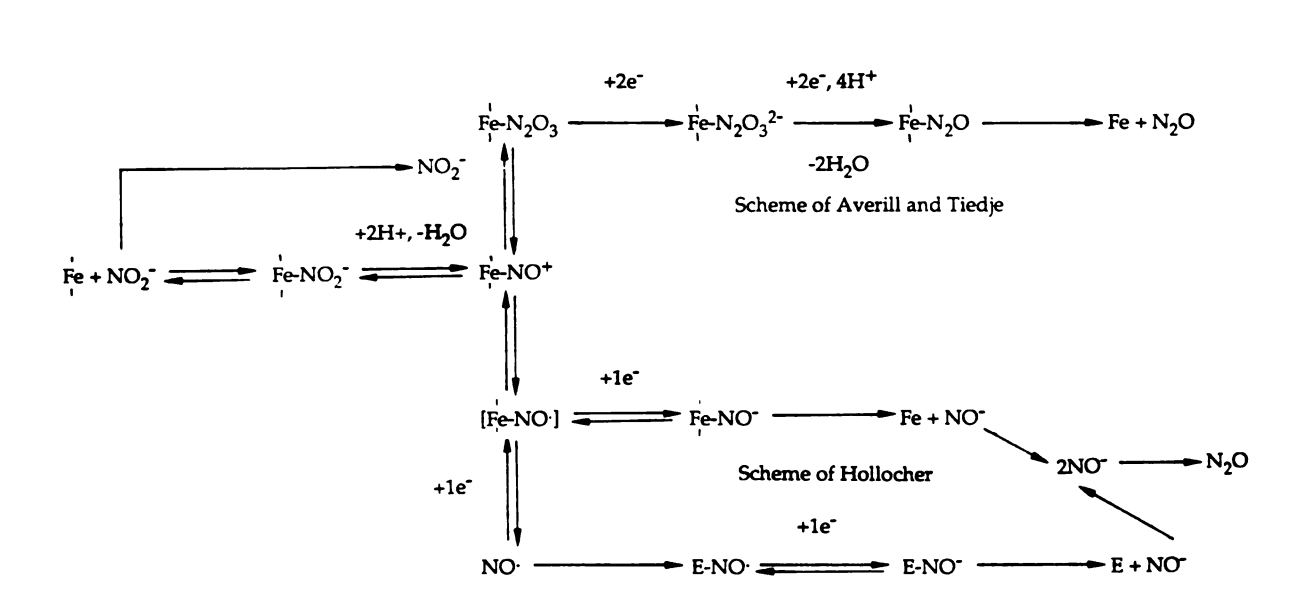
moiety.^{24, 25} In both oxidized and reduced forms of the enzyme, heme \underline{c} and heme \underline{d}_1 groups in each subunit are oriented perpendicularly to each other with a closest distance of 13-15 Å.^{26, 27} All four heme prosthetic groups are found at one end of the protein molecule.²² Heme \underline{c} is covalently bonded to the polypeptide backbone by two thioether linkages to cystine. The iron atom

of heme \underline{c} is six-coordinate and low spin in both Fe(II) and Fe(III) oxidation states and the axial ligands are thought to be histidine and methionine. Heme \underline{d}_1 is noncovalently associated in the protein pocket. In the absence of exogenous ligands, the Fe(II) heme \underline{d}_1 is high spin and is thought to be five-coordinate with a nearby axial N donor, possibly, an imidazole residue. ²⁸ The Fe(III) \underline{d}_1 has been suggested as low spin and presumably six-coordinated with an additional endogenous protein residue or a water molecule providing the other axial ligand. ²⁹ In vivo this enzyme, while water soluble after isolation, is normally associated with cell membrane and its physiological electron donor is cytochrome \underline{c}_{551} and/or a blue copper protein azurin. ^{10, 42} The kinetics work to date supports the idea that the heme \underline{c} sites are associated with electron uptake, while the heme \underline{d}_1 sites are responsible for electron donation to exogenous ligands, i.e. the substrates of the enzyme, such as oxygen and nitrite.

This enzyme is only produced anaerobically in the presence of nitrite and serves its intended function as nitrite reductase. Once formed, it can also donate electrons to molecular oxygen, reducing oxygen to water, thus functions also as cytochrome oxidase. The turnover number of cytochrome cd_1 as oxygen reductase under the physiological condition corresponds to 600 moles of oxygen consumption per mole of the enzyme per minute at 37 °C . Under anaerobic condition, one mole of this enzyme reduces 4,000 moles of nitrite to nitrogen oxides per minute at the same temperature. Thus its nitrite reductase activity is about sixfold more than its oxidase activity. The constitutive cytochrome-oxidases are found always more active than cytochrome cd_1 as the oxygen reductase. Most recently, another nonphysiological property, the carbon monoxide oxygenase activity, of cytochrome cd_1 was studied by Timkovich and Thrasher. andeet_1

C. On the Mechanism of Nitrite Reduction

Although nitrite reduction is the alleged function of cytochrome \underline{cd}_1 , controversy has arisen about the nature of the physiological intermediates or products in the course of reduction. Mainly, there are three proposed pathways concerning how NO_2^- is converted to N_2O , Scheme 2. The first,



Scheme 2. The mechanism of nitrite reduction.

also the oldest, proposes two enzymes: a nitrite reductase and a nitric oxide reductase with NO as the obvious intermediate.⁴ This pathway offers no explanation how the N-N bond is formed. The second pathway, proposed by Averill and Tiedje,³² requires that the conversion be carried out by one enzyme and that N-N bond formation occurs before reduction. The third pathway, proposed by Hollocher,³³, ³⁴ can also be carried out by a single enzyme, and suggests that reduction of nitrite to nitroxyl occurs, followed by dimerization of nitroxyl (NO⁻) to form N₂O. This pathway could

accommodate a separate NO reductase. These three schemes have coexisted since 1982 but it has not yet been resolved as to which one is actually responsible for denitrification, since this determination is not trivial. Evidence of the pros and cons for each proposal has been presented in the literature. $^{32-39}$ It can be simply pointed out that the key reaction of N-N bond formation must be intimately associated with the heme \underline{d}_1 -nitrosyl [Fe-NO+] complex, which in turn, must depend on the nature of the \underline{d}_1 heme prosthetic group.

D. Heme d₁

The green heme cytochrome cytochrome cd1 from Pseudomonas aeruginosa was first observed by Horio and coworkers in 1958. It was first classified as an " a_2 -type" heme for having a typical absorption maximum around 630 nm according to the designation Keilin assigned for cytochromes absorbing in the red region.⁴⁰ This heme was first isolated by Yamanaka and Okuniki in 1961,41 and its visible spectra in both oxidized and reduced forms and of pyridine, CN-, NO and CO derivatives were carefully documented at the same time.⁴² It was frequently compared with and related to another green heme, Barrett's green heme from Aerobacter aerogenes and Escherichia coli,43 which was also designated as "a2". Since Barrett had previously determined his heme \underline{a}_2 to be an iron chlorin it was assumed that "heme \underline{a}_2 " from Pseudomonas aeruginosa and other denitrifying bacteria must also be a chlorin. To avoid confusion with aa3 hemes of mammalian cytochrome oxidase heme \underline{a}_2 was renamed " \underline{d} " after 1970. Lemberg and Barrett noticed the spectral and solubility differences that exist between the "classical heme <u>d</u> (\underline{a}_2) ", as obtained from sources such as \underline{E} , \underline{coli} , and the extractable heme of pseudomonas nitrite reductase and therefore suggested the name heme d1 to

distinguish the latter.⁴⁴ However, the idea of heme \underline{d}_1 being a chlorin with a structure like 2 was unchallenged in more than two decades. Timkovich in 1984^{45, 46} managed to isolate and purify enough material to allow a careful structure determination with the aid of modern instruments.

The \underline{d}_1 structure concluded by Timkovich has also a chlorin core as shown by 3 with the most unusual arrangement of substituents. This structure is considered surprising since it defies all known biosynthetic pathways by which the other porphyrinoids come into being. To date there are no known exceptions to the fact that all the naturally occurring tetrapyrrolic macrocycles derive their substituent pattern from uroporphyrinogin III and structure 3 is obviously not one of them. After a careful examination on the spectra data published, C. K. Chang³ in 1985 proposed the revolutionary structure 1 for heme \underline{d}_1 , which possesses a porphyrindione (dioxo- isobacteriochlorin) core structure hitherto unknown in the biological world. This structure not only fits all the spectroscopic and analytical data better but also is compatible with the common porphinoid biosynthetic pathway.

II. OBJECTIVES OF THE PRESENT WORK

The principal objectives of our study are to understand the structure and function of \underline{d}_1 heme prosthetic group in cytochrome \underline{cd}_1 nitrite reductases. Specifically we intended to study the following:

- 1. Further characterization of heme d_1 structure. To verify the proposed porphyrindione (dioxo-isobacteriochlorin) structure of the d_1 moiety by chemical derivatization of the natural pigment and by comparing its spectral properties side-by-side with those of well-characterized synthetic model compounds.
- 2. Synthesis of d_1 prosthetic group and its structural and functional analogues. To provide definitive proof of structure and produce a copious supply of heme \underline{d}_1 and its analogues for other experiments.
- 3. Physicochemical properties of heme d_1 and model systems. To build a knowledge base of the intrinsic properties and reaction profile of heme \underline{d}_1 and to identify unique properties not present in the other systems. Using synthetic heme \underline{d}_1 and its analogues, we plan to examine the spectral properties of these compounds by UV-Vis, NMR, IR, and RR spectroscopies, and determine their redox chemistry by electrochemical means. Throughout these studies, whenever necessary, comparative studies on chlorin and isobacteriochlorin compounds will be carried out such that the attributes of the porphyrindione system can be evaluated.
- 4. Reconstitution of cytochrome cd_1 and other protein with synthetic d_1 and its analogues. To replace protoheme of myoglobin with \underline{d}_1 -type hemes to allow studies of heme \underline{d}_1 in a well defined protein environment. To replace the natural heme \underline{d}_1 in cytochrome \underline{cd}_1 with synthetic heme \underline{d}_1 and other related hemes so that the functional role of heme \underline{d}_1 moiety may be revealed. Cytochrome \underline{cd}_1 will be grown and isolated from \underline{P} . aeruginosa or \underline{P} . stutzeri.

Standard measurements and reactivity assays will be performed with reconstituted enzymes to document any structure-function relationships. In particularly, the ability to produce N_2O will be monitored in the reconstituted systems.

III. RESULTS AND PRESENTATION

Significant progress has been made during the last three years toward the above objectives. Our proposal that the green-colored heme \underline{d}_1 is not a chlorin but a porphyrindione (dioxo-isobacteriochlorin) has been fully substantiated; the suggested structure has been proven entirely correct; total synthesis of this new chromophore is now achieved; redox and coordination chemistry has been studied; native heme \underline{d}_1 and cytochrome \underline{cd}_1 have been isolated from Pseudomonas stutzeri; apoprotein of cytochrome \underline{cd}_1 has been reconstituted successfully with both native and synthetic heme \underline{d}_1 as well as a number of \underline{d}_1 analogues and related hemes.

In the following chapters, Chapter 2 provides further evidence on the heme \underline{d}_1 structure as we proposed, describing the synthesis and properties of several model compounds. The methodologies employed for the formation of 1,3-dione core structure and acrylic side chain are described in detail. Chapter 3 describes the total synthesis of heme \underline{d}_1 from different approaches and the convenient synthesis of a \underline{d}_1 analogue from coproporphyrin IV. In Chapter 4, the steric and the structural isomers of \underline{d}_1 are compared, the questions concerning the native form as well as biosynthetic origin of this novel heme are also discussed. Chapter 5 is devoted to the physicochemical property of \underline{d}_1 and its model systems in comparison with those of the other porphyrinoids, especially chlorin and isobacteriochlorin systems. Chapter 6

deals with the reconstitution of cytochrome \underline{cd}_1 nitrite reductase with both native and synthetic heme \underline{d}_1 in an effort to understand the mechanism of nitrite reduction. Finally, some thoughts on the future work are presented in Chapter 7.

IV. NOMENCLATURE OF HEME \underline{d}_1 AND RELATED PORPHYRINS

The nomenclature of porphyrinoids with keto group(s) on the ring has not been standardized. Neither the names "geminiporphyrine-diketone and geminiporphyrine-monoketone" as Inhoffen^{47, 48} used nor "oxochlorin and dioxo-isobacteriochlorin" as Johnson^{49, 50} named are convenient and specific. The prefix "oxo-", in fact, could be confused with "oxyporphyrin" or "oxophlorin", which denotes a porphyrin with an oxygen attached to the methine bridge. Furthermore, we now know that these ketone derivatives have very little chemical properties in common with those of the corresponding chlorins, isobacteriochlorins, or bacteriochlorins.⁵¹ It is probably more appropriate to consider them "quinones" of porphyrins, hence we propose the use of "porphyrinone" and "porphyrindione". In addition, we suggest the trivial names "dioneheme" for heme d_1 (pronounced either like dye-own-heme or d-1-heme) and the "6-acrylo-1,3-porphyrindione" for the metal-free \underline{d}_1 , a modification of Timkovich's "acrylochlorin".^{45, 46} The prefix numbers "6-" and "1,3-" are used to specify the positions of the acrylic side chain and the keto groups on the ring. The advantage of our nomenclature is that all common names of precursor porphyrins can be retained and put to work. For example, the monoketone derivative of mesoporphyrin (5) is named as "mesoporphyrinone" and the diketone derivative (6) is named as "1,3-mesoporphyrindione", and the diketone 7 from coproporphyrin IV is "2,3-coproporphyrin(IV)-dione".

MeO₂C
$$\frac{\alpha}{2}$$
 $\frac{\alpha}{311}$ $\frac{\alpha}{311}$

MeO₂C
$$O_2$$
Me O_2 C O_3 Me O_4 C O_4 Me O_4 C O_5 Me O_5

As illustrated in the structure 4 of metal free heme \underline{d}_1 , we use the conventional Fischer 1, 2, 8 system for the substituents, and the positions of the two keto groups are assigned as "1,3-". The four pyrrole rings are numbered A, B, C and D clockwise starting from the up-left ring bearing the first keto group and the four meso positions are indicated as α , β , γ and δ accordingly. For convenience, the position assignment of the substituents of heme \underline{d}_1 (structure 4) is taken as a standard, thus the acrylic side chain is at position 6 on ring C and the propionic chain is at position 7 on ring D. All the substituents, including the ring keto group, of other porphyrins, porphyrinones and porphyrindiones are numbered accordingly throughout this work.

CHAPTER 2

FURTHER CHARACTERIZATION OF HEME d₁ STRUCTURE

I. EVIDENCE OF THE 1,3-PORPHYRINDIONE STRUCTURE OF HEME \underline{d}_1

Absorption Spectra

The most persuasive evidence in favor of a non-chlorin structure of \underline{d}_1 is from the visible spectrum of this natural pigment in the form of its free base methyl ester. Examination of more than twenty of the naturally occurring or synthetic chlorins revealed that the chlorin visible spectra are remarkably homogeneous in that the overall pattern is relatively unperturbed by electronic effects of the peripheral substituents. However the overall shape of the \underline{d}_1 spectrum does not resemble that of any chlorin compound, but that of a typical isobacteriochlorin, such as sirohydrochlorin, 52 except that all peaks are red shifted. This leads to a less known isobacteriochlorin-type compound: a 1,3-porphyrindione 8 (dioxo-isobacteriochlorin) 53 whose absorption peaks are significantly red shifted from ordinary isobacteriochlorins. Metal complexes of the natural heme \underline{d}_1 and compound

8 are made and their visible spectra are measured quantitatively. As shown in <u>Figure 3a</u> and <u>3b</u>, the neutral, free base spectra of the two are dissimilar in

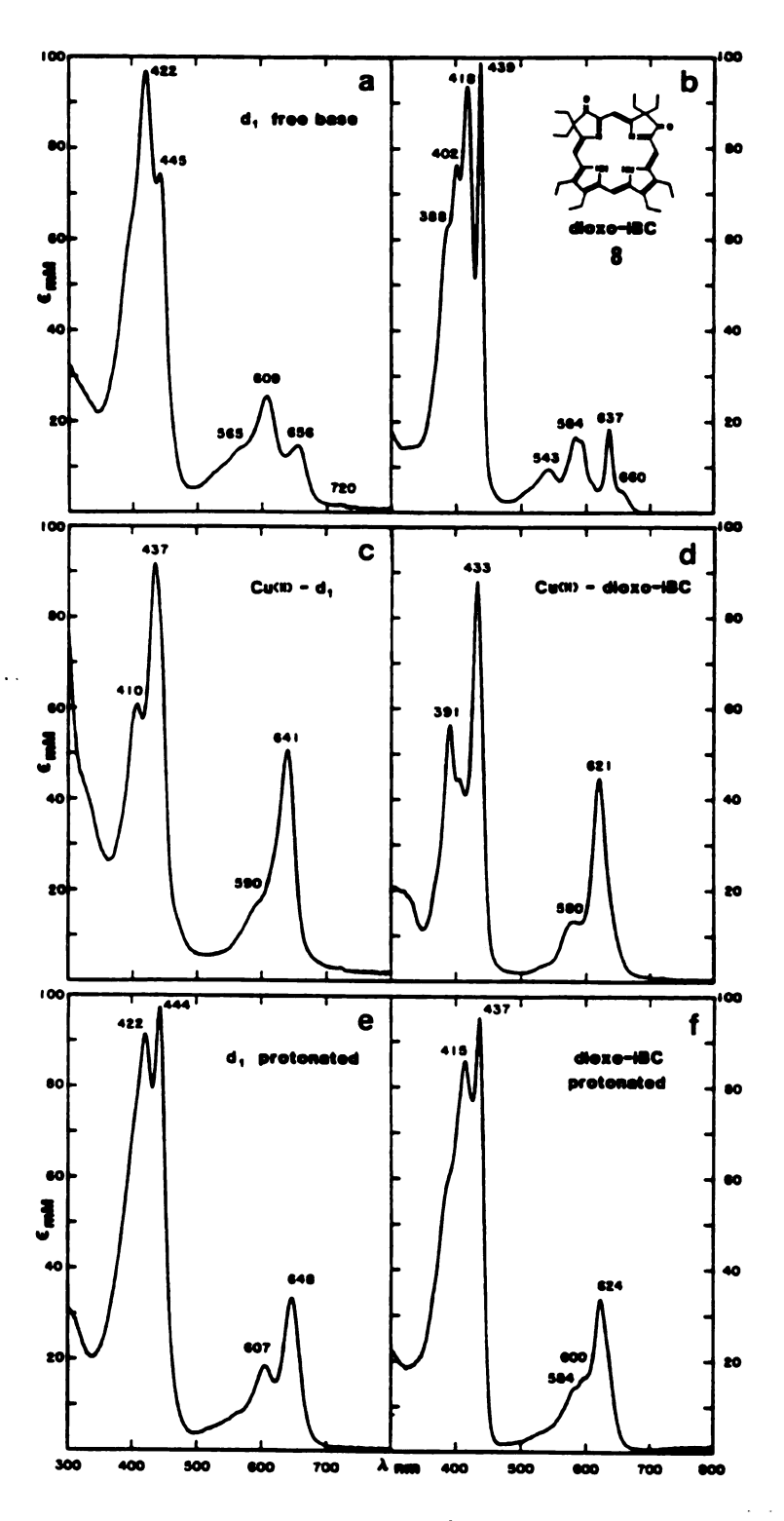


Figure 3 UV-vis absorption spectra of heme d₁ versus 1,3-OEPdione 8 in CH₂Cl₂.

both Soret and visible regions. However, the multiplicity of bands seen in the free bases due to the broken of symmetry by the central protons and vibronic overtone diminishes when the rings are protonated and metallated. The correspondence between \underline{d}_1 and 8 become more apparent when these forms are compared as shown in Figure 3c-3f. The low extinction coefficient of the Soret absorption bands and particularly the low ratio of A_{Soret} versus $A_{vis\ band}$ seen in both compounds certainly argues forcibly for the unlikelihood of chlorins or porphyrins. A consistent feature of the spectrum comparisons is the ca. 20 nm red shift of the highest wavelength of \underline{d}_1 . The proposed structure 4 does contain the extra conjugation of the acrylate which could account for the red shift. As shown in Figure 4, when this olefinic substituent of heme \underline{d}_1 is hydrogenated by treatment with H_2 -PtO₂, the band shifts to a wavelength coincident with that of dione 8.

High Resolution Fast Atom Bombardment Mass Spectra

One of the key questions of Timkovich's original assignment 3^{45} is the inability to obtain the parent MS ion of 714; an "(M-2)+" of 712 was observed instead. This was attributed to the loss of inner pyrrolic protons, an event observed in the other porphyrins.⁵² The 6-acrylo-1,3-porphyrindione structure 4, has two less hydrogen than 3 and therefore fits perfectly with the observation. New fast atom bombardment mass spectra were obtained in a matrix that consistently gives $(M+1)^+$ ions for porphyrins.⁵⁵ Mass units for the protic methyl ester, (M+1) = 713, the 2H_3 methyl ester (725, 726, and 727 corresponding to two 1H , one 1H and one 2H , or two 2H at the inner pyrrolic NH's), the copper chelate of the protic methyl ester (773), and the copper chelate of the ethyl ester (829) are only consistent with structure 4.

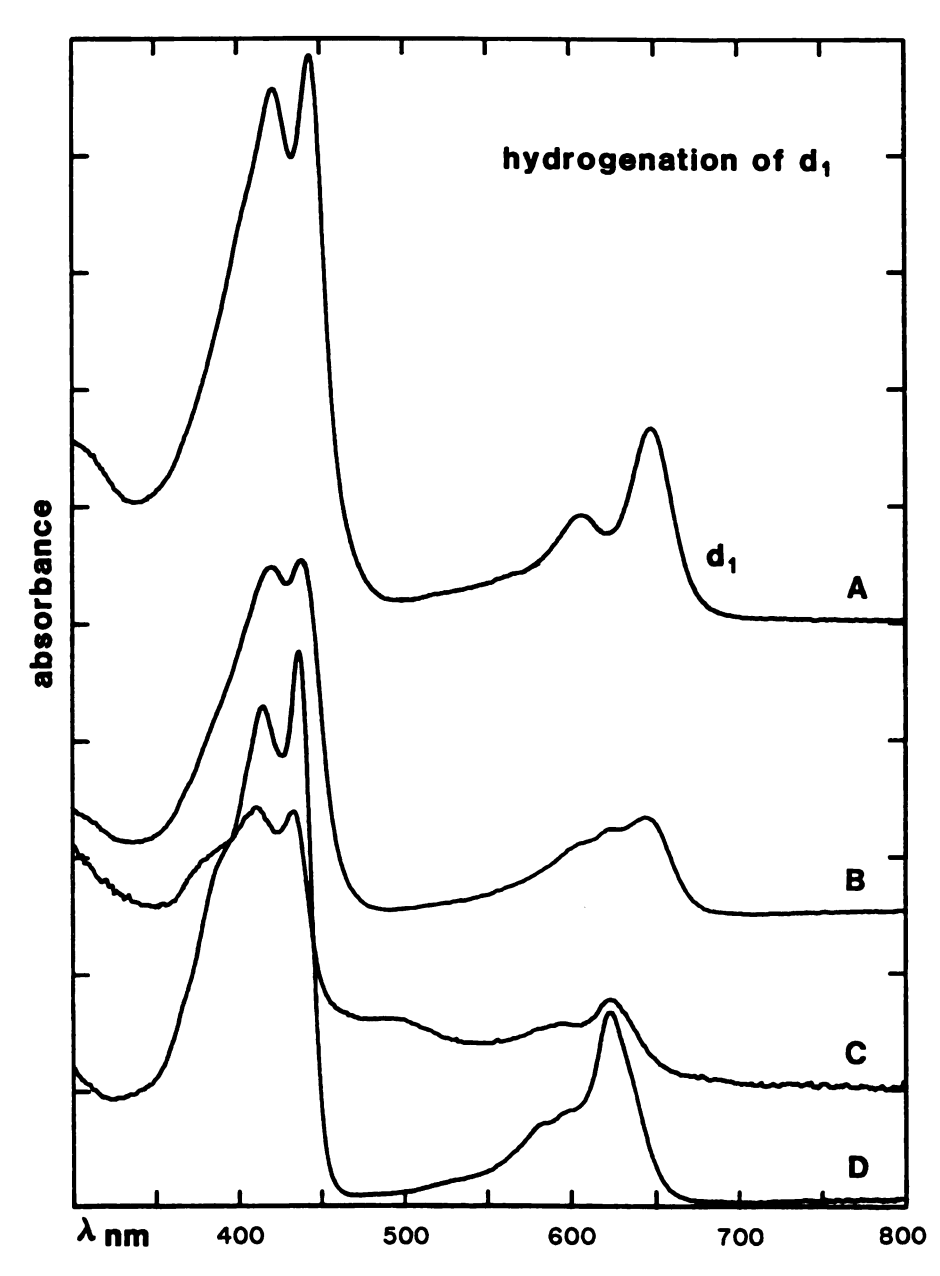


Figure 4 UV-vis absorption spectrum changes of heme \underline{d}_1 during hydrogenation in formic acid/Pt. (A) \underline{d}_1 before hydrogenation; (B) after 30 s; (C) after 90 s; (D) model compound 8 in formic acid. The \underline{d}_1 ring was also hydrogenated during the time, leading to decreased absorption.

¹³C-NMR spectra

The natural abundance 13 C-NMR of about 2 mg of natural \underline{d}_1 methyl ester, after 708,625 transients (11 days), yielded a spectrum shown in Figure 5.

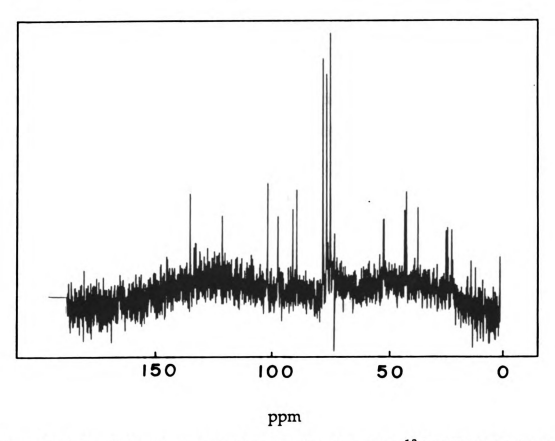


Figure 5. Natural abundance, broad-band proton-decoupled ¹³C-NMR of the free base methyl ester of d₁ in CDCl₃ at 32 °C. The chemical shifts are given in Table 1.

The chlorin structure 3 has two hydroxymethyl groups on the β -pyrrole carbons while structure 4 proposes acetate esters. The expected ¹³C chemical shift is very different for the methylene carbons of these two moieties. Methyl groups on the saturated β -pyrrolic carbons in model porphyrins are usually very close to 23 ppm.^{56, 57} The incremental shift for replacing an H with -CO₂R is about 20 ppm, predicating 43 ppm for -<u>C</u>H₂CO₂R. The incremental shift for replacement with -OH is 48 ppm, predicating 71 ppm for

- $\underline{C}H_2OH$. The spectrum of \underline{d}_1 showed no evidence of any peaks near 71 ppm while two distinct resonances are evident at 43 ppm giving compelling support for the structure 4.

With the above data we were in a position to dismiss the chlorin structure for heme \underline{d}_1 . However, further work was still required to ascertain that \underline{d}_1 does have a 1,3-porphyrindione core structure and the conjugating acrylic side chain is attached at the position 6 of ring C as we proposed. Therefore, we turned to synthesizing well-characterized model compounds.

II. STUDY WITH MODEL COMPOUNDS

Initially, model compounds 9 and 10 were designed to duplicate the structure character of 4. Model 9, with a 1, 3-dione nucleus and with one acetate function attaching to each of its two tertiary carbons, has the elements of the northern half of 4, its NMR spectra would be invaluable for verification purpose. Compound 10, with an acrylic side chain setting at the desired position on ring C, besides providing useful NMR data, should give a visible spectrum virtually identical to what has been observed with \underline{d}_1 . To verify the position of the acrylic side chain in relation to the two keto groups, a regioisomeric compound 11 of 10 was also considered necessary.

To obtain these model compounds we were facing two challenging problems, that is, developing an elegant pathway to form the 1,3-porphyrindione core structure and establishing an effective method to introduce selectively the acrylic side chain to the ring C of the macrocycle.

A. Formation of the 1, 3-Porphyrindione Skeleton

We suggested originally that the keto groups in structure 1 of \underline{d}_1 are possibly derived from a pinacolic rearrangement of vicinal diol or epoxide.³ Precedence of such reactions in porphyrin so far has been limited to only a few systems.

Hans Fischer and his students⁵⁸ reported in 1930 a novel method to obtain green-colored chlorin from porphyrin. They reacted mesoporphyrin IX in concentrated sulfuric acid with hydrogen peroxide and yielded a product which was designated as "dioxymesoporpyrin" even though the elementary analysis results were ambivalent in showing whether one or two oxygen atoms had been added to the porphyrin. Indeed they later concluded that the green product resulted from this acidic medium contains only one extra oxygen atom and called it "anhydrochlorin".⁵⁹ The structure they proposed, formulated as a epoxide ring cross a pyrrole double bond, was again incorrect. Johnson^{49, 50} and Inhoffen,^{47, 48} about 20 years ago, independently reinvestigated such oxidation reaction using symmetrical etioporphyrin and octaethylporphyrin (OEP) and established that the true identity of the major product from this hydrogen peroxide-sulfuric acid oxidation is a keto chlorin (porphyrinone) formed by a pinacol rearrangement of the intermediate diol or epoxide. By our inference, Fischer's "dioxymesoporphyrin" must also be some sort of keto derivative but the exact products of the mesoporphyrin oxidation was far from clear. For being an unsymmetrically substituted porphyrin, mesoporphyrin could produce up to 8 isomeric porphyrinones. Furthermore, as reported originally by Inhoffen and Nolte, 47, 48 and more recently by Chang 60 using OEP, the oxidation reaction does not stop at the monoketone level; diketones, and even triketones, arise almost simultaneously under the reaction condition optimized for porpyhrinone. With OEP there are five diketones and four triketones identified; for mesoporphyrin, there could be 14 diketone regioisomers alone statistically without counting the diastereomers! The sheer number of anticipated isomeric products from mesoporphyrin must have dissuaded attempts to reexamine this reaction for after more than a half century, Fischer's pioneering yet unsolved work stands unsettled.

A central question concerning the pinacol rearrangement is the migratory aptitude when the substituents involved are not equivalent, 61 such as in the mesoporphyrin's case, therefore OEP is inapplicable to address this question. Hans Fischer 58, 62 demonstrated that hydroxylation of type-IX porphyrin can be achieved with osmium tetroxide although the resultant isomeric dihydroxyl compounds were not individually identified. Recently, our group devised a convenient method 63 with OsO₄ to effective dihydroxylation of porphyrins to obtain chlorin diols. These diols indeed rearranged in acidic medium to give excellent yields of corresponding porphyrinones. Although this synthetic study is more useful in preparing for heme d and its model compounds, 64 it offers a potential way to prepare porphyrindione. Employing a variety of specifically synthesized porphyrins, C. Sotiriou of our group 65 completed a series of experiments aiming at elucidating the reactivity as well as the migratory aptitude of the biologically important porphyrin side chains. The results are cited here:

1). Relative reactivity of the pyrrole double bond towards dihydroxylation is

proportional to, barring electronic effect, the size of the substituents, the larger the substituent, the slower the rate, thus: H = Methyl (Me) > Ethyl (Et) > Acetic (A) > propionic (P).

2). Migratory aptitude of the substituents is mainly related to their electronic effect; hydrogen, ethyl, alkyl including propionate side chain will migrate over methyl group and acetate side chain has a lower mobility than methyl. These general rules hold true in most porphyrins.

Although the two-step OsO₄ oxidation-acid catalyzed pinacol rearrangement may offer some control over the unwanted porphyrinone isomers, it is not useful for producing the 1,3-dione of the isobacteriochlorin-type derivatives. In the presence of excess amounts of osmium tetraoxide only tetrahydroxybacteriochlorin was observed. Even deuteroporphyrin, which has built-in steric advantages, was found to react with an excess of OsO₄ to yield only the tetrahydroxybacteriochlorin without any trace of isobacteriochlorin. This reaction pattern may be due to the preferred diagonal π-electron delocalization pathway presents in all porphyrins, which prompts the saturation of the two isolated, diagonal pyrrole β,β' -double bonds with minimum lost of π -energy. A similar argument has been advanced to account for the exclusively diagonal reduction of the tetraphenylchlorin by diimide to yield bacteriochlorin.66 In a medium of sulfuric acid, however, porphyrin could become doubly protonated, the influence of the valence tautomerism would become insignificant, and isobacteriochlorin may be formed. Indeed, in the reaction of OEP with hydrogen peroxide-sulfuric acid, the combined yield of three dioxoisobacteriochlorins (1,3-porphyrindiones) is better than that of two dioxobacteriochlorins (1,5- and 1,6-porphyrindiones).60 Therefore the H₂O₂-H₂SO₄ oxidation was applied in an attempt to prepare model

compounds 9 from porphyrin tetraacetate 12 and the core structure of 10 from mesoporphyrin IX respectively.

1. On the H₂O₂-H₂SO₄ oxidation of porphyrin tetraacetate

The porphyrin tetraacetate 12 was synthesized through a 2+2 dipyrrylmethene condensation pathway, Scheme 3, following Fischer's classical method.^{67, 68} The dipyrrylmethene 14 was easily obtained in crystalline form by brominating pyrrole 13 in acetic acid. Heating 14 in fused methylsuccinic acid at 130° for 6 hours, gave porphyrin 12 in a yield of 12%. However, the four symmetrically substituted acetate groups render this compound not only poorly soluble in most organic solvents, but also unexpectedly inert toward H₂O₂-H₂SO₄ oxidation and subsequent pinacolic rearrangement. Only a very low yield of porphyrinone 15 was obtained together with some Y-lactone compound 16 after a prolonged reaction of 12 in the hydrogen peroxide-sulfuric acid medium. No trace of the desired porphyrindione 9 was detected. An alternative OsO₄ oxidation of this porphyrin gave only a poor yield of dihydroxychlorin 17, which refused to undergo pinacolic rearrangement to 15 in concentrated sulfuric acid but cyclized instead almost quantitatively to lactone 16. These results indicated clearly that the four electron-withdrawing acetate side chains have rendered the pyrrole double bond inactive toward H₂O₂ oxidation as well as osmic The pinacolone formation was found sluggish due to the electron-deficiency on the ring, which might destabilize the cation necessary for rearrangement, thus the reaction tends to form the thermodynamically stable 5-membered lactone 16. Similar results were also observed in our later experiments.

Scheme 3

2. On the H_2O_2 - H_2SO_4 oxidation of mesoporphyrin

We were optimistic on the oxidation of mesoporphyrin with hydrogen peroxide-sulfuric acid based on the consideration that no strong electron-withdrawing group like acetate are present and that the pinacolic rearrangement of the diols would be dictated by the specific migratory aptitudes of the substituents. As mentioned earlier, both ethyl and propionate side chains in a vic-dihydroxychlorin have a higher migratory aptitude as compared with the methyl group. Because that the diol formation is highly sensitive to the size of the side chain, the "northern diols" should be preferred versus the "southern" diols and the desired 1,3-porphyrindione 6 would be the favored product.

Thus, mesoporphyrin dimethyl ester dissolved in concentrated sulfuric acid was reacted with H₂O₂, and after about 30 minutes the solution was neutralized by sodium acetate. The solid product, collected by filtration, contained most of the ketone products with intact propionic esters. Chromatography of this material on silica gel went surprisingly well, and nine different compounds, excluding the unreacted mesoporphyrin, were obtained (Scheme 4); the total yield was about 30% (reproducible in three separated runs).⁶⁸ Structure identification in most cases was straightforward, aided by UV-vis absorption and ¹H-NMR spectra. The differentiation of monoketones 5 and 18 and also 20 and 21 was accomplished by nuclear Overhauser enhancements (NOE),63,69 which was also of great value in confirming the assignment of 3,7-dione 22. The overall products distribution shows that indeed our anticipated reactivity and migratory aptitudes hold remarkably well with only two exceptions, the 2,3-dione 19 and 1,8-dione 24, but even in these two, one of the keto group is in the "correct" place. We suspect that 19 and 24 may arise from the respective precursors 5 and 18; the

Scheme 4

subsequent pinacol rearrangement went to the "wrong" direction because the formation of adjacent diketones is energetically favorable, which offsets the regular migratory trend. In all diketones, the presence of diastereomers can be detected by NMR (bifurcation of the pyrroline substituent signals), but attempts to separate them have not been successful.

The clarification of the old literature problem has ample rewards. First, the demonstration that the oxidation of mesoporphyrin behaves in a predictable and reproducible manner and the separation and identification of individual regioisomers can be accomplished by using routine laboratory facilities and techniques immediately provide access to a rich source of all types of porphyrinone and porphyrindione derivatives. Secondly, the availability of these compounds suggests expeditious synthetic strategies for reduced porphyrin macrocycles. ^{63, 69} The monoketones and diketones are convenient precursors to alkylated chlorins and isobacteriochlorins such as bonellin⁷⁰ and sirohydrochlorin. ^{71, 72} Above all, the 1,3-porphyrindione 6 with the core structure of model compound 10, has been successfully prepared, albeit at an unimpressive yield (4.5%).

3. OsO₄ oxidation of Zn(II) porphyrinone

The disadvantage of the above H_2O_2 - H_2SO_4 oxidation of the β -substituted porphyrins, such as mesoporphyrin, is that it produces a complex mixture of isomeric products containing one, two, and three keto groups on the ring with uniformly low yields. Porphyrinone, such as 26 from octaethylporphyrin (OEP), can be prepared with significantly higher yield by an alternative 2-step reaction via OsO_4 oxidation and acid catalyzed pinacolic rearrangement. However, further oxidation of 26 by OsO_4 invariably leads to bacteriochlorin-type compound 27, which upon

rearrangement gives two isomeric products, 1,5-porphyrindione 28 and 1,6-porphyrindione 29.

We found that the osmium tetroxide addition preference can be altered dramatically in favor of isobacteriochlorin-type 1,3-porphyrindione 8 formation simply by metallation of the ring (Scheme 5). The zinc complex of 26 was found to react with OsO₄ (1.5 equivalent) in CH₂Cl₂ containing 1% pyridine to give predominantly dihydroxyporphyrinone 30 (>60% yield), which can be treated with sulfuric acid to give 1,3-dione 8. A small amount of the ring D diol 31 was also obtained which rearranged to yield about equally 8 and 32. If the synthetic goal is 8, the crude dihydroxylation products can be used directly in the pinacol rearrangement as the ratio of dione 8 to 32 is usually greater than thirty-fold. That the osmate addition mainly occurred at ring B of 26 is possibly a consequence of the electron-withdrawing effect of the carbonyl group rendering the adjacent ring D double bond less reactive. It is also noteworthy that during the pinacol rearrangement of 30 or its free base, none of the possible 1,4-dione 33 was observed. The sterically unfavorable arrangement of the four geminal ethyl groups in 33 might be the reason for its absence.

Insertion of other metal ions such as Cu(II) and Ni(II) has the same effect on switching the osmate addition pattern but the yields of the osmate esters were less satisfactory. The remarkable alteration of the site of attack by metallation in the chlorin-type system appears to be a general phenomenon. Previously it has been observed that the diimide reduction of free base tetraphenylchlorin (TPC) produces only tetraphenylbacteriochlorin whereas Zn(II) TPC gives exclusively Zn(II) tetraphenylisobacteriochlorin.⁷³ Similarly, reduction of the Ni(II) pheophorbide family of chlorin by Raney nickel promotes the formation of isobacteriochlorin.⁷⁴ Whitlock and Oster

Scheme 5

suggested that the saturation of a diametrical pyrrole double bond in the free base chlorin may be prompted by the diagonal π -electron delocalization pathway that bypasses the outer β - β ' double bonds of the pyrroline ring and its opposite partner, leading to the bacteriochlorin formation with minimum loss of π -energy.^{65, 73} The preference of this valence tautomer would be diminished when the system become metallated, or protonated as in our H_2O_2 - H_2SO_4 system. However this hypothesis did not explain why the double bond saturation occurs exclusively at the adjacent ring in the metal complex since one would expect that the absence of a preferred π -delocalizing pattern only favors a more random attack. Neither did the previous MO calculations of Zn(II)TPC show a significant difference in π -electron density between the opposite and adjacent β - β ' double bonds.⁶⁵ The cause of the selectivity remains unclear.

The selective saturation of porphyrinone double bond has made possible the synthesis of a variety of 1,3-porphyrindiones bearing peripheral substituents at the specific positions. As we have shown that dione 6, with the core structure of model compound 10, could be prepared by the H_2O_2 - H_2SO_4 oxidation of mesoporphyrin, with a <5% yield after repeatedly separation from a mixture of no less than nine ketone products. With the zinc method Scheme 6, dione 6 was prepared from mesoporphyrin cleanly with a much higher overall yield and the unreacted mesoporphyrin and porphyrinone 5 could always be recovered for recycling. The intermediacy of porphyrinone 5 seems to be necessary. Attempts to react zinc mesoporphyrin directly with an excess of OsO₄ have only resulted in intractable pigments. The two-stage oxidation via isolated porpyrinone has also imparted a high degree of regioselectivity for the isobacteriochlorin-type 1,3-dione formation. In the present case, if the isomeric porphyrinone 38 is used, the major

Scheme 6

product is 41, despite the steric advantage for osmic attack at ring A. In comparison with mesoporphyrin, the osmate selectivity of northern ring A and B versus southern ring C and D is about 4 to 1. The pinacolic rearrangement product from 40 is exclusively 3,5-porphyrindione 41, apparently reversing the migratory aptitude of methyl < propionate observed in the case of simple vic-dihydroxychlorin but fully agreeing with the above observation with porphyrindione 8, that the formation of the 1,3-dione is preferred to its 1,4-dione regioisomer. This observation has a strong influence on our later synthetic strategies to the d_1 structure 4, since we recognize that the best way to form 1,3-porphyrindione is to take advantage of both tendencies: the migratory aptitude of the substituents involved in the pinacolic rearrangement and the preferential formation of 1,3-porphyrindione from isobacteriochlorin-type vic-dihydroxyporphyrinone, as illustrated in the formation of 6 here. However if the migratory aptitudes of the substituents involved are not in agreement with the rearrangement direction, the 1,3-dione formation is still highly possible, as in the case of dione 41, since formation of the 1,4-dione is not detected. This strategy is best utilized later in the synthesis of the heme d_1 analogue 130.

B. Formation of the Acrylic Side Chain

There has been no precedence example of converting a porphyrin propionate side chain directly to an acrylic functionality. Acrylic porphyrins are usually synthesized by applying Kenovenagel-type condensation or Wittig reaction to corresponding formylporphyrins.⁷⁵ The necessary formylporphyrins can be obtained by electronic substitution of peripherally unsubstituted hemes with dichloromethyl ether,⁷⁶ or by degradation of vinylporphyrins with oxidants.⁷⁷ Owing to the inaccessibility of peripherally

unsubstituted porphyrins, especially those with the position of formyl group specified, a multistep total synthesis has often become an unavoidable choice.⁷⁸

Originally, a total synthesis pathway was contemplated to approach the model compound 10 (Scheme 7). The starting porphyrin 45 was to be assembled by a stepwise method from pyrrole 43, 44 and dipyrrylmethene 42. The dichloromethyl ether reaction would bring 45 to its formyl derivative 46, which would then be converted to a 1,3-porphyrindione 47, further to model compound 10. Since the electron-withdrawing -CHO was expected to retard the hydroxylation and lead to side reactions, we planned, as a backup, to replace the -CHO with a CH₂CHClCO₂Me group. After the formation of the 1,3-dione core structure, a strong base, such as DBU [1,8-diazabicyclo(5,4,0) undec-7ene] might generate the acrylic acid.

This scheme is obviously tedious and requires a substantial amount of time and effort to accomplish. After several attempts aiming at the synthesis of porphyrin 45 without yielding satisfactory results, we turned to another direction seeking a way to form acrylic side chain directly from the propionic side chain on a 1,3-porphyrindione.

As shown in Scheme 8, a reaction of the free base of 1,3-dione 8 with 1.5 equivalent of OsO₄ gave surprisingly only one single compound whose structure was determined by ¹H- NMR and NOE measurements to be diol 48. Presumably for the same reason as mentioned for the diol 30 formation, the ring D is less favored toward osmic attack due to the electron withdrawing effect of the keto group adjacent to it. This result is contradictory to the structure presumed by Inhoffen and Nolte who thought ring D diol 49 is the product. When diol 48 was treated with sulfuric acid, a triketone 50 was obtained. However, if heated in dilute hydrochloric acid, another chain of

Scheme 8

events took place; the diol 48 underwent elimination to generate the pyrrole double bond with the concomitant formation of an alcohol at the α -position of one of its ethyl groups on the ring. Possibly, the reaction went through an intermediate stage of exocyclic alkenes prior to dehydration (Scheme 9), a pathway perhaps similar to the suggested mechanism in Inhoffen's chlorophyll \underline{b} synthesis.⁷⁹

Two alcohols were isolated and identified as 51 and 52 with similar yields. Compound 52 was found to be quite inert toward dehydration and remained unchanged even after a lengthy reaction time, but to form readily its methoxy derivative 54 in the presence of methanol and catalytic amount of acid or on TLC plates. In contrast, compound 51 underwent smoothly dehydration to give a vinyl porphyrindione 53.

When 1,3-mesoporphyrindione 6 was treated with OsO_4 , the dihydroxylation occurred overwhelmingly at the ring C to give diol 55. Heating this compound in diluted hydrochloric acid resulted in almost quantitative formation of model compound 10 with the acrylic double bond formed at the ring C propionate side chain (Scheme 10). Even there were two alcohol intermediates possible, the β -hydroxylpropionate derivative 56 predominated. The formation of an acrylic side chain conjugating with the aromatic macrocycle seems to be thermodynamically favored so that it drives the reaction to 10 without stopping at 56 and this must have depressed the formation of hydroxymethyl isomer 57.

C. Spectroscopic Studies of Model Compounds

The UV-visible spectra of model compound 8, 53, and 10 are compared in <u>Figure 6</u>. It is obvious that the absorbance maxima are red shifted, especially in the visible region. There are about 10 nm shift toward red for

Scheme 9

Scheme 10

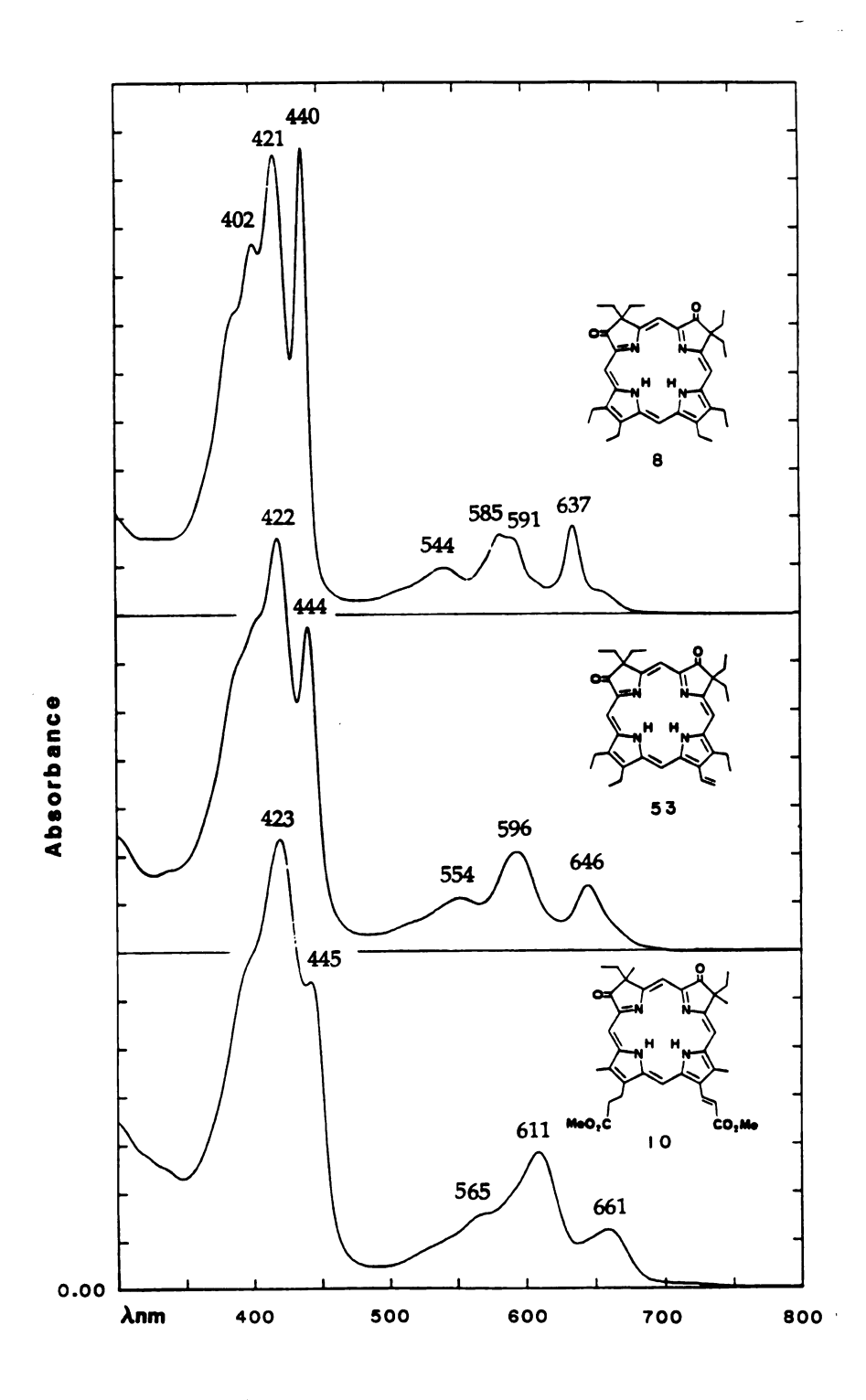


Figure 6 UV-vis absorption spectra of 1,3-dione 8, 53 and 10 in CH₂Cl₂.

all the dione absorption bands with the addition of a vinyl group and more than 20 nm shift with an additional carbonyl group. Model compound 10 has a visible spectrum virtually indistinguishable from that of d_1 (Figure 3a) arguing that these two compounds possess the same π -system. expected that the influence of the electronegative acrylic acid is both prominent and specific, i. e., the correct spectrum can only be obtained by an unique arrangement of the acrylic auxochrome in relation to the two keto groups on the ring, we were lucky to have the correct regioisomer 10 with the acrylic acid on ring C at the first try. A regio-isomer with the acrylic group on ring D was not obtained until we had achieved the total synthesis of \underline{d}_1 . The spectra of 10 in the forms of its copper complex and acid salt are given in Figure 7, they are nearly identical to those of the natural d_1 (Figure 3c and 3e). To scrutinize further, iron complex was prepared for 10 and three representative spectra (hemin chloride, alkaline ferriheme and pyridine hemochrome) were taken as shown in Figure 8. These spectra were compared with literature spectra of d_1 (Figure 1, 2 and 3 of Yamanaka and Okunuki¹¹⁴ and Figure 3 and 5c of Walsh et al¹¹⁵). The similarity between d_1 and model compound 10, again, borders on the identical. It is noticed that the triply split Soret band of the pyridine hemochrome has not been observed before with any porphyrin and chlorin hemes.

A comparison of the 1 H-NMR spectra of 10 and those of heme \underline{d}_{1} also shows a similarity that is striking for molecules of such complexity (Figure 2). One of the main reasons of Timkovich's original interpretation of the \underline{d}_{1} data went astray was the observation of \underline{d}_{1} meso resonances as grouped into two distinct pairs. This is almost universally observed for chlorin model compounds with the upfield pair representing the two meso protons adjacent to the sole saturated pyrrole. In most isobacteriochlorin, such as

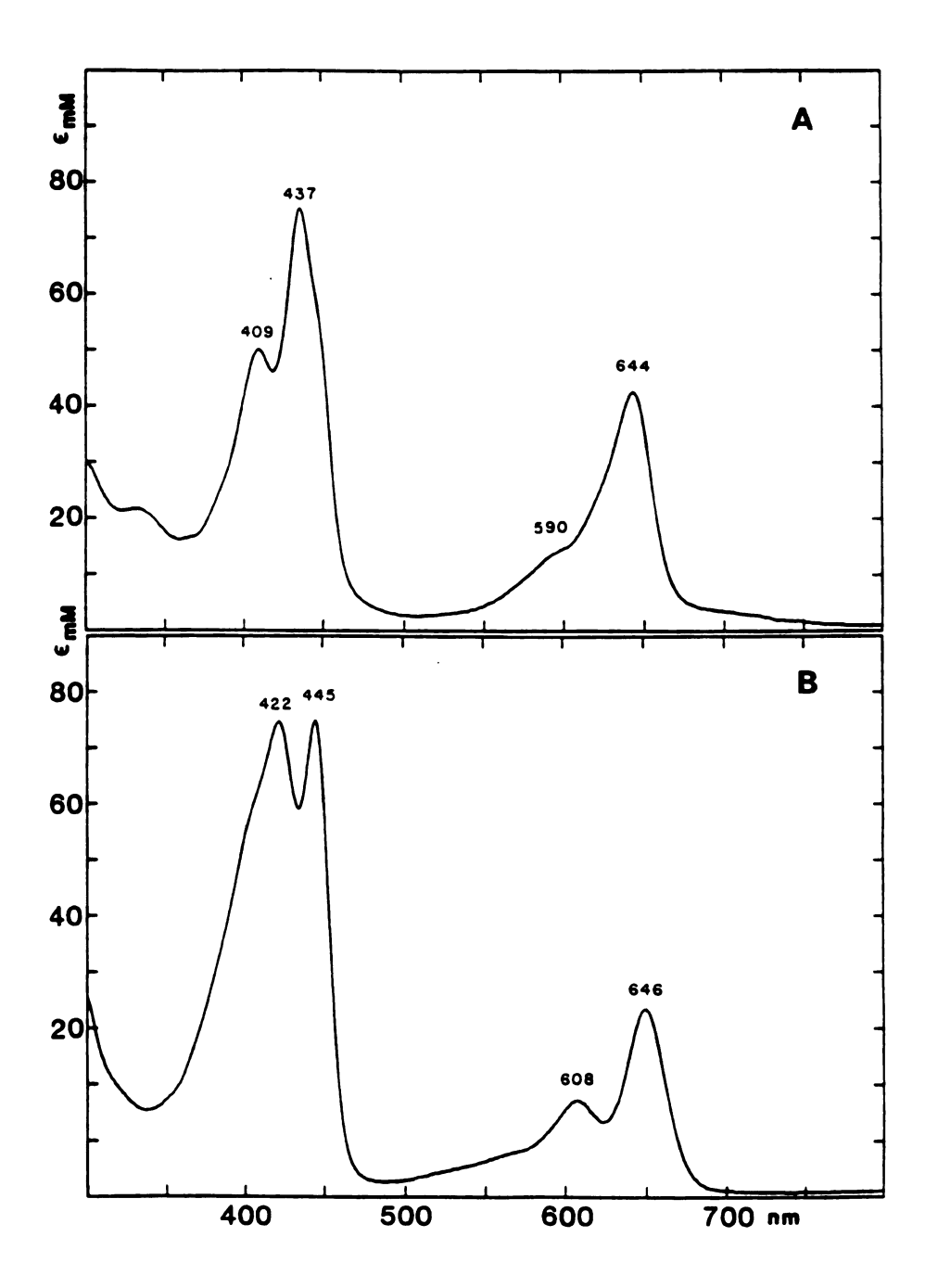


Figure 7 UV-vis absorption spectra of model compound 10 (A) in the form of Cu(II) chelate in CHCl₃ and (B) as the protonated form in formic acid.

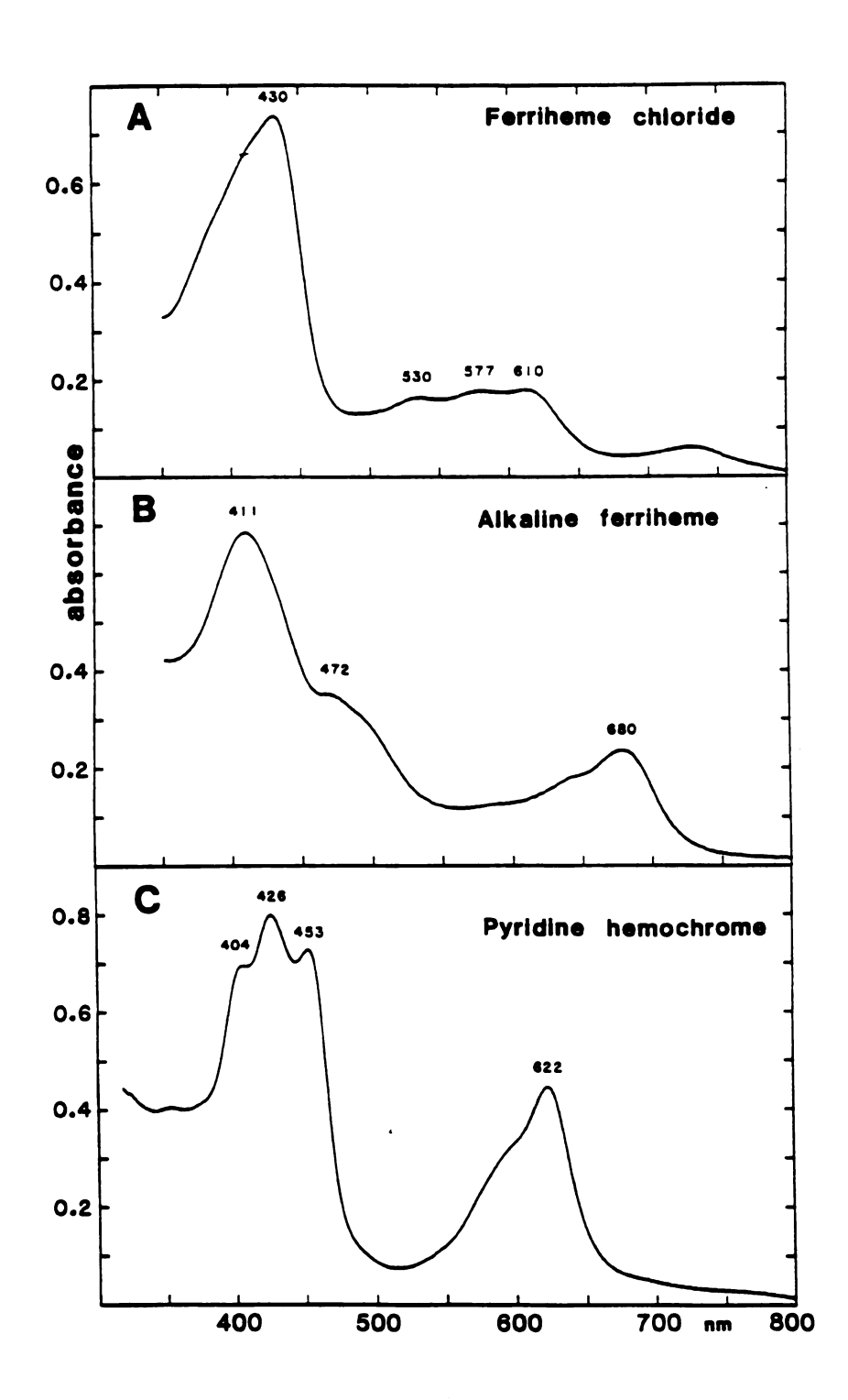


Figure 8 UV-vis absorption spectra of 10, (A) ferriheme chloride in acetone with a trace amount of HCl; (B) alkaline ferriheme in CH₂Cl₂/acetone containing tetrabutylammonium hydroxide; (C) pyridine hemochrome in CH₂Cl₂/pyridine.

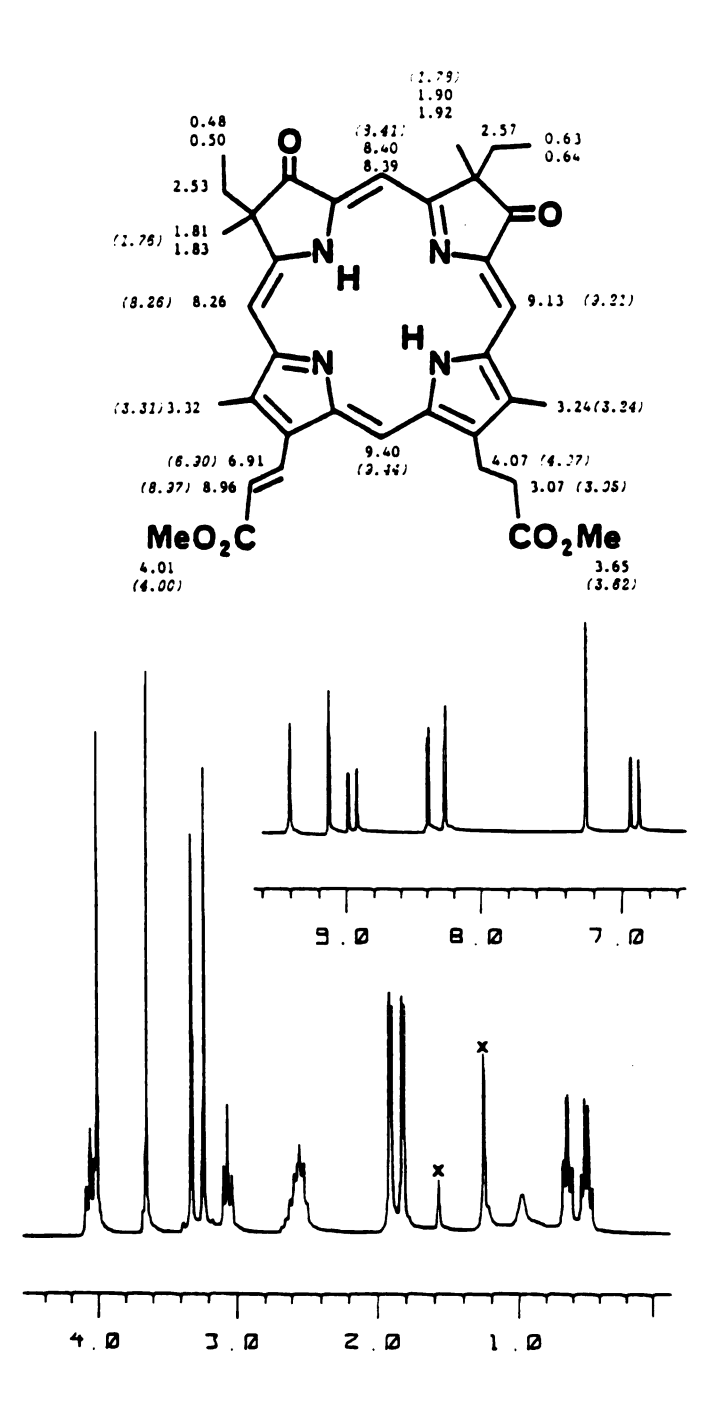


Figure 9 250 MHz ¹H-NMR spectrum of model compound 10 in CDCl₃ (The bifuration of the peaks of the pyrroline ethyl and methyl groups is an indication of the presence of diastereomers). The numbers in parenthesis are the chemical shifts of natural d₁.

sirohydrochlorin,⁷¹ the usual pattern is one meso proton down-field (the one between the unsaturated pyrroles), a pair at the intermediate shift (the two between a saturated and an unsaturated pyrrole), and one relatively upfield (the one between the two saturated pyrroles). In 1,3-porphyrindiones, the deshielding effects of the carbonyl oxygens have distorted the usual isobacteriochlorin pattern into an apparent chlorin pattern. The 3-carbonyl oxygen has deshielded α -proton from its furthest upfield normal position to a shift comparable to β -proton, while the 1-carbonyl has deshielded δ -proton to a range comparable to that of γ . The 1 H-NMR of model compound 10 has also clarified the question of chemical shift for the NH resonances of \underline{d}_1 . In 10, they appear at 0.97 ppm, which is unusually more downfield for the inner NH protons of porphyrin, but presumably reflects the decreased ring current and electron-withdrawing effect of the carbonyl groups on the ring. The corresponding chemical shift of \underline{d}_1 around 0.9 ppm had been dismissed as residue impurity.

The 13 C-NMR of model compound 10 is shown in Figure 10. The resonances are assigned based on analogies to known models 64 , 63 in Table 1 and contrasted with the spectra of its precursor compound 6 and that of natural \underline{d}_1 . It has been pointed out that the meso carbons are sensitive to the level of the saturation of the porphyrin core as well as precise substituents. 64 The highly similar pattern of the individual meso carbon resonances between model compound 10 and \underline{d}_1 is the evidence for the common core structure. Furthermore, the resonances at 207.2 and 208.7 ppm of 10, and 209.1 and 209.3 of 6 are assigned to the carbonyls which were not observed in the original \underline{d}_1 spectrum.

The similarity between the Resonance Raman spectra of model compound 10 in the form of its Cu(II) complex and those of Cu(II) \underline{d}_1 was also

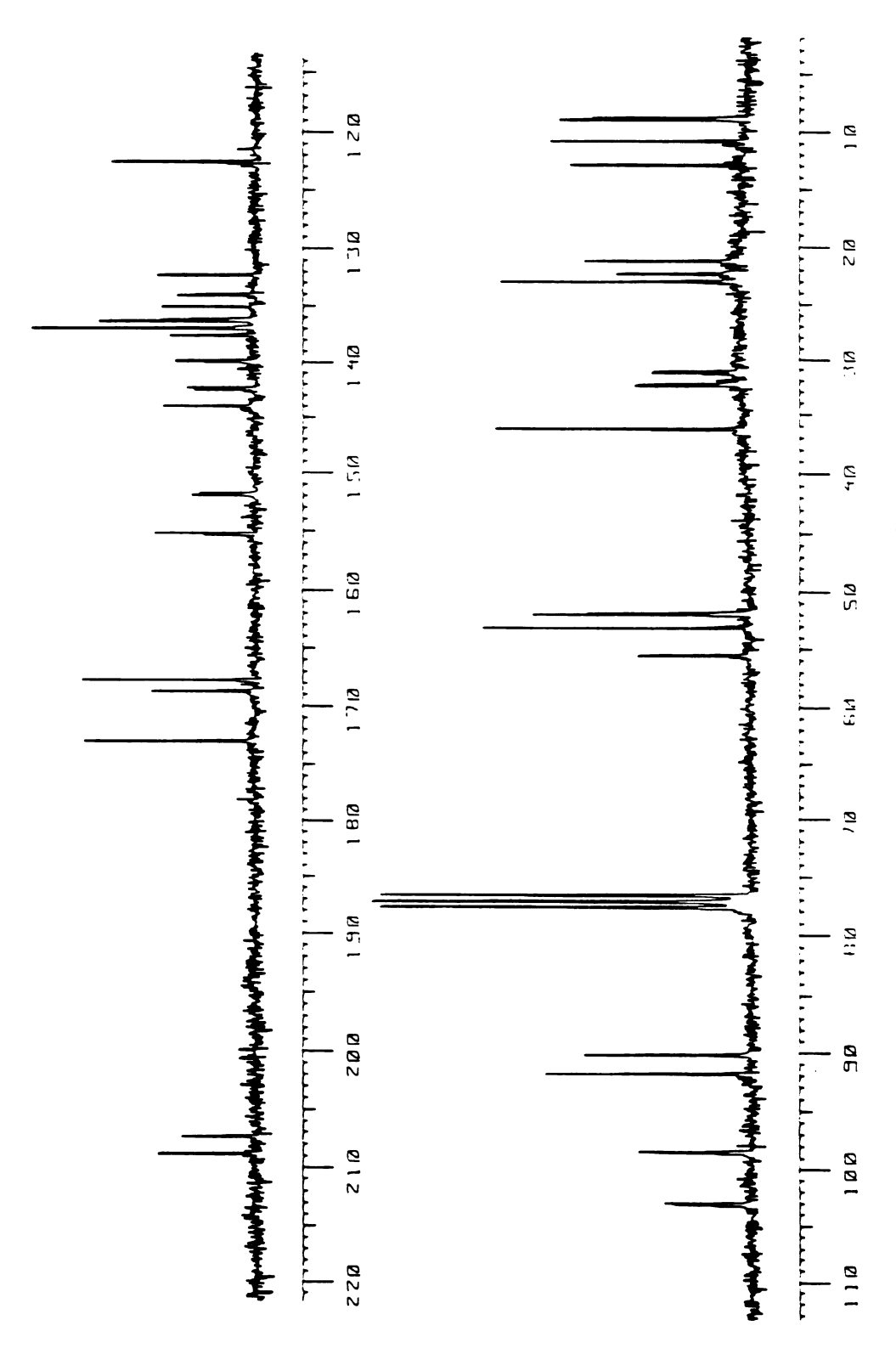


Figure 10 Natural abundance, broad-band proton-decoupled ¹³C-NMR of model compound 10 at 30 °C. Peak assignments are give in Table 1.

Table 1. $^{13}\text{C-NMR}$ chemical shifts^a of 1,3-mesoporphyrindione 6, model compound 10 in comparison with that of natural heme \underline{d}_1 tetramethyl ester.

*************	compound δ(ppm)		
carbon	dione 6	model 10	heme <u>d</u> 1
a and b (pyrrole)	131.55 (131.98, 132.03) ^b (132.24, 132.32) 135.69, 136.74 136.92, 137.10 139.52 (144.16, 144.24) (147.45, 147.59) (161.72, 161.87)	132.22 (133.87, 133.93) 134.90 (136.07, 136.19) 136.84, 137.46 139.72 (142.19, 142.34) (151.66, 151.78) (155.07, 155.19)	134.7, 137.1
-Ç- (tertiary)	53.11 <i>,</i> 55.73	53.03, 55.42	***************************************
<u>C</u> H ₂ <u>C</u> H ₂ <u>C</u> O <u>C</u> H ₃	36.19 21.18, 21.33 173.12 51.62	36.24 21.16 172.83 51.73	36.66 21.5
CH=CHCOCH3		173.12 122.48 143.83 51.91	172.83 122.9 51.9
CH2COCH3			41.7, 42.5
	8.86	0 72 0 0E	52.1
CH ₂ CH ₃ CH ₃ (pyrroline)	22.51, 23.00	8.73, 8.85 22.29, 23.01	23.4, 24.1
•••••	10.71, 11.06	10.72, 12.81	11.2, 13.2
CH ₃ (pyrrole) -C=O (ring)	209.15, 209.29	207.25, 208.71	11.4, 13.4
•••••			
meso-H	91.31, 96.86, 99.01, 99.11	90.03, 91.67 98.33 (102.88, 102.9)	90.2, 91.9 98.5, 102.9

^aReferenced against the center of CHCl₃ (77.0 ppm). ^bPairs in parenthsises indicate bifurcation due to diastereomers.

observed and will be discussed in Chapter 5.

III. EXPERIMENTAL

General

¹H- and ¹³C-NMR were obtained at 250 MHz on a Bruker WM-250 instrument. Spectra were mostly recorded in CDCl₃; the residue CHCl₃ was used as the internal standard set at 7.24 ppm. Nuclear Overhauser enhancement (NOE) was measured by difference between a spectrum with preirradiation on a target peak minus a spectrum with equivalent preirradiation at a dummy position. Magnitudes of NOEs were calculated as the area of the enhanced resonance in difference spectra divided by the area in the control spectrum with no enhancement. Mass spectra were obtained using a Finnigan 4021 GC-MS (direct insertion probe, 70ev, 200-300 °C), or a JEOL HX 110-HF spectrometer equipped with a fast atom bombardment (FAB) A matrix of thioglycerol-dithioerythreitol-dithiothreitol, 2:1:1, containing 0.1% trifloroacetic acid was used for the FAB-MS. Visible absorption spectra (in CH_2Cl_2 or $CHCl_3$) were measured with a Cary 219 or a Shimadzu 160 spectrophotometer. IR spectra were obtained from KBr pellets or NaCl films on a Nicolet IR/42 spectrometer. Melting points were obtained on an electrothermal melting point apparatus and are uncorrected. Preparative TLC plates were purchased from Analtech (silica gel G, 1000 or $1500 \mu m$).

A. Synthesis and oxidation of porphyrin tetramethyl acetate

5-Bromo-2,4'-di-(2-methoxycabonylmethyl)-2',4,5'-trimethyl-2,2'-dipyrryl-

methenium bromide (14)

To a solution of 26.7 g (0.1 mol) of pyrrole 13 in 160 ml of AcOH, 15 ml (2.9 mol) of bromine in 50 ml of AcOH were added in 15 min with stirring. The mixture was stirred for another 1 h after the addition. Then the large part of the solvent was removed by vacuum and the concentrated solution was allowed to stand at room temperature until dipyrrylmethenium bromide (13) was crystallized. The product was collected by filtration and vacuum dried. yield, 15.0 g, 46%; mp 173-175 (dec.); ¹H-NMR & 2.07, 2.37, 2.70 (3 H each, s, Me), 3.48, 3.82 (2 H each, s, CH₂CO₂), 3.69, 3.71 (3 H each, s, CO₂CH₃), 7.31 (1 H, s, methine), 7.95, 8.06 (1 H each, br s, NH); MS (direct probe 70 eV) m/e 410 (M⁺).

2,4,6,8-tetramethyl-porphyrin-1,3,5,7-tetramethyl acetate (12)

The above dipyrrylmethenium 14, 13.0 g (0.02 mol), and 250 g of methylsuccinic acid were ground together into fine powder and dried under vacuum for 8 h. The mixture was then fused in an oil bath for 6 h at 130 °C protecting from moisture. To the cooled black melt 150 ml of MeOH and 100 ml of CHCl₃ were added, dry HCl gas was then bubbled into the solution for 10 min. After standing for 4 h, the solution was diluted by addition of anther 200 ml of CHCl₃, washed first with saturated NaOAc aqueous solution (2 x 150 ml), then with water (2 x 100 ml), and dried over Na₂SO₄. The solvent was removed by vacuum and the residue was chromatographed on a silica gel column (60-250 mesh). The methylsuccinic acid was eluted out with MeOH/CH₂Cl₂ (1/100) and the porphyrin 12 was rinsed out with 5%MeOH/CH₂Cl₂. To achieve a better purification result the crude porphyrin was column chromatographed once more under the similar condition then crystalized from MeOH-CH₂Cl₂. Yield, 0.75 g (11%); ¹H-NMR

 δ -3.7 (2H, s, NH), 3.7 (12 H, s, CH₃), 3.8 (12H, s, CH₂CO₂CH₃), 5.1(8H, s, CH₂CO₂CH₃), 10.2 (4H, s, meso); UV-vis λ max (rel. int.) 401 nm (1.00), 499 (0.12), 533 (0.08), 569 (0.07), 623 (0.05); MS, found m/e 655.7233 for (M+H)⁺, C36H38N4O6 requires 655.7342.

<u>Tetramethyl-2,3,5,7-tetramethylporphyrinone-2,4,6,8-tetraacetat</u>e (**15**) and trimethyl-2-hydroxyl-1,3,5,7-tetramethyl-chlorin-1,2-(γ -lactone)-4,6,8-triacetate (**16**)

 H_2O_2 - H_2SO_4 oxidation of porphyrin 12 was carried out in the same way as will be described later in the mesoporphyrin's reaction. Only less than 5% of 15 and small amount of γ -lactone 16 were obtained and no other oxidation products were detected from the reaction system.

(15) ¹H-NMR δ 1.95 (3 H, s, Me saturated), 2.97 (3 H, s, CH₂CO₂CH₃ saturated) 3.50, 3.59, 3.62 (3 H each, ring Me), 3.75, 3.78, 3.82 (3 H each, CH₂CO₂CH₃), 3.89, 4.00 (1 H each, dd, J=17.5 Hz CH₂CO₂ saturated), 4.98, 5.04 (2 H each, s, CH₂CO₂), 5.01, 5.07 (1 H each, dd, J=17.5 Hz CH₂CO₂), 9.10, 9.85, 9.90, 9.98 (1 H each, s, meso α , δ , β , γ), -2.88, -2.83 (1 H each, br s, NH); UV-vis λ max (rel. int.) 405 nm (1.00), 505 (0.08), 543 (0.07), 587 (0.05), 642 (0.18).

(16) ¹H-NMR δ 2.37 (3 H, s, Me saturated), 3.41, 3.46, 3.57 (3 H each, s, ring Me), 3.70, 3.75, 3.81 (3 H each, s, CO₂CH₃), 4.83, 4.86 (2 H each, s, CH₂CO₂), 4.89, 4.99 (1 H each, dd, J=17.6 Hz, CH₂CO₂), 9.15, 9.17, 9.74, 9.87 (1 H each, s, meso δ , α , γ , β), -2.85 (2 H, br s, NH); UV-vis λ max (rel. int.) 392 nm (1.00), 495 (0.11), 540 (0.04), 585 (0.05), 640 (0.26).

B. H₂O₂-H₂SO₄ oxidation of mesoporphyrin

Mesoporphyrin IX dimethyl ester (350 mg) was dissolved in concentrated sulfuric acid (30 ml d=1.84) in an ice bath. To this solution under stirring was added 6% $\rm H_2O_2$ (2 ml) dropwise such that the temperature of the reaction mixture was kept below 10 °C. After the addition was complete (15 min), the dark red solution was stirred an additional 10 min in an ice bath and then at room temperature for 25 min or until the solution became dark green. The reaction was quenched by pouring the mixture into a large beaker containing NaOAc (20 g) and crushed ice. After standing at room temperature for 2 h, the solids were collected by filtration, washed with water, and dried (ca. 200 mg). The filtrate was concentrated in vacuo and mixed with acidified methanol (200 ml of MeOH+2 ml of $\rm H_2SO_4$) and chloroform (100 ml) to effect esterification. This mixture, after washing with water, afforded about 150 mg of solid material containing small amounts of unreacted mesoporphyrin dimethyl ester, together with other intractable oxidation products. Therefore, in later reaction runs, the acid filtrate was discarded.

The solid oxidation product was chromatographed on a 2 x 10 in. silica gel column eluted with methanol/methylene chloride (2/98). A fairly pure porphyrinone 18 was obtained from first 20-30 ml eluent, and the rest of pigments were collected into three fractions. Each fraction was concentrated and chromatographed again on preparative TLC plates (CH₂Cl₂ with 1% MeOH) to give eight additional compounds. Alternatively, as a group, the diones can be cleanly separated from monoketones on a silica gel column by using methylene chloride containing 5% of formic acid as eluent. Subsequent separations can be carried out on preparative TLC plates. The nine keto products are tabulated roughly according to their Rf values are given in Scheme 4.

3-Mesoporphyrinone dimethyl ester (18) Yield, 29.5 mg (8.2%); ¹H-NMR

δ 0.41 (3 H, t, CH_2CH_3 saturated), 1.82 (3 H, t, CH_2CH_3), 2.07 (3 H, s, Me saturated), 2.77 (2 H, q, CH_2CH_3 saturated), 3.26 (4 H, m, $CH_2CH_2CO_2$), 3.48, 3.55, 3.58 (3 H each, s, Me), 3.68 (6 H, s, CO_2CH_3), 4.02 (2H, q, CH_2CH_3), 4.25, 4.40 (2 H each, q, $CH_2CH_2CO_2$), 9.14, 9.86, 9.88, 9.90 (1 H each, s, meso β, α, δ and γ), -2.96 (2 H, br s, NH); UV-vis λ max (ϵ M) 642 nm (34600), 585 (5800), 547 (12400), 508 (8800), 407 (165200); MS found m/e 611.3242 for (M+H)+, ϵ C36H43N4O5 requires m/e 611.3236.

1-Mesoporphyrinone dimethyl ester (5) Yield, 35.6 mg (9.9%); ¹H-NMR δ 0.41 (3 H, t, CH_2CH_3 saturated), 1.80 (3 H, s, CH_2CH_3), 2.06 (3 H, s, Me saturated), 2.75 (2 H, q, CH_2CH_3) saturated), 3.21 (4 H, m, $CH_2CH_2CO_2$), 3.45, 3.56, 3.59 (3 H each, s, Me), 3.62, 3.65 (3 H each, s, CO_2CH_3), 4.01 (2 H, q, CH_2CH_3), 4.22, 4.38 (2 H each, q, $CH_2CH_2CO_2$), 9.10, 9.80, 9.82, 9.92 (1 H each, s, meso α, δ, β, and γ), -2.97, -2.81 (1 H each, br s, NH); UV-vis λ max (EM) 642 nm (33300), 585 (6000), 547 (12000), 508 (10000), 407 (175000); MS (direct probe, 70 eV), m/e 610 (M⁺).

1,3-Mesoporphyrindione dimethyl ester (6) Yield, 16.8 mg (4.5%); 1 H-NMR δ 0.50, 0.70 (3 H each, s, Me saturated), 2.62 (4 H, m, CH₂CH₃saturated), 3.11 (4 H, m, CH₂CH₂CO₂), 3.27, 3.32 (3H each, ring Me), 3.60, 3.63 (3 H each, s, CO₂CH₃), 4.16 (4H, m CH₂CH₂CO₂), 8.42, 8.63, 9.28, 9.51 (1 H each, s, meso β , α , δ , γ), -0.04 (2H, br s, NH); UV-vis λ max (EM) 638 nm (16800), 592 (15300), 584 (15700), 544 (9600), 438 (97000), 417 (94000), 402 (74800); MS found m/e 627.3178 for (M+H)+, C36H43N4O6 requires m/e 627.3185.

2,3-Mesoporphyrindione dimethyl ester (19) Yield, 7.5 mg (2%); 1 H-NMR δ 0.55 (6H, t, CH₂CH₃ saturated), 1.95, 1.97 (3 H each, s, Me

saturated), 2.68 (4 H, q, $\underline{\text{CH}}_2\text{CH}_3$ saturated), 3.22 (4 H, t, $\underline{\text{CH}}_2\text{CH}_2\text{CO}_2$), 3.46 (6 H, s, Me), 3.62 (3 H, s, $\underline{\text{CO}}_2\underline{\text{CH}}_3$), 4.37 (4H, t, $\underline{\text{CH}}_2\text{CH}_2\text{CO}_2$), 8.90 (2H, s, meso β and δ), 9.74, 9.90 (1 H each, s, meso α and γ), -1.63 (2H, br s, NH); UV-vis λ max (EM) 622 (18000), 592 (9400), 435 (102000), 417, (133000); MS found m/e 627.3194 for (M+H)+, C36H43N4O6 requires m/e 627.3185.

6-Mesoporphyrinone dimethyl ester (20) Yield, 4.5 mg (1.2%); ¹H-NMR δ 1.53, 2.10 (1 H each, m, $\underline{CH_2CH_2CO_2}$ saturated), 1.79, 1.80 (3 H each, t, $\underline{CH_2CH_3}$), 2.10 (3H, s, Me), 3.09 (2H, t, $\underline{CH_2CH_2CO_2}$ saturated), 3.22 (2 H, t, $\underline{CH_2CH_2CO_2}$), 3.24, 3.44, 3.60 (3 H each, s, ring Me), 3.62, 3.64 (3 H each, s, $\underline{CO_2CH_3}$), 3.90, 4.04 (2 H each, q, $\underline{CH_2CH_3}$), 4.34 (2H, t, $\underline{CH_2CH_2CO_2}$),9.17, 9.82, 9.86, 9.90 (1 H each, s, meso β, γ, δ and α), -2.92 (2 H, br s, NH); UV-vis λmax (εм) 642 nm (33300), 585 (6000), 547 (12000), 508 (10000), 407 (175000); MS found m/e 611.3245 for (M+H)+. C36H43N4O5 requires m/e 611.3236.

7-Mesoporphyrinone dimethyl ester (21) Yield, 4.5 mg (1.2%); 1 H-NMR 5 1.50, 2.08 (1 H each, m, C H₂CH₂CO₂ saturated), 1.78, 1.80 (3 H each, t, CH₂CH₃), 2.10 (3 H, s, Me saturated), 3.08 (2 H, t, CH₂CH₂CO₂ saturated), 3.23 (2 H, t, CH₂CH₂CO₂), 3.25, 3.43, 3.59 (3 H each, s, ring Me), 3.60, 3.70 (3 H each, s, CO₂CH₃), 3.87, 4.02 (2 H each, t, C CH₂CH₃) 4.34 (2 H, t, C CH₂CH₂CO₂), 9.12, 9.78, 9.80, 9.90 (1 H each, s, meso 5 5, 7 6, 7 7 and 6 7), -2.95, -2.84 (1 H each, br s, NH); UV-vis 7 8 max (7 8 max (7 8 max (7 9 eV) 610 (7 9 eV) 610 (7 9.

3,7-Mesoporphyrindione dimethyl ester (22) Yield, 9.5 mg (2.6%); 1 H-NMR δ 0.44 (3 H, t, CH₂CH₃ saturated),1.56, 2.15 (1 H each, m, CH₂CH₂CO₂ saturated), 1.75 (3 H, t, CH₂CH₃), 1.99, 2.02 (3 H each, s, Me saturated), 2.71, (2

H, q, <u>CH</u>₂CH₃), 3.02 (2 H, t, CH2<u>CH</u>₂CO₂ saturated), 3.29 (2 H, t, CH₂<u>CH</u>₂CO₂), 3.49, 3.50 (3 H, s, ring Me), 3.51, 3.75 (3 H, s, CO₂<u>CH</u>₃), 3.93 (2 H, t, <u>CH</u>₂CH₃), 4.29 (2 H, t <u>CH</u>₂CH₂CO₂), 9.05, 9.06, 9.66, 9.74 (1 H each, s, meso δ, β, γ, and α), -2.78, -2.74 (1 H each, s, br s, NH); UV-vis λ max (εм) 685 nm (95000), 652 (7300), 622 (6800), 556 (10700), 514 (8100), 486 (5700), 411 (187000), 401 (164000); MS, found m/e 627.3198 for (M+H)+, C36H43N4O6 requires m/e 627.3185.

1,7-Mesoporphyrindione dimethyl ester (23) Yield, 7.0 mg (1.9%); 1 H-NMR δ 0.61 (3 H, t, CH₂CH₃ saturated), 1.70 (3 H, t CH₂CH₃), 1.76, 2.15 (1 H each, m, CH₂CH₂CO₂ saturated), 1.95, 1.96 (3 H each, s, Me saturated), 2.63 (2 H, q, CH₂CH₃ saturated), 2.94 (2 H, t, CH₂CH₂CO₂ saturated), 3.13 (2 H, t CH₂CH₂CO₂), 3.43, 3.44 (3 H each, s, ring Me), 3.46, 3.72 (3 h each, s, CO₂CH₃), 3.75 (2 H, q, CH₂CH₃), 4.14 (2 H, t, CH₂CH₂CO₂), 8.57, 8.78, 9.32, 9.52 (1 H each, s, meso α, δ, γ, and β), -0.61 (2 H, br s, NH); UV-vis λ max (εм) 637 nm (15800), 592 (14400), 583 (15000), 544 (9100), 437 (92000), 417 (90000), 402 (72000); MS (direct probe 70 eV), m/e 626 (M⁺).

1,8-Mesoporphyrindione dimethyl ester (24) Yield, 2.0 mg (0.5%); 1 H-NMR δ 0.52, (3H, m, CH₂CH₃ saturated), 1.77 (3 H, t, CH₂CH₃), 1.82, 2.20 (1 H each, m, CH₂CH₂CO₂ saturated), 1.98, 2.01 (3 H each, s, Me saturated), 2.68 (2H, q, CH₂CH₃ saturated), 3.00 (2 H, t, CH₂CH₂CO₂ saturated), 3.17 (2 H, t, CH₂CH₂CO₂)3.34, 3.37 (3 H each, s, ring Me), 3.57, 3.65 (3 H, s, CO₂CH₃), 3.91 (2 H, t, CH₂CH₃CO₂), 8.93, 8.97, 9.66, 9.80 (1 H each, s, meso γ, α, δ, and β); UV-vis λ max (EM) 623 nm (19000), 592 (5900), 436 (100000), 417 (135000); MS, found m/e 627.3910 for (M+H)+, C36H43N4O6 requires m/e 627.3185.

C. Preparation of 1,3-porphyrindione from zinc porphyrinone*

Typically, 1 mmol of porphyrinone was dissolved in 100 ml of CHCl₃ and 50 ml of MeOH, and to this solution 2 ml of saturated Zn(OAc)₂ methanol solution and a pinch of NaOAc were added. The solution was brought to refluxing and causing the brown-color to turn gradually into green. The completion of zinc insertion can be monitored by TLC or by UV-vis spectrum (the bands of the free base at 406, 546, and 508 nm should disappear). The excess of zinc acetate was then washed away with water (3 x 100 ml) and the solvent was evaporated.

The residue was vacuum dried and redissolved in 100 ml of dry methylene chloride. To this solution 1 ml of dry pyridine and 380 mg (1.5 mmol) of osmium tetroxide in 0.38 ml of anhydrous ether was added, and the mixture was allowed to stir at room temperature, under nitrogen, in the dark for 20 h. It was then quenched with methanol (50 ml) and bubbled with H₂S for 10 min to decompose the osmic ester. The precipitated osmium sulfide was removed by filtration, and the crude product in the filtrate was chromatographed on a silica gel column. Unreacted Zn(II) porphyrinone was eluted first with 1% MeOH/CH₂Cl₂, and the slower moving dihydroxy compounds were then rinsed down quickly by increasing the amount of methanol in the eluent.

To effect pinacolic rearrangement, the diol containing fractions were brought to dryness and treated with ~10 ml of sulfuric acid directly. The central zinc ion was replaced by protons during this time. After stirring for a few minutes at room temperature, the acid solution was carefully diluted with 100 ml of methanol in an ice bath with continual stirring. The solution was further diluted with 150 ml of CH₂Cl₂ and washed with saturated

NaOAc solution (3 x 100 ml), water (2 x 100 ml), and brought to dryness. The residue was chromatographed once again on preparative TLC (1~2% $MeOH/CH_2Cl_2$) to separate the major 1,3-dione from a small amount of 2,3-dione.

In both OEP and mesoporphyrin systems the yield of dihydroxy compounds were usually higher than 60%, and the yield of 1,3-dione from diols through pinacolic rearrangement was above 80% while that of the 2,3-dione was less than 5%.

*The above procedure can only be applied to porphyrinones with alkyl side chains or other substituents with the similar electronic property. When electron-withdrawing substituents are involved stronger acidic condition has to be used to effect the rearrangement and more isomeric products are formed (to be discussed in chapter 3).

D. Acrylate side chain formation

2,2,4,4,5,7,8-heptaethyl-6-vinyl-1,3-porphyrindione (53)

Osmium tetroxide (384 mg, 1.5 mmol) in 3.84 ml of ether and 1.5 ml of pyridine were added to a solution of 566 mg (1 mmol) of dione 7 in 150 ml of CH₂Cl₂, and the reaction was allowed to proceed, under argon, in the dark, at room temperature for 24 h. The solution was then treated with 50 ml of methanol and bubbled with H₂S for 10 min. The precipitated osmium sulfide was removed by filtration on celite and the crude product was dried by vacuum before chromatographed on a silica gel column. Unreacted green dione 8 (55%) was eluted first with 1% MeOH/CH₂Cl₂ and the dark-grey dihydroxy compound 48 was eluted off with 5% MeOH/CH₂Cl₂; yield, 222

mg, 37%; ¹H-NMR δ 0.41, 0.44, 0.56, 0.64, 0.71, (3 H each, t, CH_2CH_3 sat.), 1.41 (3 H, s, CH_2CH_3 sat.), 1.47, 1.48 (3 H each, t, CH_2CH_3), 2.21, 2.45 (6 H each, m, CH_2CH_3 sat.), 3.35 (4 H, m, CH_2CH_3), 3.81, 4.09 (1 H each, br s. OH), 7.12, 7.57, 7.68, 8.48 (1 H each, s, β , α , γ , δ); UV-vis λ max (εм) 669 nm (8800), 611 (6700), 547 (8200), 516 (6400), 417 (38500), 385 (48800), 368 (39700).

Diol 48 (222 mg, 0.37 mmol) was dissolved in 50 ml of dioxane with 3 ml of diluted hydrochloric acid (5%). The mixture was heated on a steam bath until the dark-grey solution turned into a bright-green color. The reaction was allowed to go for another 10 min before cooled down and diluted with 100 ml of CH_2Cl_2 . The organic solution was washed twice with water and evaporated to dryness. Separation on TLC plate (1% MeOH/CH₂Cl₂) gave the fast moving band of vinyl dione 53 followed by the two α -hydroxyethyl dione 51 and 52. An α -methoxyethyl dione 54 was also separated, which was found derived from 52 on the plate in the presence of methanol and can be easily made by treating 52 with acidified methanol. The structures of above products were confirmed by NOE.

- (51) Yield, 34 mg, 16%; 1 H-NMR δ 0.35 (3 H, t, CH₂CH₃ sat.), 0.97 (9 H, m, CH₂CH₃ sat.), 1.39 (9 H, m CH₂CH₃) 2.29 (3 H, d, CHOHCH₃), 2.84 (8 H, m, CH₂CH₃), 3.40 (6 H, m, CH₂CH₃), 6.34 (1 H, q, CHOHCH₃), 8.25, 8.50, 9.02, 9.92 (1 H, each, s, meso, β , α , δ , γ); UV-vis λ max (rel. int.) 401 (0.82), 418 (1.00), 441 (0.93), 549 (0.17), 591 (0.28), 640 (0.25).
- (52) Yield, 67 mg, 31%; 1 H-NMR δ 0.38, 0.43 (3 H each, t, CH₂CH₃ sat.), 0.55 (6 H, t, CH₂CH₃ saturated), 1.67 (9 H, m, CH₂CH₃), 2.11 (3 H, d, CHOHCH₃), 2.55 (8 H, m, CH₂CH₃), 3.73 (6 H, m, CH₂CH₃), 6.23 (1 H, q, CHOHCH₃), 8.30, 8.47, 9.18, 9.96 (1 H each, s, meso β , α , δ , γ); UV-vis λ max (rel. int.) 401 (0.83), 419 (1.00), 439 (0.94), 548 (0.18), 587 (0.30), 640 (0.27).

- (53) Yield, 79 mg, 38%; 1 H-NMR δ 0.42, 0.55 (6 H each, t, CH₂CH₃ sat.), 1.67 (9 H, m, CH₂CH₃), 2.54 (8 H, m CH₂CH₃ sat.), 3.71 (6H, m, CH₂CH₃), 6.09 (2 H, dd, CH=CH₂), 7.85 (1 H, dd, CH=CH₂), 8.34, 8.46, 9.17, 9.49 (1 H each, s, meso β , α , δ , γ), 1.50 (2 H, br s, NH); UV-vis λ max (rel. int.) 422 nm (1.00), 444 (0.82), 554 (0.17), 596 (0.28), 646 (0.22).
- (54) Yield, 24 mg, 11%; 1 H-NMR δ 0.41, 0.56 (6 H each, t, CH₂CH₃ sat.), 1.67 (9 H, m, CH₂CH₃), 2.09 (3 H, d, CH(OCH₃)CH₃), 2.57 (8 H, m CH₂CH₃), 3.50 (3 H, s. OCH₃), 3.73, (6 H, m, CH₂CH₃), 5.61 (1 H, d, CHOHCH₃), 8.33, 8.49, 9.21, 10.02 (1 H each, s, meso β , α , δ , γ); UV-vis λ max (rel. int.) 4.02 (0.80), 4.19 (1.00), 4.39 (0.87), 5.46 (0.17), 5.88 (0.25), 6.39 (0.21).

<u>Dimethyl-1,3-mesoporphyrindione-6-acrylate-7-propionate</u> (10)

The 1,3-mesoporphyrindione (6) was treated with OsO₄ in the same way as described above to effect the dihydoxylation. Typically, 100 mg (147 mmol) of 5 gave 42 mg (59 mmol) of 5,6-dihydroxyl-1,3-mesoporphyrindione 55. The dehydration was accomplished smoothly by heating 55 in 10 ml of dioxane with 2.5 ml of 5% HCl (or alternatively, refluxing 55 in 50 ml of benzene with a few drops of concentrated hydrochloric acid). After the distinctive color change from grey to bright-green color change had taken place, 1 ml of concentrated sulfuric acid in 10 ml of MeOH was added to the reaction solution. The mixture was heated for another 5 min on steam bath and then set aside for 4 h to ensure esterification of propionic side chain. The solution containing crude product was combined with 50 ml of CH₂Cl₂ and washed with water and vacuum dried. The crude product was further purified on a TLC plate (1%MeOH/CH₂Cl₂) to give the green pigment 10, 32 mg.

- (55) Yield, 40%; ¹H-NMR δ 0.45, 0.64 (3 H each, t, CH_2CH_3 saturated), 1.52, 1.57, 1.68, (3 H each, s, Me saturated), 2.22 (4 H, m, CH_2CH_3), 2.40 (2 H, m, $CH_2CH_2CO_3$) as saturated), 2.79 (2 H, t, $CH_2CH_2CO_3$), 2.85 (3 H, s, ring Me), 2.92 (2 H, m, $CH_2CH_2CO_3$ sat.), 3.52 (2 H, t, $CH_2CH_2CO_3$), 3.62, 3,74 (3 H, s, CO_3CH_3), 3.98 (2 H, t, $CH_2CH_2CO_3$), 7.10, 7.56, 7.69, 8.44 (1 H each, s, meso β, α, γ, δ), 3.55, 3.82 (1 H each, br s, OH); UV-vis λmax (rel. int.) 368 nm (0.82), 383 (1.00), 412 (0.87), 507 (0.14), 540 (0.18), 604 (0.16), 659 (0.21).
- (10) Yield, 80%; ¹H-NMR δ 0.48, 0.50 (3 H, t, CH₂CH₃ sat.), 0.63, 0.64 (3 H, t, CH₂CH₃ sat.), 1.81, 1.83 (3 H, s Me sat.), 1.90, 1.12 (3 H, s, Me sat.), 2.55 (4 H, m, CH₂CH₃), 3.07 (2 H, t, CH₂CH₂CO₂), 3.24, 3.32 (3 H each, s, ring Me), 3.65 (3 H, s, CH₂CH₂CO₂CH₃), 4.01 (3 H, s, CH=CHCOCH₃), 4.07 (2 H, t, CH₂CH₂CO₂), 6.91, 8.96 (1 H each, d, CH=CHCO₂), 8.26 (1 H, s, meso β), 8.39, 8.40 (1 H, s, meso α), 9.13 (1 H, s, meso δ), 9.40 (1 H, s, meso γ), 0.97 (2 H, br s, NH); UV-vis λ max (rel. int.) 423 nm (1.00), 446 (0.71), 568 (0.34), 611 (0.32), 661 (0.21); MS found m/e 625.2946 for (M+H)+, C46H41N4O6 requires 625.3030.

CHAPTER 3

TOTAL SYNTHESIS OF HEME d_1

I. RATIONALE OF THE SYNTHETIC STRATEGY

At first, it might seem easy to achieve the total synthesis of \underline{d}_1 as the major synthetic hurdles, e.g., the formation of 1,3-dione core structure and the introduction of acrylic double bond, have already been overcome. All that left was to replace the ethyl side chains in model compound 10 by acetic acid groups. In principle, a double OsO_4 oxidation-pinacolic rearrangement of a porphyrin diacetate like 58 would furnish the core structure 59 of heme

 \underline{d}_1 . However, in view of the difficulties experienced in the synthesis of model compound 9, where electron-withdrawing acetate side chains were

involved, we expected that the \underline{d}_1 synthesis may not be so simple. Nevertheless, we chose to make a symmetric porphyrin such as 60 first to study the property of porphyrin bearing two acetic side chains and to see if the desired 1,3-dione structure can be formed. To circumvent the difficulties associated with acetic side chains, porphyrins such as 61 and 62 with the masked acetic functions (in the form of chloroethyl side chains here) were also considered.

If the pinacolic rearrangement pathway should fail, we also planned alternatively to examine the direct oxygenation of the unsubstituted β -positions on an isobacteriochlorin. We thought that an isobacteriochlorin like 63 would undergo oxygenation to yield the \underline{d}_1 core structure 59. Several syntheses of unsubstituted isobacteriochlorin had been reported by Battersby's group.^{80, 81} It is possible to follow their procedures to prepare a simple model compound such as 64 to see if this idea would work. If so, we would then incorporate the other substituents and prepare 63 by this approach.

II. FROM 1,4-PORPHYRIN DIACETATE -- A TEST

The 1,4-porphyrin diacetate 60 was first synthesized in 36% yield by the

condensation of symmetric 5,5'-dimethyl-dipyrrylmethenium bromide 65 with 5,5'-dibromo-dipyrromethenium perbromide 66 in formic acid with one equivalent of bromine (Scheme 11). Compound 65 was easily prepared by the self-condensation of pyrrole 67 upon refluxing in a mixture of formic acid and hydrobromic acid for 2 h. Dipyrrylmethene 66 was best prepared via its benzyl ester precursor by catalytic hydrogenolysis and subsequent bromination.⁸²

Scheme 11

Reaction of porphyrin 60 with 1.2 equivalent of OsO_4 in CH_2Cl_2 , followed with H_2S effected dihydroxylation at two possible positions to give northern diol 67 (13%) and southern diol 68 (48%). The electron -withdrawing effect of the acetate side chains may have rendered the osmic attack at the northern pyrroles unfavorable. The two diols were separated on preparative TLC plate and 67 was then treated with concentrated sulfuric acid. While porphyrinone 69 was isolated as a minor product, a green colored major fraction was identified as the γ -lactone 70. This compound was found resistant to pinacolic rearrangement in acid and to hydrolysis in basic medium. Another minor product 71 was found with a hydroxymethyl substituent which might be formed by a similar dehydration-hydration

mechanism as described in Chapter 2. Further reaction of the zinc complex of 69 with OsO₄ and followed with sulfuric acid yielded predominately the 3,5-porphyrindione 73 derived obviously from ring-C diol 72 with the migration of methyl group. No trace amount of 1,3-dione 59 was detected. Some starting porphyrinone 69 as well as a hydroxymethyl porphyrinone 74 were also isolated from the reaction mixture (Scheme 12).

The result of the reaction of porphyrin 60 in H₂O₂-H₂SO₄ was messy and gave no indication of the formation of any porphyrindiones and a prolonged reaction only resulted in decomposition. Apparently the strong electron-withdrawing effect of the two acetic groups, plus the "wrong arrangement" of the substituents at the northern pyrroles have prevented the formation of the desired 1,3-dione 59 from this porphyrin.

III. FROM PORPHYRIN WITH MASKED ACETIC SIDE CHAINS--A BYPASS

A. <u>1,4-Bis-(2-chloroethyl)-porphyrin</u>

Porphyrin 61, chosen for reasons of convenient preparation and separation of its isomeric products in the later reaction steps, was synthesized by a pathway similar to that used in preparing 60. This porphyrin has been made previously by Smith⁸³ and Battersby's group⁸⁴ using different approaches.

The 2-ethyl acetate side chains of pyrrole 67 which was synthesized as described in experimental part, were selectively reduced with diborane to hydroxyethyl groups which were then reacted with thionyl chloride to form the 2-chloroethyl derivative 75. The bis-(2-chloroethyl)-dipyrrylmethenium bromide 76 was obtained in the same way as described above, and condensed similarly in a "2+2" pattern with 66 to generate 61 in a yield of 32% (Scheme

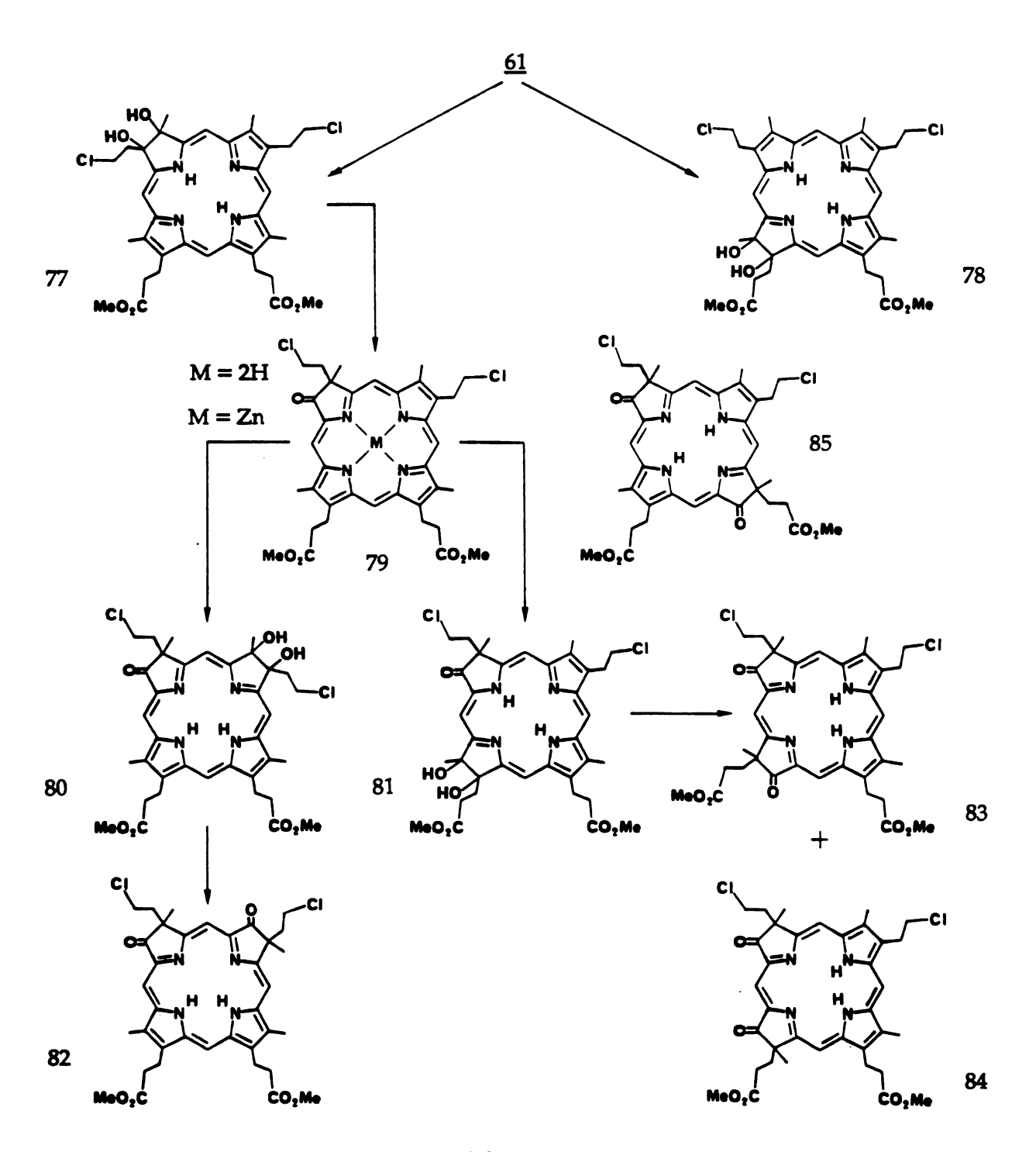
Scheme 12

<u>13</u>).

Scheme 13

The reaction of porphyrin 61 with osmium tetroxide, Scheme 14, produced the northern diol 77 (11%) and the southern diol 78 (31%) respectively. The acid catalyzed pinacol rearrangement of 77 was accomplished smoothly in sulfuric acid to give exclusively porphyrinone 79 with the migration of chloroethyl group which was verified by NOE measurement. OsO₄ oxidation of the zinc complex of 79 gave mainly two vic-diols at its ring B (80) and ring D (81) in a ratio about 2 to 1 with a total yield of 25%. The mixture of this two diols were treated with H₂SO₄ directly without separation since they had been found not very stable in the ordinary working-up process. About 48% of the porphyrinone 79 was found regenerated from the rearrangement reaction mixture, and the other major products included 1,3-dione 82 (8%), 1,7-dione 83 (14%) and 1,8-dione 84(7%).

Replacing the of acetate side chain by chloroethyl group did not seem to improved the electron-deficient problem significantly, as the yield of the northern diol 77 was still lower than that of the south. The surprising result was vic-diol 92 going back to porphyrinone 79 rather than giving the "normal" pinacolic product. Also the reaction between the zinc complex of porphyrinone 79 and OsO₄ did not follow the empirical rules observed in the



Scheme 14

model compound study: not only ring B, but also ring D diol has been formed. However, the differential formation of isobacteriochlorin-type compound by zinc insertion still held true, there was no bacteriochlorin-type compound such as 1,6-dione 85 has been detected. The low yield of 1,3-porphyrindione 82 was probably resulted from the reluctant migration of the ring B methyl group of 80 since the methyl group has a lower mobility than that of the chloroethyl group. To achieve a higher yield of 1,3-dione 82 the positions of these two groups on ring B should be exchanged to suit their intrinsic migratory tendencies, i. e., a porphyrin like 62 is needed.

B. <u>1,3-Bis-(2-chloroethyl)-porphyrin</u>

Porphyrin 62 was synthesized by derivatization of protoporphyrin IX according to literature method⁸⁵ with modifications (Scheme 15). The two

Scheme 15

reactive vinyl groups of protoporphyrin were converted to the chloroethyl side chains by oxidation with $Tl(NO_3)_3$ to the diacetal 86 and to dialdehyde 87, followed by reduction to 88 with NaBH₄, and then by chlorination with PhCOCl-DMF to 62, each step giving essentially a quantitative yield.

Osmium tetroxide oxidation of porphyrin 62 (Scheme 16) offered all four possible vic-diols; ring A 89 (6.8%), ring B 90 (6.9%), ring C 91 (22%) and ring D 92 (26%). The two northern diols were separated from the two south and subjected to acid catalyzed pinacolic rearrangement directly without further separation. The two porphyrinone, 93 and 94, were obtained in very high yield (~90%). We learned from the 1,4-bis-(2-chloroethyl)-porphyrin pathway that for porphyrinone with such substituents, the osmic attack would occur on both pyrroles flanking to the keto group, so both zinc complexes 93 and 94 could offer 1,3-dione 82 even though the former would be the major producer. Thus OsO₄ oxidation of the mixture 93 and 94 and rearrangement produced six porphyrindiones in addition to the regenerated starting porphyrinones 93 (16%) and 94 (17%). Among them, 1,3-porphyrindione 82 was obtained in highest yield (22%), others including 3,5-dione 95 (17%), 3,7-dione 96 (5%), 1,8-dione 97 (4%), 2,3-dione (3%) 98 and 1,7-dione 99 (2%). The structures of these compounds were identified by their visible spectra and the NOE measurements. According to the position of the second keto group introduced, we could deduce that dione 109 and 99 must be derived porphyrinone 93, whereas 95, 96 and 98 from 94. 3,7-porphyrindione 96 was the first bacteriochlorin-type product observed in the zinc porphyrinone oxidation. Although the percentage yield of 96 was not so significant, the appearance of this compound implied that less electron-rich substituents, even like the chloroethyl group, could render the regioselectivity of osmic attack toward zinc porphyrinone less specific. This

Scheme 16

phenomenon has been seen at least in one other case (vide infra).

C. Oxidation of 1,3-Porphyrindione Side Chains

In order to transform the chloroethyl group to acetate side chain, porphyrinone 79 was first tested (Scheme 17).

Heating of 79 in pyridine with KOH resulted in the formation of compound 100 with a hydroxyethyl group derived from the saturated ring A chloroethyl side chain by a nucleophilic substitution, and a vinyl group through the elimination of a HCl from the aromatic ring B chloroethyl side chain. The latter transformation was successfully used in the heme deprosthetic group synthesis to regenerate the vinyl groups from the protected chloroethyl forms. The alcohol side chain of 100 was converted to an aldehyde 101 by Swern oxidation in a good yield (>70%). To oxidize 101 further to acid, in its ester form 102, several reagents, such as argentic oxide (AgO)87 and pyridinium dichromate (PDC)88 have been tried. PDC oxidation gave 102 in a yield of 55% and the argentic method gave a slightly lower yield. PDC was also found to oxidize alcohol 100 in DMF directly to 102 after a lengthy reaction time. The vinyl group survived throughout these reactions.

Unfortunately, this mild procedure turned out to be impractical when 1,3-dione 82 was applied. As shown in Scheme 18, reaction of this compound with KOH in pyridine produced the 2,4--bis-hydroxyethyl-1,3-porphyrindione 103 as a mixture of cis and trans isomers with poor yield (<45%). Attempt to oxidize 103 directly to the diacid of 59 with PDC ended up with a bleached solution containing unidentified species. Even the result of Swern oxidation was messy, only a poor yield of dialdehyde compound 104 could be detected. Oxidation by using AgO led also to miserable decomposition.

IV. FROM 1,3-PORPHYRIN DIACETATE - REACHING THE GOAL

Although the foregoing experiments, either from 1,4-porphyrin diacetate or from porphyrins with masked acetic functions, did not provide a practical synthesis of heme \underline{d}_1 , they were educational. Having failed to bypass the "acetate problem", we had to press forward in the face of difficulties -- starting again from porphyrins with acetic side chains. Since we had already made porphyrinone diacetate 69 from 1,4-porphyrin diacetate 60 it should not be impossible to make 1,3-porphyrindione 59 if the migratory aptitude of all the substituents involved in pinacolic rearrangement are in tune with the migratory direction favoring the 1,3-dione formation.

Porphyrin 58, which fits the above requirement was therefore constructed. The two acetate substituents of this porphyrin at the right positions are expected to direct the subsequent double migration of the adjacent methyl groups to generate the desired 1,3-dione nucleus. Owing to the reluctance of the pinacolic rearrangement caused by the two electron-withdrawing acetate groups, stronger acidic medium was considered to force the reaction.

As shown in <u>Scheme 19</u>, the dialdehyde porphyrin 87, obtained previously, was oxidized with the Jones reagent and esterified in acidified methanol to provide porphyrin 58 in 92% yield.

OsO₄ attacked porphyrin 58 at all four pyrrole rings. After the separation of the unreacted 58 on a silica gel column, the two northern diols (105 and 106, 20%) were further separated from the two southern diols (107 and 108, 51%) on preparative TLC plates. The two southern diols were found unstable on TLC plates and could only be isolated as the spiro γ -lactone derivatives 109 and 110. The southern diols and their lactone derivatives could be

Scheme 19

recycled, however, by reducing with a mixture of AcOH-HI-H₃PO₂ to recover porphyrin 58.^{63, 89}

In order to achieve a higher yield for the pinacolic rearrangement of the northern diols, several strong acidic media were tested. We found that by using sulfuric acid alone, only less than 15% of porphyrinones 111 and 112 could be obtained with the major products being the inert γ-lactone 113 and 114; using Nafion or Magic acid, diol decomposition was observed. The reaction condition was finally optimized by treating the diols with FSO₃H-H₂SO₄-fuming H₂SO₄ (10:10:1), and porphyrinones 111 and 112 were obtained as the major products (45%) with the amount of lactones 113 and 114 reducing to about 10%. The separation of 111 and 112 was accomplished on TLC plates by "over-developing", and the ratio of these two porphyrinones was about one to one. It is necessary to purify porphyrinone 111 at this stage or the multiple isomeric products derived from 112 would surely add more difficulties to the already tedious separation in the next step.

Porphyrinone 111 was metalated with zinc(II) acetate in CH₃Cl-MeOH and the zinc complex was oxidized with 1.5 equivalent of OsO₄. The oxidation products were quickly separated from the unreacted zinc porphyrinone on a silica gel column by flash chromatography under argon. Following the zinc removal by washing with aqueous HCl solution (10%), the purple colored porphyrinone diol 115 (18%), which was unstable on TLC plate, was separated from its ring C regioisomer 116 (15%) and ring D 117 (12%) on a chromatotron protecting from air and light. Rearrangement of 127 in concentrated sulfuric acid containing 10% of fluorosulfonic acid generated the desired 1,3-porphyrindione 59 (as the mixture of cis and trans diastereomers) in a modest yield of 12%. Other compounds isolated from the reaction mixture included the regenerated porphyrinone 111 (20%), a

 γ -lactone 118 (8%), a porphyrinone α -hydroxyacetate 119 (15%) and an α -hydroxymethyl porphyrinone 120 (4%) (Scheme 20). Formation of 119 and 120 was probably from a process analogous to that we encountered in the acrylate side chain formation (Chapter 2, B).

As we mentioned earlier for zinc complexes bearing less electron-rich substituents, such as chloroethyl groups in compound 79, the osmic attack on the porphyrinone is less selective. In the present case, with the strong electron-withdrawing acetate side chains, the reaction is even less selective and the dihydroxylation occurred at all the three pyrrole rings without remarkable preferences. These results have therefore overridden the empirical rules observed in our model compound study where only simple alkyl substituents were involved. However, the advantage of using the zinc method is still obvious: without zinc insertion, the OsO₄ oxidation would overwhelmingly lead to the bacteriochlorin-type ring C diol 117, and the desired ring B diol 115 would not have been formed at all.

The presence of acetate substituents further hindered the second pinacolic rearrangement on ring B of 115 as demonstrated by the low yield of 1,3-dione 59 even under the best condition tested. When the above FSO₃H-H₂SO₄-fuming H₂SO₄ (10:10:1) mixture, which worked best in the first pinacol rearrangement, was applied here, the predominate product was the regenerated porphyrinone 111. By using sulfuric acid with only 10% of FSO₃H, this "reduction" was largely prevented. The similar reduction has been observed in the rearrangement of porphyrinone diols bearing chloroethyl substituents (section 3).

The precise mechanism for the reduction, like most alcohol reduction, is obscure. We believe that the diol may be reduced via the intermediate b-j (Scheme 21) which are favored by the electron-withdrawing acetate group as

Scheme 20

Scheme 21

well as by a very electron-negative porphyrinone core structure. In strong acid, benzylic alcohols are known to undergo reduction by nucleophilic substitution.⁹⁰

Porphyrinone diol 115 was unstable and difficult to purify. To avoid the unnecessary loss, the mixture of diols obtained from the OsO₄ oxidation of Zn(II) porphyrinone 111 was treated with H₂SO₄-FSO₃H(10%) directly to effect the rearrangement. More than eight compounds were isolated in this manner and the structures and yields are given in Scheme 22. In addition to the three compounds derived from 115 as described above, 1,7-dione 121, 1,8-dione 122 and porphyrinone 6-acrylate 125 were derived from porphyrinone diol 116, and 1,5-dione 123 and 1,6-dione 124 were produced from diol 117. All these porphyrindiones were obtained as diastereomeric mixtures.

The cis-1,3-dione 59a and its trans isomer 59b were separable by TLC plates, approximately in a ratio of 1.5 to 1. Their structure assignments will be described in next chapter. These compounds were found rather stable, even a prolonged developing on TLC plate in air did not result in noticeable decomposition or isomerization.

The formation of acrylic double bond was accomplished by separately treating 59a and 59b with 1.5 equivalent of OsO_4 in methylene chloride to effect the dihydroxylation followed by reacting with a catalytical amount of HCl in boiling benzene (Scheme 23). In both cases, two regioisomers, with the acrylate substituent either on ring C or ring D were isolated in a ratio about 5 to 1. The formation of diols 127a and 127b, once again, demonstrated the reduced selectivity of the osmic attack duo to the acetate substituents. We use the prefix "iso-" in naming the ring-D acrylic compounds, thus there are $cis-\underline{d}_1$ (128a=4a) and $cos d_1$ (128b=4b), $cis-iso-\underline{d}_1$ (129a) and $cos d_1$ (129b).

Scheme 22

Scheme 23

Among above four isomers only cis- \underline{d}_1 (128a) with the structure 4 as we proposed is truly identical with the natural \underline{d}_1 tetramethyl ester in a careful comparison of ¹H and ¹³C NMR spectra, UV-Visible absorption, HPLC and TLC.

V. A \underline{d}_1 ANALOGUE FROM COPROPORPHYRIN IV

The most successful example of applying all the methodologies developed in the \underline{d}_1 synthesis was the preparation of homo- \underline{d}_1 130 in which two pyrroline propionate replaced the acetate side chains. Compound 130 may be used as substitutes and spectral probes for heme \underline{d}_1 in a variety of experiment conditions including protein reconstitution. The total yield of 130 from the same reaction pathway is significantly higher than that of \underline{d}_1 owing to the replacement of troublesome acetic side chains by the less electron-withdrawing propionic side chains.

As shown in Scheme 24, the symmetric coproporphyrin IV tetramethyl ester,*starting compound, was conveniently synthesized through a condensation of dipyrrylmethenes 132 and 66 in a yield of 47%. Compound 132 was made by standard method from corresponding pyrrole 131in formic acid with hydrobromic acid.

Scheme 24

The OsO₄ oxidation generated two diol compound 133 and 134, with the northern isomer 133 being the favored product, which upon pinacolic rearrangement in sulfuric acid produced predominately porphyrinone 135. Further reaction of 135 with osmium tetraoxide after zinc insertion gave three diols with the ring B isomer 136 as the major product. Treating the mixture of diols with H_2SO_4 - FSO_3H (9:1) led to the formation of 1,3-dione 139 with the migration of methyl group (32%, yield), together with the regenerated porphyrinone 135 (20%) and other keto regioisomers (Scheme 25).

The formation of acrylic side chain was accomplished as usual by further reaction with OsO_4 , followed by dehydration in boiling benzene with a small amount of hydrochloric acid. The homo- \underline{d}_1 130 was obtained almost quantitatively without any indication of the formation of its ring D regioisomer 144, however, a minor hydroxymethyl compound 145 was observed (Scheme 26).

Scheme 25

In conclusion, the successful synthesis of heme \underline{d}_1 and its stereo and regioisomers as well as its structural isomers not only established the \underline{d}_1 structure we proposed, but also provided us a reasonable supply of materials to study physical properties and functions of this green heme in biological systems.

VI. EXPERIMENTAL

A. Porphyrin-1/A-diacetate system

<u>Tetramethyl-2,3,5,8-tetramethyl-porphyrin-1,4-diacetate-5,6-dipropionate</u> (60)

4,4'-di-ethoxycarbonylmethyl-3,3',5,5'-tetramethyl-2,2',-dipyrrylmethenium bromide 65, 12.9 g (0.051 mol), and 5,5'-dibromo-3,3'di-methoxycarbonylmethyl-4,4'-dimethyl-2,2'-dipyrrylmethenium bromide 66, 29.1 g (0.05 mol), were suspended in formic acid (250 ml, 98-100%) and treated with 2.6 ml of bromine. The mixture was refluxed in an oil bath for 3 h and the solvent was then allowed to boil off over a period of 1 h with a stream of air. To the dried reaction residue were added 500 ml of methanol and 10 ml of concentrated sulfuric acid, followed by 40 ml of trimethyl orthoformate. After standing overnight, protected from moisture, the reaction mixture was diluted with 600 ml of CH₂Cl₂ first and then 400 ml of concentrated aqueous NaOAc solution. The organic layer was separated, washed once again with 300 ml of NaOAc solution and then with water (3 x After evaporation of the solvent, the crude product was chromatographed on a silica gel column (50 to 250 mesh) using 1% MeOH/CH₂Cl₂ as eluent first then gradually increasing methanol to 5%. A dark non-fluorescent forerun was discarded and the moving of porphyrin band on column can be monitored by using an UV-lamp to ensure a complete collection. The porphyrin containing fractions were combined and brought to dryness in vacuo and then crystallized from CH₂Cl₂-MeOH. yield, 12.3 g, 36%; ¹H-NMR δ 3.25 (4 H, t, CH₂CH₂CO₂), 3.44, 3.57 (6 H each, s, Me), 3.66 (6 H, s, $CH_2CH_2CO_2CH_3$), 3.73 (6 H, s, $CH_2CO_2CH_3$), 9.79 (1 H, s, meso α), , 9.91 (2 H, s, meso β , δ), 9.96 (1 H, s, meso γ), -4.06 (2 H, br s, NH); UV-vis λmax (rel. int.) 399 (1.00), 498 (0.10), 531 (0.07), 568 (0.06), 622 (0.05); MS found m/e 683.7840 for $(M+H)^+$, C38H43N4O8 requires 683.7884.

Dihydroxychlorin 67 and 68

Osmium tetroxide (600 mg, 2.4 mmol) in anhydrous ether (6 ml) was added to a methylene chloride (200 ml) solution of porphyrin 60 (1.36 g, 2.0 mmol). Dry pyridine (1 ml) was added subsequently, and the mixture was allowed to stir at room temperature, under argon, in the dark for 20 h. The reaction was then quenched with 100 ml of methanol and bubbled with H₂S for 10 min. The precipitated black osmium sulfide was removed by filtration through celite, and the crude product in the filtrate was brought to dryness and chromatographed on a silica gel column. Unreacted porphyrin was eluted first with 1% MeOH/CH₂Cl₂. The faster moving isomer which turned out to be northern diol 67 was eluted then with 2% MeOH/CH₂Cl₂ and the slower moving southern diol 68 was rinsed down with 4% MeOH/CH₂Cl₂. Diol 67 was further purified on preparative TLC plates, developed with 5% EtOAc/CH₂Cl₂. Yield: unreacted porphyrin 60, 476 mg (35%), northern diol 67 186 mg (13%), southern diol 68, 687 mg (48%).

Tetramethyl-3,4-dihydroxyl-2,3,5,8-tetramethylchlorin-1,4-diacetate-6,7-dipropionate (67) 1 H-NMR δ 1.91 (3 H, s, Me sat.), 3.15 (4 H, t, $\underline{\text{CH}_{2}\text{CH}_{2}\text{CO}_{2}}$), 3.20, 3.38, 3.41 (3 H each, s, ring Me), 3.62, 3.67 (3 H each, s, $\underline{\text{CH}_{2}\text{CO}_{2}\text{CH}_{3}}$), 3.94 (3 H, s, $\underline{\text{CH}_{2}\text{CO}_{2}\text{CH}_{3}}$), 4.18 (4 H, m, $\underline{\text{CH}_{2}\text{CO}_{2}}$ sat., $\underline{\text{CH}_{2}\text{CH}_{2}\text{CO}_{2}}$) 4.56, 4.68 (1 H each, d, J=16 Hz, $\underline{\text{CH}_{2}\text{CO}_{2}}$), 9.04, 9.10, 9.57, 9.73 (1 H each, s, meso α , β , γ , δ), 12.88 (2 H, br s, NH); UV-vis λ max (rel. int.) 392 nm (1.00), 494 (0.11), 521 (0.04), 589 (0.05), 642 (0.29); MS found m/e 717.8043 for (M+H)+, C38H45N4O10 requires 717.8031.

dipropionate (68) ¹H-NMR δ 2.14 (3 H, s, Me sat.), 2.54, 2.75 (2 H each, m, $CH_2CH_2CO_2$), 3.23, 3.33, 3.36 (3 H each, s, ring Me), 3.48 (3 H, s, $CH_2CH_2CO_2CH_3$ sat.), 3.65 (3 H, s, $CH_2CH_2CO_2CH_3$), 3.70, 3.71 (3 H each, s, $CH_2CO_2CH_3$), 4.05 (2 H, m, $CH_2CH_2CO_2$), 4.58, 4.67 (1 H each, d, J=16 Hz, CH_2CO_2), 4.71 (2 H, s, CH_2CO_2), 8.91 (2 H, s, meso β , γ), 9.53, 9.62 (1 H each, s, meso α , δ), -2.29, -2.36 (1 H each, br s, NH); UV-vis λ max (rel. int.) 392 nm (1.00), 497 (0.10), 522 (0.03), 588 (0.04), 640 (0.26); MS found m/e 717.8025 for (M+H)+, C38H45N4O10 requires 717.8013.

Porphyrinone 69, lactone 70 and methoxymethyl compound 71

To the north diol 67 (186 mg, 0.26 mmol) was added 20 ml of concentrated sulfuric acid, and the mixture was stirred for 2 h at room temperature before being quenched with 100 ml of methanol in an acetone/dry-ice bath. The solution was then allowed to stand for 5 h, protected from moisture, to ensure the re-esterification. The solution was further diluted with 200 ml of CH_2Cl_2 and washed with aqueous NaOAc (25%, 3 x 150 ml) and water (3 x 150 ml). The solvent was evaporated and the residue was chromatographed on preparative TLC plates, developed with 2% $MeOH/CH_2Cl_2$. The fastest moving brown band was porphyrinone 69 (43 mg, 24%), followed by red colored hydroxymethyl porphyrin 71 (16 mg, 9%) and lactone 70 (83 mg, 47%).

Tetramethyl-2,4,5,8-tetramethyl-porphyrinone-1,4-diacetate-6,6-dipropionate (69) 1 H-NMR δ 1.94 (3 H, s, Me sat.), 2.94 (3 H, s, CO₂CH₃ sat.), 3.18, 3.25 (2 H each, t, CH₂CH₂CO₂), 3.46, 3.54, 3.59 (3 H each, s, ring Me), 3.65, 3.66 (3 H each, s, CH₂CH₂CO₂CH₃), 3.98, 3.89 (1 H each, d, J=16 Hz, CH₂CO₂ sat.), 4.22, 4.37 (2 H each, t, CH₂CH₂CO₂), 5.02 (2 H, s, CH₂CO₂), 9.07, 9.86, 9.92, 9.94 (1 H each, s, meso β , α , γ , δ), -2.82, -2.97 (2 H, br s, NH); UV-vis λ max

(rel. int.) 404 nm (1.00), 506 (0.09), 543 (0.09), 587 (0.06), 614 (0.04), 643 (0.24); MS m/e found 699.7854, C38H43N4O9 requires 699.7878.

Trimethyl-1-hydroxy-2,3,5,8-tetramethyl-1,2-(γ -lactone)chlorin-4-acetate-6,7-dipropionate (70) 1 H-NMR d 2.35 (3 H, s, Me sat.), 2.87 (4 H, m, $\frac{CH_{2}CH_{2}CO_{2}}{CH_{2}CO_{2}}$), 3.08, 3.26, 3.44 (3 H each, s, ring Me), 3.55 (2 H, m $\frac{CH_{2}CO_{2}}{CO_{2}}$ sat.), 3.53, 3.61 (3 H each, s, $\frac{CH_{2}CH_{2}CO_{2}CH_{3}}{CH_{2}CO_{2}CH_{3}}$), 3.74 (3 H, s, $\frac{CH_{2}CO_{2}CH_{3}}{CH_{2}CO_{2}}$), 4.83, 4.84 (1 H, each, s, $\frac{CH_{2}CO_{2}}{CO_{2}}$), 9.11, 9.13, 9.15, 9.60 (1 H each, s, meso α , β , γ , δ), -3.10 (2 H, br s, NH); UV-vis λ max (rel. int.) 390 (1.00), 493 (0.10), 541 (0.03), 587 (0.04), 640 (0.24); MS found m/e 685.7633 for (M+H)+, C37H41N4O9 requires 685.7607.

Tetramethyl-3-hydroxymethyl-2,5,8-trimethylporphyrin-1,4-diacetate-6,7-dipropionate (71) 1 H-NMR δ 3.26, 3.27 (2 H each, t, $\underline{CH_2CH_3CO_2}$), 3.59 (3 H, s, ring Me), 3.64 (6 H, s, ring Me), 3.65 (6 H, s, $\underline{CH_2CH_2CO_2CH_3}$), 3.74, 3.75 (3 H, s, $\underline{CH_2CO_2CH_3}$), 4.36, 4.41 (2 H each, t, $\underline{CH_2CH_2CO_2}$), 5.04, 5.15 (2 H each, s, $\underline{CH_2CO_2}$), 5.94 (2 H, s, $\underline{CH_2OH}$), 10.04, 10.06, 10.16, 10.29 (1 H each, s, meso); UV-vis λ max (rel, int.) 401 nm (1.00), 499 (0.10), 534 (0.07), 568 (0.06), 622 (0.05), 642 (0.043); MS found m/e 699.7847 for (M+H)+, C38H43N4O9 requires 699.7878.

<u>Tetramethyl-3,5-porphyrindione-1,4-diacetate-6,7-dipropionate</u> (73)

Starting with 69, the zinc insertion, OsO4 oxidation and sulfuric acid catalyzed rearrangement were accomplished as described previously. Chromatographic separation on TLC plates, developed with 2% MeOH/CH₂Cl₂, gave 3,5-dione 73 as the major product in pair of cis and trans isomers. Yield, 44%; ¹H-NMR 1.61, 2.15 (1 H each, m, CH₂CH₂CO₂), 181, 193

(3 H each, s, Me sat.), 2.89 (2 H, t, $CH_2CH_2CO_2$ sat.), 3.09 (2 H, t, $CH_2CH_2CO_2$), 3.17 (3 H, s, CO_2CH_3 sat.), 3.35, (2 H, t, $CH_2CH_2CO_2$), 3.37, 3.41 (3 H each, s, ring Me), 3.62 (3 H, s, $CH_2CH_2CO_2CH_3$), 3.73 (3 H, s, $CH_2CO_2CH_3$), 3.90 (2 H, m, CH_2CO_2 sat.), 4.09 (2 H, t, $CH_2CH_2CO_2$), 481 (2 H, s, CH_2CO_2), 858, 865, 943, 955 (1 H each, s, meso γ , β , α , δ), -0.50 (2 H, br s, NH); UV-vis λ max (rel. int.) 416 nm (1.00), 437 (0.83), 546 (0.13), 587 (0.19), 639 (0.21); MS found m/e 715.7836 for (M+H)+, C38H43N4O10 requires 715.7872.

B. 1,4-Bis-(2-chloroethyl)-porphyrin system

Ethyl-diacetoacetate

In a 2 L flask were placed 138 g (1 mol) of K_2CO_3 , 30 g (0.18 mol) mol (crushed up finely), 100 g (1 mol) of 2, 4-pentanedione, 167 g (1 mol) of ethyl bromoacetate and 350 ml of 2-butanone. The mixture was heated slowly to reflux. After about 30 min, the refluxing became vigorous but subsided gradually. The reaction was continued for 4 h and then the mixture was cooled and diluted with 1 L of acetone. The inorganic salts were filtered off and washed further with acetone. The solvent was evaporated with a rotavapor and the orange colored crude product was distilled under vacuum. Yield, 153 g (82%). 1H -NMR (as ketone -- enol tautomers) δ 1.27 (3 H, t, $CO_2CH_2CH_3$), 2.15, 2.18, 2.27 (6 H, s, CO_2CH_3), 2.86, 2.89, 3.24, 3.26 (3 H, d, s, $CHCH_2$), 4.14 (2 H, q, CH_2CH_3).

Ethyl acetoacetate oxime

136 g of ethyl acetoacetate was dissolved in 300 ml of acetic acid and the solution was cooled in an ice bath. The saturated aqueous solution of sodium nitrite, 73 g (1.06 mol), was added dropwise with stirring and the temperature was controlled below 20 °C. The reaction was continued for

another 2 h after the addition. The orange-colored oxime solution was kept at low temperature or used immediately.

Ethyl-4-ethoxycarbonylmethyl-3,5-dimethylpyrrole-2-carboxylate

To the well stirring solution of ethyl-diacetoacetate (186 g, 1 mol) in 350 ml of AcOH was added the above oxime solution (1.05 mol) dropwise while adding zinc powder (200 g, 3.06 mol) such that to maintain the reaction temperature between 90 to 95 °C. After the addition, the reaction mixture was heated for 1 h before being poured onto 1000 g of ice. The crude product was precipitated as a yellow solid which was collected by filtration and washed with water. The solid was then redissolved in 500 ml of CH₂Cl₂, filtered again to remove zinc powder and dried over Na₂SO₄. After evaporation of solvent the pyrrole was crystallized from ethanol. Yield, 103.7 g (41%); MP, 85-87 °C; ¹H-NMR δ, 1.21 (3 H, t, CH₂CO₂CH₂CH₃), 1.32 (3 H, t, CO₂CH₂CH₃), 2.21, 2.26 (3 H each, s, Me), 3.34 (2 H, s, CH₂CO₂), 4.09 (2 H, q, CH₂CO₂CH₂CH₃), 4.27 (2 H, q, CO₂CH₂CH₃), 8.97 (1 H, br s, NH).

Ethyl-3-(2-hydroxyethyl)-3,5-dimethylpyrrole-2-carboxylate

Boron trifloride-ether complex (130 ml) was added dropwise to a solution of sodium borohydride (25 g) in diglyme (50 ml), and the diborane generated was flushed with a slow steam of nitrogen into a solution of foregoing pyrrole (25.3 g, 0.1 mol) in 100 ml of THF. The reaction was continued for 45 min, methanol was then carefully added to quench the excess B_2H_6 until effervescence ceased. The solvent was evaporated and the crude product pyrrole was crystallized form methanol. Yield, 18.7 g (89%); MP, 109-111 °C; ¹H-NMR δ 1.26 (3 H, t, CO₂CH₂CH₃), 2.20, 2.23 (3 H each, s, Me), 2.57, 3.51 (2 H each, t, CH₂CH₂OH), 4.19 (2 H, q, CO₂CH₂CH₃), 10.11 (1 H,

br s, NH).

Ethyl-3-(2-chloroethyl)-2,4-dimethylpyrrole-5-carboxylate (75)

The above hydroxyethylpyrrole pyrrole (10.05 g 0.05 mol) was dissolved in 200 ml of benzene, 20 g of anhydrous K_2CO_3 , and 6 ml of thionyl chloride were added subsequently. The mixture was heated under refluxing for 3 h. After cooling, the solution was filtered to remove the inorganic salts and the filtrate was brought to dryness. The crude product was crystallized from methanol to give 10.3 g of pyrrole 75, 90%. MP, 110-112 °C; ¹H-NMR δ 1.22 (3 H, t, $CO_2CH_2CH_3$), 2.11, 2.15 (3 H each, s, Me), 2.72, 3.38 (2 H each, t, CH_2CH_3Cl), 4.17 (2 H, q, $CO_2CH_2CH_3$), 8.60 (1 H, br s, NH).

4,4'-bis-(2-chloroethyl)-3,3',5,5'-tetramethyl-2,2'-dipyrrylmethenium bromide (76)

Pyrrole 75, 11.5 g (0.05 mol), in 30 ml of formic acid (98-100%) was heated on a steam bath. To this solution 7 ml of concentrated hydrobromic acid (48%) was added in one portion and the heating was continued for about 2 h until gas evolution ceased. On standing at room temperature overnight the dipyrrylmethenium salts were crystallized as a dense chunky solid. It was collected by filtration, washed with cold methanol to yield 5.1 g of 76, (50%). MP, 217-219 °C; ¹H-NMR δ 2.28, 2.66 (6 H each, s, Me), 2.96, 3.38 (2 H each, t, CH₂CH₂Cl), 7.08 (1 H, s, methine), 8.01 (2 H, s, NH).

<u>Dimethyl-1,4-bis-(2-chloroethyl)-2,3,5,8-tetramethylporphyrin-6,7-di-</u> <u>propionate (61)</u>

The condensation of 4.06 g (0.01 mol) of dipyrrylmethenium bromide 76 and 5.83 g (0.01 mol) of dipyrrylmethenium bromide 66 was carried out in the

same way as described in the synthesis of porphyrin 60. The porphyrin 61 obtained from column chromatography was crystallized from CH₂Cl₂-MeOH as sparkling purple blades, 2.12g (32%). MP, sintered at 202 °C and melted at 208 °C (lit. MP 201-203 °C); 1 H-NMR 3.26 (4 H, t, CH₂CH₂CO₂), 3.49, 3.57 (6 H each, s, ring Me), 3.66 (6 H, s, CH₂CH₂CO₂CH₃), 4.06 (4 H, t, CH₂CH₂CO₂), 4.36 (8 H, m, CH₂CH₂Cl), 9.81, 9.83, 9.89, 10.01 (1 H each, s, meso), -3.99 (2 H, br s, NH); UV-vis λ max (rel. int.) 400 nm (1.00), 498 (0.13), 532 (0.10), 568 (0.08), 620 (0.06); MS (direct probe) m/e 663 (M⁺).

Dihydroxylchlorin 77, 78, porphyrinone 79, 1,3-porphyrindione 82, 1,7-porphyrindione 83 and 1,8-porphyrindione 84.

To a solution of 1,4-bis-(2-chloroethyl)-porphyrin 61, 6.63 g (10 mmol) in 200 ml of CH₂Cl₂, pyridine (5 ml) was added, followed by 3.10 g (12 mmol) of OsO₄. The reaction was stirred in the dark, under nitrogen, for 24 h before being diluted with 100 ml of methanol and quenched with H₂S. The oxidation products were chromatographed on a silica gel column. Porphyrin 61 (1.52 g, 23% recovered) was eluted first with methylene chloride while the mixture of the two dihydroxylchlorins were washed out with 2% MeOH/CH₂Cl₂. This mixture was then chromatographed on TLC plates, developed with 8% EtOAc/CH₂Cl₂, to separate the fast moving northern diol 77 (0.767 g, 11%) from the southern diol 78 (2.16 g, 31%). The distinction of 77 and 78 was based on derivatization: the southern isomer underwent dehydration in dioxane with diluted acid to form an acrylate side chain, which gave the specific proton NMR peak at 4.10 ppm (CH=CH₂CO₂CH₃) together with two pairs of doublet at 6.92 and 9.09 ppm (CH=CHCO₂).

The above north diol 77 (1.1 mmol) was stirred with 10 ml of concentrated sulfuric acid for 30 min to effect the pinacolic rearrangement

followed by re-esterification with methanol. The porphyrinone **79** was obtained in a yield of 680 mg (91%) after being chromatographed on TLC plates.

The zinc insertion was carried out by reacting 79 with zinc acetate in 100 ml of CHCl₃ and 20 ml of methanol. After 30 min refluxing, the mixture was concentrated, the zinc complex was precipitated by the addition of methanol and filtered in virtually quantitative yield.

To a solution of the above zinc complex in 150 ml of CH_2Cl_2 , 2 ml of pyridine and 380 mg (1.5 mmol) of osmium tetroxide were added and the reaction was allowed to proceed in the dark, under argon, for 24 h at room temperature. The reaction mixture was worked up by treating with methanol and H_2S as described before and chromatographed on silica gel column (1% MeOH/CH₂Cl₂, then 4% MeOH/CH₂Cl₂). Yield, recovered Zn(II) 79, 379 mg (51%), and a mixture of two diols (80 and 81), 350 mg (45%).

The mixture of zinc diols (0.45 mmol) was dissolved 10 ml of concentrated H_2SO_4 and allowed to stir at room temperature for 30 min. After being cooled in a dry ice-acetone bath, 100 ml of MeOH (100 ml) was added carefully to the solution, which was then partitioned between CH_2Cl_2 (200 ml) and water (100 ml). The organic layer was separated, washed with aqueous sodium acetate (25%, 2 x 100 ml), water (2 x 100 ml), dried over Na_2SO_4 and evaporated to dryness, to give, after separation on TLC plates (1% MeOH/ CH_2Cl_2), 146 mg (48%) of regenerated porphyrinone 79, 25 mg (8%) of 1,3-dione 82, 44 mg (14%) of 1,7-dione 83 and 22 mg (7%) of 1,8-dione 84.

Dimethyl-1,4-bis-(2-chloroethyl)-1,2-dihydroxyl-2,3,5,8-tetramethyl-chlorin-6,7-dipropionate (77) ¹H-NMR δ 2.03 (3 H, s, Me sat.), 2.65, 3.20 (2 H each, m, <u>CH₂CH₂Cl sat.</u>), 2.77, 2.79 (2 H each, t, CH₂<u>CH₂CO₂</u>), 3.15, 3.16, 3.24 (3

H each, s, ring Me), 3.62, 3.68 (3 H each, s, CO_2CH_3), 3.90 (8 H, m, CH_2CH_2C l and $CH_2CH_2CO_2$), 8.65, 8.66, 9.29, 9.31 (1 H each, s, meso α , δ , γ , β); UV-vis λ max (rel. int.) 393 nm (1.00), 494 0.11), 521 (0.05), 589 (0.06), 642 (0.29).

Dimethyl-1,4-bis-(2-chloroethyl)-7,8-dihydroxyl-2,3,5,8-tetramethyl-chlorin-6,7-propionate (78) 1 H-NMR δ 2.01 (3 H, s, Me sat.), 2.50 (2 H, m, $\underline{\text{CH}_{2}\text{CH}_{2}\text{CO}_{2}}$ sat.), 3.01, 3.29 (2 H each, t, $\underline{\text{CH}_{2}\text{CH}_{2}\text{CO}_{2}}$), 3.03, 3.18, 3.25 (3 H each, s, ring Me), 3.57, 3.71 (3 H, each, s, $\underline{\text{CO}_{2}\text{CH}_{3}}$), 3.94 (2 H, t, $\underline{\text{CH}_{2}\text{CH}_{2}\text{CO}_{2}}$), 3.78 -4.22 (8 H, m, $\underline{\text{C}}\underline{\text{H}_{2}\text{CH}_{2}\text{Cl}}$), 8.72, 8.77, 9.30, 9.35 (1 H each, s, meso γ , δ , α , β); UV-vis λ max (rel. int.) 392 nm (1.00), 495 (0.12), 522 (0.04), 588 (0.05), 641 (0.27).

Dimethyl-2,4-bis-(2-chloroethyl)-2,3,5,8-tetramethyl-porphyrinone-6,7-dipropionate (79) 1 H-NMR δ 2.16 (3 H, s, Me sat.), 2.40, 3.28 (1 H each, m, $\underline{CH_2CH_2Cl}$ sat.), 3.22 (4 H, t, $\underline{CH_2CH_2CO_2}$), 3.32 (2 H, m, $\underline{CH_2CH_2Cl}$), 3.40, 3.53, 3.55 (3 H each, s, ring Me), 3.66, 3.67 (3 H each, s, $\underline{CO_2CH_3}$), 4.18 (4 H, m, $\underline{CH_2CH_2CO_2}$), 4.26, 4.42 (2 H each, t, $\underline{CH_2CH_2Cl}$), 9.16, 9.66, 9.85, 9.86 (1 H each, s, α , β , δ , γ), -3.01 (2 H, br s, NH); UV-vis λ max (rel. int.) 409 nm (1.00), 510 (0.10), 548 (0.11), 589 (0.08), 615 (0.06), 644 (0.25); MS (direct probe 70 eV), m/e 679 (M⁺).

Dimethyl-2,4-bis-(2-chloroethyl)-2,4,5,8-tetramethyl-1,3-porphyrindione-6,7-dipropionate (82) 1 H-NMR δ 1.95, 1.94 (3 H each, s, Me sat.), 3.25 (12 H, m, $\underline{\text{CH}_{2}\text{CH}_{2}\text{Cl}}$ sat., $\underline{\text{CH}_{2}\text{CH}_{2}\text{CO}_{2}}$), 3.34, 3.36 (3 H each, s, ring Me), 3.58, 3.60 (3 H each, s, $\underline{\text{CH}_{2}\text{CH}_{2}\text{CO}_{2}\text{CH}_{3}}$), 4.23 (4 H, m, $\underline{\text{CH}_{2}\text{CH}_{2}\text{CO}_{2}}$), 8.61, 8.79, 9.41, 9.45 (1 H each, s, meso β , α , δ , γ), -0.67 (2 H, br s, NH); UV-vis λ max (rel. int.) 418 nm (1.00), 439 (0.94), 545 (0.13), 592 (0.18), 637 (0.22); MS found m/e 696.6521 for (M+H)+, C36H41N4O6Cl2 requires 696.6574.

Dimethyl-1,4-bis-(2-chloroethyl)-2,3,5,8-tetramethyl-1,7-porphyrindione-6,7-dipropionate (83) 1 H-NMR δ 1.76, 2.10 (1 H each, m, CH₂CH₂CO₂ sat.), 1.95, 1.97 (3 H each, s, Me sat.), 2.89 (2 H, m, CH₂CH₂CO₂sat.), 3.01, 3.32 (6 H, m, CH₂CH₂Cl sat. and CH₂CH₂CO₂), 3.35, 3.42 (3 H each, s, ring Me), 3.45 (3 H, s, CO₂CH₃ sat.), 3.70 (3 H, s, CO₂CH₃), 4.00-4.50 (6 H, m, CH₂CH₂Cl and CH₂CH₂CO₂), 8.59, 8.78, 8.33, 9.51 (1 H each, s, meso α , δ , γ , β), -0.60 (2 H, br s, NH); UV-vis λ max (rel. int.) 403 nm (0.75), 419 (1.00), 440 (0.94), 545 (0.14), 593 (0.20), 638 (0.24); MS found m/e 696.6492 for (M+H)+, C36H41N4O6Cl2 requires 696.6574.

C. 1,3-Bis-(2-chloroethyl)-porphyrin system

<u>Dimethyl-1,3-bis-(2,2-dimethoxyethyl)-2,4,5,8-tetramethylporphyrin-6,7-dipropionate (86)</u>

To a solution of protoporphyrin IX dimethyl ester (5.91 g, 0.01 mol) in 1.5 L of methylene chloride and 250 ml of methanol was added 15.5 g (0.035 mol) of $Tl(NO_3)_3.3H_2O$ dissolved in 500 ml of Methanol. The solution was stirred at 40 °C for 10 min and the white $TlNO_3$ was precipitated out.

Hydrogen sulfide was then bubbled into the solution for 10 min followed by addition of 25 ml of concentrated HCl to destroy the Tl(III)-porphyrin complex. The mixture was stirred for 5 min and then filtered to remove the solid inorganic salt. The organic filtrate was washed with aqueous sodium acetate (25%, 2 x 200 ml), water (3 x 300 ml) and then brought to dryness. Porphyrin 86 was recrystallized from CH_2Cl_2 -MeOH with a yield of 6.65 g (95%). MP, 230-232 °C; ¹H-NMR δ 3.28, 3.32 (2 H each, t, $CH_2CH_2CO_2$), 3.45, 3.47 (6 H each, s, $CH(OCH_3)_2$), 3.57, 3.59. 3.60, 3.62 (3 H each, s, ring Me), 3.66, 3.68 (3 H each, s, CO_2CH_3), 4.09, 4.20 (2 H each, d, $CH_2CH(OCH_3)_2$), 4.34, 4.39 (2 H each, t, $CH_2CH_2CO_2$), 5.08, 5.14 (1 H each, t, $CH_2CH(OCH_3)_2$), 10.00, 10.03, 10.06, 10.09 (1 H each, s, meso), -4.02 (2 H, br s, NH); UV-vis λ max (EM) 400 nm (169800), 498 (12300), 533 (7900), 567 (5500), 621 (3300);

<u>Dimethyl-1,3-bis-(hydrogencarbonylmethyl)-2,4,5,8-tetramethyl-6,7-dipropionate (87)</u>

Porphyrin 86, 3.6 g (0.05 mol) was dissolved in 1000 ml of tetrahydrofuran and the solution was heated to reflux, followed by addition of 36 ml of diluted hydrochloric acid (4.5 ml of concentrated HCl in 31.5 ml of water) in one portion. The mixture was refluxed for 5 min and then cooled immediately in an ice bath. The solution was diluted with 1000 ml of chloroform, and washed with aqueous sodium acetate (25%, 500 ml) and water (2 x 800 ml). The solvent was evaporated under vacuum and the residue was crystallized from CH_2Cl_2 -MeOH (or used directly to undergo either reduction by NaBH₄ to 88 or oxidation by Jones reagent to porphyrin 58). Isolated yield, 2.56 g (81.3%); 1 H-NMR δ 3.23 (4 H, t, $CH_2CH_2CO_2$), 3.37 (6 H, s, Me), 3.49, 3.50 (3 H each, s, Me), 3.66 (6 H, s, CO_2CH_3), 4.29, 4.30 (2 H each, t, $CH_2CH_2CO_2$), 4.75, 4.80 (2 H each, d, CH_2CHO), 9.55, 9.62, 9.80, 9.24 (1 H

each, s, meso), 10.10, 10.13 (1 H each, t, CHO), -4.35 (2 H, br s, NH).

<u>Dimethyl-1,3-bis-(2-dihydroxyethyl)-2,4,5,8-tetramethylporphyrin-6,7-dipropionate (88)</u>

The foregoing porphyrin dialdehyde diester (87) (containing a small amount of monoester), without further purification, was stirred in a mixture of THF and MeOH (4:1) in an ice bath and treated with 10.5 g of NaBH₄ in cold methanol. The reaction was allowed to proceed for 10 min before 35 ml of acetic acid was carefully added to quench the excess borohydride. The solvent was evaporated under vacuum and the residue was treated with acidified methanol (5 ml H₂SO₄ in 200 ml MeOH). After 8 h, the acidic solution was diluted with 500 ml of CH₂Cl₂, washed with 500 ml of NaOAc solution (25%), then with water (3 x 500 ml). After dried by vacuum, the crude product was chromatographed on a neutral alumina column (Brockman Grade III) with CHCl₃ to separate a small amount of unreacted acetal porphyrin, and the porphyrin dialcohol 88 was eluted with 3% MeOH/CHCl₃ to give a yield of 2.28 g (73%). 1 H-NMR δ 3.25 (4 H, t, $CH_2CH_2CO_2$), 3.57 (12 H, s, ring Me), 3.65 (6 H, s, CO_2CH_3), 4.23 (4 H, t, <u>CH</u>₂CH₂CO₂), 4.37 (8 H, m <u>CH</u>₂CH₂OH), 9.98, 10.01, (2 H each, s, meso), -3.82 (2 H, br s, NH). UV-vis λ max (rel. int.) 399 nm (1.00), 499 (0.11), 533 (0.08), 566 (0.06), 620 (0.05).

<u>Dimethyl-1,3-bis-(2-chloroethyl)-2,4,5,8-tetramethylporphyrin-6,7-dipropionate (62)</u>

To a solution of above porphyrin dialcohol 88 (2.5 g, 4 mmol) in 500 ml of dry DMF was added 30 ml of benzoyl chloride. The mixture was heated at 98 °C for 1 h under nitrogen and then allowed to be cooled. Water (600 ml)

and triethylamine (40 ml) were added. The precipitated porphyrin 62 was collected by filtration and washed with water. The crude porphyrin was passed through a short silica gel column and then crystallized from CH_2Cl_2 -MeOH. Yield, 2.38 g (90%); MP 216-218 °C (lit. 216-217 °C); ¹H-NMR δ 3.24, 3.26 (2 H each t, $CH_2CH_2CO_2$), 3.46, 3.50, 3.53, 3.56 (3 H each, s, ring Me), 3.66, 3.67 (3 H each, s, CO_2CH_3), 4.19-4.38 (12 H, m CH_2CH_2C l and $CH_2CH_2CO_2$), 9.75, 9.82, 9.87, 9.96 (1 H each, s, meso); UV-vis λ max (rel. int.) 399 nm (1.00), 498 (0.11), 533 (0.08), 567 (0.06), 621 (0.05); MS (direct probe 70 eV), m/e 663 (M⁺).

Porphyrinone 93 and 94

Porphyrin 62, 6.63 g (10 mmol), in 400 ml on CH₂Cl₂ and 5 ml of pyridine was treated with 3 g (12 mmol) of osmium tetroxide under the same condition as described before. After working up, the mixture of the oxidation products was chromatographed on a silica gel column, eluted with 1% MeOH/CH₂Cl₂ to give 1.59 g (24%) of unreacted porphyrin 62. The faster moving northern diols were separated partially from the slower moving southern diols. Further purification on TLC plates with 8% EtOH/CH₂Cl₂ gave a combined yield of 1.25 g (18%) for the northern diols and 3.34 g (48%) for the southern diols.

The mixture of the two northern diols (1.79 mmol) was dissolved in 15 ml of concentrated sulfuric acid and stirred at room temperature for 30 min. Porphyrinone 93 and 94 were obtained, after working up and separation by chromatography, in a total yield of 91%, 559 mg for 93 and 547 mg for 94. To achieve a higher yield of 1,3-dione the mixture of these two porphyrinones can be used directly without separation for the next step.

Dimethyl-1,3-bis-(2-chloroethyl)-2,4,5,8-tetramethyl-1-porphyrinone-

6,7-dipropionate (93) 2.09 (3 H, s, Me sat.), 2.88, 3.28 (1 H each, m, $\underline{CH_2CH_2Cl}$ sat.), 3.20 (6 H, m, $\underline{CH_2CH_2Cl}$ sat. and $2\underline{CH_2CH_2CO_2}$), 3.45, 3.57, 3.62 (3 H each, s, ring Me), 3.63, 3.65 (3 H each, s, $\underline{CH_2CO_2CH_3}$), 4.21, 4.24, 4.36, 4.45 (2 H each, t, $\underline{CH_2CH_2Cl}$ and $2\underline{CH_2CH_2CO_2}$), 9.11, 9.84, 9.87, 9.95 (1 H each, s, meso α , δ , β , γ), -2.92, -2.98 (1 H each, br s, NH); NOE test: selective irradiation of 8-Me at 3.45 ppm caused an increase of 9.7% in intensity for δ -proton, and irradiation of 4- and 5-Me at 3.57 and 3.62 ppm gave β -meso proton an increase of 9.8% and 10.8%, respectively; UV-vis λ max (rel. int.) 407 nm (1.00), 508 (0.09), 547 (0.10), 588 (0.07), 645 (0.23).

Dimethyl-1,4-bis-(2-chloroethyl)-2,4,5,8-tetramethyl-3-porphyrinone-6,7-dipropionate (94) 1 H-NMR δ 2.09 (3 H, s, Me sat.), 2.86, 3.29 (1 H each, m $\frac{CH_{2}CH_{2}Cl}{Cl}$ sat.), 3.23, (6 H, m, $\frac{CH_{2}CH_{2}Cl}{Cl}$ sat. and $\frac{2CH_{2}CH_{2}CO_{2}}{Cl}$, 3.42, 3.51, 3.57 (3 H each, s, ring Me), 3.67 (6 H, s, $\frac{CH_{2}CH_{2}CO_{2}CH_{3}}{Cl}$, 4.21, 4.55 (4 H each, m, $\frac{CH_{2}CH_{2}Cl}{Cl}$, and $\frac{2CH_{2}CH_{2}CO_{2}}{Cl}$, 9.12, 9.77, 9.82, 9.87 (1 H each, s, meso β , α , δ , γ), -2.92, -3.01 (1 H each, br s, NH); UV-vis λ max (rel. int.) 407 nm (1.00), 508 (0.10), 547 (0.11), 587 (0.08), 643 (0.24).

1,3-Dione 82, 3,5-dione 95, 3,7-dione 96, 1,8-dione 97, 2,3-dione 98 and 1,7-dione 99

Zinc insertion to the forgoing porphyrinones 105 and 106 was accomplished as usual in CHCl₃-MeOH with Zn(OAc)₂. The mixture of these two complexes (744 mg, 1 mmol), was treated with osmium tetroxide (380 mg, 1.5 mmol) to effect dihydroxylation as described previously in a total yield of 404 mg (52%). 305 mg (41%) of the unreacted starting material was recovered. The rearrangement of diols were carried out in the concentrated sulfuric acid (15 ml), yielding mainly six porphyrinones, in addition to the regenerated porphyrinones (133 mg, 33%), with the 1,3-dione 82 as the major

product after separation.

Dimethyl-2,4-bis-(2-chloroethyl)-2,4,5,8-tetramethyl-1,3-porphyrindione-6,7-dipropionate (82) It was found the same as that obtained form 1,4-bis-(2-chloroethyl-porphyrin system. Yield, 79 mg (22%).

Dimethyl-1,4-bis-(2-chloroethyl)-2,4,6,8-tetramethyl-3,5-porphyrindione-6,7-dipropionate (95) Yield, 61 mg (17%); 1 H-NMR δ 1.74, 2.20 (1 H each, m, 1 CH₂CH₂CO₂ sat.), 1.94, 1.97 (3 H each, s, Me sat.), 2.98 (2 H, m, 1 CH₂CH₂CO₂ sat.), 3.03 to 3.35 (4 H, m 1 CH₂CH₂Cl sat.), 3.21 (2 H, m, 1 CH₂CH₂CO₂), 3.39 (3 H, s, 1 CH₂CH₂CO₂CH₃ sat), 3.37, 3.44 (3 H each, s, ring Me), 3.64 (3 H, s, 1 CH₂CH₂CO₂CH₃), 4.08, 4.18, 4.31 (2 H each, t, 1 CH₂CH₂Cl, and 1 CH₂CH₂CO₂), 8.64, 8.74, 9.40, 9.50 (1 H each, s, meso 1 CH₂CH₂Cl, and 1 CH₂CH₂CO₂), 1 CH₂CH₂CO₂DH₃ (1 H each, s, meso 1 CH₂CH₂CO₂DH₃DH₃CH₂CO₂DH₃DH₃CH₂CO₂DH₃DH₃CH₂CO₃DH₃DH₃CH₃CO₃DH₃DH₃CH₃CO₃DH₃DH₃CH₃CO₃DH₃DH₃CH₃CO₃DH₃DH₃CH₃CO₃DH₃DH₃CH₃CO₃DH₃DH₃CH₃CO₃DH₃DH₃CH₃CO₃DH₃CH₃CO₃DH₃DH₃CH₃CO₃DH₃CO₃DH₃CH₃CO₃DH₃CH₃CO₃DH₃CO₃DH₃CH₃

Dimethyl-1,4-bis-(2-chloroethyl)-2,4,5,8-tetramethyl-3,7-porphyrindione-6,7-dipropionate (96) Yield, 18 mg (5%); 1 H-NMR δ 1.54, 2.12 (1 H each, m, $CH_{2}CH_{2}CO_{2}$), 2.05 (6 H, s, Me sat.), 2.95, 3.30 (4H, m, $CH_{2}CH_{2}CI$ sat.), 3.28 (3 H, s, $CO_{2}CH_{3}$ sat.) 3.04 (2 H, t, $CH_{2}CH_{2}CO_{2}$ sat.), 3.26 (2 H, t, $CH_{2}CH_{2}CO_{2}$), 3.54, 3.56 (3 H each, s, ring Me), 3.76 (3 H, s, $CO_{2}CH_{3}$, 4.27, 4.31, 4.44 (2 H each, t, $CH_{2}CH_{2}CI$ and $CH_{2}CH_{2}CO_{2}$), 9.08, 9.09, 9.67, 9.77 (1 H each, s, meso δ , β , γ , α), -2.70, -2,75 (1 H each, br s, NH); UV-vis λ max (rel. int.) 402 nm (0.86), 411 (1.00), 483 (0.05), 511 (0.06), 553 (0.07), 623 (0.05), 652 (0.06), 686 (0.52).

Dimethyl-2,3-bis-(2-chloroethyl)-2,4,5,8-tetramethyl-1,8-porphyrindione (97) Yield, 14 mg (4%); 1 H-NMR δ 1.67, 2.18 (1 H each, m, $\underline{\text{CH}}_{2}\text{CH}_{2}\text{CO2}$ sat.), 2.00, 2.02 (3 H each, s, Me sat.), 3.00 (2 H, t, $\underline{\text{CH}}_{2}\underline{\text{CO}}_{2}$ sat.), 3.09-3.35 (4 H, m,

<u>CH₂CH₂Cl</u> sat.), 3.16 (2 H, t, CH₂CH₂CO₂), 3.35, (3 H, s, CO₂CH₃ sat.), 3.57, 3.61 (3, H each, s, ring Me), 3.63 (3 H, s, CO₂CH₃), 4.11, 4.21, 4.56 (2 H each, t, CH₂CH₂Cl and CH₂CH₂CO₂), 8.91, 8.89, 9.63, 9.84 (1 H each, s, meso γ , α , δ , β), -1.60 (2 H, br s, NH); UV-vis λ max (rel. int.) 416 nm (1.00), 436 (0.75), 541 (0.06), 591 (0.10), 623 (0.16), 690 (0.04).

Dimethyl-1,4-bis-(2-chloroethyl)-1,4,5,8-tetramethyl-2,3-porphyrindione-6,7-dipropionate (98) Yield, 11 mg (3%); 1 H-NMR δ 1.98 2.00 (3 H each, s, Me sat.), 2.90-3.35 (8 H, m, $_{CH_{2}CH_{2}Cl}$ Cl sat.), 3.21 (4 H, t, $_{CH_{2}CH_{2}CO_{2}}$), 3.46 (6 H, s, ring Me), 3.60 (6 H, s, $_{CO_{2}CH_{3}}$), 8.92 (2 H, s, meso β , δ), 9.66, 10.00 (1 H each, s, meso α , γ), -1.60 (2 H, br s, NH); UV-vis λ max (rel. int.) 416 nm (1.00), 435 (0.76), 591 (0.10), 625 (0.17), 686 (0.06).

Dimethyl-3,3-bis-(2-chloroethyl)-2,4,5,8-tetraethyl-1,7-porphyrindione-5,7-dipropionate (99) Yield, 7 mg (2%); 1 H-NMR δ 1.75, 2.11 (1 H each, m, $CH_{2}CH_{2}CO_{2}$), 1.97, 1.99 (3 H each, s, Me sat.), 2.93, (2 H, t, $CH_{2}CH_{2}CO_{2}$ sat.), 3.02-3.83 (4 H, m, $CH_{2}CH_{2}CI$), 3.11 (2 H, t, $CH_{2}CH_{2}CO_{2}$), 3.44 (3 H, s, $CO_{2}CH_{3}$ sat), 3.45, 3.71 (3 H each, s, ring Me), 3.71 (3 H, s, $CO_{2}CH_{3}$), 4.12, 4.21 (6 H, m, $CH_{2}CH_{2}CI$) and $CH_{2}CH_{2}CO_{2}$), 8.58, 8.79, 9.33, 9.58 (1 H each, s,meso α , δ , γ , β), -0.53 (2 H, br s, NH); UV-vis λ max (rel. int.) 418 nm (1.00), 439 (0.93), 544 (0.12), 592 (0.18), 636 (0.21).

D. Oxidation of porphyrinone and 1,3-porphyrindione side chains Dimethyl-2-hydroxymethyl-2,3,5,8-tetramethyl-2-vinylporphyrinone-6,7-dipropionate (100)

To a solution of 2,4-bis-(2-chloroethyl)-porphyrinone **79** (68 mg, 0.1 mmol) in 40 ml of pyridine, under argon, 0.8 g of KOH in 3 ml of water was

added and the solution was refluxed for 5 h. The mixture was then cooled and evaporated to dryness under vacuum. The residue was dissolved in 20 ml of methanol with 0.5 ml of sulfuric acid and allowed to stand at room temperature for 6 h. The crude product was worked up by washing the solution with aqueous sodium acetated and then water, dried over Na₂SO₄, evaporated under vacuum, chromatographed on a TLC plate to give 56 mg (90%) of 112. 1 H-NMR δ 2.10, (3 H, s, Me sat.), 2.90-3.20 (4 H, m, C H₂CH₂OH), 3.17, 3.18 (2 H each, t, C CH₂CO₂), 3.42, 3.51, 3.62 (3 H each, s, ring Me), 3.61, 3.64 (3 H each, s, C CO₂CH₃), 4.18, 4.29 (2 H each, t, C H₂CH₂CO₂), 6.30 (2 H, dd, C CH= C CH₂), 8.19 (1 H, dd, C H= C H₂), 9.19, 9.84, 9.90, 9.97 (1 H each, s, meso α , β , δ , γ), -2.92 (2 H, br s, NH); UV-vis λ max (rel. int.) 412 (1.00), 511 (0.11), 550 (0.09), 596 (0.07), 652 (0.24); MS (direct probe, 70 eV), m/e 625 (M⁺).

<u>Dimethyl-2-(hydrogencarbonylmethyl)-2,3,5,8-tetramethyl-4-vinyl-porphyrin-one-6,7-dipropionate (101)</u>

A solution of 10 ml of CH_2Cl_2 and 0.4 ml 0.44 mmol of oxalyl chloride was stirred in an dry-ice/acetone bath under nitrogen. 0.68 ml (8.8 mmol) of dimethyl sulfoxide in 2 ml of CH_2Cl_2 was added. The mixture was allowed to stir for 5 min before porphyrinone 112 (31 mg, 0.05 mmol) in 5 ml of CH_2Cl_2 was added. After stirring for another 15 min, 0.28 ml 20 mmol) of triethyl amine was added and the reaction mixture was gradually warmed up to room temperature. The solution was diluted with 20 ml of CH_2Cl_2 , washed with saturated NaCl solution (20 ml), aqueous HCl (5%, 2 x 20 ml), Na_2CO_3 (5%, 20 ml), water, and then brought to dryness. Separation on TLC plate, developed with 1% $MeOH/CH_2Cl_2$, gave 101 in a yield of 24 mg (78%). ^1H-NMR δ 2.00 (3 H, s, Me sat.), 3.19, 3.22 (2 H each, t, $CH_2CH_2CO_2$), 3.43, 3.58, 3.61 (3 H each, s, ring Me), 3.62, 3.64, (3 H each, s, CO_2CH_3), 3.98 (2 H, dd, J=17)

Hz, $\underline{CH_2CO_2}$), 4.22, 4.38 (2 H each, t, $\underline{CH_2CH_2CO_2}$), 6.32 (2 H, dd, $\underline{CH=CH_2}$), 8.22 (1 H, dd, $\underline{CH=CH_2}$), 9.09, 9.90, 9.95, 9.99 (1 H each, s, meso α, β, δ, γ), -2.95, -2.87 (1 H each, d, NH); UV-vis λ max (rel. int.) 412 (1.00), 512 (0.11), 548 (0.09), 594 (0.07), 651 (0.23); MS (direct probe, 70 eV), m/e 623 (M⁺).

<u>Trimethyl-2,3,5,8-tetramethyl-4-vinylporphyrinone-2-acetate-6,7-</u>dipropionate (<u>102</u>)

To a solution of porphyrinone aldehyde **101** (20 mg, 0.03 mmol) in 15 ml of THF with 1 ml of water, 15 mg (0.12 mmol) of argentic oxide was added and the mixture was stirred at room temperature for 30 h. The solid was then filtered and the green filtrate was bought to dryness under vacuum. The residue was dissolved in 20 ml of methanol with 0.5 ml of sulfuric acid and allowed to stand for 5 h before being diluted with 30 ml of CH₂Cl₂. The solution was washed with aqueous sodium acetate (25%, 2 × 20 ml), water (3 × 20 ml) and then evaporated to dryness. The crude product was purified on TLC plate (1%MeOH/CH₂Cl₂) to give 15 mg (76%) of **102**. ¹H-NMR δ 2.04 (3 H, s, Me sat.), 2.87 (3 H, s, CH₂CO₂CH₃), 3.23 (4 H, m, CH₂CH₂CO₂), 3.57, 3.63 (3 H each, s, ring Me), 3.65 (6 H, s, CH₂CO₂CH₃), 3.67 (2 H, dd, CH₂CO₂), 4.26, 4.40 (2 H each, t, CH₂CH₂CO₂), 6.33 (2 H, dd, CH₂=CH), 8.22 (1 H, CH₂=CH), 9.25, 9.91, 10.04, 10.08 (1 H each, s, meso α , β , δ , γ), -2.91 (2 H, br s, NH); UV-vis λ max (rel. int.) 413 nm (1.00), 514 (0.12), 548 (0.08), 594 (0.07), 652 (0.25); MS (direct probe 70 eV), 653 for (M⁺).

<u>Dimethyl-2,4-bis-(2-hydroxyethyl)-2,4,5,8-tetramethyl-1,3-porphyrin-dione-6,7-dipropionate</u> (103)

2,4-Bis-(2-chloroethyl)-1,3-porphyrindione 82 (69 mg, 0.1 mmol) was treated with KOH as described above led to 103 in a total yield of 44% as a

mixture of cis and trans isomers. The two compound were separated on TLC plates after a prolonged developing time to give the slower moving band assigned as cis-dione 103a (13 mg) and faster moving component as the-trans isomer 103b (16 mg).

(103a) ¹H-NMR 1.94, 1.98 (3 H each, s, Me sat.), 2.80-3.14, 3.55, (8 H, m, $\underline{\text{CH}_2\text{CH}_2\text{OH}}$), 3.10 (4 H, m, $\underline{\text{CH}_2\text{CH}_2\text{CO}_2}$), 3.29, 3.34 (3 H each, s, ring Me), 3.60, 3.62 (3 H each, $\underline{\text{CO}_2\text{CH}_3}$), 4.17, 4.18 (2 H each, t, $\underline{\text{CH}_2\text{CH}_2\text{CO}_2}$), 8.52, 8.72, 9.35, 9.62 (1 H each, s, meso, β , α , δ , γ); UV-vis λ max (rel. int.) 413 nm (1.00), 436 (0.73), 487 (0.10), 544 (0.13), 588 (0.16), 636 (0.17); MS (direct probe, 70 eV), 658 (M⁺).

(103b) ¹H-NMR 1.92, 1.95 (3 H each, s, Me sat.), 2.75-3.05, 3.54 (8 H, m, $\underline{\text{CH}_2\text{CH}_2\text{OH}}$), 3.08, 3.11 (3 H each, s, ring Me), 3.60, 3.62 (3 H each, s, $\underline{\text{CO}_2\text{CH}_3}$), 4.17, 4.18 (2 H each, t, $\underline{\text{CH}_2\text{CH}_2\text{CO}_2}$), 8.46, 8.66, 9.30, 9.55 (1 H each, s, meso, β , α , δ , γ); UV-vis λ max (rel. int.) 415 nm (1.00), 437 (0.87), 545 (0.19), 588 (0.26), 637 (0.26); MS (direct probe, 70 eV), 658 (M⁺).

E. Heme d_1 synthesis from porphyrin-2,4-diacetate

<u>Tetramethyl-1,3,5,8-tetramethylporphyrin-2,4-diacetate-6,7-dipropionate</u> (58)

Porphyrin 87 (3.12 g, 5 mmol) was dissolved in 400 ml of acetone with 5 ml of formic acid and stirred in an ice-NaCl bath. To this solution 38 ml of Jones reagent, which was made of 6.79 g of CrO₃, 6 ml of H₂SO₄ and 50 ml of water, was added slowly and the solution was allowed to stir for another 15 min. Large part of the solvent was evaporated under vacuum (the temperature of the bath was controlled below 40 °C) and the residue was redissolved in 300 ml of methanol followed by addition of 5 ml of concentrated sulfuric acid. After standing for 8 h at room temperature the

solution was further diluted with 400 ml of CH_2Cl_2 and washed first with aqueous NaOAc (25%, 2 × 200 ml), and then with water (3 × 300 ml). The solvent was removed under vacuum and the crude product was chromatographed on a silica gel column, eluted with 1% MeOH/CH₂Cl₂. crystallization from CH_2Cl_2 -MeOH gave porphyrin 58 in a yield of 3.13 g (92%); ¹H-NMR δ 3.26 (4 H, t, $CH_2CH_2CO_2$), 3.53, 3.56, 3.58, 3.60 (3 H each, s, ring Me), 3.64, 3.66 (3 H each, s, $CH_2CH_2CO_2CH_3$), 3.73, 3.75 (3 H each, s, $CH_2CO_2CH_3$), 4.34, 4.37 (2 H each, t, $CH_2CH_2CO_2$), 4.90, 4.96 (2 H each, s, CH_2CO_2), 9.94, 9.97, 9.99, 10.00 (1 H each, s, meso), -3.94 (2 H, br s, NH); UV-vis λ max (rel. int.) 400 nm (1.00), 498 (0.12), 532 (0.09), 567 (0.08), 621 (0.06); MS found m/e 683.7865 for (M+H)+, C38H42N4O8 requires 683.78934.

Dihydroxychlorin 105 and 106

Osmium tetroxide (2 g, 7.8 mmol) was added to a solution of porphyrin 58 (4.5 g, 6.6 mmol) in 20 ml of CH₂Cl₂ and 5 ml of pyridine. The reaction was allowed to proceed, under nitrogen, in the dark, at room temperature for 20 h. The solution was diluted with 100 ml of methanol and then bubbled with H₂S for 15 min. The precipitated osmium sulfide was filtered on celite and the filtrate was brought to dryness under vacuum. The residue was subjected chromatographic separation on a silica gel column. Most of the unreacted porphyrin was eluted first with 1% MeOH/CH₂Cl₂ and the faster moving north diols were separated from the south isomers to a large extent. The slower moving south diols was completely eluted with 5% MeOH/CH₂Cl₂. The northern diol containing fractions were further separated on preparative TLC plates (6% EtOAc/CH₂Cl₂) to give the northern diols 105 and 106, (945 mg, 20%), and the southern diols 107 and 108, (3.36 g

51%), combined with the fractions obtained from the column. In addition, 990 mg (22%) of porphyrin 58 was recovered. The mixture of the two northern diols could be separated on TLC plate after a prolonged developing time, with diol 105 as the faster moving band, but usually were applied without separation for the next reaction to avoid decomposition.

Tetramethyl-1,2-dihydroxy-1,3,5,8-tetramethylchlorin-2,4-diacetate-6,7-dipropionate (105) 1 H-NMR 1.96 (3 H, s, Me sat.), 3.12, 3.16 (2 H each, t, $CH_{2}CH_{2}CO_{2}$), 3.30 (3 H, s, $CH_{2}CO_{2}CH_{3}$ sat.),3.37, 3.39, 3.65 (3 H each, s, ring Me), 3.70, 3.72 (3 H each, s, $CH_{2}CO_{2}CH_{3}$), 3.94 (3 H, s, $CH_{2}CO_{2}CH_{3}$), 4.15 (6 H, m, $CH_{2}CO_{2}$ and two $CH_{2}CH_{2}CO_{2}$), 4.68, 4.78 (1 H each, d, $CH_{2}CO_{2}$), 9.03, 9.19, 9.61, 9.67 (1 H each, s, meso δ , α , γ , β), -2.79 (2 H, br s, NH); UV-vis λ max (ϵ M) 392 (191000), 495 (13500), 520 (2500), 589 (3900), 642 (44800); MS found m/e 717.8077 for (M+H)+, C38H44N4O10 requires 717.8032.

Tetramethyl-3,4-dihydroxy-1,3,5,8-tetramethylchlorin-2,4-diacetate-6,7-dipropionate (106) 1 H-NMR δ 1.95 (3 H, s, Me sat.), 3.03 (3 H, s, CO₂CH₃ sat.), 3.15 3.17 (2 H each, t, CH₂CH₂CO₂), 3.42 (3 H, s, CO₂CH₃ sat.), 3.48 (6 H, s, ring Me), 3.65 (3 H,s, ring Me), 3.67, 3.74 (3 H each, s, CH₂CH₂CO₂CH₃), 3.95 (3 H, s, CH₂CO₂CH₃), 4.19 (2H, s, CH₂CO₂), 4.18, 4,32 (2 H each, t, CH₂CH₂CO₂), 4.78, 4.89 (1 H each, d, CH₂CO₂), 9.02, 9.16, 9.66, 9.72 (1 H each, s, meso α, β, γ, δ), -2.73 (2 H, br s, NH); UV-vis λ max (εм) 392 nm (198000), 494 (13600), 590 (4100), 642 (45700); MS found m/e 717.8055 for (M+H)+, C38H44N4O10 requires 717.8032.

Porphyrinone 111, 112 and lactone 113, 114

The mixture of north diols 117 and 118 (1.43 g, 2 mmol) was dissolved in

an acid medium made of 10 ml of H_2SO_4 , 10 ml of FSO_3H and 1 ml of fuming H_2SO_4 , and the mixture was stirred, in the dark, at room temperature for 5 h. The acid solution was then frozen in a dry-ice/acetone bath and quenched carefully with 200 ml of methanol with shaking. The solution was warmed up slowly to room temperature and allowed to stand for 6 h before further diluted with 300 ml of CH_2Cl_2 . The organic solution was partitioned and washed with aqueous sodium acetate (25%, 3 × 200 ml), then washed with water (3 × 300 ml), dried over Na_2SO_4 , and brought to dryness. Separation on preparative TLC plates (6% $EtOAc/CH_2Cl_2$, or 1% $MeOH/CH_2Cl_2$) gave porphyrinone 111 as the fastest moving band followed by its regioisomer 112 and then lactones 113 and 114.

Tetramethyl-2,3,5,8-tetramethylporphyrinone-2,4-diacetate-6,7-dipropionate (111) Yield, 335 mg (24%); 1 H-NMR δ 1.95 (3 H, s, Me sat.), 2.96 (3 H, s, CH₂CO₂CH₃), 3.20, 3.23 (2 H each, t, CH₂CH₂CO₂), 3.46, 3.56, 3.57 (3 H each, s, ring Me), 3.63, 3.66 (3 H each, s, CH₂CH₂CO₂CH₃), 3.78 (3 H, s, CH₂CO₂CH₃), 3.90, 4.00 (1 H each, d, CH₂CO₂), 5.04 (2 H, s, CH₂CO₂), 9.13, 9.89, 9.92, 9.95 α , δ , β , γ), -2.87, -2.93 (1 H each, br s, NH); UV-vis λ max (ϵ M) 406 nm (169000), 507 (9500), 544 (12000), 588 (5900), 644 (32400); MS found m/e 699.7832 for (M+H)+, C38H43N4O9 requires 699.7878.

Tetramethyl-1,4,5,8-tetramethylporphyrinone-2,4-diacetate-6,7-dipropionate (112) Yield, 293 mg (21%); 1 H-NMR δ 1.95 (3 H, s, Me sat.), 2.97 (3 H, s, CH₂CO₂CH₃), 3.26 (4 H, m, CH₃CH₃CO₂), 3.46., 3.55, 3.60 (3 H each, s, ring Me), 3.66, 3.67 (3 H each, s, CH₂CH₂CO₂CH₃), 3.81 (3 H, s, CO₂CH₃), 3.88, 3.98 (1 H each, d, CH₂CO₂), 4.23, 4.38 (2 H each, t, CH₂CH₂CO₂), 4.99, 5.09 (1 H each, d, CH₂CO₂), 9.07, 9.85, 9.86, 9.94 (1 H each, s, meso β , γ , α , δ), -2.79, 2.91 (1 H each, s, NH); UV-vis λ max (ϵ M) 405 nm (17300), 506 (9600), 544 (11800),

586 (5900), 642 (34800); MS found m/e 699.7845 for (M+H)+, C38H43N4O9 requires 699.7878.

Trimethyl-2-hydroxy-1,2-(γ -lactone)-1,3,5,8-tetramethylchlorin-4-acetate-6,7-dipropionate (113) Yield, 82 mg (6%); 1 H-NMR δ 2.36 (3 H, s, Me sat.), 2.91, 2.96 (2 H each, t, CH₂CH₂CO₂), 3.13, 3.34, 3.35 (3 H each, s, ring Me), 3.49, 3,59 (1 H each, d, CH₂CO₂), 3.56, 3.61 (3 H each, s, CH₂CH₂CO₂CH₃), 3.71 (3 H, s, CH₂CO₂CH₃), 3.92, 3.93 (2 H each, t, CH₂CH₂CO₂), 4.73 (2 H, s, CH₂CO₂), 9.09, 9.12, 9.23, 9.56 (1 H each, s, meso δ , α , γ , β), -3.22 (2 H, br s, NH); UV-vis λ max (rel. int.) 391 nm (1.00), 494 (0.11), 540 (0.04), 587 (0.05), 641 (0.26); MS found 685.7654 for (M+H)+, C37H41N4O9 requires 685.7607.

Trimethyl-4-hydroxy-3,4-(γ -lactone)-1,3,5,8-tetramethylchlorin-2-acetate-6,7-dipropionate (114) Yield, 68 mg (5%); 1 H-NMR δ 2.36 (3 H, s, Me sat.), 3.03 (4 H, t, CH₂CH₂CO₂), 3.28, 3.40, 3.56 (3 H each, s, ring Me), 3.53, 3.70 (1 H each, d, CH₂CO₂), 3.59, 3.63 (3 H each, s, CH₂CH₂CO₂CH₃), 3.81 (3 H, s, CH₂CO₂CH₃), 4.91, 5.01 (1 H each, d, CH₂CO₂), 9.14, 9.17, 9.51, 9.77 (1 H each, s, meso α , β , γ , δ), -2.92 (2 H, br s, NH); MS found m/e 685.7683 for (M+H)⁺, C37H41N4O9 requires 685.7607.

1,3-Dione 59, porphyrinone lactone 118, hydroxymethyl porphyrinone 119,porphyrinone α-hydroxyacetate 120, 1,7-dione 121, 1,8-dione 122, 1,5-dione 123, 1,6-dione 124 and porphyrinone acrylate 125.

Porphyrinone 111 (1.75 g, 2.5 mmol) was dissolved in 150 ml of CHCl₃ and 20 ml of MeOH and the solution was brought to reflux for 5 min before 1.0 g of Zn(OAc)₂ and 0.1 g of NaOAc in 10 ml of MeOH were added. After about 30 min refluxing, (the reaction was monitored by TLC test since the Rf

value of the green-colored Zn(II) complex is smaller than that of the brown-colored starting compound), the mixture was cooled, washed with water (3 \times 100 ml), dried under vacuum, and crystallized from CH₂CH₂-MeOH in a virtually quantitative yield.

To the solution of the above zinc complex in 100 ml of CH_2Cl_2 plus 5 ml of pyridine, 960 mg (3.75 mmol) of OsO_4 was added, and the reaction was allowed, as usual, to proceed in the dark, under argon for 30 h at room temperature. The reaction mixture was quenched with 50 ml of MeOH, bubbled with H_2S , and then filtered on celite. The filtrate was dried under vacuum and chromatographed quickly on a silica gel column protecting form light. Argon was used to pack the column and flush the diols out after the front moving unreacted zinc porphyrinone (916 mg, 46%) had been eluted. To the slower moving fractions, dilute HCl solution (10%, 200 ml) was added and the solution was shaken for a few minutes (to remove the zinc) and then washed with water. The porphyrinone diols were separated to a large extent by using a chromatotron (0~5 % MeOH/ CH_2Cl_2 gradient) under argon to give about 18% of the violet diol 115, and the green colored diol 116 and 117 in a total yield of 27%.

The foregoing diol 115 (354 mg, 0.45 mmol) was treated with 10 ml of sulfuric acid containing 1 ml of fluorosulfonic acid. the mixture was stirred in the dark for 2 h before being chilled in a dry-ice/acetone bath. To this solution was added carefully 100 ml of cold methanol and the solution was let to stand at room temperature for 6 h. Further diluted with 200 ml of CH_2Cl_2 , the solution was partitioned and washed with aqueous sodium acetate (25%, 2 x 200 ml) and then washed with water (3 x 200 ml). The solvent was removed by vacuum and the residue was chromatographed on TLC plates (1% MeOH/ CH_2Cl_2) to give 1,3-dione 59, in a total yield of 38 mg

(12%), consisting of the cis and trans isomers, along with regenerated porphyrinone 123 (62 mg, 20%), γ -lactone 118 (24 mg, 8%), α -hydroxyacetate 119 (45 mg, 15%) and α -hydroxymethyl derivative 120 (13 mg, 4%). The cis and trans isomers of 1,3-dione 59 were further separated on TLC plate, developed by 5% EtOAc/CH₂Cl₂ or 1% MeOH/CH₂Cl₂ for a prolonged time, in the dark, until the two green bands were separated. The faster moving band was attributed to the trans isomer 59b (18 mg), while the slower one, cis 59a (16 mg).

When the mixture of Zn(II) diol 115, 116, and 117 were treated with H_2SO_4 -FSO₃H (9:1) directly without demetallation and prior separation, more than nine compounds were isolated from the reaction mixture. Among them, four known compounds: 1,3-done 59 (6%), γ -lactone 118 (4%), porphyrinone hydroxyacetate 119 (7%), hydroxymethyl porphyrinone 120 (2%) were obtained approximately in the same ratio as that in the previous reaction, five other compounds: 1,7-dione 133 (17%), 1,8-dione 134 (6%), 1,5-dione 123 (4%), 1,6-dione 124 (9%) and porphyrinone 7-acrylate 125 (3%) were identified as the major products.

Tetraethyl-3,4-dihydroxy-2,3,5,8-tetramethylporphyrinone-2,4-diacetate -6,7-dipropionate (115) 1 H-NMR δ 1.64, 1.69 (3 H each, s, Me sat.), 2.92, 3.00 (3 H each, s, CH₂CO₂CH₃), 2.95 (4 H, m, CH₂CH₂CO₂), 2.90, 3.23 (3 H each, s, ring Me), 3.43, 3.54 (1 H each, d, CH₂CO₂), 3.53 (2 H, s, CH₂CO₂), 3.59, 3.60 (3 H each, s, CH₂CH₂CO₂CH₃), 7.46, 7.79, 8.70, 8.83 (1 H each, s, meso α, β, δ, γ). UV-vis λ max (ϵ M) 400 nm (75200), 415 (88500), 436 (91300), 540 (9700), 584 (14500), 592 (14200), 638 (15500); MS found m/e 733.7894 for (M+H)+, C38H45N4O11 requires 733,8025.

dipropionate (**59a**) ¹H-NMR δ 1.83, 1.85 (3 H each, s, Me sat.), 3.10 (4 H, m, $CH_2CH_2CO_2$), 3.07, 3.13 (3 H each, s, $CH_2CO_2CH_3$), 3.26, 3.28 (3 H each, s, ring Me), 3.57, 3.61 (3 H each, s, $CH_2CO_2CH_3$), 3.75, 3.76 (1 H each, s, CH_2CO_2), 3.75, 3.87 (1 H each, d, CH_2CO_2), 4.15 (4 H, t, $CH_2CH_2CO_2$), 8.46, 8.87, 9.38, 9.56 (1 H each, s, meso β , α , δ , γ), -0.21 (2 H, br s, NH); UV-vis λ max (**EM**) 417 nm (99500), 437 (98000), 542 (9700), 591 (15600), 637 (17000), MS found m/e 715.7832 for (M+H)+, C38H43N4O10 requires 715.7872.

Trans-tetramethyl-2,4,5,8-tetramethyl-1,3-porphyrindione-2,4-diacetate-6,7-dipropionate (59b) 1 H-NMR δ 1.80, 1.81 (3 H each, s, Me sat.), 3.07, 3.11 (2 H each, t, $CH_{2}CH_{2}CO_{2}$), 3.17, 3.19 (3 H each, s, $CH_{2}CO_{2}CH_{3}$), 3.24, 3.28 (3 H each, s, ring Me), 3.58, 3.61 (3 H each, s, $CH_{2}CH_{2}CO_{2}CH_{3}$), 3.77, 3.78 (1 H each, s, $CH_{2}CO_{2}$), 3.79, 3.90 (1 H each, d, $CH_{2}CO_{2}$), 4.11, 4.12 (2 H each, t, $CH_{2}CH_{2}CO_{2}$), 8.40, 8.61, 9.34, 9.50 (1 H each, s, meso β , α , δ , γ), 0.15 (2 H, br s, NH); UV-vis λ max (ϵ M) 416 (98000), 437 (92000), 544 (9700), 589 (15700), 638 (16900); MS found m/e 715.7826 for (M+H)+, C38H43N4O10 requires 715.7872.

Trimethyl-4-hydroxy-3,4-(γ -lactone)-2,3,5,8-tetramethylporphyrinone -2-acetate-6,7-dipropionate (118) 1 H-NMR δ 1.75, 2.14 (3 H each, s, Me sat.), 2.86, 2.89 (2 H each, t, CH₂CH₂CO₂), 3.01, 3.07 (3 H each, s, ring Me), 3.17 (3 H, s, CH₂CO₂CH₃), 3.42, 3.52 (1 H each, d, CH₂CO₂), 3.53, 3.54 (3 H each, s, CH₂CH₂CO₂CH₃), 3.70 (2 H, s, CH₂CO₂), 3.72 (4 H, m, CH₂CH₂CO₂), 7.86, 8.39, 9.00, 9.05 (1 H each, s, meso α , β , δ , γ), 0.85 (2 H, br s, NH); UV-vis λ max (rel. int.) 379 (0.78), 391 (0.86), 411 (1.00), 503 (0.09), 543 (0.11), 587 (0.13), 634 (0.21); MS found m/e 667.7489 for (M+H)+, C37H40N4O10 requires 667.7453.

Tetramethyl-2,3,5,8-tetramethylporphyrinone-2-acetate-4-(α -hydroxy)-acetate-6,7-dipropionate (119) ¹H-NMR δ 1.97, (3 H, s, Me sat.), 2.97 (3 H, s,

CH₂CO₂CH₃), 3.17, 3.22 (2 H each, t, CH₂CH₂CO₂), 3.41, 3.57, 3.64 (3 H each, s, ring Me), 3.63 (6 H, s, CH₂CH₂CO₂CH₃), 3.75 (3 H, s, CH₂CO₂CH₃), 3.92, 4.01 (1 H each, d, CH₂CO₂), 4.18, 4.35 (2 H each, t, CH₂CH₂CO₂), 6.78 (1 H, s, CHOH), 9.18, 9.93, 9.94, 10.06 (1 H each, s, meso α , δ , γ , β), -2.99 (2 H, br s, NH); UV-vis λ max (EM) 406 (185000), 506 (13000), 543 (12400), 591 (6000), 647 (35600); MS found m/e 715.7898 for (M+H)+, C38H43N4O10 requires 715.7872.

Tetramethyl-3-hydroxymethyl-1,5,8-trimethylporphyrinone-2,4-diacetate -6,7-dipropionate (120) 1 H-NMR δ 1.93 (3 H, s, Me sat.), 2.95 (3 H, s, CH₂CO₂CH₃ sat.), 3.22, 3.24 (2 H each, CH₂CH₂CO₂), 3.57, 3.61 (3 H each, s, ring Me), 3.65, 3.74 (3 H each, s, CH₂CH₂CO₂CH₃), 3.76 (3 H, s, CH₂CO₂CH₃), 3.90, 4.00 (1 H each, d, CH₂CO₂), 4.33, 4.39 (2 H each, t, CH₂CH₂CO₂), 5.04 (2 H, s, CH₂CO₂), 5.75 (2 H, s, CH₂OH), 9.10, 9.90, 10.02, 10.09 (1 H each, s, meso α, β, δ, γ), -2.87, -2.95 (1 H each, br s, NH); UV-vis λ max (rel. int.) 4.05 nm (1.00), 505 (0.11), 541 (0.10), 590 (0.08), 646 (0.26); MS found m/e 715.7837 for (M+H)+, C38H43N4O10 requires 715.7872.

Tetramethyl-2,3,5,8-tetramethyl-1,7-porphyrindione-2,4-diacetate-6,7-dipropionate (121) 1 H-NMR δ 1.60, 2.20 (1 H each, m, $_{CH_{2}CH_{2}CO_{2}}$), 1.81, 1.83 (3 H each, s, Me sat.), 2.87, 3.07 (2 H each, t, $_{CH_{2}CH_{2}CO_{2}}$), 315 (3 H, s, $_{CH_{2}CO_{2}CH_{3}}$ sat.), 3.26, 3.37 (3 H each, s, ring $_{CH_{3}}$), 3.41 (3 H, s, $_{CH_{2}CH_{2}CO_{2}CH_{3}}$ sat.), 3.70 (3 H, s, $_{CH_{2}CH_{2}CO_{2}CH_{3}}$), 3.75 (3 H, s, $_{CH_{2}CO_{2}CH_{3}}$), 3.79 (2 H, s, $_{CH_{2}CO_{2}}$), 4.07 (2 H, t, $_{CH_{2}CH_{2}CO_{2}}$), 4.76 (2 H, s, $_{CH_{2}CO_{2}}$), 8.42, 8.68, 9.23, 9.48 (1 H each, s, meso $_{C}$, $_{C}$

Tetramethyl-2,3,5,7-tetramethyl-1,8-porphyrindione-2,4-diacetate-6,7-dipropionate (122) 1 H-NMR δ 1.70, 2.40 (1 H each, m, $_{CH_{2}}$ CH₂CO₂ sat.), 1.88, 1.97 (3 H each, s, Me sat.), 2.96 (2 H, t, $_{CH_{2}}$ CH₂CO₂ sat.), 3.10 (3 H, s, $_{CH_{2}}$ CO₂CH₃ sat.), 3.30 (2 H, t, $_{CH_{2}}$ CH₂CO₂), 3.34 (3 H, s, $_{CH_{2}}$ CH₂CO₂CH₃ sat.), 3.44, 3.54 (3 H each, s, ring Me), 3.62 (3 H, s, $_{CH_{2}}$ CH₂CO₂CH₃), 3.77 (3 H, s, $_{CH_{2}}$ CO₂CH₃), 3.81, 3.83 (1 H each, d, $_{CH_{2}}$ CO₂), 4.18 (2 H, t, $_{CH_{2}}$ CH₂CO₂), 4.96 (2 H, s, $_{CH_{2}}$ CO₂), 8.86, 9.91, 9.64, 9.81 (1 H each, s, meso $_{Y}$, $_{Q}$, $_{Q}$, $_{Q}$, $_{Q}$); UV-vis $_{Q}$ Max (rel. int.) 413 nm (1.00), 435 (0.80), 545 (0.05), 590 (0.09), 619 90.16), 685 (0.04); MS found m/e 715.7816 for (M+H)+, C38H43N4O10 requires 715.7872.

Tetramethyl-2,3,6,8-tetramethyl-1,5-porphyrindione-2,4-diacetate-6,7-dipropionate (123) 1 H-NMR δ 1.59, 2.10 (1 H each, m, $_{CH_2CH_2CO_2}$), 1.89, 2.02 (3 H each, Me sat.), 3.01 (2 H, t, $_{CH_2CH_2CO_2}$ sat.), 3.05 (3 H, s, $_{CH_2CO_2CH_3}$ sat.), 3.14 (2 H, t, $_{CH_2CH_2CO_2}$), 3.28 (3 H s, $_{CH_2CH_2CO_2CH_3}$ sat.), 3.49, 3.52 (3 H each, s, ring Me), 3.62 (3 H, s, $_{CH_2CH_2CO_2CH_3}$ sat.), 3.81 (3 H, s, $_{CH_2CO_2CH_3}$), 3.87, 3.96 (1 H each, d, $_{CH_2CO_2}$), 4.25 (2 H, t, $_{CH_2CH_2CO_2}$), 4.97 (2 H, s, $_{CH_2CO_2}$), 9.04, 9.11, 9.66, 9.77 (1 H each, s, meso $_{Y}$, $_{α}$, $_{δ}$, $_{β}$), -2.71 (2 H, br s, NH); UV-vis $_{λ}$ max (rel. int.) 409 nm (1.00), 482 (0.04), 509 (0.06), 551 (0.06), 622 (0.04), 651 (0.05), 685 (0.50); MS found m/e 715.7865 for (M+H)+, C38H43N4O10 requires 715.7872.

Tetramethyl-2,3,5,8-tetramethyl-1,6-porphyrindione-2,4-diacetate-5,7-dipropionate (124) 1 H-NMR δ 1.57, 2.21 (1 H each, m, $_{CH_{2}CH_{2}CO_{2}}$ sat), 1.97, 1.98 (3 H each, s, Me sat.), 2.97 (2 H, t, $_{CH_{2}CH_{2}CO_{2}}$) sat.), 3.05 (3 H, s, $_{CH_{2}CO_{2}CH_{3}}$), 3.16 (2 H, t, $_{CH_{2}CH_{2}CO_{2}}$), 3.32 (3 H, s, $_{CH_{2}CH_{2}CO_{2}CH_{3}}$), 3.47 (6 H, s, ring Me), 3.72 (3 H, s, $_{CH_{2}CH_{2}CO_{2}CH_{3}}$), 3.77 (3 H, s, $_{CH_{2}CO_{2}CH_{3}}$), 3.85, 3.87 (1 H each, d, $_{CH_{2}CO_{2}}$ sat.), 4.23 (2 H, t, $_{CH_{2}CH_{2}CO_{2}}$), 4.87 (2 H, s, $_{CH_{2}CO_{2}}$), 8.87, 8.93, 9.60, 9.74 (1 H each, s, meso $_{CH_{2}CH_{2}CO_{2}}$), -2.14, -2.21 (1 H each, br s,

NH); UV-vis λmax (rel. int.) 399 nm (0.40), 420 (1.00), 483 (0.04), 549 (0.06), 616 (0.05), 645 (0.04), 677 (0.27); MS found m/e 715.7832 for (M+H)⁺, C38H43N4O10 requires 715.7872.

Tetramethyl-2,3,5,8-tetramethylporphyrinone-2,4-diacetate-7-acrylate-6-propionate (125) 1 H-NMR δ 1.95 (3 H, s, Me sat.), 2.99 (3 H, s, CH₂CO₂CH₃), 3.15 (2 H, t, CH₂CH₂CO₂), 3.40, 3.54 (3 H each, s, ring Me), 3.67 (6 H, s, ring Me and CH₂CH₂CO₂CH₃), 3.78 (3 H, s, CH₂CO₂CH₃), 3.89, 3.97 (1 H each, d, CH₂CO₂), 4.05 (3 H, s, CH=CHCH₃), 4.16 (2 H, t, CH₂CO₂CH₃), 4.98 (2 H, s, CH₂CO₂), 7.12, 9.23 (1 H each, d, CH=CHCO₂), 9.08, 9.90, 9.94, 9.95 (1 H each, s, meso α , β , δ , γ), -2.50 (2 H, br s, NH); UV-vis λ max (rel. int.) 409 nm (1.00), 509 (0.08), 546 (0.09), 599 (0.05), 658 (0.24); MS found 697.7743 for (M+H)+, C38H41N4O9 requires 697.7719.

<u>Cis-d₁ 128a, trans-d₁ 128b, cis-iso-d₁ 129a, trans-iso-d₁ 129b</u>

Osmium tetroxide (14 mg, 0.056 mmol) was added to a solution of cis-1,3-dione 59a (20 mg, 0.028 mmol) in 10 ml of dry CH₂Cl₂ and 0.2 ml of pyridine. The mixture was stirred, in the dark, under argon, at room temperature for 20 h before being diluted with 10 ml of MeOH and quenched by H₂S gas. The precipitated black osmium sulfide was removed by filtration on celite. The solvent was evaporated and the residue was chromatographed on a small silica gel column (2 x 10 cm). The column was first eluted with 1% MeOH/CH₂Cl₂ to collect the fast moving green band, the starting dione 59a (8 mg, 40%), then with 2% MeOH/CH₂Cl₂ to obtain the slower moving grey-colored diols. The diol containing fractions were brought to dryness under vacuum and the residue was redissolved in 10 ml of benzene. To the refluxing benzene solution, 5 drops of concentrated hydrochloric acid was

added, and the grey-colored solution turned gradually into bright green indicating the dehydration had occurred. The reaction was monitored by TLC until the grey-colored diols had become undetectable (about 30 min). The solvent was evaporated under vacuum and the residue was chromatographed on a preparative silica gel TLC plate, developed with 1% MeOH/CH₂Cl₂. Two bands were observed on plate: the faster moving bright green band as the major product turned out to be cis- d_1 128a (8 mg, 67%), whereas the slower moving pigment with a deeper green color was identified as cis-iso- d_1 129a (3 mg, 25%).

The trans-1,3-dione 59b (18 mg) was treated OsO₄ and worked up exactly as described above, giving 6 mg of trans- \underline{d}_1 128b, 2 mg of trans-iso- \underline{d}_1 129b, and 9 mg of the starting material recovered.

Cis- \underline{d}_1 (Tetramethyl-2,4,5,8-tetramethyl-1,3-porphyrindione-cis-2,4-diacetate-6-acrylate-7-propionate) (128a=4) 1 H-NMR δ 1.77, 1.79 (3 H each, s, Me sat.), 3.03 (2 H, t, CH₂CH₂CO₂), 3.13, 3.17 (3 H each, s, CH₂CO₂CH₃), 3.22, 3.30 (3 H each, s, ring Me), 3.61 (3 H, s, CH₂CH₂CO₂CH₃), 3.73 (3 H, s, CH₂CO₂CH₃), 3.70, 3.78 (1 H each, d, J=17 Hz, CH₂CO₂), 3.75 (2 H, s, CH₂CO₂), 4.00 (3 H, s, CH=CHCO₂CH₃), 4.04 (2 H, t, CH₂CH₂CO₂), 6.90, 8.96 (1 H each, d, J=16 Hz, CH=CHCO₂), 8.26, 8.42, 9.21, 9.42 (1 H each, s, meso β , α , δ , γ), UV-vis λ max (rel. int.) 422 nm (1.00), 446 (0.72), 610 (0.29), 660 (0.17); MS found m/e 713.7745 for (M+H)+, C38H41N4O10 requires 713.7713.

Trans- \underline{d}_1 (Tetramethyl-2,4,5,8-tetramethyl-1,3-porphyrindione-trans-2,4-diacetate-6-acrylate-7-propionate) (128b) 1 H-NMR δ 1.74, 1.78 (3 H each, s, Me sat.), 3.04 (2 H, t, CH₃CH₂CO₂), 3.21, 3.22 (3 H each, s, CH₂CO₂CH₃), 3.22, 3.29 (3 H each, s, ring Me), 3.62 (3 H, s, CH₂CO₂CH₃), 3.71, 3.79 (1 H each, d, J=17, CH₂CO₂), 3.77 (2 H, s, CH₂CO₂), 3.99 (3 H, s, CH=CHCO₂CH₃), 4.04, (2 H, t,

CH₂CH₂CO₂), 6.88, 8.93 (1 H each, d, J=16 Hz, <u>CH</u>=<u>CH</u>CO₂CH₃), 8.20, 8.36, 9.18, 9.38 (1 H each, s, meso β , α , δ , γ); UV-vis λ max (rel. int.) 423 nm (1.00), 445 (0.70), 611 (0.32), 660 (0.71); MS found m/e 713.7756 for (M+H)+, C38H41N4O10 requires 713.7713.

Cis-iso- \underline{d}_1 (Tetramethyl-2,4,5,8-tetramethyl-1,3-porphyrindione-cis-2,4-diacetate-7-acrylate-6-propionate) (**129a**) ¹H-NMR δ 1.77, 1.78 (3 H each, s, Me sat.), 3.05 (2 H, t, CH₂CH₂CO₂), 3.13, 3.15 (3 H each, s, CH₂CO₂CH₃), 3.17, 3.38 (3 H each, s, ring Me), 3.64 (3 H, s, CH₂CH₂CO₂CH₃), 3.71 (2 H, s, CH₂CO₂), 3.72, 3.80 (1 H each, d, J=17 Hz, CH₂CO₂), 3.99 (3 H, s, CH=CHCO₂CH₃), 4.02 (2 H, t, CH₂CH₂CO₂), 6.93, 9.02 (1 H each, d, J=16Hz, CH=CHCO₂), 8.21, 8.38, 9.26, 9.40 (1 H each, s, meso β , α , δ , γ); UV-vis λ max (rel. int.) 419 nm (1.00), 443 (0.75), 537 (0.12), 573 (0.14), 603 (0.15), 651 (0.19); MS found m/e 713.7729 for (M+H)⁺, C38H41N4O10 requires 713.7713.

Trans-iso- \underline{d}_1 (Tetramethyl-2,4,5,8-tetramethyl-1,3-porphyrindione-trans-2,4-diacetate-7-acrylate-6-propionate) (129b) ¹H-NMR δ 1.74, 1.75 (3 H each, s, Me sat.), 3.05 (2 H, t, CH₂CH₂CO₂), 3.13, 3.21 (3 H each, s, CH₂CO₂CH₃), 3.22, 3.36 (3 H each, s, ring Me), 3.64 (3 H, s, CH₂CH₂CO₂CH₃), 3.73 (2 H, s, CH₂CO₂), 3.73, 3.80 (1 H each, s, meso β , α , δ , γ); UV-vis λ max (rel. int.) 420 nm (1.00), 443 (0.70), 538 (0.09), 573 (0.15), 604 (0.17), 652 (0.19); MS found m/e 713.7784 for (M+H)+, C38H41N4O10 requires 713.7713.

F. Coproporphyrin IV system

(The work-up procedures were similar to the 1,3-dione 59, 82 and \underline{d}_1 synthesis except those otherwise described.)

4,4'-Bis-(2-methoxycarbonylethyl)-3,3',5,5'-tetramethyl-2,2'-dipyrryl-

methenium bromide (132)

t-Butyl-3-(2-methoxycarbonylethyl)-2,4-dimethylpyrrole-5-carboxylate (131) (28.1 g, 0.1 mol) was treated with 14 ml of hydrobromide acid in 50 ml of formic acid to effect the self-condensation and worked up in the same way as described in the preparation of dipyrrylmethenium 76. Compound 132 was obtained in a yield of 18.1 g (80%). MP, 209-211 °C; MS (direct probe, 70 eV), 373 for (M⁺).

Coproporphyrin IV tetramethyl ester

The above dipyrrylmethenium bromide **132** (5.0 g, 11 mmol) was condensed with dipyrrylmethenium bromide **66** (5.8 g, 10 mmol) in 50 ml of formic acid containing 5.2 ml of bromine under refluxing. Following the same procedure as described in the synthesis of porphyrin **60** and **61** led to the formation of coproporphyrin IV in a yield of 3.3 g (46.5%). MP, 173-174 °C (lit. 174°C). ¹H-nmr δ 3.22, 3.29 (4 H each, t, CH₂CH₂CO₂), 3.52, 3.61 (6 H each, s, ring Me), 3.68 (12 H, s, CO₂CH₃), 4.31, 4.40 (4 H each, t, CH₂CH₂CO₂), 9.89 (1 H, s, meso α), 9.94 (2 H, s, meso β and δ), 10.01 (1 H, s, meso γ), -3.98 (2 H, s, br. NH); UV-vis λ max (rel. int.) 399 nm (1.00), 498 (0.10), 531 (0.07), 567 (0.06), 620 (0.05); MS (direct probe, 70eV) 710 m/e for (M⁺).

Coproporphyrinone tetramethyl ester (135)

The reaction of coproporphyrin IV tetramethyl ester (3.5 g, 5 mmol) with osmium tetroxide (1.52 g, 6 mmol) gave the north diol 133, which was identified as the faster moving band on TLC plate, in a yield of 1.45 g (39%) and the south diol 0.97 g (26%). Pinacolic rearrangement of 133 was carried out in sulfuric acid for 2 h, forming the porphyrinone 135 as the major product (1.06g, 75%). 1 H-NMR δ 1.50, 2.08 (1 H each, m, CH₂CH₂CO₂), 2.09 (3

H, s, Me sat.), 3.06 (2 H, t, $CH_2CH_2CO_2$ sat.), 3.23 (6 H, t, $CH_2CH_2CO_2$), 3.27 (3 H, s, CO_2CH_3 sat.), 3.47, 3.56, 3.58 (3 H each, s, ring Me), 3.64, 3.67, 3.69 (3 H each, s, CO_2CH_3), 4.23, 4.37, 4.38 (2 H each, t, $CH_2CH_2CO_2$), 9.14, 9.84, 9.85, 9.60 (1 H each, s, meso α, δ, β, γ), -2.91, -3.02 (1 H each, br s, NH); NOE, a selective irradiation of the ring-B Me (3.47 ppm) caused the adjacent α-proton at 9.14 ppm to increase in intensity (6%); UV-vis λ max (rel. int.) 405 nm (1.00), 507 (0.08), 546 (0.08), 586 (0.05), 613 (0.03), 642 (0.21); MS found 727.8445 for (M+H)+, C40H47N4O9 requires 727.8419.

1,3-Coproporphyrin(IV)-dione dimethyl ester (139)

Zinc insertion of porphyrinone 135 was carried out with Zn(OAc)₂ in CHCl₃-MeOH as described before. Osmium tetroxide oxidation of 1 mmol (791 mg) of Zn(II) porphyrinone and subsequent rearrangement in sulfuric acid-fluorosulfonic acid (9:1) resulted in the formation of 1,3-dione 139 (cis and trans isomers) as the major product (237 mg, 32% from porphyrinone 135), together with small amounts of 1,7-dione 140 (29 mg 4%), 1,4-dione 142 (22 mg, 3%), 1,8-dione 141 (25 mg, 3%), 7-acrylate derivative 143 (35 mg, 5%) and other by-products.

1,3-Coproporphyrin(IV)-dione tetramethyl ester (139) ¹H-NMR δ 1.74, 2.13 (2 H each, m, $\underline{CH_2CH_2CO_2}$ sat.), 1.93, 1.95 (3 H each, s, Me sat.), 2.91, (4 H, m, $\underline{CH_2CH_2CO_2}$ sat.), 3.10, 3.12 (2 H each, t, $\underline{CH_2CH_2CO_2}$), 3.33, 3.46 (3 H each, s, ring Me), 3.40, 3.43 (3 H each, s, $\underline{CH_2CH_2CO_2CH_3}$ sat.), 3.62, 3.71 (3 H each, s, $\underline{CH_2CH_2CO_2CH_3}$), 4.12, 4.19 (2 H each, t, $\underline{CH_2CH_2CO_2}$), 8.58, 8.77, 8.33, 9.59 (1 H each, s, meso β , α , δ , γ ,), -0.72 (2 H, br s, NH); NOE, irradiating the δ -proton at 8.39 ppm caused the Me singlet (3.46 ppm) to increase in intensity. UV-vis λ max (rel. int.) 403 nm (0.73), 419 (0.96), 439 (1.00), 543 (0.10), 593 (0.16), 636

(0.20); MS found m/e 743.8452 for $(M+H)^+$, C40H47N4O10 requires 743.8413.

1,7-Coproporphyrin(IV)-dione tetramethyl ester (140) ¹H-NMR δ 1.70, 2.14 (2 H each, m, CH₂CH₂CO₂ sat.), 1.93, 1.94 (3 H each, s, Me sat.), 2.91 (4 H, m, CH₂CH₂CO₂ sat.), 3.13, 3.15 (2 H each, t, CH₂CH₂CO₂), 3.31, 3.35 (3 H each, s, ring Me), 3.41, 3.42 (3 H each, s, CH₂CH₂CO₂CH₃ sat.), 3.59, 3.62 (3 H each, s, CH₂CH₂CO₂CH₃), 4.14, 4,18 (2 H each, t, CH₂CH₂CO), 8.56, 8.74, 9.35, 9.66 (1 H each, s, meso α , δ , γ , β); NOE, irradiating the γ -proton at 9.35 ppm caused the triplet at 4.18 ppm to increase in intensity. UV-vis λ max (rel. int.) 418 nm (0.94), 439 (1.00), 545 (0.13), 592 (0.18), 637 (0.21); MS found m/e 743.8743 for (M+H)⁺, C40H47N4O10 requires 743.8413.

1,8-Coproporphyrin(IV)-dione tetramethyl ester (141) ¹H-NMR δ 1.62, 2.18 (2 H each, m, CH₂CH₂CO₂ sat.), 1.99, 2.00 (3 H each, s, Me sat.), 3.00 (4 H, m, CH₂CH₂CO₂ sat.), 3.16, 3.19 (2 H each, t, CH₂CH₂CO₂), 3.34, 3.37, 3 H each, s, ring Me), 3.36, 3.47 (3 H each, s, CH₂CH₂CO₂CH₃ sat.), 3.62, 3.64 (3 H each, s, CH₂CH₂CO₂CH₃), 4.23, 4.34 (2 H each, t, CH₂CH₂CO₂), 8.94, 8.99, 9.65, 9.86 (1 H each, s, meso α , γ , δ , β), -1.80 (2 H, br s, NH); UV-vis λ max (rel. int.) 416 nm (1.00), 435 (0.78), 592 (0.08), 624 (0.17), 690 (0.04); MS found m/e 743.8345 for (M+H)⁺, C40H47N4O10 requires 743.8413.

1,4-Coproporphyrin(IV)-dione tetramethyl ester (142) ¹H-NMR δ 1.70, 2.25 (2 H each, m CH₂CH₂CO₂ sat.), 1.83 (6 H each, s, Me sat.), 3.02 (4 H, t, CH₂CH₂CO₂ sat.), 3.12 (6 H, s, ring Me), 3.38 (6 H, s, CH₂CH₂CO₂CH₃ sat.), 3.61 (6 H, s, CH₂CH₂CO₂CH₃), 3.95 (4 H, t, CH₂CH₂CO₂), 7.57, 9.25 (1 H each, s, meso α , γ), 8.88 (2 H, s, meso β and δ), 0.83 (2 H, br s, NH); UV-vis λ max (rel. int.) 406 nm (1.00), 424 (0.43), 523 (0.07), 560 (0.11), 599 (0.13), 651 (0.33);

MS found m/e 743.8469 for $(M+H)^+$, C40H47N4O10 requires 743.8413.

7-Acrylo-coproporphyrin(IV)-one tetramethyl ester (143) 1 H-NMR δ , 1.60, 2.15 (1 H each, m, $_{CH_{2}CH_{2}CO_{2}}$ sat.), 2.08 (3 H, s, Me sat.), 3.08 (2 H, m, $_{CH_{2}CH_{2}CO_{2}}$ sat.), 3.18 (4 H, m, $_{CH_{2}CH_{2}CO_{2}}$), 3.25, (3 H, s, $_{CH_{2}CH_{2}CO_{2}CH_{3}}$ sat.), 3.61 (6 H, s, ring Me), 3.64 (3 H, s, ring Me), 3.62, 3.72 (3 H each, s, $_{CH_{2}CH_{2}CO_{2}CH_{3}}$), 4.03 (3 H, s, $_{CH=CHCO_{2}CH_{3}}$), 4.32 (4 H, m, $_{CH_{2}CH_{2}CO_{2}}$), 6.99, 9.23 (1 H each, d, $_{CH=CHCO_{2}}$), 9.17, 9.74, 9.94, 10.05 (1 H each, s, meso α , β , δ , γ), -2.81, -2.87 (1 H each, s, NH); UV-vis λ max (rel. int.) 412 nm (1.00), 512 (0.10), 549 (0.09), 597 (0.06), 657 90.24); MS m/e 725.8213 for (M+H)+, C40H45N4O9 requires 725.8260.

Homo-d₁ (6-Acrylo-1,3-coproporphyrin(IV)-dione tetramethyl ester) (130)

1,3-Dione 139 (75 mg, 0.1 mmol) was treated with OsO_4 (38 mg, 0.15 mmol) under the condition as described previously, yielding 36 mg (48%) of 130, together with 3 mg of hydroxymethyl dione (145).

(130) ¹H-NMR 1.65, 2.20 (2 H each, m $\underline{CH_2CH_2CO_2}$ sat.), 1.88, 1.93 (3 H each, Me sat.), 2.83 (4 H, m, $\underline{CH_2CH_2CO_2}$, sat.), 3.26 (2 H, t, $\underline{CH_2CH_2CO_2}$), 3.36, 3.38 (3 H each, s, $\underline{CH_2CH_2CO_2CH_3}$ sat.), 3.40, 3.43 (3 H, each, ring Me), 3.70, (3 H, s, $\underline{CH_2CH_2CO_2CH_3}$), 4.00 (3 H, s, $\underline{CH=CHCO_2CH_3}$), 4.03 (2 H, t, $\underline{CH_2CH_2CO_2CO_2}$), 6.90, 9.40 (1 H each, d, $\underline{CH=CHCO_2}$), 8.45, 8.55, 9.18, 9.51 (1 H, s, meso β , α , δ , γ); UV-vis λ max (rel. int.) 422 nm (1.00), 446 (0.70), 608 (0.28), 658 (0.16); MS found m/e 741.8279 for (M+H)⁺, C40H45N4O10 requires 741.8254.

CHAPTER 4

ON THE STRUCTURE OF HEME d_1

I. THE STERIC AND REGIO ISOMERS OF HEME \underline{d}_1

A. Cis- and trans-d₁ -- Stereochemistry Deduced from NMR Shift Reagent

The visible spectra of the diasterotropic cis- \underline{d}_1 128a and trans- \underline{d}_1 128b are virtually identical. The ¹H-NMR spectra of the two have recognizable differences as shown in <u>Table 2</u> and <u>Figure 11</u>. The peaks of meso protons of the trans isomer 128b are significantly upfield shifted and all the methyls, including those of methyl ester of the acetate, are also shifted to different positions in comparison with those of cis isomer 128a or the natural \underline{d}_1 .

The lanthanide ¹H-NMR shift reagent, such as Eu(fod)₃, which can provide useful information on the configuration and conformation problems, was used to study the stereochemistry of \underline{d}_1 via the two precursors cis-dione 59a and trans-dione 59b. ¹H-NMR were taken from a solution of either dione, to which an increasing amount of Eu(fod)₃ was added until the solution was saturated, therefore no more induced shift could be observed. It is known that the chemical shifts induced by lanthanide are resulted predominately from a dipolar (pseudocontact) mechanism.⁹¹ For a porphyrin with 6,7-dipropionate substituents, the lanthanide is believed to associate with the two carbonyl oxygens, either simultaneously as a bidentate complex or, in a statistical sense, with either one or the other, thus inducing a dramatic down-field shift of the γ -meso proton.⁹² We inferred that the possibility of Eu(fod)₃ associating with the two keto groups on the ring⁹³

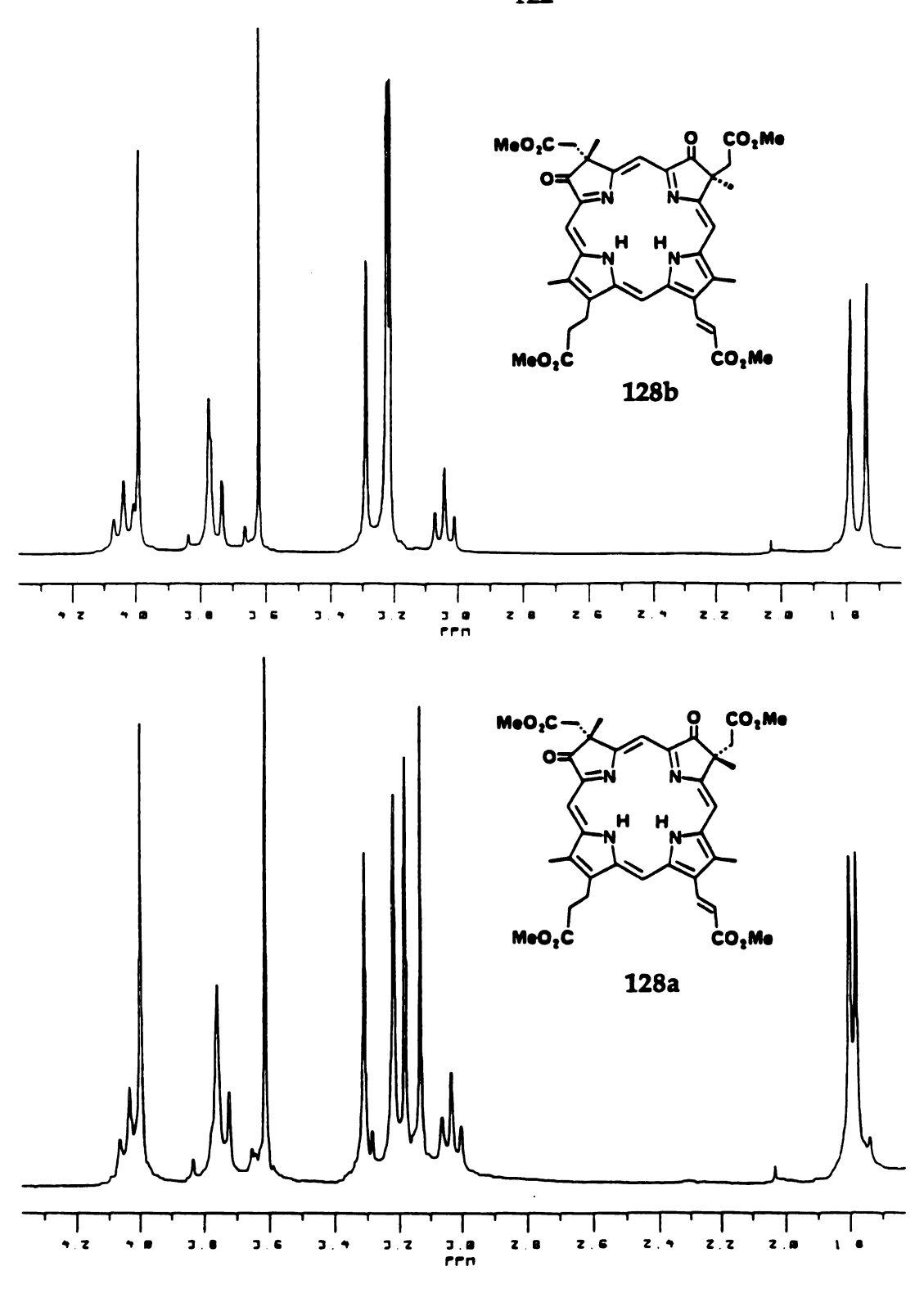


Figure 11 250 MHz ¹H-NMR spectra of cis-<u>d</u>₁ (128a) versus trans-<u>d</u>₁ (128b) in CDCl₃.

might be the same for both cis and trans isomer, but the interaction between the shift reagent and the two acetate substituents on the isomers would be different. The relative magnitude of the induced shifts of the α -proton should establish the distance between the two acetate groups and permit the assignment of their stereochemistry. In the case of cis dione **59a**, in which the two acetate groups are on the same side of the macrocycle, Eu(fod)₃ should have a higher affinity and thus, the α -meso proton should have a larger shift than that of the trans isomer. Figure **12** tabulates the Eu(fod)₃ induced

Figure 12. The Eu(fod)₃ induced chemical shift (in ppm) of meso protons of the cis-dione 59a and trans 59b (in parentheses). Eu(fod)₃ conc.=0~10 mM.

chemical shifts (in ppm) of meso protons of the cis-dione 59a and 59b (in parentheses). In deed, the α -proton clearly saw the largest difference between the induced shifts, $\Delta \Delta = 1.38 \cdot 1.18 = 0.20$ ppm. In contrast, the difference observed between the isomers at the β or the δ proton is negligible. Since 59a has the largest shift, itself and the acrylate derived from which, i. e. 128a, should have a cis conformation. Based on this result, the stereochemistry of heme \underline{d}_1 is assigned as cis with respect to the two acetic side chains. The definite proof, of cause, must await an X-ray crystallography study.

B. Cis- and trans-iso- d₁ -- Location of the Acrylic Side Chain

The electronegative acrylate side chain has a prominent effect on the visible spectrum of the porphyrindione core. As shown in Figure 13, the spectrum of iso- \underline{d}_1 (129a) is significantly different from that of \underline{d}_1 (128a=4a). The bands at the Soret region have a different shape as well as a shift and the bands in visible region appear in a quite different pattern. Distinguishable ¹H-NMR spectra are also observed for iso- \underline{d}_1 (Table 2). The position of the acrylate was verified by NOE measurements. For example, selective irradiation of the 8-methyl singlet (δ =3.38 ppm) on ring D of cis-iso- \underline{d}_1 (129a), resulted in a 5% increase in intensity on the neighboring δ -H singlet at 9.26 ppm, 4% and 3.5% on the acrylate double bond protons. At the time when we proposed the structure 1 for heme \underline{d}_1 , the position of the acrylic acid in relation to the two keto groups on ring A and B was tentative, now with the side by side comparison of the spectra of 128a and 129a, combined with the result from NOE measurements, the location of this substituent is firmly established.

II. ON THE NATIVE FORM OF \underline{d}_1

An important question concerning the proposed structure 1 for \underline{d}_1 is whether the 1,3-porphyrindione structure is the native form of the heme, or it arises from a diol by a pinacol-pinacolone rearrangement during its purification. There are several lines of evidence against a possibility of an in vitro rearrangement. It is obvious that the conditions used for the isolation of the free base methyl ester are not as harsh as is necessary for diol rearrangement in model compounds and \underline{d}_1 synthesis. The chiral 2 and 4

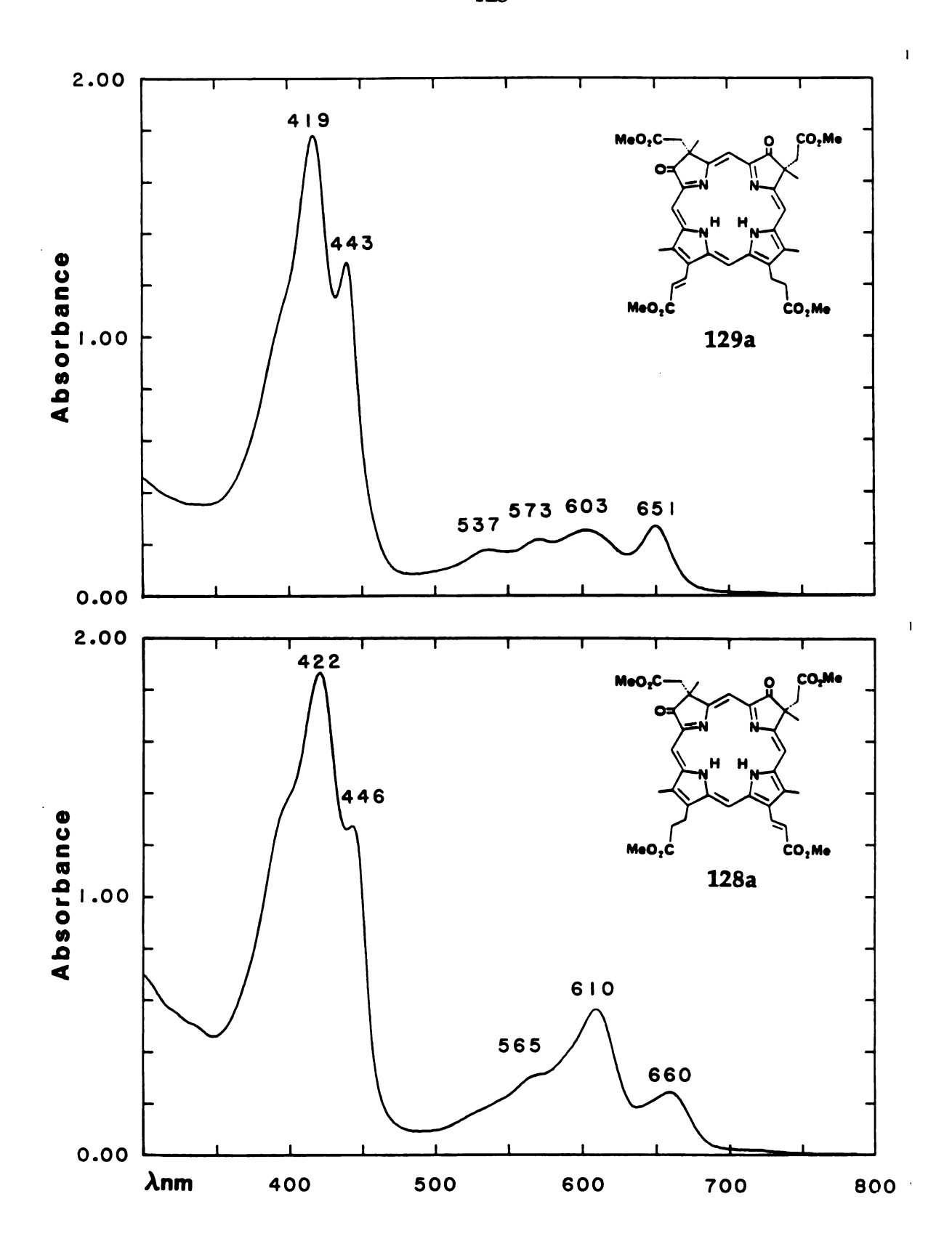


Figure 13 UV-vis absorption spectra of cis-d₁ (128a) versus cis-iso-d₁ (129a) in CH₂Cl₂.

Table 2. 1 H-NMR chemical shifts of heme d $_{1}$ free base and its stereo- and regioisomers. Chemical shifts at 25°C in parts/million in CDCl $_{3}$ withCHCl $_{3}$ as internal standard (δ =7.24).

δ(ppm)	compound						
proton	cis-d ₁	trans-d ₁	cis- iso-d ₁	trans- iso-d ₁	H#	mı	ultiplicity
meso a	8.418	8.363	8.377	8.318	1	s	
β	8.267	8.204	8.214	8.155	1	S	
ξ	9.429	9.384	9.403	9.347	1	S	
δ	9.211	9.180	9.258	9.214	1	S	
-CH=CHCO ₂ CH ₃	6.902	6,883	6.927	6.909	1	d	J=16.2 Hz
	8.962	8.934	9.019	8.991	1	d	, 10.212
	3.996	3.990	3.987	3.984	3	s	
-CH ₂ CH ₂ CO ₂ CH ₃	4.046	4.037	4.025	4.012	2	t	J=7.4 Hz
	3.035	3.036	3.053	3.044	2	t	, ,,,,,,,,,,,,,,,,,,,,,,,,,,,,,,,,,,,,,
	3.612	3.616	3.641	3.643	3	s	
2-CH ₂ CO ₂ CH ₃	3.781	3.788	3. 7 98	3.802	1	d	J=17.6 Hz
	3.696	3.710	3.721	3.735	1	d	j=17.0112
	3.126	3.209	3.131	3.128	3	s	
4-CH ₂ CO ₂ CH ₃	3.751	3. <i>7</i> 71	3.712	3.732	2	S	•
	3.176	3.204	3.174	3.219	3	s	
2-CH ₃	1.790	1.784	1.784	1.752	3	S	•
4-CH ₃	1.776	1.735	1.774	1.747	3	s	
5-CH ₃	3.307	3.385	3.145	3.223	3	S	•••••••••
8-CH ₃	3.223	3.217	3.385	3.362	3	s	

 β -carbons give rise to diastereomers unavoidably in porphyrindiones synthesized by rearrangement when different substituents are involved, but there is no evidence for diastereomeric resonances in the extracted \underline{d}_1 . Similarity of the meso proton chemical shifts in the free base methyl ester and a diamagnetic Fe^{2+} form of \underline{d}_1 in a freshly prepared crude extract argues against subsequent chemical transformation.⁴⁵ This argument was stringently tested by comparing the differences in meso proton shifts between free base and diamagnetic iron complexes of model compounds. As shown in Table 3, the shifts produced on going from metalloporphyrin to free base are generally small and especially small for \underline{d}_1 , and they do not grossly distort the profile of resonances. Above all, the synthetic \underline{d}_1 has been found in full function in the reconstituted \underline{cd}_1 nitrite reductase, as will be discussed in Chapter 5, thus it leaves no doubt about the consistency of \underline{d}_1 structure before and after its isolation.

Table 3. Meso prton chemical shift differences between hemes and free bases.^a

meso	<u>d</u> ₁	1,3-OEPdione 8	protoporphyrin IX
α	0.16	0.51	0.18
β	0.12	0.66	0.26
Υ	-0.15	0.46	0.49
δ	-0.18	0.44	0.06

^aFree base shifts were in CDCl₃ at 20 °C. Heme shifts were in 1:1 $D_2O-[D5]$ pyridine at 20 °C.

III. ON THE BIOSYNTHETIC ORIGIN OF \underline{d}_1

The unprecedented keto structure of heme \underline{d}_1 poses many challenging questions. The first would be "How is heme \underline{d}_1 formed in nature?" Biosynthetically, all tetrapyrrolic macrocycles found in nature derive their acid side chains and substitution patterns from a single intermediate, uroporphyrinogen III, which itself is cyclized enzymically from four units of porphobilinogen.² In animals and plants the formation of protoporphyrin IX and chlorophylls requires the decarboxylation of uroporphyrinogen III to yield coproporphyrinogen III, which by oxidative decarboxylation produces protoporphrinogen IX. On the other hand, an alternative pathway produces sirohydrochlorin from which another set of pigments, such as vitamin \underline{B}_{12} and \underline{F}_{430} are formed. Now the question is "By which route is heme \underline{d}_1 biosynthesized, via protoporphyrin or sirohydrochlorin (Scheme 27)?"

Since the biological existence of the gem-diol structure has been substantiated by the recently established heme \underline{d} structure 64 of E. coli, it can be assumed that the keto groups in \underline{d}_1 could be obtained from a pinacolic rearrangement via a gem-dihydroxy derivative of protoporphyrin. Such a "protoporphyrin route" is essentially what we have followed in the laboratory synthesis. Nevertheless, owing to the difficulties we experienced in preparing \underline{d}_1 (extremely acidic conditions, mixture of diastereomers, etc.), we have doubt about the feasibility of this route in a natural setting.

If heme \underline{d}_1 is derived from the "sirohydrochlorin route", its configuration should be automatically defined by the precursor. Indeed the cis stereochemistry about the two angular acetic side chains concluded by our work, as well as the overall substituent arrangement, suggests that the \underline{d}_1

biosynthesis may be just another branch of the intricate uroporphyrinogen III $--\underline{B}_{12}$ pathway.

The two possibilities regarding the \underline{d}_1 biosynthesis may be distinguished experimentally by tracing the source of the two angular methyl groups. If the protoporphyrin-related pinacolic rearrangement is involved, the methyl groups should come from the 1,3-acetic acid side chains of uroporphyrinogen III. In contrast, if the sirohydrochlorin is the precursor, the methyl groups are transferred to uroporphyrinogen III from SAM (S-adenosylmethionine). The isotopic labeling technique, which has been successfully used in the \underline{B}_{12} biosynthesis,² will produce direct evidence concerning the pathway of \underline{d}_1 synthesis in living system.

Scheme 27

CHAPTER 5

PHYSICOCHEMICAL PROPERTIES OF HEME \underline{d}_1 AND MODEL SYSTEMS

I. GENERAL CONSIDERATION

Having proven the unprecedented "porphyrindione" structure of \underline{d}_1 , we must raise questions like 'Why is this structure needed?' 'Are there any obligatory roles of this structure in the dissimilatory nitrite reduction?' An obvious approach to the answers is to compare the properties of this new macrocycle with other better known porphyrinoids. An enormous amount of effort has been devoted to document just about every conceivable properties of porphyrins. It seems that every new spectroscopic technique introduced to chemistry and biophysics in the last three decades has been applied to porphyrins and their multitude metal complexes. We cannot, of cause, duplicate all these measurements on porphyrinones and porphyrindiones since it is unnecessary to do so. However, some preliminary results have been collected from the studies with spectroscopic techniques such as UV-vis, ¹H- and ¹³C-NMR, IR and RR, and the molecular structures, the redox potentials and the PK3 values of these compounds have been determined. This chapter is a summary of the physicochemical studies so far carried out on the d1 and related compounds in an attempt to build up a framework for future investigation. Some results covered in this chapter are cited from literature work published previously by our group and our collaborators in order to present a general review.

It is intriguing to recognize that both siroheme and heme \underline{d}_1 prosthetic

group have the isobacteriochlorin-type core structure, yet they differ with regard to their spectroscopic, redox and chemical properties. Porphyrinones and porphyrindiones have generally been viewed as derivatives of chlorin, isobacteriochlorin or bacteriochlorin, therefore, the differences between these two systems, whenever observed, are emphasized throughout this chapter.

II. ABSORPTION SPECTRA

A. Spectral Features of Porphyrinones

A typical visible spectrum of porphyrinone, that of 135, is illustrated in Figure 14, and the data taken from eighteen others, plus two hydroporphyrins as comparison, are listed in Table 4. The spectra of Cu(II)-metallated and protonated porphyrinones are given in Table 5 for general reference.

Like those of their chlorin cousins, the spectra of porphyrinones are very much consistent in that the overall pattern is relatively unperturbed by electronic effects. The intense singlet near-UV band, still called Soret band, is found around 407 nm with a molar extinction efficient in the order of 1.5 to 2.0 x 10⁵, which is 4 to 5 times more intense than the visible bands above 450 nm. The peak at the longest wavelength (band I) is observed at 643 nm (± 2 nm) and is always more intense than the other bands in this region. Band II usually appears as the least intense one, whereas Band IV is broad with a shoulder on its blue side. The spectral features of porphyrinones differ from that of a typical chlorin⁵⁴ in that the Soret band as well as Band I of chlorin are observed at shorter wavelength, about 15 nm toward blue, but with a similar molecular extinction coefficient as that of porphyrinone.

Substituents on the porphyrinone periphery can effect the absorption

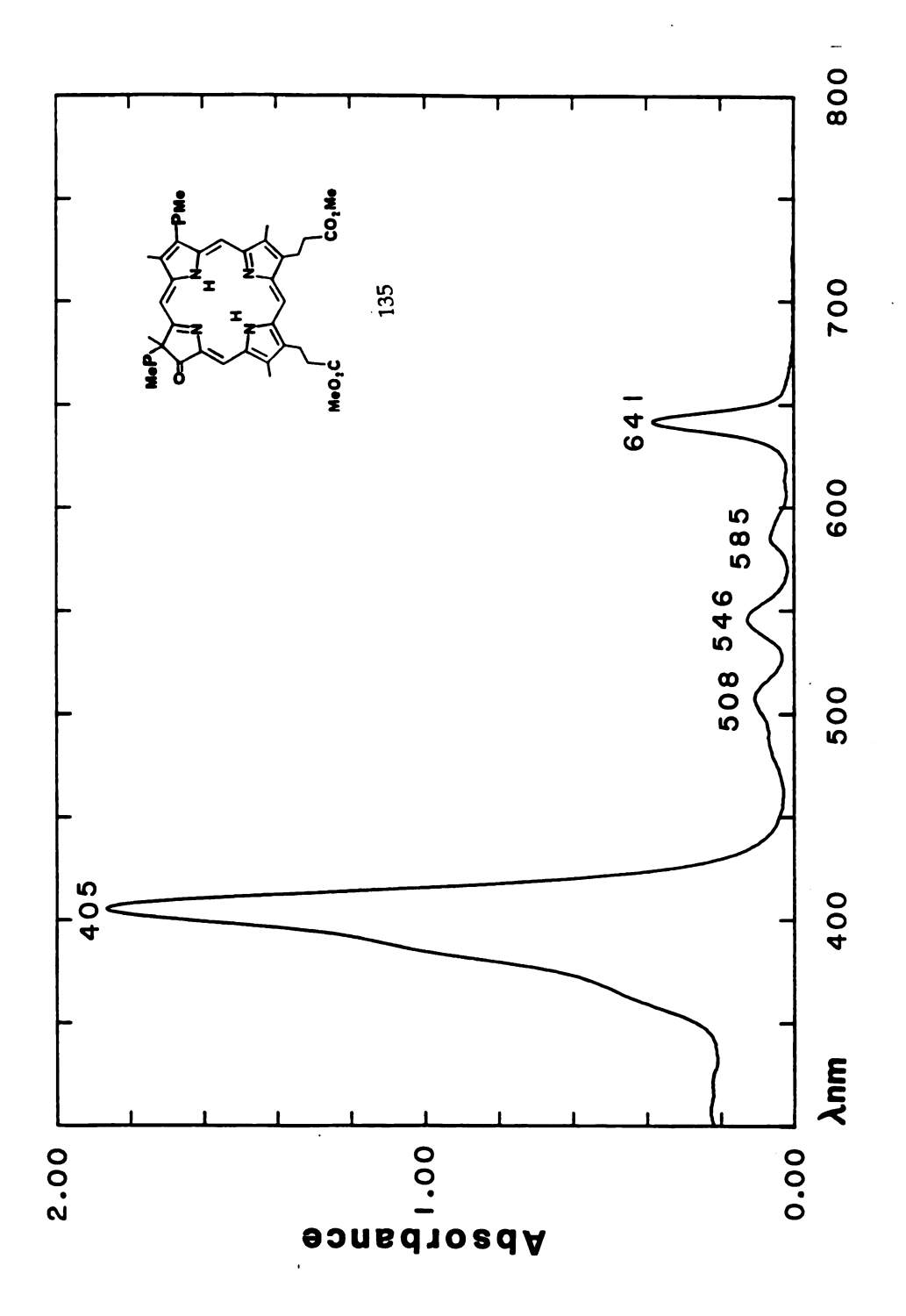


Figure 14 UV-vis absorption spectrum of porphyrinone 135 in CH₂Cl₂.

Table 4. Visible spectra of various porphyrinones in comparison with chlorins.

The relative intensity of the bands is indicated in parenthesis.

___________ band (nm) IV Ш II compound Soret Ι 407 510 549 586 642 octaethylporphyrinone 26 (.23)(1.00)(.09)(.10)(.07)5 407 508 547 585 642 1-mesoporphyrinone (1.00)(.08)(.09)(.06)(.22)407 508 547 585 642 3-mesoporphyrinone 18 (1.00)(.07)(.09)(.05)(.22)2,3-(bis-2-chloroethyl)-93 407 508 547 588 645 1-porphyrinone (1.00)(.09)(.10)(.07)(.25)1,4-(bis-2-chloroethyl)-547 587 643 94 407 508 2-porphyrinone (.08)(.24)(1.00)(.10)(.11)1-porphyrinone-507 2,4-diacetate 111 406 544 589 645 (.07)(.23)(1.00)(.09)(.10)3-porphyrinone-2,4-diacetate 545 406 506 587 643 112 (.09)(.09)(.23)(1.00)(.07)1-porphyrinone-2-acetate-4-(1-hydroxy)-acetate 120 407 506 544 591 647 (1.00)(.09)(.08)(.06)(.25)2,4-bis-(2-chloroethyl)-8-hydroxymethyl-408 508 546 590 646 3-porphyrinone (.17)(.16)(1.00)(.13)(.33)2-(2-hydroxyethyl)-511 550 596 652 4-vinyl-1-porphyrinone 100 412 (1.00)(.11)(.09)(.07)(.24)4-vinyl-1-porphyrinone 102 412 512 548 594 -2-aecaldehyde 651 (1.00)(.11)(.09)(.07)(.23)1-mesoporphyrinone-520 565 585 641 6-acrylate 414 A (1.00)(.07)(.12)(.09)(.20)

Table 4 (contd.)

3-mesoporphyrinone- 7-acrylate	В	416 (1.00)	524 (.08)	563 (.17)	583 (.10)	640 (.18)
1-coproporphyrinone- 6-acrylate	143	417 (1.00)	526 (.07)	565 (.12)	585 (.09)	641 (.19)
1-porphyrinone- 2,4-diacetate-6-acrylate		415 (1.00)	521 (.11)	563 (.15)	587 (.12)	643 (.22)
2-hydroxyl-1,2-(γ-lacton	e)-	(====,	()	(120)	(/	(/
chlorin-4-acetate	113	391 (1.00)	494 (.11)	540 (.04)	587 (.05)	641 (.26)
4-hydroxyi-3,4-(γ-lacton	e)-					
chlorin-2-acetate	114	390 (1.00)	493 (.10)	541 (.03)	587 (.04)	640 (.24)
1,2-dihydroxylchlorin-						
2,4-diacetate	105	392 (1.00)	494 (.10)	522 (.04)	590 (.04)	642 (.28)
3,4-dihydroxylchlorin-		(2000)	(-20)	((*** = /	(0,
2,4-diacetate	106	392 (1.00)	495 (.11)	521 (.04)	589 (.05)	643 (.27)
1,1-dihydro-gem- octaethylchlorin	С	391	495 (.09)	521 (.06)	589 617 (.05) (.06)	643
1-methyl-gem-		(1.00)	(.07)	(.00)	(.05) (.06)	(.29)
octaethylchlorin	D	391 (1.00)	496 (.09)	522 (.05)	589 615 (.05) (.05)	643 (.32)

Table 5. Visble spectra of Cu-metallated and protonated porphyrinones in comparison with chlorins. The relative intensity of the bands is indicated in parenthesis.

band (nm) Soret Q compound Cu(II)-572 octaethylporphyrinone 26 414 616 378 (.08)(.28)(.28)(1.00)Cu(II)-570 379 414 616 3-mesoporphyrinone 18 (.25)(1.00)(.07)(.27)Cu(II)-1-methylgem-OEC 494 530 569 388 612 D (1.00)(.07)(.06)(80.)(.33)3H+octaethylporphyrinone 26 401 416 535 570 623 (1.00)(.83)(.07)(.08)(.15)3H+-3-mesoporphyrinone 18 399 416 535 548 569 620 (.06) (.06) (.08) (1.00)(.09)(.15)3H+-1,1-dihydro-525 gem-OEC 394 406 619 С (.07)(1.00)(.09)(.17)3H+-1-methylgem-OEC 407 D 394 524 619 (1.00)(.09)(.06)(.18) spectra. An exocyclic double bond, such as a vinyl group, shifts the absorption bands to longer wavelength (up to 8 nm). Introducing a conjugated acrylic side chain would red-shift the Soret band by 7 nm and also change the pattern of visible bands: band III and IV are 16 nm red-shifted but I and II are virtually unchanged.

The γ -lactone compounds, such as 113 and 114, obtained as a by-product of the pinacolic rearrangement of some vic-diols have a spectrum very similar to that of a chlorin with its band III diminished and shifted to a longer wavelength.

B. Spectral Features of Porphyrindiones

Dominated by the relative positions of the two keto groups on the macrocycle, the isomeric diones give totally different spectra from one another. In Figure 15 and 16, the spectra of all five isomeric porphyrindiones are illustrated. Not only the isobacteriochlorin-type 1,3- 2,3- and 1,4-dione but all so the bacteriochlorin-type 1,5- and 1,6-dione exhibit distinct absorption spectra due to different molecular symmetries are involved in their structures. Not surprisingly even the metal complexes and protonated forms of these regioisomeric diones have quite different spectra. In Table 6, the spectral data of some Cu(II) and acid salt of diones are tabulated. As illustrated in Figure 17 and 18, the spectra of Cu(II) 1,3-dione versus Cu(II) 2,3-dione, the protonated 1,3-dione versus protonated 1,4-dione, both couples exhibit very distinct spectral features. These results suggest immediately the extensive π-overlap of the two oxo groups with the ring system, forming a marocycle skeleton different from the typical porphyrin or isobacteriochlorin system.

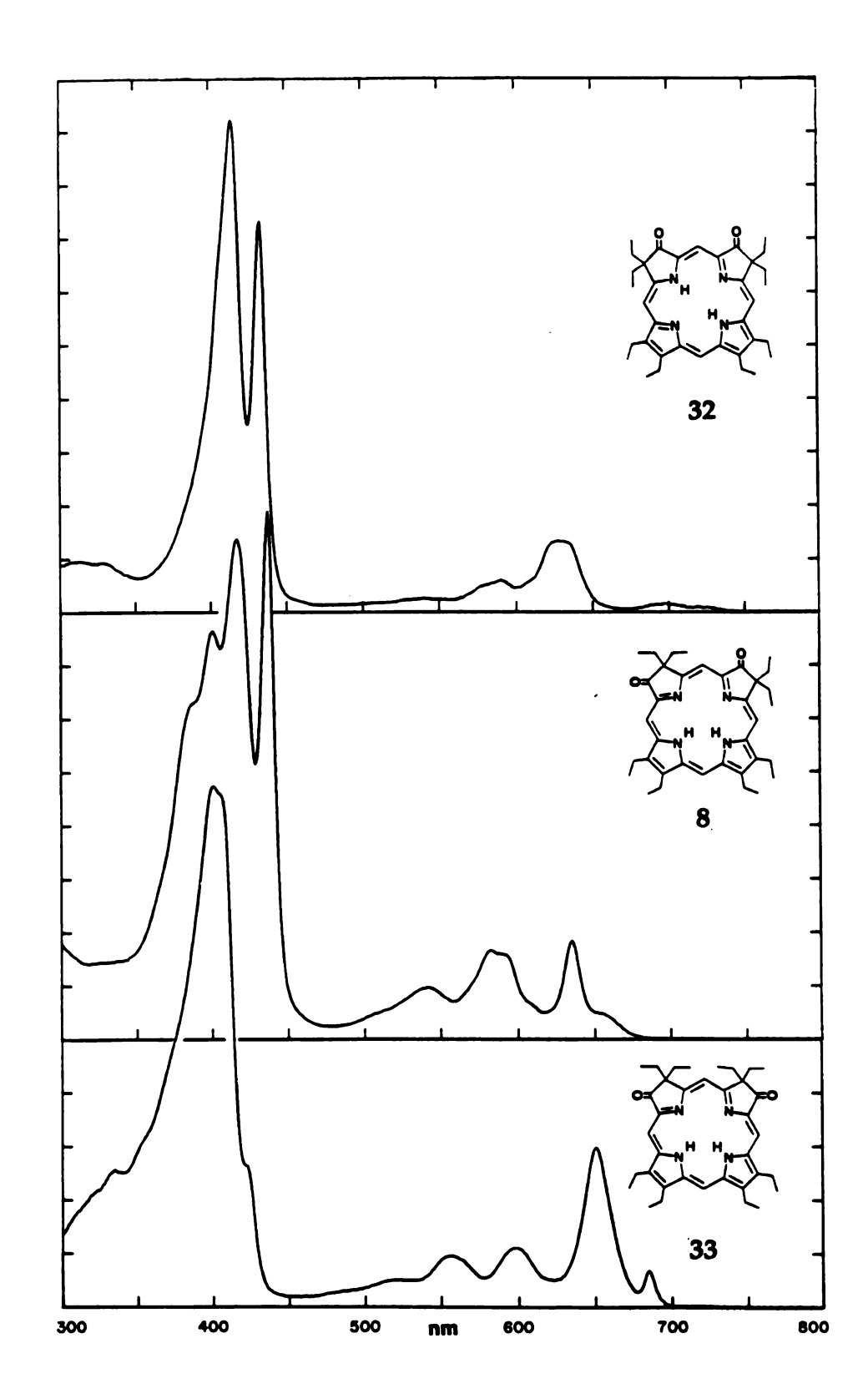


Figure 15 UV-vis absorption spectra of 2,3-dione (32), 1,3-dione (8) and 1,4-dione (33) in $\mathrm{CH_2Cl_2}$.

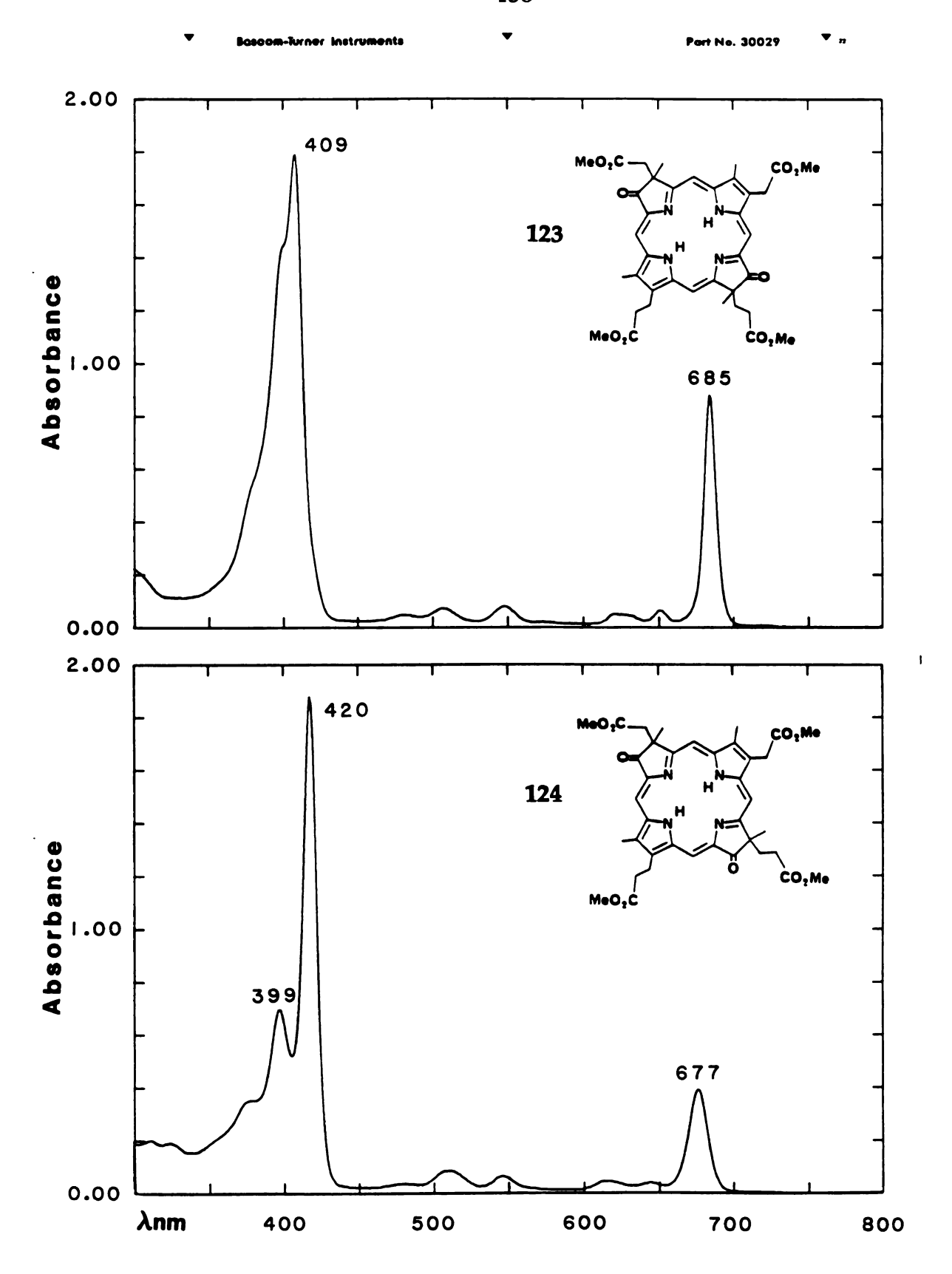


Figure 16 UV-vis absorption spectra of 1,5-dione (123) and 1,6-dione (124) in CH₂Cl₂.

Table 6. Visible spectra of Cu(II)-metallated and protonated porphyrindiones. The relative intensity of the bands is indicated in parenthesis.

	band (nm)						=====	=====
compound				Soret			Q	
Cu(II)-octaethyl- 1,3-porphyrindione	8		391 (.71)	433 (1.00)		501 (.10)	580 (.19)	621 (.52)
Cu(II)-1,3-porphyrin- dione-2,4-diacetate	59a		389 (.65)	430 (1.00)		(.10)	575 (.18)	617 (.54)
Cu(II)-cis-d ₁	128a		4 10 (.61)	438 (1.00)				643 (.58)
Cu(II)-octaethyl- 2,3-porphyrindione	32		395 (.71)	430 (1.00)	441 (.93)	543 (.10)	581 (.12)	691 (.64)
Cu(II)-octaethyl- 1.5-porphyrindione	28		381 (.48)	426 (1.00)		524 (.06)	667 (.12)	701 (.76)
Cu(II)-octaethyl- 1,6-porphyrindione	29		380 (.80)	420 (1.00)	442	542	585 (.21)	666 (.34)
3H ⁺ -octaethyl- 1,3-porphyrindione	8		413 (.80)	436 (1,00)			596 (.21)	629 (.76)
3H+-octaethyl- 2,3-porphyrindione	32		413 (.80)	439 (1.00)			618 (.18)	657 (.22)
3H+-octaethyl- 1,4-porphyrindione	33		399 (1.00)	42 0	523 (.07)	568 (.10)	604 (.17)	648 (.52)
3H ⁺ -octaethyl- 1,3,5-porphyrintrione	50		•	424 (1.00)	. ,		624 (.24)	679 (.17)
3H+1,3-dimethyl-gem- octaethyl- isobacteriochlorin	E	368 (.46)	385 (.45)	405 (1.00)	492 (.09)	518 (.07)	587 (.12)	632 (.38)

octaethyl- 1,3-dimethyl-gemisobacteriochlorin

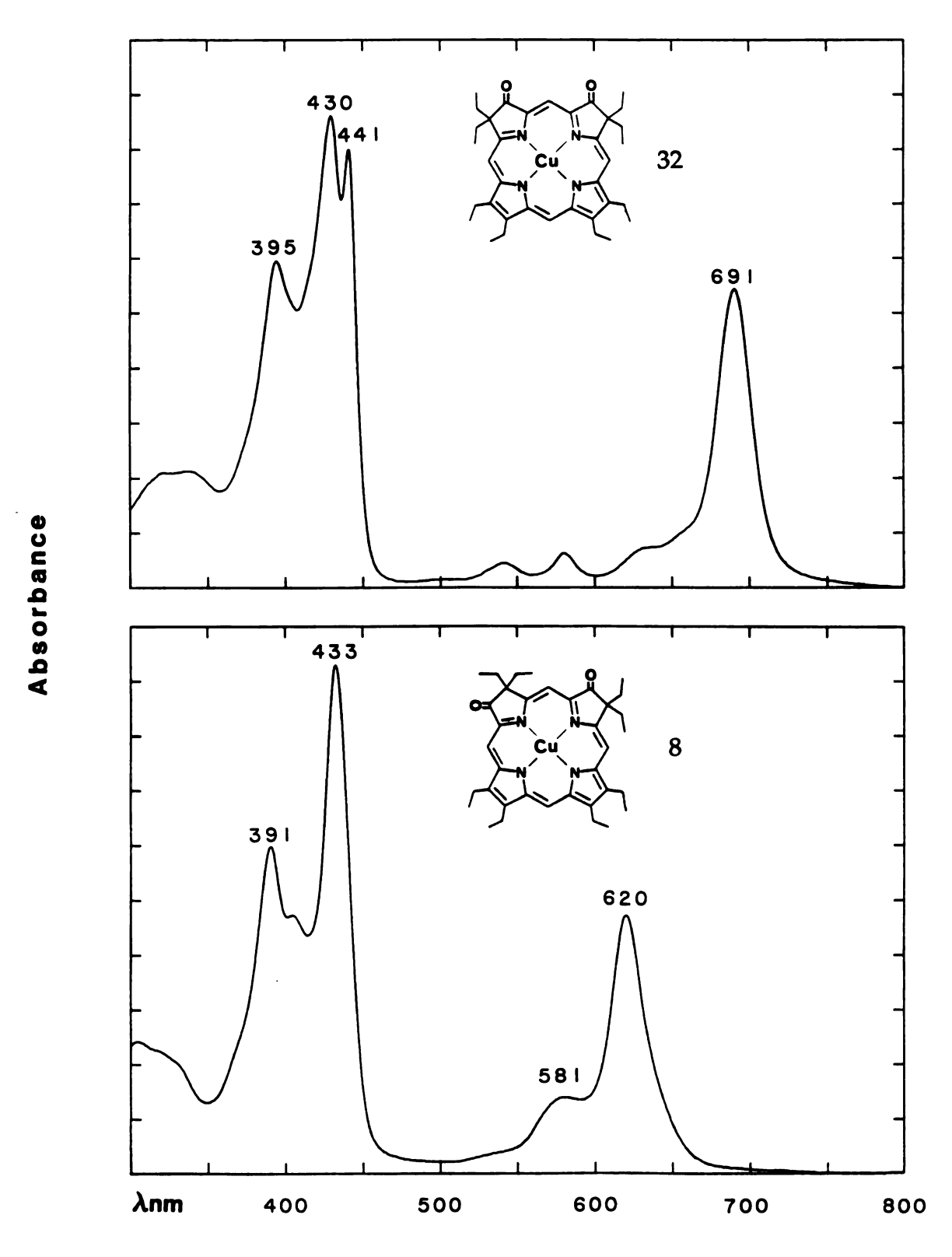


Figure 17 UV-vis absorption spectra of Cu (II) 2,3-dione (32) and 1,3-dione (8) in CH₂Cl₂.

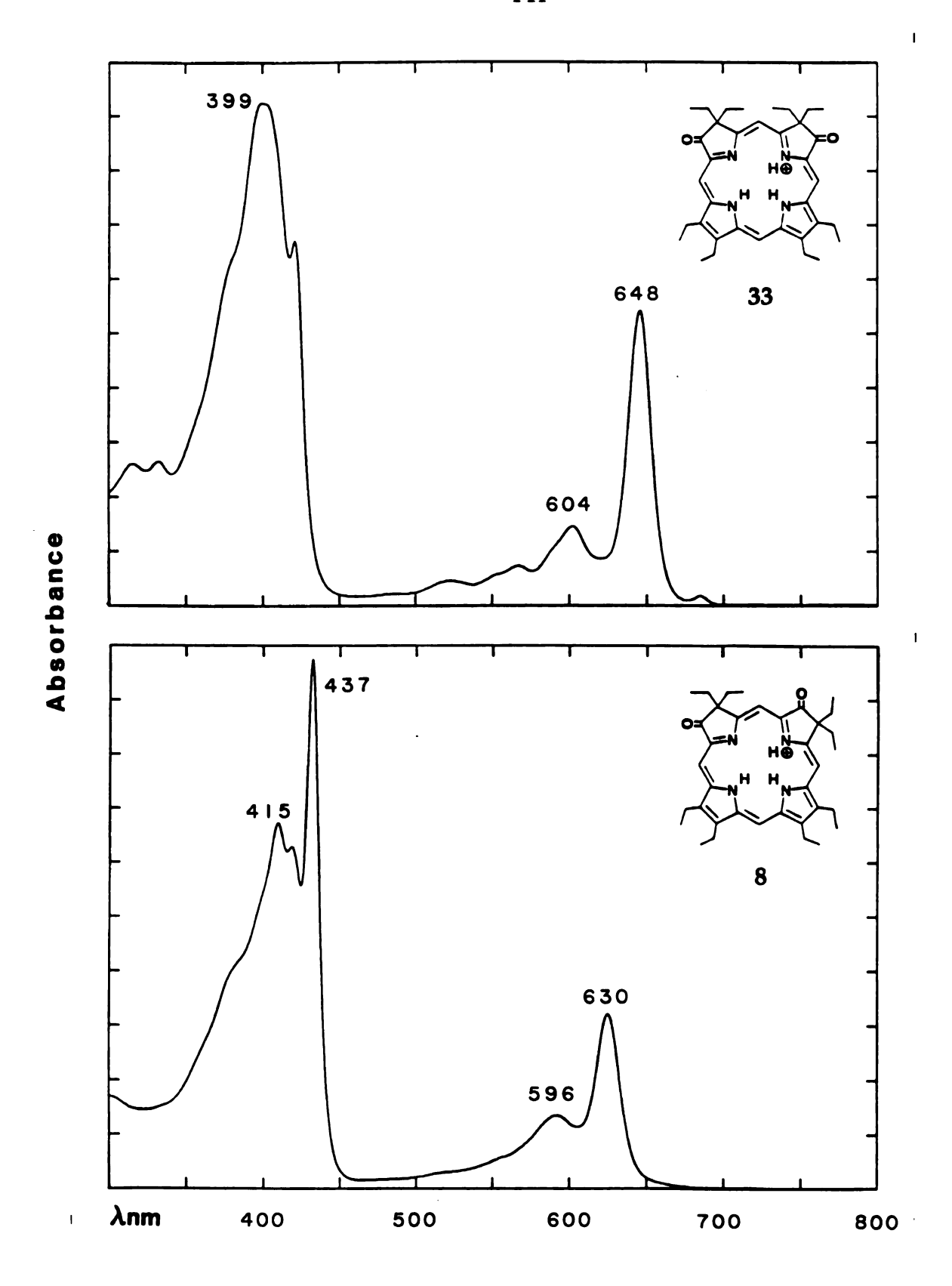


Figure 18 UV-vis absorption spectra of 1,4-dione (33) and 1,3-dione (8) in CH_2Cl_2 with CF_3CO_2H (1%).

The Soret region of the 1,3-dione seems to be composed of at least four distinguishable bands: a sharpest and most intense band at 439 nm, another one at 418 nm and two shoulder bands at 402 and 388 nm. In the visible region, there are five bands observed. The molecular extinction coefficient of the Soret band (ε =85,000 to 90,000) of 1,3-dione is significantly lower than that of the 2,3- and 1,4-diones.

In comparison with the 1,3-dione, a typical isobacteriochlorin has a single broad Soret band at a much shorter wavelength around 376 nm⁶⁰. The positions of the major visible bands of isobacteriochlorin are not so much dissimilar with those of the 1,3-dione but the relative intensity of 635 nm peak is higher in isobacteriochlorin.

Peripheral electronic effects are summarized in <u>Table 7</u>. The spectrum of the monoketone-lactone compound 118 maintains virtually the basic features of the Soret region of the 1,3-dione, but its visible bands are more scattered with Band I becoming the most intense peak. The influence of a conjugated vinyl group on the 1,3-dione spectrum is significant: a vinyl group at ring C, position 6, can diminish the multiple Soret to two bands, and can shift all visible bands about 10 nm bathchromically, giving a spectrum similar to that of \underline{d}_1 . The presence of an acrylic side chain at this position brings about the the spectrum of \underline{d}_1 as we described before, having virtually a single Soret band at 422 nm with a 446 nm shoulder and all the visible bands red-shifted by 20 nm. The unusually low extinction coefficient (ε =82,000) of the Soret band and the low ratio of the Soret band versus visible bands (~3.2) are the unique features of "6-acrylo-1,3-porphyrindione".

III. NUCLEAR MAGNETIC RESONANCE SPECTROSCOPY

Table 7. Visible spectra of 1,3-porphyrindiones in comparison with isobacteriochlorins. The relative intensity of the bands are indicated in the parenthesis.

		band (nm)						
compound			soret			visibl	le	
1,3-octaethyl-								
porpohyrindione*	8	403	421	440	544	585	591	637
		(.80)	(1.00)	(1.00)	(.13)	(.21)	(.17)	(.23)
1,3-mesoporphyrin-	6	402	417	438	543	584		638
dione		(.86)	(1.00)	(.97)	(.15)	(.21)		(.22)
2,4-bis-(2-chloroethyl)								
1,3-porphyrindione*	82		418	439	545		592	637
			(1.00)	(.94)	(.13)		(.18)	(.21)
2,4-bis-(2-hydroxyethy	1)-							
1,3-porphyrindione	88		415	437	545	588		637
			(1.00)	(.87)	(.19)	(.26)		(.26)
cis-1,3-porphyrindione	<u>-</u> -							
2,4-diacetate	59a		417	437	542		591	637
			(1.00)	(.98)	(.11)		(.17)	(.19)
trans-1,3-porphyrindic	ne-							
2,4-diacetate	59b		416	437	544	589		638
			(1.00)	(.82)	(.11)	(.16)		(.17)
5-(1-methoxylethyl)-								
1,3-porphyrindione	52	402	419	439	546	588		639
		(.80)	(1.00)	(.87)	(.17)	(.25)		(.21)
5-(1-hydroxylethyl)-								
1,3-porphyrindione	54	401	418	439	548	587		640
		(.82)	(1.00)	(.93)	(.17)	(.28)		(.25)

Table 7 (contd.)

6-vinyl-octaethyl-									
1,3-porphyrindione	53		422	444		554		596	646
			(1.00)	(.82)		(.17)		(.28)	(.22)
1,3-mesoporphyrindion	ne-								
6-acrylate	10		423	445				611	661
			(1.00)	(.71)				(.32)	(.21)
cis-d ₁	128a		422	446				61 0	660
			(1.00)	(.72)				(.29)	(.17)
trans-d ₁	128b		423	44 5				611	6 60
			(1.00)	(.7 0)				(.32)	(.71)
cis-iso-d ₁	129a		419	443	537	573		603	651
			(1.00)	(.75)	(.12)	(.14)		(.15)	(.19)
tran-iso-d ₁	129b		420	443	538	573		604	652
			(1.00)	(.70)	(.15)	(.15)		(.17)	(.19)
4 hydroxyl 2.4 (x/ loote									
4-hydroxyl-3,4-(γ-lacto 1-porphyrinone-	ne/-								
2,4-diacetate	118	379	391	411	503	543	587		634
2, 1- macetate	110	(.81)	(.86)	(1.00)	(.09)	(.11)	(.13)		(.21)
1,3-dimethyl-gem-		(.01)	(.00)	(1.00)	(.02)	(.11)	(.10)		(.21)
octaethyl-		373			511	546	589		636
isobacteriochlorin	E	(1.00)			(.16)	(.25)	(.38)		(.09)
	Ē	(1.00)			(.10)	(.20)	()		(.07)
sirohydrochlorin		377		482sh	513	547	589		635
		(1.00)		(.07)	(.10)	(.18)	(.28)		(.02)
=======================================		======	.====	=====	=====		,	=====	:====

A. ¹H-NMR Spectra

Removal of the peripheral double bonds and introduction of keto groups to the macrocycle lead to a decrease in the ring current, as indicated by the upfield shift of the outer meso proton signals and a down field shift of the inner N-H signals. A trend of upfield shift for almost all of the peaks of the peripheral substituents, attached either to the pyrrole or to the saturated pyrroline rings, is also observed as going from porphyrin, to porphyrinone, and to porphyrindione (Table 8). The decrease of ring current is moderate in porphyrinone and bacteriochlorin-type dione but is very pronounced in the isobacteriochlorin-type 1,3-dione. Comparing with the features observed for dione 59a, the peaks in the spectrum of \underline{d}_1 are even more upfield shifted indicating the powerful conjugation of acrylate side chain with the ring π -system.

In general, the peaks of porphyrindiones are less spread out and are often not first order. They are further complicated by the magnetic nonequivalence of the methylene protons of the side chains because of the asymmetric quaternary β carbon atom on the pyrroline ring. An additional complicating factor in these compounds is the possible spin-spin coupling between the substituents.

The two methylene protons on the acetate side chains of porphyrin 58 exhibit only a single peak, thus two peaks are observed at 3.73 and 3.75 ppm respectively. However, in porphyrinone 111, these protons on pyrroline ring A are not only upfield shifted to ~3.95 ppm, but also split into a AB-type doublet-doublet with a J-value of 17 ppm. On pyrrole ring B, they remains as a singlet with almost no shift. In the spectra of dione 59a both set of methylene peaks appear around 3.70 ppm, with splitting only coming from ring A acetate. The splitting of the methylene protons might be caused by the

Table 8. 1 H-NMR chemical shifts of heme \underline{d}_1 related porphyrin, porphyrinone and porphyrindiones. Chemical shifts at 25^0 C in parts/million in CDCl $_3$ with CHCl $_3$ as internal standard (δ =7.24 ppm).

	compound δ(ppm)									
proton	PH ₂ 58	MK-1 111	MK-2 112	1,6-DK 124	1,8-DK 122	1,3-DK 59a	1,7-DK 121			
meso a p	10.00s 9.99s 9.97s 9.94s	9.95s 9.92s 9.89s 9.13s	9.94s 9.86s 9.85s 9.07s	9.74s 9.60s 8.93s 8.87s	9.81s 9.65s 8.91s 8.86s	9.56s 9.38s 8.67s 8.46s	9.48s 9.22s 8.68s 8.42s			
-CH ₂ CH ₂ CO ₂ CH ₃	4.37t 4.35t 3.26t 3.26t 3.24s 3.66s	4.38t 4.23t 3.23t 3,20t 3.66s 3.63s	4.38t 4.23t 3.46t 3.26t 3.67s 3.66s	4.23t 3.14t 2.97t 2.08m 1.57m 3.72s 3.32s	4.19t 3.13t 2.97t 2.21m 1.70m 3.62s 3.41s	4.15t 4.11t 3.14t 3.06t 3.61s 3.57s	4.07t 3.25t 2.87t 2.10m 1.69m 3.70s 3.25s			
-C <u>H</u> ₂ CO ₂ C <u>H</u> ₃	4.96s 4.90s 3.75s 3.73s	5.04s 4.00dd 3.90dd 3.78s 2.96s	5.09dd 4.99dd 3.98dd 3.88dd 3.81s 2.97s	4.87s 3.90dd 3.82dd 3.77s 3.05s	4.96s 3.88dd 3.80dd 3.77s 3.09s	3.87dd 3.75dd 3.76s 3.17s 3.07s	4.76s 3.79s 3.74s 3.15s			
-С <u>Н</u> ₃	3.75s 3.73s 3.66s 3.64s	3.66s 3.63s 3.58s 1.95s	3.60s 3.55s 3.46s 1.95s	3.47s 3.47s 1.97s 1.87s	3.55s 3.44s 1.97s 1.88s	3.30s 3.26s 1.85s 1.83s	3.37s 3.25s 1.93s 1.81s			
N-H	4.20b	-2.93s -2.87s	-2.91s -2.79s	2.21s 2.15s	0.06b	-0.20b				

deformation of the adjacent saturated ring which somehow inhibited the rotation of the acetate group such that the magnetic environment of the two protons became different.

In the spectrum of \underline{d}_1 , the vinylic protons on the acrylate exhibit two doublets at 6.90 and 8.96 ppm with a coupling constant of 17 Hz typical of a trans olefinic structure for the acrylate side chain.

In most isobacteriochlorin, 60 the usual pattern of meso protons is one going down-field (the one between the unsaturated pyrroles, y), a pair at the intermediate shift (the two between a saturated and an unsaturated pyrrole, β , δ), and one relatively upfield (the one between the two saturated pyrroles, a). In 1,3-porphyrindiones, the deshielding effects of the carbonyl oxygens have distorted the usual isobacteriochlorin pattern. The 3-carbonyl oxygen has deshielded α -proton from its furthest upfield normal position to a shift comparable to β -proton, while the 1-carbonyl has deshielded δ -proton to a range comparable to that of y. The deshielding effect of the carbonyl group is best seen in the monoketone's case as shown in Figure 19: one of the two original upfield peaks attributed to the meso protons flanking the reduced pyrrole ring is shifted down-field to the region of the two protons by the pyrrole rings, thus giving a "3:1" pattern which has been universally observed in the spectra of all porphyrinones. The ¹H-NMR chemical shifts of the meso protons from the spectra of some selected porphyrinones, porphyrindiones, chlorin, and isobacteriochlorin are listed in Table 9 for comparison.

B. ¹³C-NMR Spectra

The ¹³C spectra data of the selected porphyrin, porphyrinone and porphyrindione are summarized in <u>Table 10</u>. Rather than discussing each

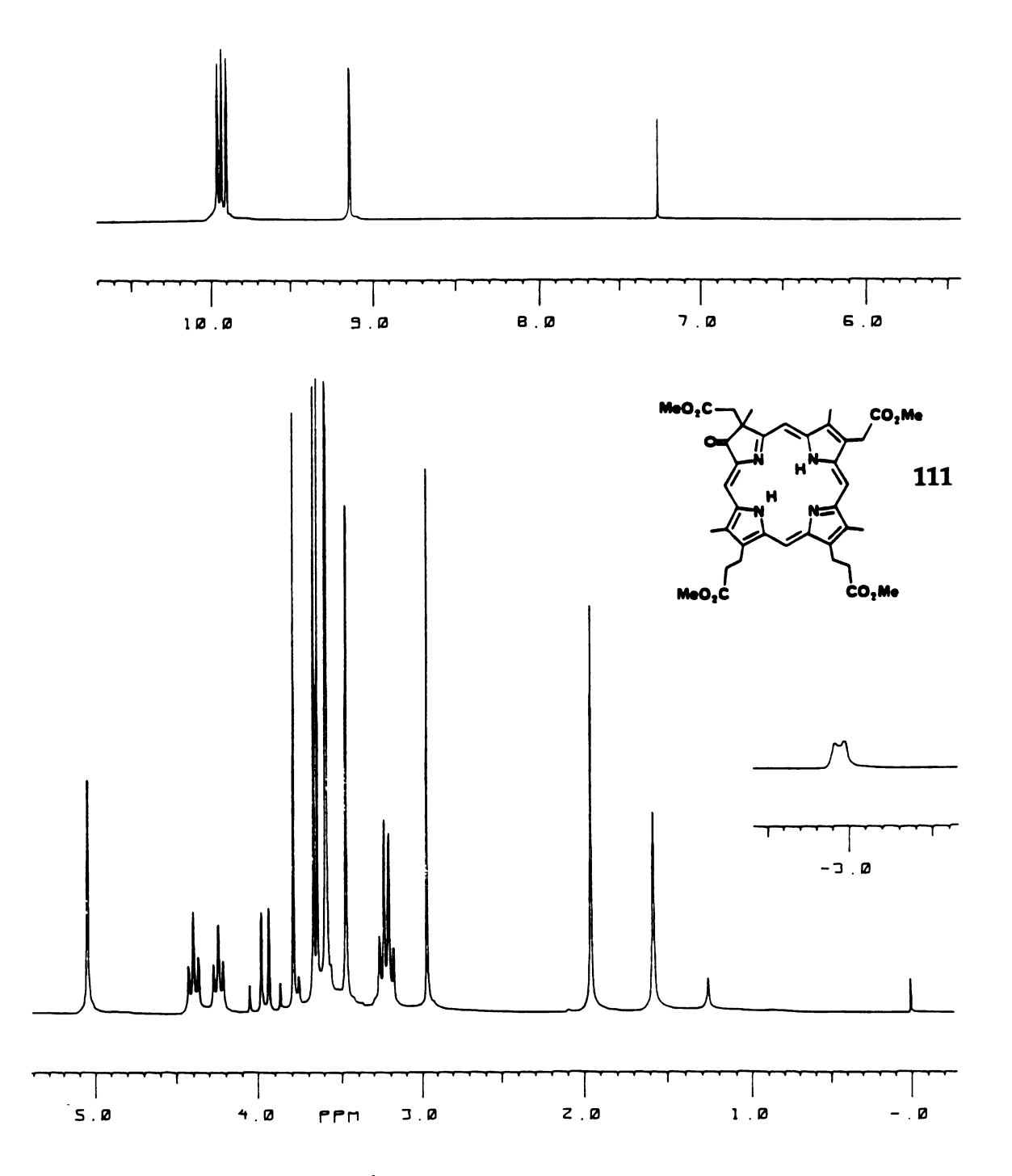
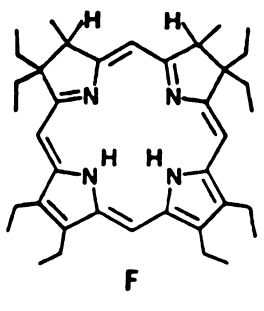


Figure 19 250 MHz ¹H-NMR spectrum of porpnyrinone 111 in CDCl₃.

Table 9. ¹H-NMR schmical shifts of meso protons of porphyrindiones in comparison with their analogous bacteriochlorins and isobacteriochlorins.

=======================================	======	========		======================================	======	
			meso pro	meso protons (δ)		
compound		α	β	Υ	δ	
OEPone	26	9.13	9.14	9.86	9.83	
1,3-OEPdione	8	8.58	8.39	9.24	9.37	
2,3-OEPdione	32	9.59	8.83	9.79	8.83	
1,4-OEPdione	33	8.81	7.24	9.05	7.42	
1,5-OEPdione	28	9.05	9.71	9.05	9.71	
1,6-OEPdione	29	8.78	8.78	9.59	9.59	
MeOEC	D	8.71	8.87	8.87	9.69	
1,3-DMOEiBC	E	6.56	7.13	8.35	7.28	
2,3-DMOEiBC	F	6.70	7.15	7.15	8.38	
1,4-DMOEiBC	G .	6.44	7.29	7.29	8.35	
1,5-DMOEBC	н	8.52	8.52	8.67	8.67	
ois 1.2 diams	<u> </u>	0 47	8.46	0.56	0.20	
cis-1,3-dione	59a	8.67	0. 4 0	9.56	9.38	
sirohydrochlori	in	6.78	7.36	8.53	7.46	



2,3-DMOEiBC

1,4-DMOEiBC

1,5-DMOEiBC

Table 10. ¹³C-NMR chemical shifts of selected porphyrin, porpnyrinone and porphyrindione.

	compound δ (ppm)							=====
carbon	porpl 5		porphy 11	rinone 1	dion 59		d ₁ free 128	base a
α and β (pyrrole)	136.55 138.16	136.25 137.41 138.23 137.67	133.32 134.58 138.61 141.08	132.58 133.73 135.86 139.14 146.20 153.34	131.40 131.84 136.11 144.90 145.20 161.13	135.05 137.76 167.63 145.56	132.49 134.60 136.87 167.63	135.50
-C- (tertiary)	•••••	•••••	52.15	•••••	49.42	•••••	49.51	•••••
-CH ₂ CH ₂ COCH ₃	173.48	•••••	172.97	173.33	173.20	••••	172.93	•••••
-CH2CH2COCH3	51.63		51.42		51.78		51.77	
O - <u>C</u> H ₂ CH ₂ COCH ₃	32.36 21.69	32.14 21.62	36.71 21.51	36.27 21.10	36.24 21.36	21.12	36.27 21.25	
О -CH= <u>C</u> HCO <u>C</u> H ₃							122.67	52.00
O -CH <u>2</u> COCH₃	171.92	171.83	171.16	170.45	170.54	170.34	170.42	
О -CH₂CO <u>C</u> H₃	52.2 5	52 .21	51.24	50.98	51.59		51.68	51.48
O - <u>C</u> H₂COCH₃	36.83		42.12	31.87	41.67	41.98	41.50	42.21
-CH ₃ (pyroole)	11.47	11.23	11.28	10.86	11.12	10.69	12.87	10.80
-CH ₃ (pyrroline)			23.84		23.46	23.86	23.9 3	23.24
-C=O (ring)			208.35		207.42	207.33	206.53	205.50
α,β.γ,δ (meso)	96.80 96.44	96.64 95.97	99.38 92.96	98.13 91.76	98.88 91.37		102.64 91.54	

spectrum in detail, the general features of ¹³C spectra of porphyrinone and porphyrindione are presented here.

Since the relative contribution of aromatic ring current to the final chemical shift is much less for ¹³C than ¹H, there is less ambiguity about the bond types or neighboring groups in these structures. The spectra of these compounds can be deliberately subdivided into four regions: The aliphatic carbon region with the chemical shifts in the range of 10 to 60 ppm; the meso carbon region, 90 to 105 ppm; aromatic ring carbon region, 125 to 165 ppm; and the carbonyl region in the most strongly deshielded portion of the spectrum, 170 to 210 ppm.

It is evident that the methylene carbons attaching directly to the pyrrole rings have their resonances at upper field in comparison with their counterpart attaching to the saturated pyrroline rings, for example, the methyl group on pyrrole ring appears at 11.3 ppm versus 24 ppm in the saturated ring and the methylene carbon of the acetate, 37 ppm compared to 42 ppm.

The meso carbon signals are closely spaced in porphyrins' case but are spread out in porphyrinones and porphyrindiones. They are quite sensitive to the conjugation effect of the acrylic acid substituent. In the spectrum of cis-dione **59a** the two upper field meso peaks essentially overlap at 91.30 ppm and the two down-field resonances at 96.57 and 98.88 ppm. In cis-d₁, the two upper field peaks separate by more than 1.5 ppm, 89.97 and 91.54 ppm, and the other two peaks are down-field shifted to 98.14 and 102.64 ppm respectively. Except for the 6-acrylate side chain, these two compounds are identical.

The region between 130 to 170 ppm belongs to the resonances of the α and β pyrrole carbons. In the case of porphyrin, these resonances are closely

spaced, 130 to 146 ppm, and exhibit mainly in two sets with the β carbons at the upper field. Owing to the N-H tautomerism at room temperature, these peaks, especially those of the α carbons, are close to coalescence. The N-H exchange might be slower in the porphyrinones and porphyrindiones, since the α and β bands are observed prominently. These bands are also spread out in the whole region with the α carbon next to the keto group significantly down field shifted to 167 ppm.

The signals of the carbonyl carbons on both propionate and acetate side chains are observed in the narrow region from 170 to 174 ppm, whereas the ring carbonyl carbons appear above 200 ppm.

IV. VIBRATIONAL SPECTROSCOPY

A. Infrared Spectra

The IR spectra of 1,3-porphyrindiones, including that of \underline{d}_1 itself, are quite similar to those of isobacteriochlorins, especially where the skeletal bands are positioned. The spectra of heme \underline{d}_1 , in the form of its free base and copper complex, are given in <u>Figure 20</u>, the absorption bands of \underline{d}_1 , in comparison with its precursor dione **59a**, sirohydroporphyrin and DMOEiBC are listed in Table **11**.

The strongest bands in the spectra of \underline{d}_1 from 1713 to 1741 cm⁻¹ and 1170 to 1205 cm⁻¹ are characteristic of C=O and C-OR stretching vibrations of the carboxylate esters. The typical ring C=O bands are observed at 1717 cm⁻¹ as in Cu(II) \underline{d}_1 and OEPdione 8, however this band is usually mingled with the ester bands around 1735 cm⁻¹ in diones with acetate and propionate side chains. The bands in the 2953 to 2851, 1437 to 1457, and 1350 to 1380 cm⁻¹ regions are characteristic of C-H stretching and bending vibrations of

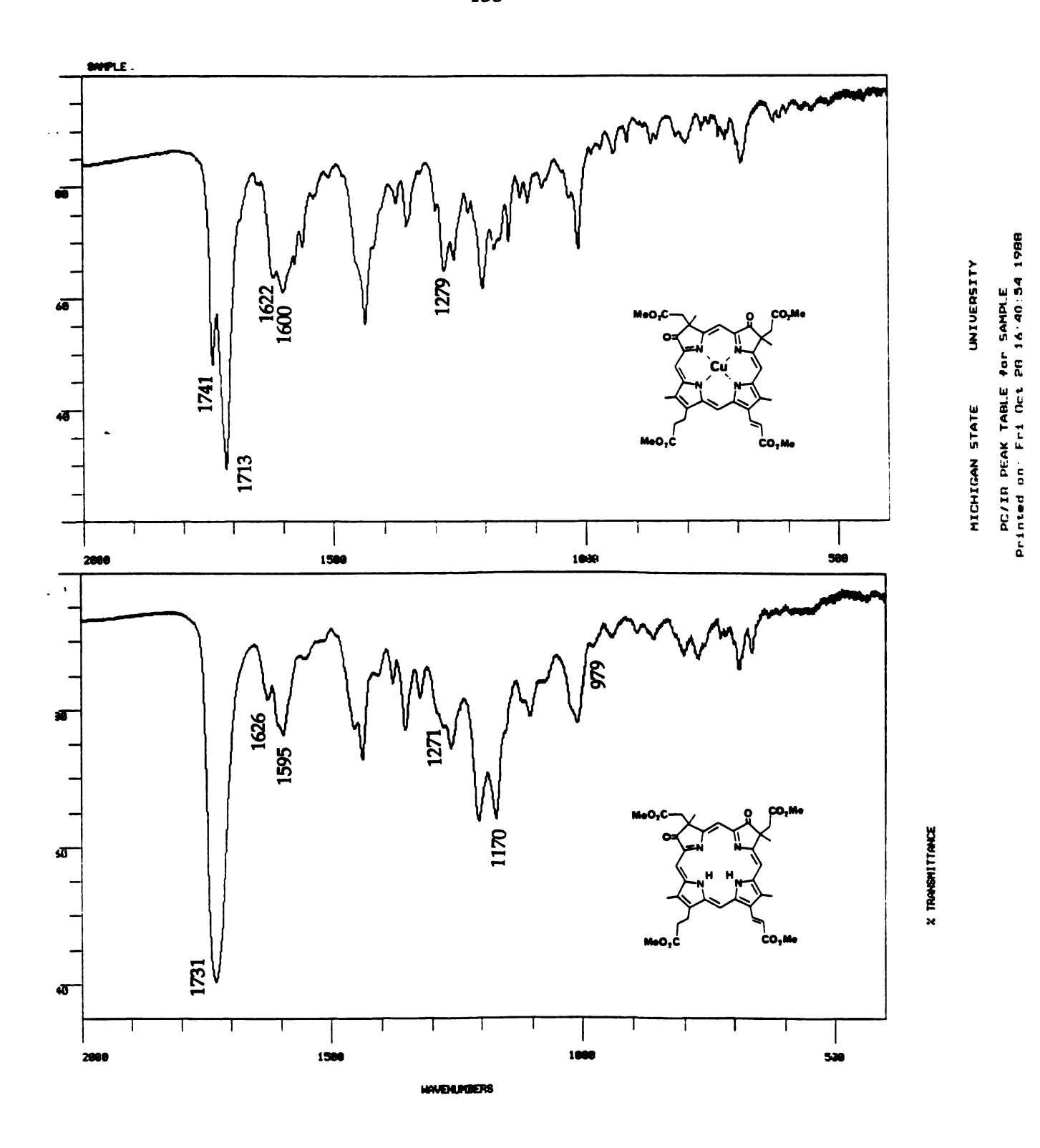


Figure 20 FT-IR spectra of \underline{d}_1 and Cu (II) \underline{d}_1 , samples were prepared as a thin films on NaCl pellets.

MICHIGAN STATE UNIVERSITY

Table 11. Infrared absorption bands of d_1 and porphyrindiones in comparison with sirohydroporphyrin and isobacteriochlorin

d ₁ (cis) 128a	d ₁ (Cu ^{II}) 128a	1,3-dione 59a	1,3-dione 8	siro-hydro- chlorin	DMOE- iBC e			
3369w 3275w	3068w 3039w	3370w 3266w			3363w 3275w			
2954m 2924s 2859m 1731s	2954m 2923s 2852m 1741s 1713s	2953m 2924s 2853m 1735s	2965m 2933s 2875m 1714s	2962s 2887m 1729s	2963m 2931s 2870m			
			1,110		1640m			
1626m 1595m 1550w	1622m 1600m 1576m 1560w	1599m 1546w	1599m 1574m 1541w	1603m	1603s 1570m			
10000	1537w 1511w	1516w	1011W		1539w 1511m 1464m			
1453m 1437m	1453w 1437m 1415w	1451m 1437m 1408w	1457m	1457m	1452m			
1377w 1353w 1324w	1375w 1351w 1328w	1376w 1351m	1380w 1332w	1375w	1397w 1381w			
1324w 1271m	1279m		1318w		1318w 1278w			
1260m	1260m 1232w	1257m	1267w 1246w	1260m	1247w			
1204m	1204m	1203m	1207m	1198m				
1170m	1181m 1168w	1175m		1178m	1188m			
	1151w 1129w 1113w		1140w		1133w 1113w			
1104w	1084w	1106w	1102w	1093m	1110			
1063w	1030w	1067w	1059w		1059w			
	1000₩	1021m	1024w					

Table	11 ((contd.)

1010m	1013m		1001w	1014m	1005
979w	986w		1001W		1003
	971w	965w			
941w	943w	940w	948w		948m
	916w	, 2011	921w		919w
893w	884w	893w	898w		887w
0,0,0	870w	0,011	864w		864w
860w	860w		00111		00111
00011	00011	851w			
		00211		835w	
	819w		820w		827w
800w	801w				U
			791w		
770w	768w	773w	777w		772w
	755w				757w
	735w		741w		
728w	726w	728w			718w
		•	710w		
702w	703w				
690w	691w	685w			685w
666w		668w	674w		666w
			639w		
			617w		

methylene and methyl groups.

Heme d₁ has a prominent band at 1595 cm⁻¹, which is identified as the skeletal band common to all isobacteriochlorin-type structures, revealed by data in Table 11. Previously, it was reported by Mason⁹⁴, who observed a strong band at 1598 cm⁻¹ from the spectrum of tetrahydroOEP. The corresponding absorption bands of bacteriochlorin-type diones are determined in lower frequency region, for example, 1593 cm⁻¹ was observed for Cu(II) 1,5-OEPdione and 1594 cm⁻¹ for 1,6-dione free base. Chlorins and porphyrinones exhibit a medium strength band in this region with slightly higher wavenumbers, as shown in Table 12, methylOEC has a band at 1610, porphyrinone 26 and 111 exhibit one at 1604 and 1606 cm⁻¹, respectively. Porphyrins rarely have bands in the 1500 to 1700 cm⁻¹ region, and such bands when present are usually broad and weak. Therefore, the band at 1600 cm⁻¹ vicinity can be considered as the diagnostic absorption for porphyrindiones and isobacteriochlorins.⁹⁵

The acrylate side chain should add two types of IR bands arising from the conjugated olefinic and ester groups. However, these bands are not so easily identified in the spectrum of \underline{d}_1 due to their overlapping with the other C=C and -COOR modes. Alternatively, the contribution from the acrylate function to the spectrum is best illustrated by comparing the spectrum of a porphyrin acrylate 146 and its precursor porphyrin 61, as shown in Figure 21.

The C=C stretching mode of acrylate stands out clearly at 1623 cm⁻¹ in the spectrum of porphyrin acrylate 146, corresponding to a band at 1626 cm⁻¹ in the spectra of \underline{d}_1 free base and 1620 cm⁻¹ of its Cu(II) complex. Notably, this band is more prominent for porphyrin acrylate since it is not marred by the strong skeletal absorption observed around 1600 cm⁻¹ in the \underline{d}_1 spectra. The ν (C=C) mode is commonly seen as a doublet for acrylates, resulting either

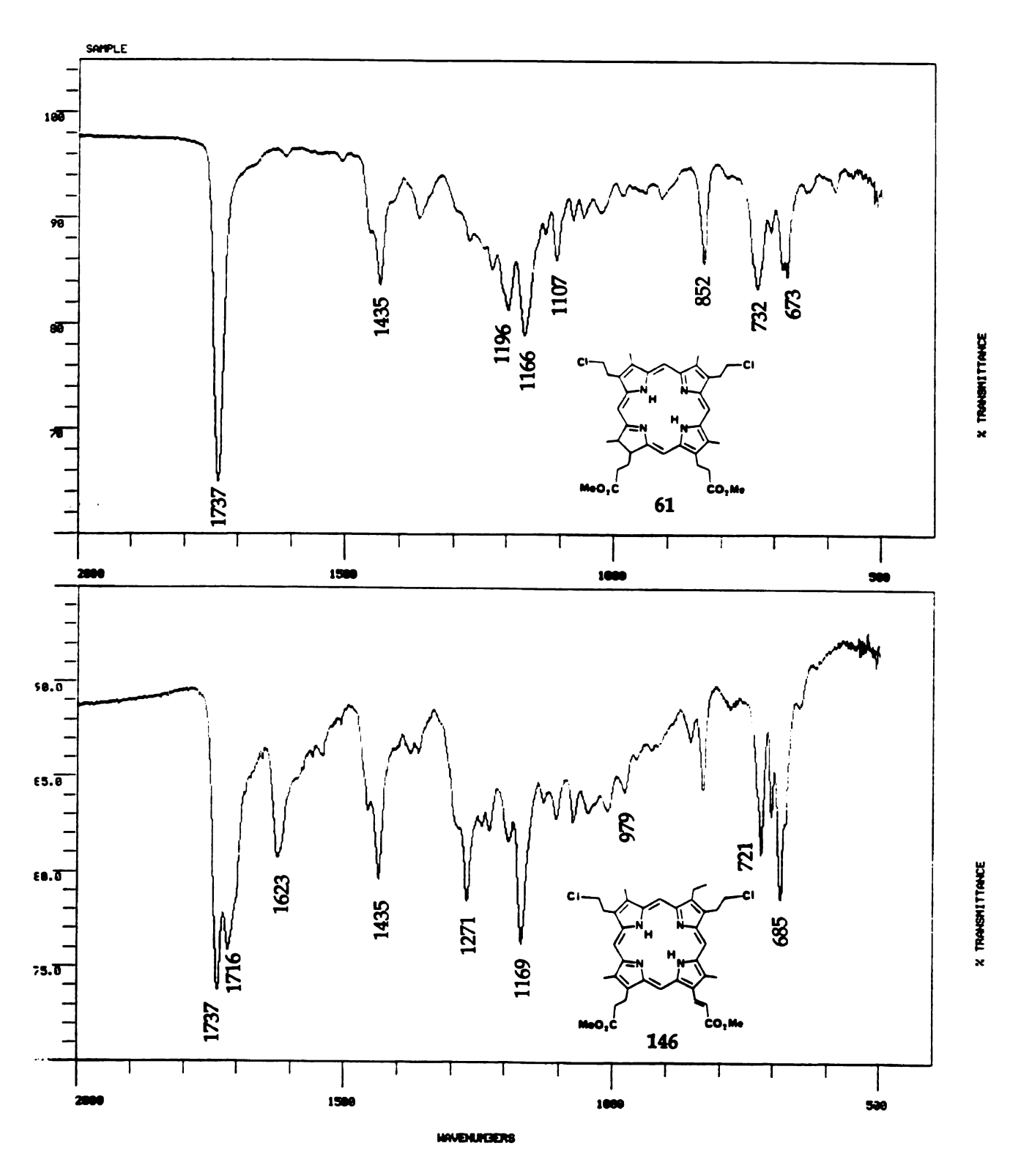


Figure 21 FT-IR spectra of porphyrin 61 and acryloporphyrin 146, samples were prepared as a thin films on NaCl pellets.

from an overtone or due to rotational isomerism;⁹⁶ however, no evidence for the second band is observed in the spectra of \underline{d}_1 and its synthetic models.

Out of plane =CH deformations are expected for trans acrylates at ~980 to 974 cm⁻¹, 96 and are observed at 979 cm⁻¹ as a weak but clear band for both \underline{d}_1 and porphyrin acrylates 146. The cis acrylate should have a band around 820 cm⁻¹, but no such absorption was ever observed in the \underline{d}_1 spectrum, suggesting a trans acrylate side chain.

The carbonyl stretching mode, $\nu(C=O)$, of the methyl acrylate group is observed at 1718 cm⁻¹, but it is usually overlapped with the $\nu(C=O)$ modes of the two ring keto groups in the spectra of \underline{d}_1 and the other porphyrinones and porphyrindiones. This band bifurcated at 1716 cm⁻¹ due to the propionate ester band as can be seen in the spectrum of porphyrin acrylate **146**. The C-O stretching modes of the acrylate group at 1310 to 1250 cm⁻¹ and 1200 to 1100 cm⁻¹ are observed at 1271 and 1270 cm⁻¹ for **146** and \underline{d}_1 respectively and around 1170 cm⁻¹ in both cases in combination with the bands of the propionate esters.

In the free base \underline{d}_1 spectrum, two N-H stretching bands are observed at 3275 and 3369 cm⁻¹ with an overtone band of the carbonyls at 3423 cm⁻¹. The presence of two ν_{N-H} suggests two nonequivalent hydrogens in the cis- \underline{d}_1 structure, as has also been proved by X-ray study which indicated both hydrogens are located at the southern ring C and ring D pyrrole nitrogen, and they are nonequivalent due to the asymmetric structure of \underline{d}_1 . This is to be compared with isobacteriochlorins where two bands with different intensities were recorded suggesting the presence of two different tautomers.⁶⁰ The N-H stretching vibrations appear as a clean single band in the region of 3335 to 3345 cm⁻¹ for porphyrinones and in 3310 to 3340 cm⁻¹ for porphyrins.

Table 12 gives the infrared absorption bands of some selective

Table 12. Infrared absorption bands of porphyrinones in comparison with chlorin.

====			===========	:==========
	acrylo-) / OTO
	porphyrinone	porphyrinone	porphyrinone	MeOEC
		111	26	D
	3342w	3338w	3336w	3341w
	2956m	2952m	2963 s	2963s
	2922m	2925m	2933m	2931m
	2852m	2857m	2872m	2868m
	1738s	1737s		
	1714s		1713s	
	1623m			
	1614m	1606m	1604m	1609s
	1588w		1586m	
	1559w	1557 w		
	1542w			1540m
	1522w	1516w	1522w	1519w
			1465m	
	1456m		1454m	1449w
	1436m	1437m		
	1402w		1403m	1397w
	1378w	1376w	1372w	1373w
				1360w
	1352w	1350m		
			1320m	1311w
	1274m	1261m	1265w	1266w
	1239w			
	1225w		1224w	1229w
	1195w	1198m	1184m	1198m
	1168m	1169m	1163w	1165w
				1153w
	1130w		1136w	

table 12 (contd.)

1101w	1109w		
		1095m	1097w
	1088w		1085w
1073w	1076w		
	1059w	1056m	1056m
	1021m		
			1014w
999w		998m	988m
	966w		
978w			
949w	952w	952m	945m
914w	91 4 w		
885w	896w	898w	896w
			885w
		862w	
855w	850w	846w	845w
838w			
		825w	824w
744w		741w	744w
		732m	732m
718m		715m	712m
	706m	703w	701w
690m		682m	685w
672m	672m	666w	664m
630w	629w		
		608w	603w

porphyrinones. Methyloctaethylchlorin (MeOEC), is also included for comparison. The similarity between these two systems are easily observed.

B. Resonance Raman Spectra

In the metal complex of porphyrindione, there is an inherent x, y inequivalence of the macrocyclic π -conjugation pathways, resulting in an absorption spectrum possessing separately allowed Q_x and Q_y visible transitions and two Soret transitions. The visible spectrum of Cu(II) \underline{d}_1 is given in Figure 3c, and as seen therein, the wavelength chosen for excitation, Ar ion-laser at 457.9 nm and Kr ion-laser at 406.7 nm, are on the different side of Soret band (437 nm). The resonance Raman spectrum of extracted natural \underline{d}_1 methyl ester and model compound 6 and 10 in their Cu(II)-metallated form are shown in Figure 22, and the spectra of copper complexes of synthetic \underline{d}_1 and dione 59a are given in Figure 23. The similarity between these two sets of spectra is obvious, however, the spectra obtained upon excitation at 457.9 nm have their lower frequency modes intensified whereas those under 406.7 nm excitation have their higher frequency bands enhanced.

It is noteworthy that the number of the resonance Raman active vibrations of \underline{d}_1 and the 1,3-dione model compounds, either with or without the acrylate side chain, far exceeds those apparent in Soret-excited scattering from metalloporphyrins. This is due to the reduction in symmetry of the chromophore from D4h to Cs, allowing the Raman-forbidden Eu vibrational modes of the higher symmetry structure to become Raman active modes in the low symmetry.

In 1981, Ching et al.⁹⁷ reported the resonance Raman spectra of cytochrome \underline{cd}_1 nitrite reductase using selective excitation to study heme \underline{c} and \underline{d}_1 . With excitation in the Soret region of heme \underline{d}_1 they observed an

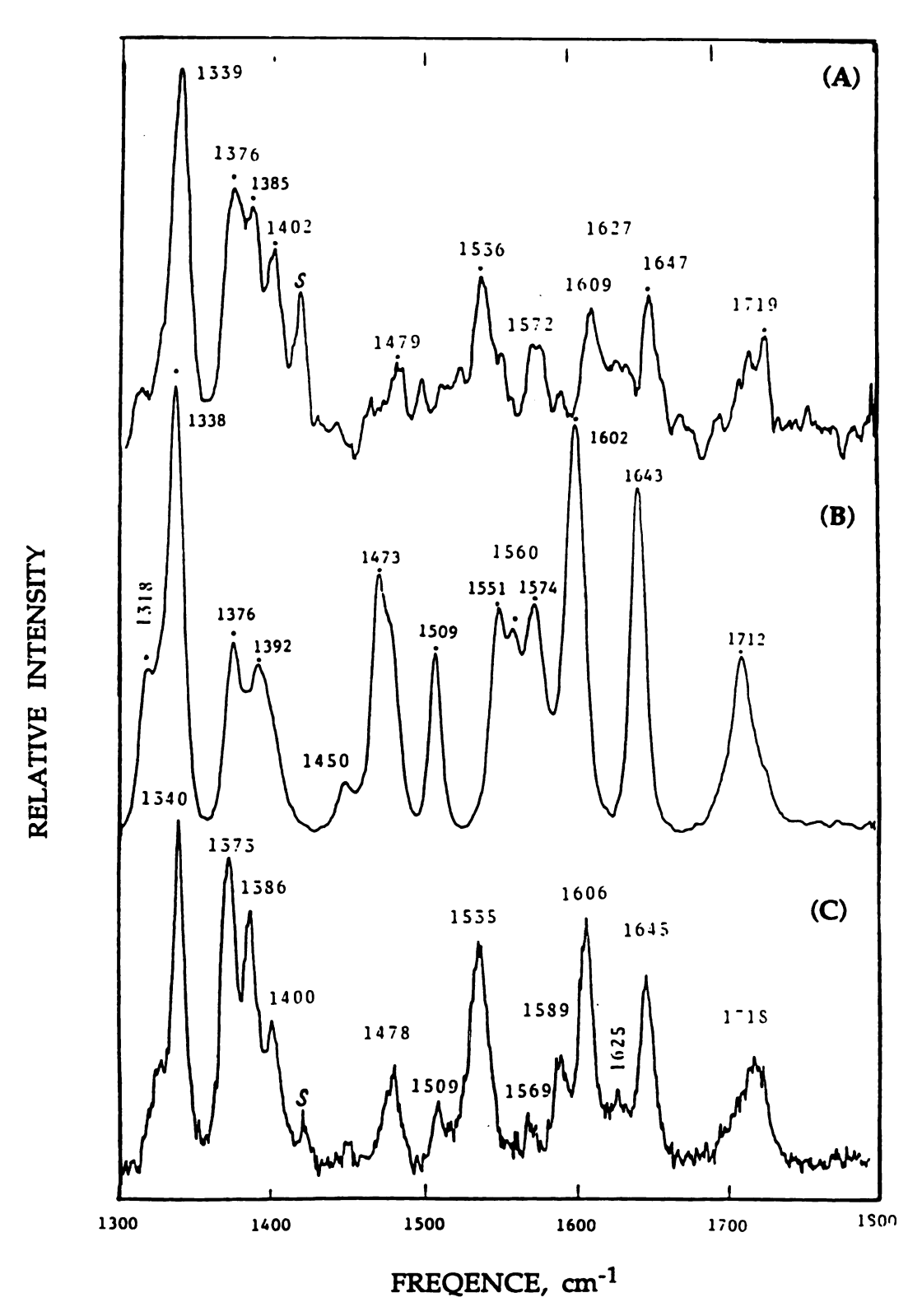


Figure 22 Resonance Raman spectra of (A) natural -d₁ Cu (II) complex; (B) 1,3-dione 6 Cu (II) complex and (C) acrylo-1,3-dione 10 Cu (II) complex at ~2 °C, sample A and B in CH₂Cl₂, and sample C as ~1 mg/100 mg KBr; 457.9 nm laser excitation (50 mW).

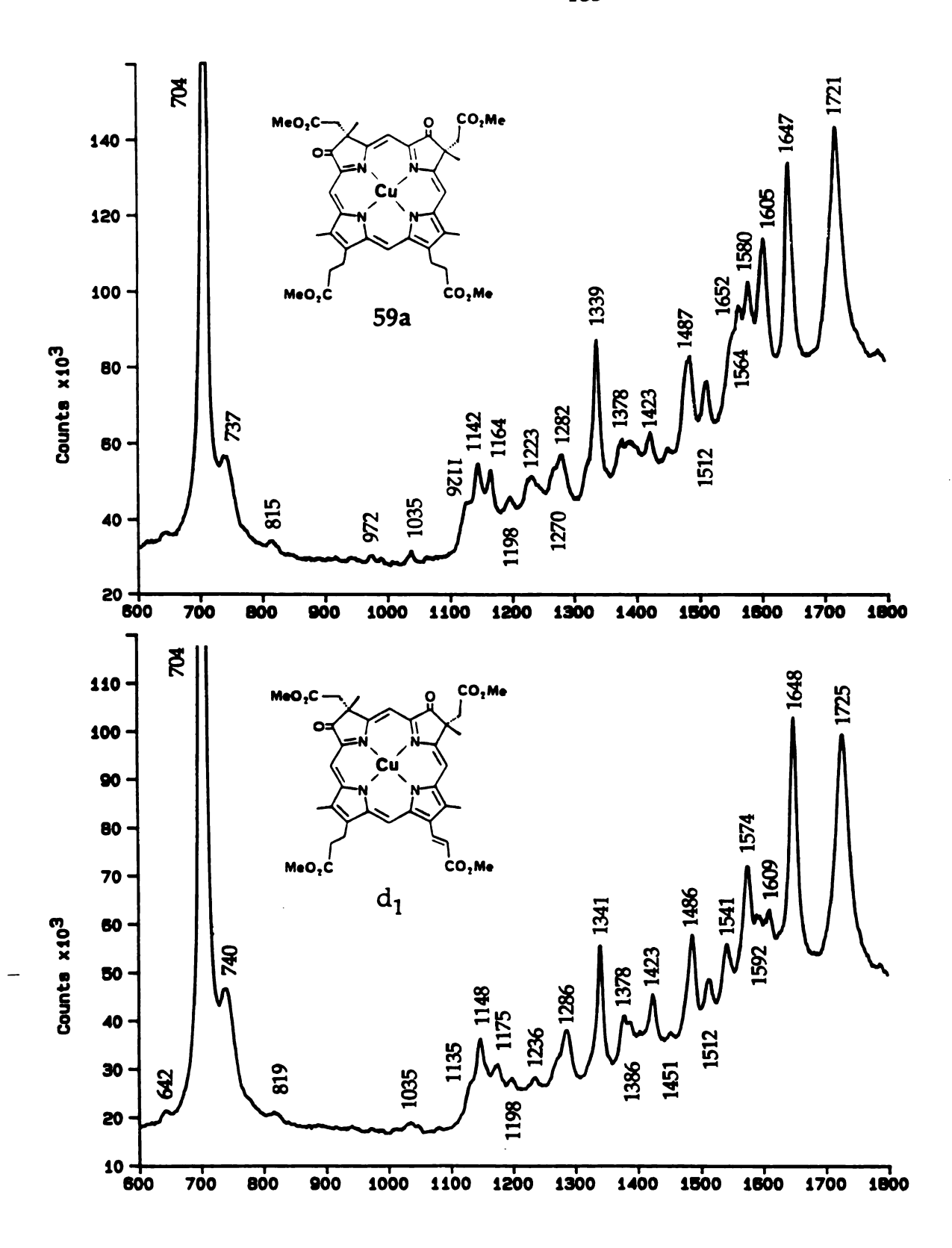


Figure 23 Resonance Raman spectra of Cu (II) complexes of synthetic \underline{d}_1 128 a and 1,3-dione 59a in $\mathrm{CH_2Cl_2}$.

unique mode at 1715 cm⁻¹ for ferrous heme, and a 1725 cm⁻¹ band with increased intensity for the ferric state, indicating a functional group interacts strongly with the heme electronic system. Since no Raman modes had ever been recorded in this region for porphyrins and hydroporphyrins, these authors suspected the presence of an carbonyl group on the heme ring, or on a chlorin ring based on RR results of porphyrindione compounds obtained previously by our coworkers at MSU.⁹⁸

The bands at 1715-1725 cm⁻¹ in the spectra of Cu(II) \underline{d}_1 can now be unambiguously assigned to the localized stretching modes, $\nu(C=0)$, of the keto groups on the ring. Because the 1725 cm⁻¹ mode in Figure 23b appears as a broad band with the highest intensity and the ~1720 cm⁻¹ feature in Figure 22a seems to have one or more shoulders at lower frequency, it is likely that these bands contain separate vibrational components, including possibly that from the acrylate ester group, similar to what observed from the IR study.

A major difference between the spectrum of Cu(II)- \underline{d}_1 and that of dione 59a occurs in the 1500-1610 cm⁻¹ region. The former exhibits a fairly intense feature at 1541 cm⁻¹ and a multiple band around 1590 cm⁻¹ with a prominent feature at 1574 cm⁻¹ as well as a weak 1609 cm⁻¹ band. However, for dione 59a, the 1541 cm⁻¹ band is absent, with an intense feature at 1605 cm⁻¹ instead and a weak one at 1564 cm⁻¹ in the multiple band region. The altered pattern of intensity between these two systems suggests differences in excited states of these macrocycles. Furthermore, since the vibrational modes in this region are dominated by the stretching of the Cb-Cb and Ca-Cm bonds, it is evident that the presence of the acrylate substituent has a remarkable influence on the π -system of the entire porphyrindione macrocycle.

The intense feature at \sim 1340 cm⁻¹ in the spectra of all the diones, including \underline{d}_1 itself, could be assigned to the oxidation-state-sensitive-band

 (ν_4) according to Cotton et al,⁹⁹ who observed the similar feature from the spectra of cytochrome <u>cd</u>₁. The presence of multiple bands in this region, at 1370-1400 cm⁻¹, is another feature of porphyrindiones. Corresponding multiple bands have also been observed in the RR spectra of siroheme¹⁰⁰ and bacteriochloropyll^{101,102} as well as in a variety of metallochlorin complexes.¹⁰³

V. X-RAY DIFFRACTION ANALYSIS

The results of an X-ray study¹⁰⁴ of 1,3-OEPdione 8 and its Cu(II) complex established the molecular structure of 1,3-porphyrindione, i.e., the core of \underline{d}_1 . The structure, atom labels, bond distances, and deviation from planarity are presented in Figure 24.

These data revealed that there is an expansion of core size because of the lengthening of the metal center to the pyrroline-N distance in comparison with corresponding porphyrins, and this is similar to that occurring in the isobacteriochlorin structure. 105 , 106 It appears to be a general phenomenon that whenever a pyrrole ring is saturated, there is up to 0.05 A center to N elongation. Thus, \underline{d}_1 and isobacteriochlorin, such as sirohydrochlorin, intrinsically have a hole size about 4% lager than a porphyrin core.

Both of the free base and Cu(II) complex of 1,3-dione 8 are nearly planar and are comparable to other Cu(II) porphyrins. The structure of the corresponding Ni(II) complex is not known, but likely to be ruffled in analogous to other Ni(II) hydroporphyrins that also have an expanded core size (Figure 25).¹

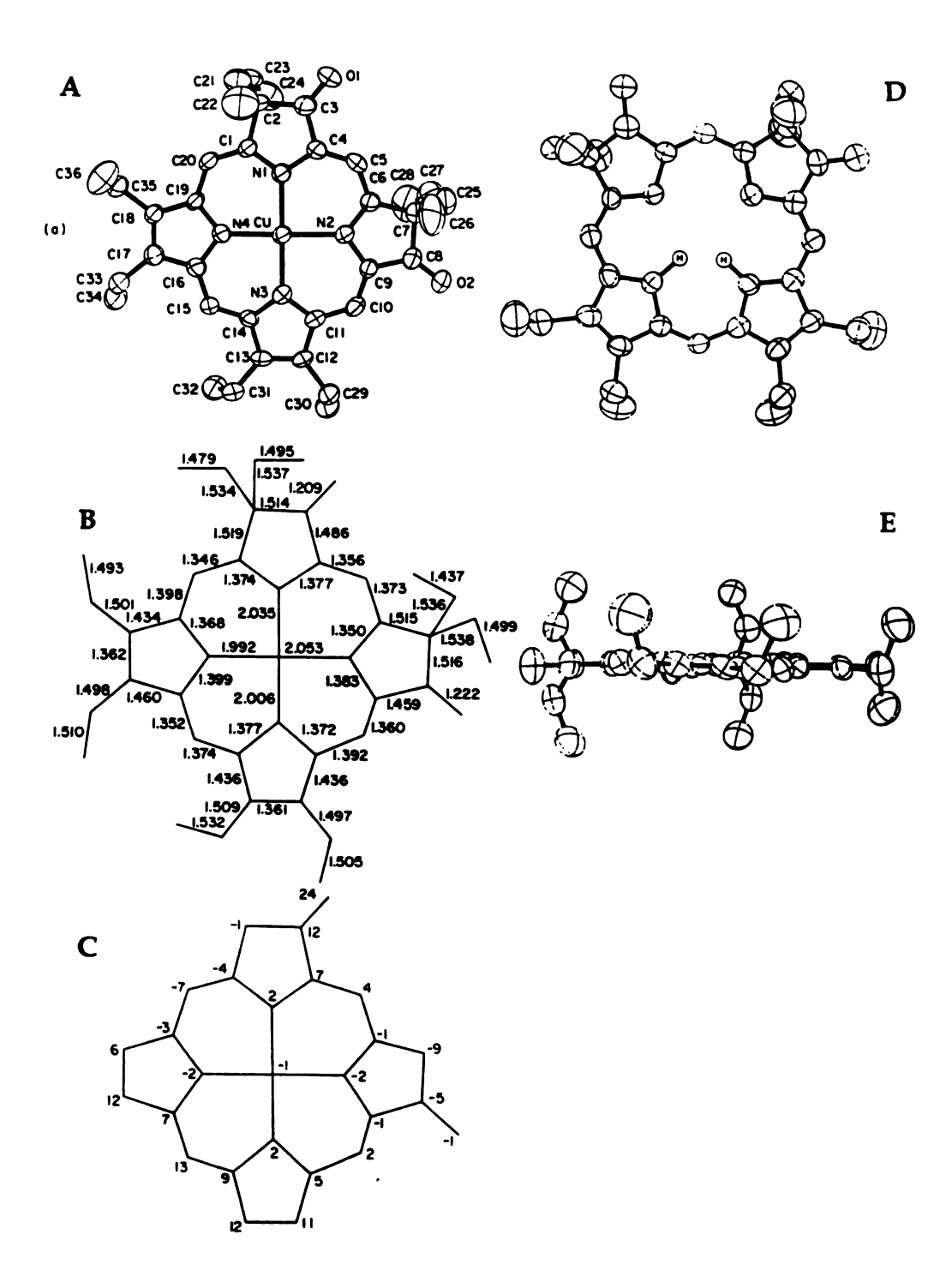


Figure 24 (A) Molecular structure and atom labels of Cu (II) 1,3-dione 8, (B) bond distance,

(C) deviation from the plane of the four nitrogens. (D) Free base of 1,3-dione 8, (E)

Another view of D.

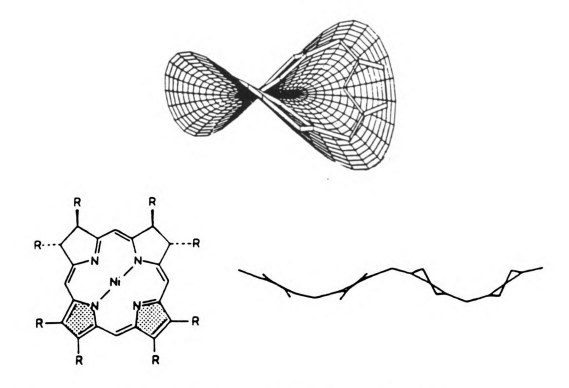


Figure 25. Geometric model of the ruffling of Ni(II) isobacteriochlorin. 1

The large core size in dione heme and siroheme should favor certain coordination reactions involving high spin-low spin transitions. Also, the combined effect of electronegative nature of dione heme and large central hole should stabilize the low valent metal complexes of \underline{d}_1 .

In a separate study of the X-ray structure of the free base 1,3-OEPdione 8^{119} a difference electron density map of the central cavity revealed that both of the inner N-H hydrogens are located at the adjacent pyrrole rings (ring C and ring D) thus completing an 18-electron aromatic system. The corresponding isobacterio- chlorin system has multiple valence tautomeric forms with the inner protons scrambled among the four nitrogens, and in some of these forms the π -conjugation is interrupted resulting in a lowered aromaticity of isobacteriochlorin, as discussed in the $^1\text{H-NMR}$ study.

IV. THE REDOX PROPERTY

The redox chemistry of porphyrinone and porphyrindiones has been examined by cyclic voltammetry. 104 The results are listed in Table 13. The porphyrinone and porphyrindiones exhibit ring oxidation potentials very similar to those of porphyrin, and in sharp contrast to those of their hydroporphyrin cousins, especially to that of isobacteriochlorins which are significantly easier to oxidize than the porphyrin (by as much as $0.6V^{107,108,125}$). An immediate consequence of this invariance is that the Fe(II)CO complex of porphyrindione oxidizes to Fe(III) with concomitant loss of CO as opposed to Fe(II)COiBC, which yields a stable Fe(II)COiBC+ π -cation radical on oxidation. Also, in contrast to the behavior of chlorins and isobacteriochlorins, which are harder to reduce than porphyrins, $^{107,\ 108}$ the porphyrinone and porphyrindiones are easier to reduce. Note that the Fe(II)/Fe(III) couples are also shifted so that the metal centered reductions become easier.

Extended Huckel MO calculations¹⁰⁴ helped rationalize the observed redox trends and indicated that the HOMOs of porphyrins, porphyrinones and porphyrindiones fall within a narrow energy range, unlike those in chlorins, bacteriochlorins and isobacteriochlorins. The calculated energies for the HOMOs of model zinc complexes are listed in <u>Table 14</u>. The more negative orbital energies correspond to harder to oxidize molecules. For reduction potentials, the more negative LUMOs will translate into easier to reduce molecules. LUMO energies are also given in <u>Table 14</u>. The calculated net charges on the metals also increase with addition of keto groups, which should therefore result in the metal being harder to oxidize, as observed. The experimental redox trends are thus reasonably well predicated by the

Table 13. Redox potentials of porphyrin, porphyrinones and porphyrindiones (vs. SCE)^a

=======================================			
compound	ring/ring+ 	Fe ³⁺ /Fe ²⁺	ring/ring ⁻
porphyrin (OEP)			
H_2	0.83		-1.46
Cu	0.73		-1.46
FeCl	0.9	-0.5 ^b	
Fe(MeIm) ₂ ^c		-0.37	
Fe(MeIm)CO		0.38 ^d	
porphyrinone (26)			
H_2	0.84		-1.36
Cu	0.68		-1.37
FeCl	0.95	-0.34 ^b	
Fe(MeIm ₎₂ c		-0.19	
Fe(MeIm)CO		0.41 ^d	
1,3-dione (8)			
H_2	0.82		-1.29
Cu	0.67		-1.27
FeCl	0.84	-0.24 ^b	
Fe(MeIm) ₂ ^c		0.06	
Fe(MeIm)CO		0.53 ^d	
MeOEiBC (E)			
H ₂	0.82		-1.19

 $^{^{}a}E_{1/2}$ obtined by cyclic votammetry at a Pt electrode in $CH_{2}Cl_{2}$ containing 0.1 M tetrabutylammonium perchlorate. $^{b}Qusi$ -reversible. $^{c}In \ 2 \ M \ N$ -methyl imidazole. $^{d}Irreversible$ loss of CO.

molecular calculations.

Zn 1, 6-dione

Table 14. The calculated energies for the LUMOs and HOMOs of model zinc complexes.

LUMO Zn porphyrin -9.195eV Zn monoketone -9.394eV Zn 1, 3-diketone -9.276eV Zn isobacteriochlorin -8.752eV -9.547eV Zn 1, 6-diketone HOMO Zn porphyrin -11.159eV Zn monoketone -11.189eV Zn chlorin -10.823eV Zn isobacteriochlorin Zn 1, 3-diketone -10.935eV -10.338eV

Zn bacteriochlorin

-10.279eV

VII. THE BASICITY OF THE CENTRAL NITROGENS

-10.953eV

The PK₃ values (addition of the first proton, PH₂ + H⁺ \longrightarrow PH₃⁺) of some porphyrindiones have been determined in 2.5% sodium dodecyl sulfate: 1.8 for model compound 8, 1.7 for dione 10 and \underline{d}_1 itself. These values are drastically less basic than that of common porphyrins (3.0-5.8) or chlorins (3.5-4.2).¹⁰⁹ The extremely weak basicity of \underline{d}_1 and corresponding diones

relative to isobacteriochlorins is derived from the strong electron-withdrawing effect of the ring-keto groups which cause the central nitrogens less basic. Similarly, the monoketone compound **26** has been reported unable to form its cation PH₃⁺ by reaction with chloroacetic acid in benzene, unlike its chlorin counterpart which is fully protonated under the same reaction condition.¹¹⁰

VIII. EXPERIMENTAL

Visible absorption spectra (in CH_2Cl_2 or $CHCl_3$) were measured with a Cary 219 or a Shimadzu 160 spectrophotometer. Spectra were plotted directly from data stored on floppy diskettes.

¹H- and ¹³C-NMR were obtained at 250 MHz on a Bruker WM-250 instrument. Spectra were mostly recorded in CDCl₃; the residue CHCl₃ was used as the internal standard set at 7.24 ppm.

IR spectra were obtained from KBr pellets (~1 mg compound/100 mg KBr) or films on NaCl pellets (by evaporating the CHCl₃ solution of the samples) on a Perkin-Elmer Model 1800 FT-IR instrument and a Nicolet IR/42 spectrometer.

Raman spectra in Figure 22 were obtained with a computer controlled Jarrell-Ash scanning spectrophotometer using a Spectra-Physics 164-05 Ar laser. Spectra were collected in back-scattering geometry on anaerobic solution samples (~1 mg/ml in CH₂Cl₂) maintained at 2 °C in a sample dewar. Alternatively, room temperature spectra were recorded on polycrystalline samples dispersed in KBr (~1 mg sample/100 mg KBr) pressed into the angular groove of a spinning sample holder. Spectra in Figure 23 were obtained from samples spining in cylindrical quartz cells and freshly

distilled CH₂Cl₂ was used as solvent. The Raman equipment included a Spex 1401 Ramalog with PMT detection and a Spex 1877 B outfitted with a EG&G model 1421 detector and OMA III computer. The laser system used is Innova 90 krypton ion laser.

Cyclic voltammetry was performed using a Bioanalytical System CV-IA unit. All measurements were carried out in CH_2Cl_2 containing 0.1 M tetrabutylammonium perchlorate at a scan rate of 200 mV/sec.

CHAPTER 6

RECONSTITUTION OF CYTOCHROMe \underline{cd}_1 WITH NATIVE AND SYNTHETIC HEME \underline{d}_1

I. PREVIOUS WORK

Yamanaka and Okunuki¹¹⁰ first studied the reconstitution of cytochrome $\underline{cd_1}$ from \underline{P} . aeruginosa with the extractable heme \underline{d}_1 group as well as other porphyrin hemes. The oxidase activity of the reconstituted protein was determined by the oxidation of reduced cytochrome \underline{c}_{551} under aerobic conditions and the nitrite reductase activity was examined by the oxidation of cytochrome \underline{c}_{551} anaerobically in the presence of nitrite. They obtained a 37% recovery of oxidase activity and 54% recovery of nitrite reductase activity with heme \underline{d}_1 reconstituted enzymes and partial activity recovery with other hemes. Hill and Wharton¹¹¹ later reconstituted the same enzyme with natural heme \underline{d}_1 by a different method and restored almost quantitatively the original oxidase activity. They also found that, except for the heme \underline{a} which yielded 5% activity after reconstitution, no other heme showed any activity.

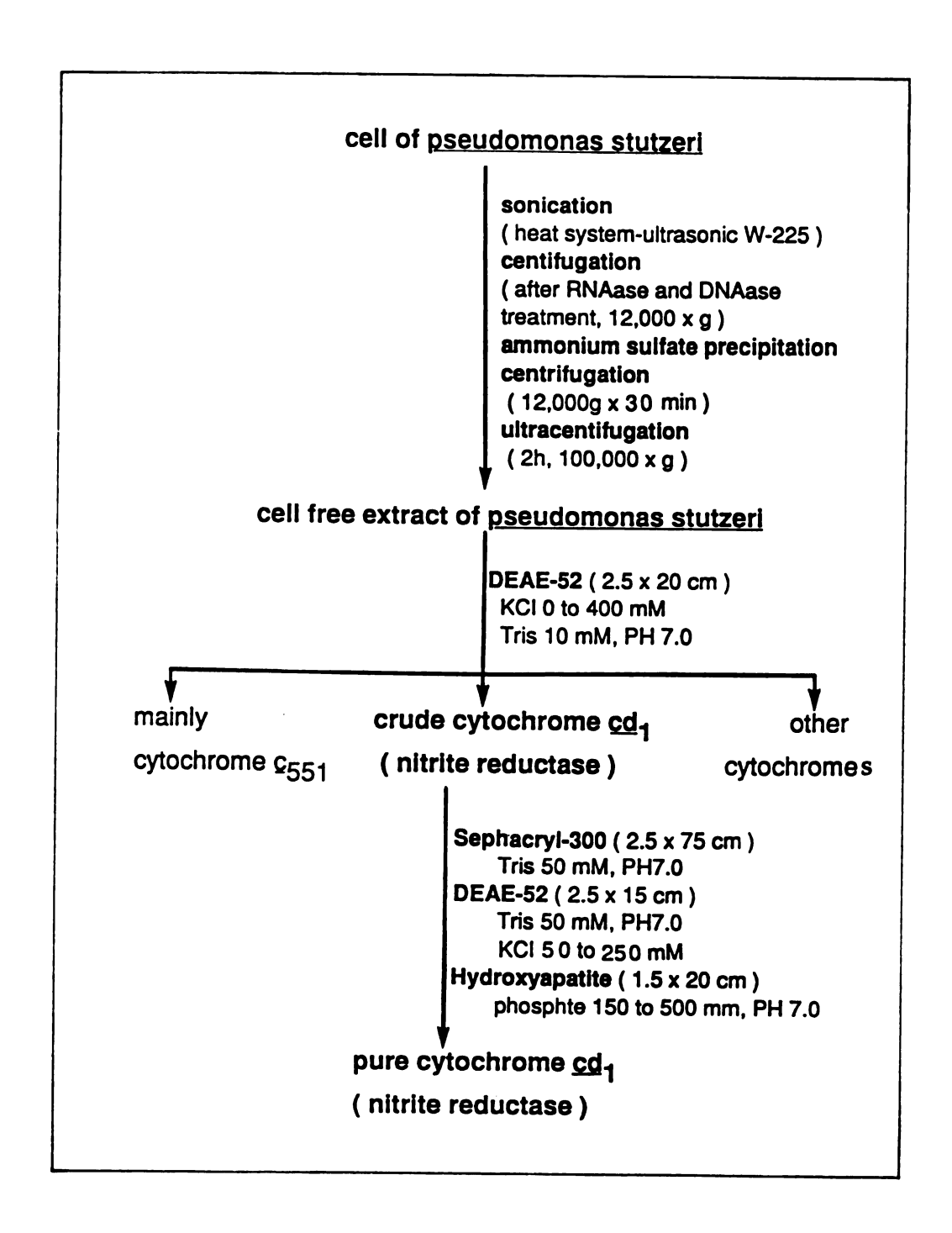
This chapter describes our reconstitution work on nitrite reductase from P. stutzeri with both native and synthetic heme \underline{d}_1 groups. The spectral properties and the NO and N₂O producing activities of the reconstituted enzymes give further evidence that the unusual dione structure of \underline{d}_1 is correct and the synthetic compound is fully functional.

II. EXPERIMENTAL

A. Preparation of Apoprotein

Nitrite reductase was prepared and purified from Pseudomonas stutzeri (strain JM 300) by the method of Weeg-Aerssens et al. 112 The overall procedure is shown in Scheme 28. Basically, 65 g of cell paste, harvested from 15 liter of tryptic soy broth containing 5 g of KNO3, 2 g of NaHCO3, 10 μ g of CuSO4 and 10 mg of FeSO4. 7H2O, yielded about 45 mg of cytochrome cd1. Since the significant loss of the green heme d1 concentration in each stage of chromatography and dialysis has been observed, above procedure can also be simplified by using just 3 steps: a DEAE-52 column to separate cytochrome c551 and other cytochromes, a Sephacryl-300 sizing column, and then directly to hydroxylapatite to obtain higher total yield of pure enzyme. If the purity of the enzyme is not strictly required, two DEAE columns only can offer an even higher yield with about ~90% purity with much less effort. All the purification and reconstitution operations were carried out in a cold room (4 °C).

The apoprotein of nitrite reductase was prepared according to the procedure developed by Hill and Wharton. Typically, 2 mg of pure enzyme in 1 ml of buffer (25 mM HEPES, PH 7.3) was treated with 5 ml of cold acidified acetone (0.024 N HCl). The apoprotein was precipitated and the green heme \underline{d}_1 was extracted into the overlying acetone solution after shaking the mixture for 1 minute. The apoprotein was separated from acetone by centrifugation at 1000 x g for 5 minute and the precipitate was extracted once more with 3 ml of acidified acetone to ensure complete removal of heme \underline{d}_1 . The protein precipitate was washed once with 3 ml of phosphate buffer (25 mM, PH 7.0). The pellet was then redissolved in



Scheme 28

phosphate buffer containing 6 M of urea with gentle stirring until a homogeneous reddish solution formed. The apoprotein solution was stored at 0 ° C for use in next step.

B. Preparation of Heme d₁

The native heme \underline{d}_1 was exacted from nitrite reductase by the procedure described above. The green acetone solution containing heme \underline{d}_1 was brought to near dryness in the dark by blowing the acetone off with a stream of nitrogen. The residue was dissolved in the phosphate buffer (25 mM, PH 7.3) and centrifuged to remove any remaining protein precipitate. The heme \underline{d}_1 solution was adjusted to PH 7.0 in an ice bath with NaOH (1 N) and stored in the dark under argon.

The iron insertion of the synthetic heme \underline{d}_1 tetramethyl ester was accomplished by the standard ferrous sulfate pyridine/acetic acid method. Hydrolysis of the methyl ester was carried out by dissolving 5 g of the ferric heme \underline{d}_1 tetramethyl ester in 10 ml of tetrahydrofuran (THF) followed by addition of 1 ml of KOH solution (1 N). The reaction solution was stirred in the dark under argon for 10 hours or until the organic layer had become almost colorless. THF was then evaporated and the PH of the aqueous solution was adjusted to 7.0 with HCl (1 N) in an ice bath. This heme solution was also stored in the dark under argon to avoid decomposition.

C. Reconstitution of Nitrite Reductase

The reconstitution was carried out according to Hill and Wharton's procedure modified as follows. To maximize the yield of incorporation of heme \underline{d}_1 into the apoprotein, excess amount of heme \underline{d}_1 , 10 to 1, was used. The heme \underline{d}_1 solution was added to the heme \underline{c} containing apoprotein

solution and the mixture was incubated with gentle stirring for 30 minute, then dialyzed with agitation for 12 hours against phosphate buffer (10 mM, PH 7.0). The dialysis medium was change twice during the period. The reconstituted enzyme was separated from the excess of heme \underline{d}_1 by passing the crude enzyme solution over a short DEAE cellulose column (DE-23, Whatman, 0.5 x 5 cm). Heme \underline{d}_1 , which has a pKa of 4.5, stick tightly at the top of the column and the reconstituted enzyme was eluted off with additional concentrated phosphate buffer (100 mM, PH 7.0). The reconstitution is very straightforward: a successful reconstitution invariably gave a well defined narrow band of the protein from the column, whereas nonbounded ones, such as that with protoheme, resulted in a very defused band.

D. Estimation of Protein

The concentration of protein was estimated by the bicinchoninic acid method of Smith et al¹¹³ using crystalline bovine serum albumin as the standard. The relative concentration of the reconstituted enzyme was also estimated by taking the ratio of the absorbance at 522 and/or 555 nm versus that of intact enzyme in the reduced state. Both methods gave comparable values. The concentration of heme \underline{d}_1 was estimated by using the published extinction coefficient of 32,100 M⁻¹ cm⁻¹ for the imidazole-ferriheme complex. Absorption spectra were recorded on a Perkin Elmer 5 or a Cary 219 spectrophotometer.

E. Activity Assay

Activity was measured by gas evolution (NO and N_2O) from nitrite with NADH/phenazine methosulfate (PMS) as the electron donor system. The

assay contained 6 μ mol NADH, 0.36 μ mol PMS and 3 μ mol NaNO₂ in a total volume of 3 ml. All stork solutions were made in HEPES buffer (50 mM. PH 7.3). A mixture of NADH and nitrite solutions was made oxygen free by repeatedly evacuating and fill with argon. The deoxygenated mixture was added anaerobically to a 25 ml serum bottle containing the PMS solution in buffer which had been flushed with argon. The reaction was initiated by addition of the enzyme, about 1 μ g. The nitrite concentration (0.5 mM) was in excess for both NO and N₂O production. Enzyme activity was based on the initial rate of NO and N₂O evolution.

Gas evolution was monitored on a Perkin Elmer 910 gas chromatograph equipped with ⁶³Ni electron capture detector and Porapak Q column under conditions previously described. Carrier flow rate was adjusted so that the approximate retention time for NO and N₂O were 1 and 2.2 minute, respectively. Under these conditions the retention times of nitric oxide and oxygen were extremely close and it was necessary to use strict anaerobic techniques for sampling and injecting the gas phase of the assay vials. We used a gastight syringe equipped with a gas lock and the needle and syringe were flushed with argon before use.

III. SPECTRAL CHARACTERIZATION

The acetone extract containing green heme \underline{d}_1 has an absorbance maximum at 427 nm (Soret band) and a broad plateau from 520 to 520 nm with the low intensity maxima at 529, 575 and 612 nm. This spectrum is essentially the same as that from \underline{P} . aeruginosa by Yamanaka and Okunuki. The spectrum of synthetic heme \underline{d}_1 in acidified acetone is indistinguishable from that of the native \underline{d}_1 as shown in Figure 26. The

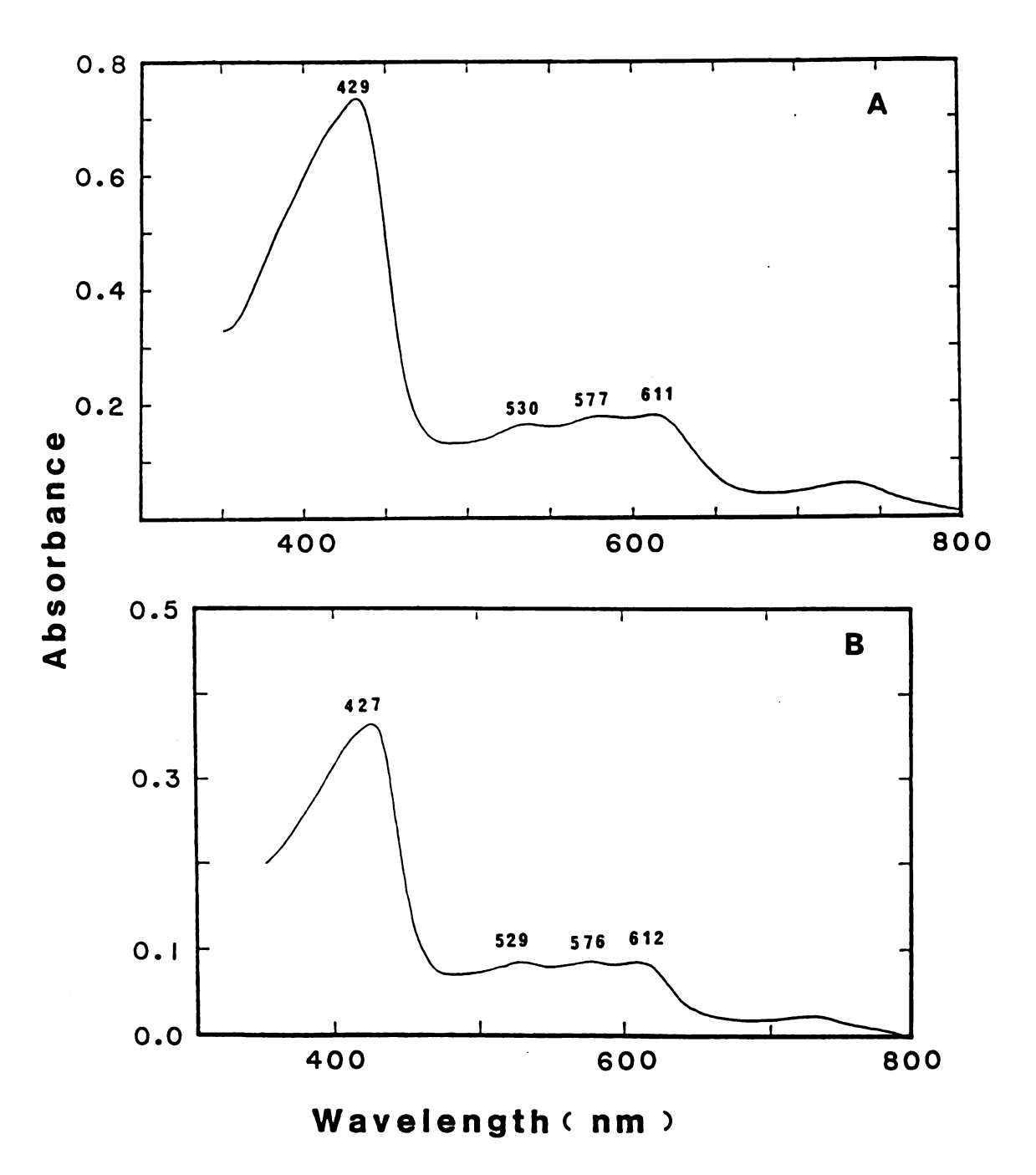


Figure 26 UV-vis spectra of Fe (III) \underline{d}_1 in acetone containing 0.024 N HCl and about 10% of water, (A) synthetic heme \underline{d}_1 ; (B) native heme \underline{d}_1 from <u>P. stutzeri</u>.

spectra of oxidized and reduced synthetic heme \underline{d}_1 in phosphate buffer at $_P H$ 7.3 is shown in Figure 27. The ferric heme has absorption maximum at 406 nm (Soret), a broad shoulder around 480 nm and a near infrared band at 781 nm. When Fe (III) was reduced to Fe (II) by $Na_2S_2O_4$, the Soret band appeared at 454 nm with a shoulder around 416 nm and the near infrared band shifted to 628 nm. These spectra are also very close to those observed by Yamanaka and Okunuki¹¹⁵ and can be used as excellent references to identify the characteristic absorbances of heme \underline{d}_1 in the spectrum of nitrite reductase. As illustrated in Figure 28. The absorption spectra of pure preparation of nitrite reductase from P. stutzeri is similar to those reported by Yamanaka and Okunuki¹¹⁶ and Hill and Wharton¹¹¹ from P. aeruginosa nitrite reductase. There are absorbance maxima at 411 nm (Soret), 524, 644 nm and a shoulder at 360 nm in the oxidized form; and at 417 nm (Soret), 460, 522, 549, 555 nm and 625-655 nm plateau in the reduced form. The 280 nm absorbance belongs to protein and the 315 nm band is derived from dithionite. The main differences between the reduced spectrum of this enzyme and that from P. aeruginosa is that the intensity of the doublet at 549 and 555 nm is reversed such that the peak at 555 nm is now more intense than the one at 549 nm, whereas in all the reported spectra of nitrite reductase from P.aeruginosa the opposite trend is observed, that is, the peak at 549 nm is higher than that at 555 or 554 nm. This feature is consistent in all of our preparations and has also been recorded in an earlier study on the nitrite reductase of another strain of P. stutzeri (Van Niel strain). 117 In addition, the broad band in the long wavelength area in the oxidized state, 644 nm, is somewhat bathochromically shifted comparing with the one in the spectra of the enzyme from P. aeruginosa that usually appears between 635 to 649 nm.

The Soret band at 417 nm in the reduced spectrum is attributed to heme \underline{c}

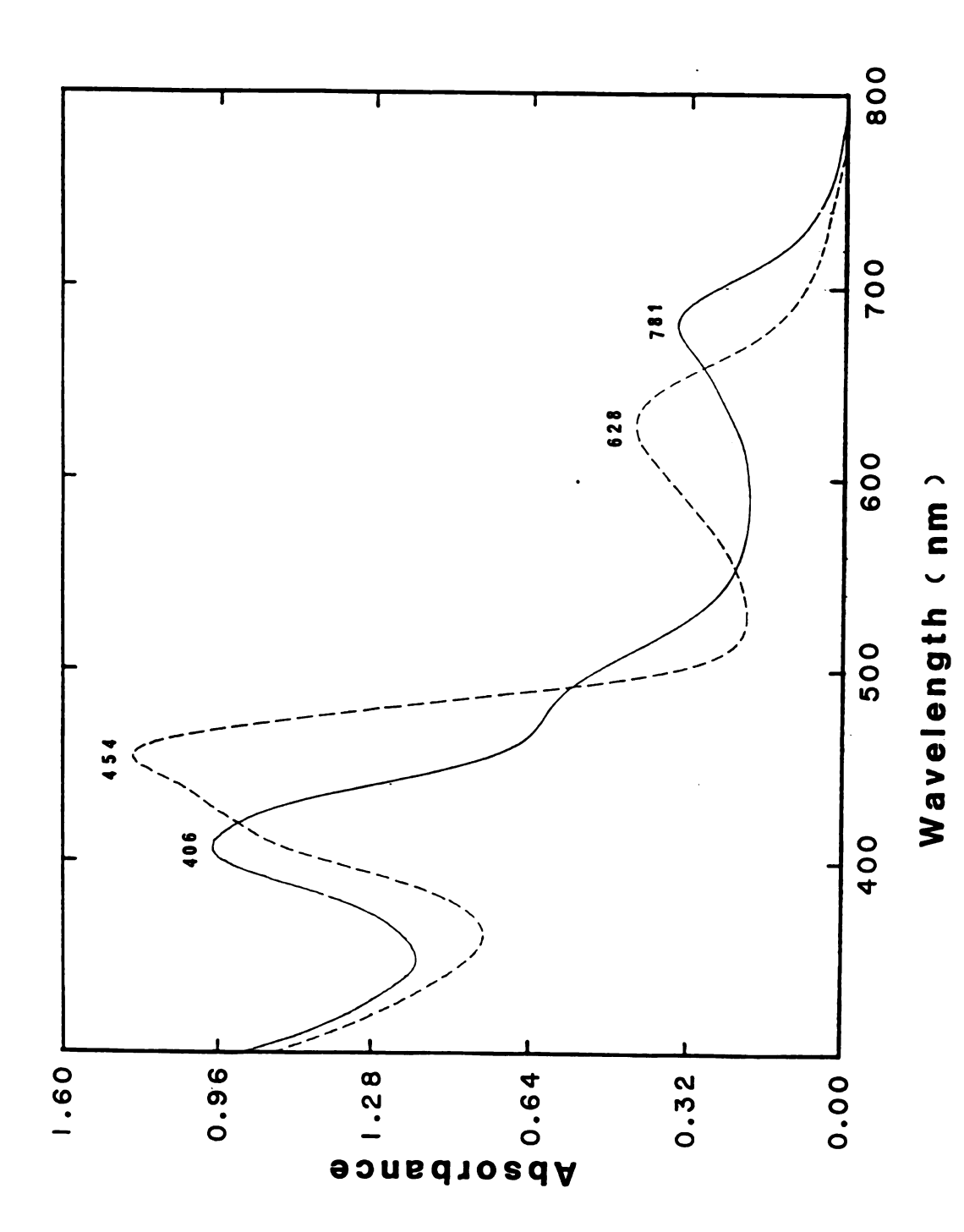


Figure 27 UV-vis spectra of synthetic d1 in 0.25 M of phosphate buffer at pH 7.3. —, oxidized; ---, reduced with Na₂S₂O₄.

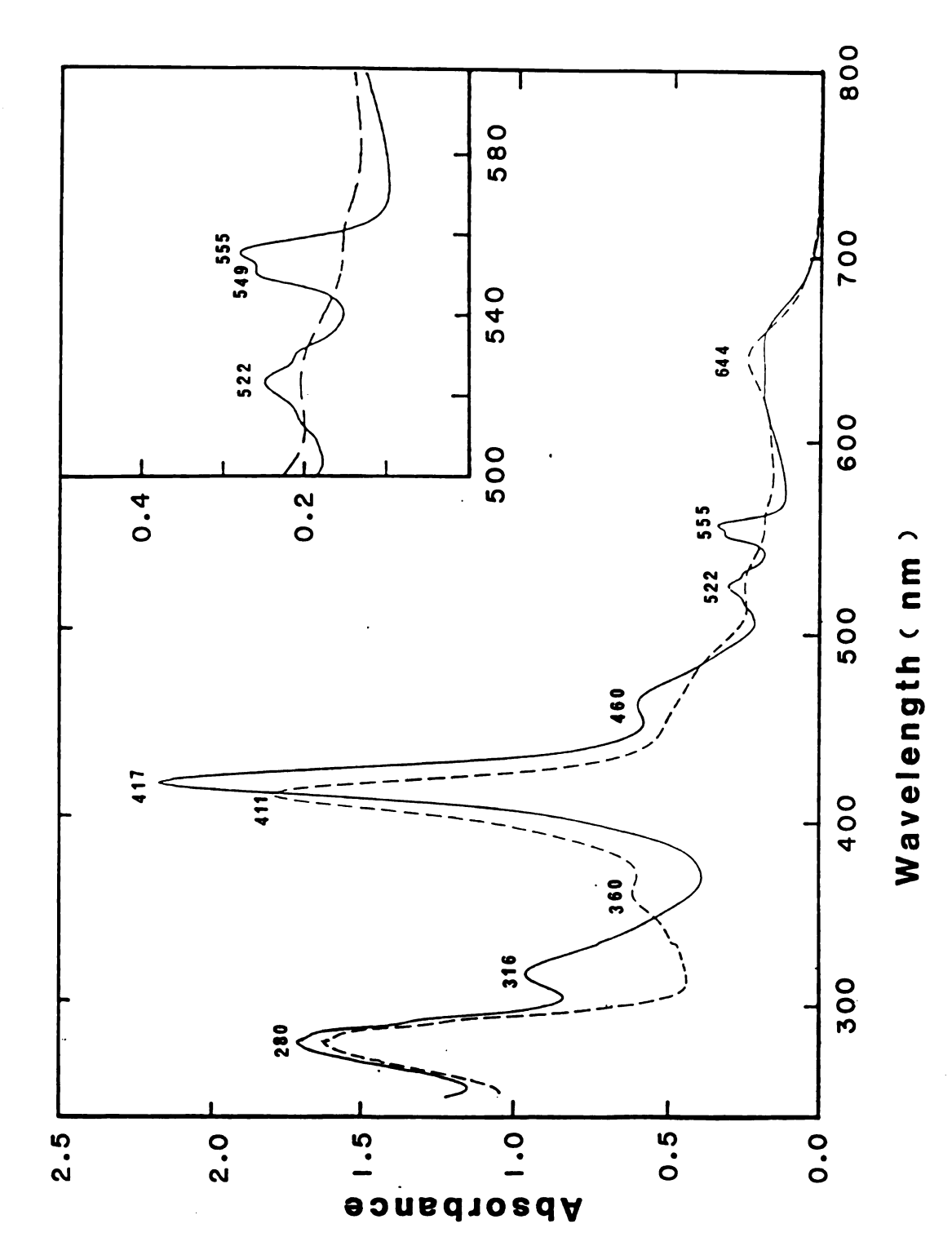


Figure 28 UV-vis spectra of pure preparation of nitrite reductase from P. stutzeri in 0.25 M phosphate buffer at $_{\rm pH}$ 7.0. ---, oxidized; --- reduced with $_{\rm Na_2}S_{\rm 2}O_{\rm 4}$.

and so is the band at 522 nm and the doublet at 549 and 555 nm. Comparison of the spectra in <u>Figure 27</u> reveals that heme \underline{d}_1 is responsible for the weak shoulder at 460 nm and the broad band near 640 nm. The spectrum of apoprotein, <u>Figure 29</u>, is deprived spectral characteristics typical of heme \underline{d}_1 . the spectra of enzymes reconstituted with the native and synthetic heme \underline{d}_1 , shown in <u>Figure 30a</u> and 30b, have regained virtually all the features of heme \underline{d}_1 . The 460 nm shoulder peak in the spectrum of the enzyme reconstituted with synthetic heme \underline{d}_1 is less prominent, indicating a slightly lower incorporation of \underline{d}_1 into the protein.

IV. Recovery of activity

The progress curves of NO and N_2O production for intact nitrite reductase and reconstituted enzymes are shown in Figure 31 and 32. The shapes of these curves are approximately the same. Because of the pattern of gas production was not linear, the values for restoration of activity were calculated from the amount of gas produced at each time point in comparison with those for the intact enzyme. The percent recovery of activity was comparable for each time point, and the mean value is reported in Table 16. The heme \underline{c} containing apoprotein remained soluble after dialysis to remove the urea and had no detectable activity during the time course of an initial rate experiment. When reconstituted with either native and synthetic heme \underline{d}_1 a large part of its nitrite reductase activity was restored: 80% and 78% respectively, for the native and synthetic heme \underline{d}_1 reconstituted enzyme. These activity recoveries are higher than the 54% obtained by Yamanaka and Okunuki¹¹⁰ in their experiment mentioned earlier.

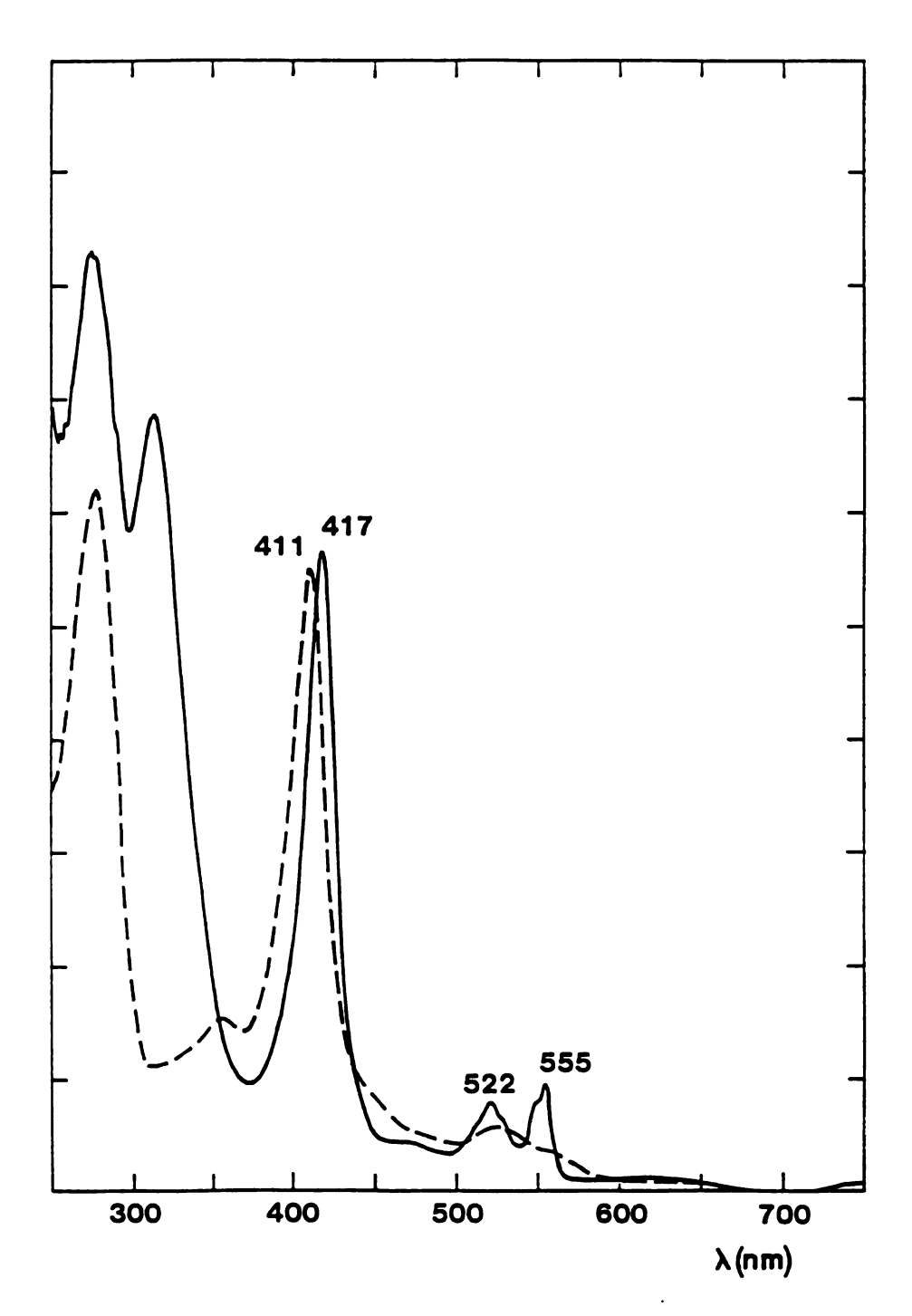


Figure 29 UV-vis spectra of apoprotein of nitrite reductase from P. stutzeri after removal of heme d₁, the apoprotein was dissolved in 0.25 M of phosphate buffer at pH 7.0. ---, oxidized; ---, reduced with Na₂S₂O₄.

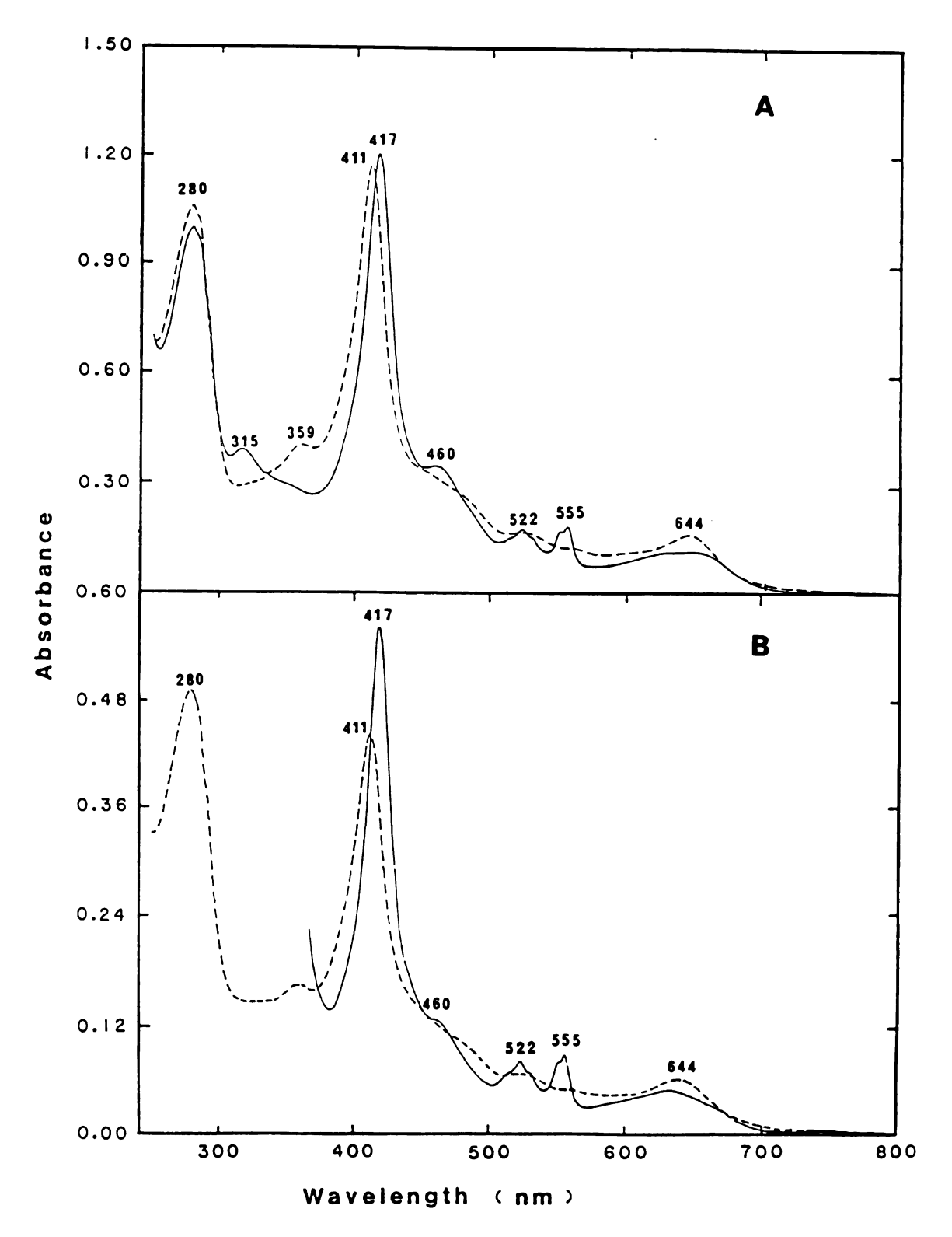


Figure 30 UV-vis spectra of reconstituted nitrite reductase in 0.25 M of phosphate buffer at $_{\rm P}$ H 7.0, (A) native $\underline{\bf d}_1$ reconstituted and (B) synthetic $\underline{\bf d}_1$ reconstituted. ---, oxidized; ---, reduced with Na₂S₂O₄.

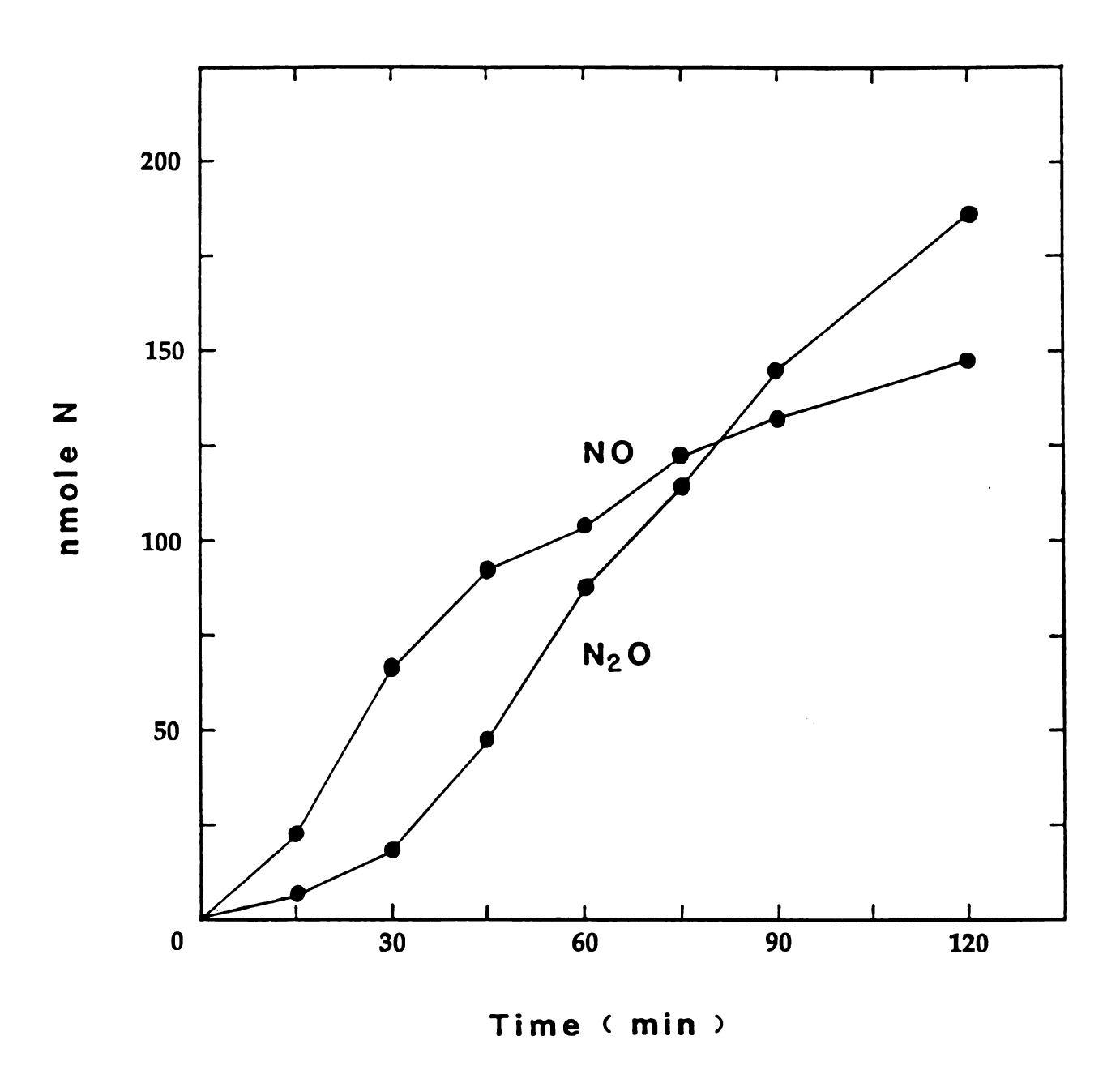


Figure 31 Progress curves of nitric oxide and nitrous oxide production from 1 mM of nitrite by intact nitrite reductase from <u>P. stutzeri</u>.

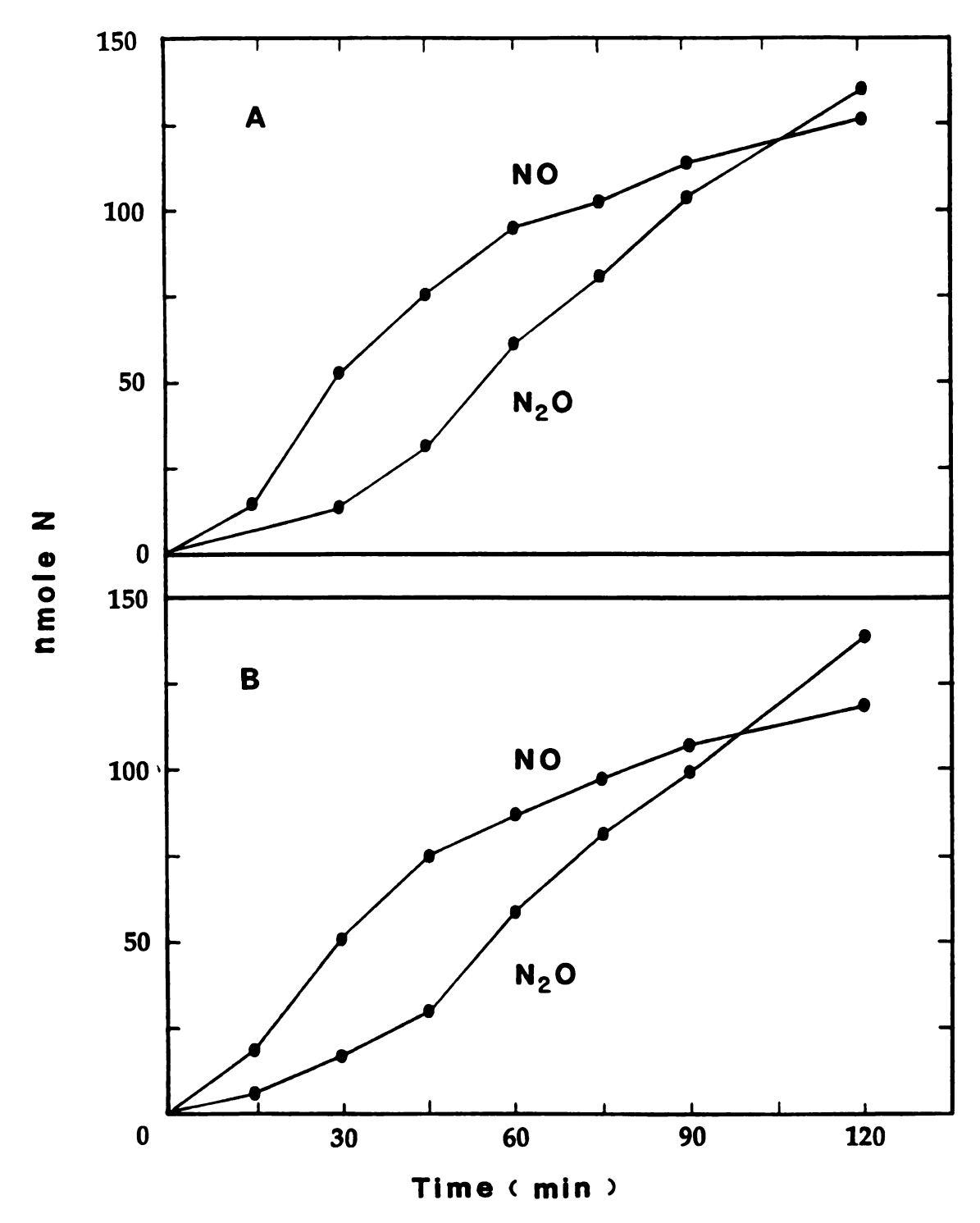


Figure 32 Progress curves of nitric oxide and nitrous oxide production from 1 mM of nitrite by the reconstituted nitrite reductase, (A) reconstituted with synthetic heme \underline{d}_1 and (B) reconstituted with native heme \underline{d}_1 .

Table 16. Recovery of nitrite reductase activity after reconstitution of the apoprotein with native and synthetic heme \underline{d}_1 .

Treatment of enzyme	Enzymic activity measured		
	NO ₂ to NO ^a	NO ₂ - to N ₂ O ^a	
Intact, enzyme	100	100	
Apoprotein	0	0	
Reconstituted, native \underline{d}_1	83(4.4) ^b	77(3.3)	
Reconstituted, synthetic \underline{d}_1	82(3.8)	73(2.5)	

a Activities are expressed in relative units. The activity of the intact enzyme represents 100%.

V. DISCUSSION

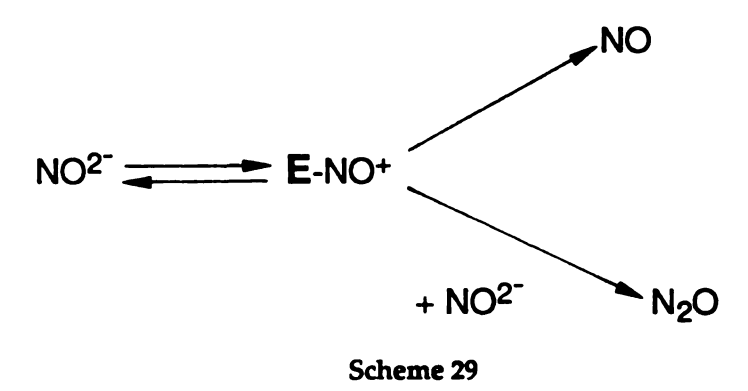
Cytochrome \underline{cd}_1 nitrite reductase reconstituted with either the native and synthetic heme \underline{d}_1 is essentially the same in most aspects. The matching of the spectral and biological properties of the synthetic heme \underline{d}_1 with those of the natural prosthetic group leaves on doubt that heme \underline{d}_1 must have the structure as we proposed. As mentioned in chapter 1, the kinetics work to date supports the idea that heme \underline{c} sites of the enzyme are associated with electron-uptake while heme \underline{d}_1 sites are responsible for electron-donation to exogenous ligands. Thus, it is expected that the apoprotein would not exhibit any nitrite reductase activity due to the removal of \underline{d}_1 prosthetic groups.

The enzymatic activities of the reconstituted enzymes were about 20% lower than that of the intact nitrite reductase, this loss is understandable considering the possible denaturation of the protein during the

b Numbers between parentheses represent the deviation from the meanvalue of two initial rate determinations within the same experiment.

reconstitution process. The ratio of A_{460nm}/A_{555nm} in the reduced spectra is 1.68 for the native and 1.48 for the synthetic heme \underline{d}_1 reconstituted enzymes as compared to 1.75 for the intact nitrite reductase. The differences indicate that the reconstitution was about 96% complete for native \underline{d}_1 and about 85% for the synthetic \underline{d}_1 . The synthetic heme \underline{d}_1 we used for the reconstitution comprised a pair of enantiomers. This might account for the lower incorporation of the synthetic heme \underline{d}_1 , since the wrong enantiomer presumably cannot fit the protein pocket as well as the correct stereo isomer so that it may dissociate easily from the binding site during purification from excess heme \underline{d}_1 .

As we mentioned in chapter 1, Averill and Tiedje³² proposed a pathway by which NO_2^- can be converted to N_2O by one enzyme (nitrite reductase), through a heme- NO^+ intermediate. This proposal is supported by evidence from ^{15}N and ^{18}O studies that show a sequential mechanism of NO_2^- addition and by studies that show two Km values for NO_2^- , 1.4 μ M for NO_2^- production and 59 μ M for N_2O production. It also appears that the reaction kinetics of the nitrite reductase are perturbed by its removal from the membrane environment and by purification. This likely affects the fate of the enzyme-bound nitrosyl intermediate which enhances the ratio of NO/N_2O produced by the purified enzyme (Scheme 29)



The results show that the apoprotein produce neither NO nor N_2O from NO_2^- , and that when reconstituted with heme \underline{d}_1 the original NO and N_2O producing activities were restored. Furthermore, the purified enzyme did not produce N_2O when NO was added as substrate.¹¹⁸ This confirms that a single enzyme can carry out the entire NO_2^- to N_2O step, and establishes that heme \underline{d}_1 in its nitrite reductase pocket is required for both NO and N_2O production. Thus N_2O production from NO_2^- does not require a nitric oxide reductase. The fact that only one-half of the nitrite reductase product was N_2O can be explained by the altered environment of the purified enzyme. The heme \underline{d}_1 extraction and reconstitution procedure did not alter the NO_2^- to N_2O product ratio.

Presently, the relationship between the prosthetic group structure and the reductase function is not well understood. Previously, porphyrin hemes, such as protoheme, hematoheme and mesoheme, have been reported to give little or no oxidase activity in the reconstituted enzyme. Some preliminary data from our reconstitution experiment indicated that the structural features of dione heme apparently are very special for the enzyme activity. Several hemes examined to date, including the 2,4-diacetic acid deuteroheme 58, porphyrinone heme 111 showed no nitrite reductase activities at all. Studies are in progress to insert other dione heme analogs (for example, altered keto and acrylic substitutions) to test the essentialness of \underline{d}_1 structural elements.

CHAPTER 7

CONCLUSION AND FUTURE WORK

I. EVALUATION OF THE PRESENT WORK

This thesis work has essentially reached the goals of our original proposal. The model compound study provided solid evidence on the structure we proposed and the methodologies developed toward the 1,3-porphyrindione core structure and acrylate side chain formation led ultimately the total synthesis of $\underline{\mathbf{d}}_1$. In retrospect, the $\underline{\mathbf{d}}_1$ synthesis might be considered as a piece of "brutal force" work since the whole pathway was a "push-through" process with a large quantity of starting materials, severe reaction conditions and also unsatisfactory yields. Nevertheless, the successful synthesis of $\underline{\mathbf{d}}_1$, together with its stereo- and regioisomers, has unequivocally proved its structure. Our physicochemical studies have shown that the most distinctive features of porphyrindions are its electronegativity due to both inductive and conjugating effect of the two keto groups and a enlarged core size brought about by the saturation of the pyrrole rings.

The study on the reconstituted cytochrome \underline{cd}_1 indicated that the synthetic heme \underline{d}_1 is fully functional in the enzyme, just like the native heme as far as the nitrite reductase activity is concerned. Another important message obtained from this study concerns the nitrite reduction mechanism. The loss of N₂O producing activity in the absence of heme \underline{d}_1 and its restoration by addition of heme \underline{d}_1 suggested that nitrite reduction may

convert NO_2^- to N_2^- O without invoking a role for nitric oxide reductase in the denitrification pathway.

II. FUTURE WORK

It is important to further understand the chemical, structural, spectroscopic characteristics of dioneheme, and its function in microbial denitrification. Future work should include the following:

- 1. The ligand coordination of heme d_1 and model systems. Using synthetic \underline{d}_1 and its analogues, we plan to prepare a variety of 5- and 6- coordinated heme complexes containing CO, O_2 , NO, CN⁻, and NO₂⁻ as axial ligand. Their formation equilibria and chelation dynamics will be studied by stopped-flow or flash photolysis techniques.
- 2. Further work on reconstitution of cytochrome cd_1 . Work on the reconstitution of cd_1 enzymes with a wide variety of synthetic dioneheme analogues and other related hemes has already begun, aiming at the relationship between the prosthetic group structure and its intrinsic reactivities in the enzyme and the mechanism concerning nitrite reduction.

 3. Intramolecular electron transfer in cytochrome cd_1 . The unique two heme arrangement with a relatively fixed distance of cytochrome cd_1 provides an ideal model to study the long range electron-transfer problem in biological systems. Pro our purposes, with regard to the binding and electron transfer steps required for the activation and reduction of NO_2^- and O_2 , the precise description of intramolecular electron transfer step is important. The key question is whether the slow heme c_1 to heme c_2 to heme c_3 transfer is a result of electron tunneling over a relatively long distance (13-15 c_3) or whether large

conformation changes are involved. The study of electron transfer rates will

be facilitated by using reconstituted cytochrome \underline{cd}_1 in which the heme \underline{d}_1 is replaced by other electron donors, such as a Zn (II) porphyrindione.

REFERENCES

- 1. Eschenmoser, A., <u>Angew. Chem. Int. Ed. Engl.</u>, 1988, 27, 5.
- 2. Battersby, A. R.; and MacDonald, E., Acc. Chem. Res., 1979, 12, 14.
- 3. Chang, C. K., J. Biol. Chem., 1985, 260, 9250.
- 4. For a general reference: Payne, W. J., "Denitrification", 1981, John Wiley & Son, New York, and Delwiche, C. C.; Bryan, B. A., Ann. Rev. Microbiol. 1979, 30, 241.
- 5. Losada, M. J., J. Mol. Catal., 1976, 1 245.
- 6. Forget, P.; Dervartanian, D. V., Biochim. Biophys. Acta, 1972, 256,600.
- 7. Iwasaki, H.; Saigo, T., Plant Cell Physiol., 1980, 21, 1573.
- 8. Matsubara, T.; Frunzke, K.; Zumft, W. G., J. Bacteriol., 1982, 149, 816.
- 9. Hirio, Y.; Higash, T.; Yamanaka, T.; Matsubara, H.; Okunuki, K., J. Biol. Chem., 1961, 236, 944.
- 10. Sawhney, y.; Nicholas, D. J. D., <u>J. Gen. Microbiol.</u>, **1978**, <u>106</u>, 119.
- 11. Matsubara, at.; Iwasuki, H., <u>J. Biochem</u>. (Tokyo), **1972**, <u>72</u>, 57.
- 12. Newton, N., <u>Biochim. Biophys. Acta</u>, **1969**, <u>185</u>, 316.
- 13. Mancinelli, R. L.; Cronin, S.; Hochstein, L. I., Arch. Microbiol., 1986, 145, 202
- 14. Kodama, T., <u>Plant. Cell Physiol.</u>, **1970**, <u>11</u>, 231, and Weeg-Aerssens, E., **1988**, Ph. D. Dissertation, Michigan State University.
- 15. Horio, T., <u>J. Biochem.</u>, **1958**, <u>45</u>, 195.
- 16. Horio, T., <u>J. Biochem.</u>, **1958**, <u>45</u>, 260
- 17. Horio, T.; Higash, T.; Matsubara, H.; Kusa, K.; Nakai, M.; Okunuki, K., Biochim. Biophys. Acta, 1958, 29, 297.
- 18. Yamanaka, T.; Ota, A.; Okunuki, K., <u>Biochim. Biophys. Acta</u>, 1960, 44, 397.
- 19. Yamanaka, T.; Ota, A.; Okunuki, K;, <u>Biochim. Biophys. Acta</u>, 1961, 53, 294.
- 20. Yamanaka, T.; Kijimoto, S.; Okunuki, K., Nature, 1962, 194, 759.

- 21. Yamanaka, T.; Kijimoto, S.; Okunuki, K., <u>I. Biochem.</u>, **1963**, <u>53</u>, 416.
- 22. Mitra, S.; Bershn, R., <u>Biochemistry</u>, **1980**, <u>19</u>, 3200.
- 23. Saraste, M.; Virtanen, I.; Kuronen, T., <u>Biochim. Biophys. Acta</u>, 1977, 492, 156.
- 24. Greenwood, C., in "Metalloporphyrins", Part I, (Harrison, P. M., ed) Verlag Chemie, 1985, pp 43-77.
- 25. Takano, T.; Dickson, R. E.; Schichman, S. A.; Mayer, T. E., <u>J. Mol. Biol.</u>, **1979**, <u>133</u>, 185.
- 26. Makinen, M. W.; Schichman, S. A.; Hill, S. C., Science, 1983, 222, 929.
- 27. Schichman, C. A.; Gray, H. B., <u>I. Am, Chem. Soc.</u>, 1981, 103, 7794.
- 28. Johnson, M. K.; Thomson, A. J.; Walsh, T. A.; Barber, D.; Greenwood, C., <u>Biochem. J.</u>, **1980**, <u>189</u>, 285.
- 29. Walsh, T. A.; Johnson, M. K.; Greenwood, C.; Barber, D.; Springall, J. P.; Thomson, A. J., <u>Biochem. J.</u>, **1977**, 177, 29.
- 30. Yamanaka, T., Nature, 1964, 204, 253.
- 31. Timkovich, r.; Thrasher, J. S., <u>Biochemistry</u>, **1988**, <u>27</u>, 5383.
- 32. Averill, B. A.; Tidjde, J. M., <u>FEBS Letter</u>, **1983**, <u>138</u>, 8.
- 33. Garber, A. E.; Hollocher, T. C., <u>J. Biol.Chem.</u>, **1982**, <u>257</u>, 4705.
- 34. Kim, C.; Hollocher, T. C., <u>J. Biol. Chem.</u>, **1984**, <u>259</u>, 2092.
- 35. Garber, A. E.; Hollocher, T. C., <u>J. Biol. Chem.</u>, **1982**, <u>257</u>, 8091.
- 36. Bryan, B. A.; Shearer, G.; Skeeters, J. L.; Kahl, D., <u>J. Biol. Chem.</u>, **1983**, 258, 8613.
- 37. Garber, A. E.; Hollocher, T. C., <u>J. Biol. Chem.</u>, 1983, <u>258</u>, 3587.
- 38. Aerssens, E.; Tidjde, J. M.; Averill, B. A., <u>J. Biol. Chem.</u> 1986, <u>261</u>, 9662.
- 39. Aerssens, E.; Tiedje, J. M.; Averill, B. A., <u>J. Am. CHem. Soc.</u> 1987, <u>109</u>, 7214.
- 40. Keilin, D., Nature, 1933, 132, 783.
- 41. Horio, t.; Higashi, T.; Yamanaka, T.; Matsubara, H.; Okunuki, K., <u>I.</u> <u>Biol. Chem.</u> **1961**, <u>236</u>, 944.
- 42. Yamanaka, T.; Okunuki, K., Biochim. Biophys. Acta, 1963, 67, 397.
- 43. Barrett, J., <u>Biochem. J.</u>, **1956**, <u>64</u>, 626.

- 44. Lemberg, R.; Barrett, J., "The Cytochromes", 1973, Acedamic Press, New York.
- 45. Timkovich, R.; Cork, M. S., Taylor, P. V., J. Biol. Chem., 1984, 259, 1577.
- 46. Timkovich, R.; Cork, M. S.; Talyor, P. V., <u>J. Biol. Chem.</u>, **1984**, <u>259</u>, 15089.
- 47. Inhoffen, H. H.; Nolte, W., Tetrahetron letter, 1967, 2185.
- 48. Inhoffen, H. H.; Nolte, W., Justus, Liebigs Ann. Chem., 1969, 725, 167.
- 49. Bonnett, R.; Dolphin, D.; Johnson, A. W.; Oldfield, D. J.; Stephenson, G. F., Pro. Chem. Soc., 1964, 371.
- 50. Johnson, A. W.; Oldfield, D. J., J. Chem. Soc., 1965, 4303.
- 51. Chang, C. K.; Barkigia, K.; Hanson, L. K.; Fajer, J., <u>I. Am. Chem. Soc.</u>, **1986**, 108, 1352
- 52. Murphy, M. J.; Siegel, L. M.; Kamin, H.; Rosenthal, D., <u>J. Biol. Chem.</u>, **1973**, 248, 2801.
- 53. Inhoffen, H. H.; Notle, W., Justus Liebigs Ann. Chem., 1969, 725, 167.
- 54. Gouterman, M.; 1978, in "The Porphyrins", (Dolphin, D., ed.)Vol. III, Academic Press, New York, pp 1-165
- 55 Musselman, B. D.; Waltson, J. T.; Chang, C. K., J. Org. Mass Spectrom., 1986, 21, 215.
- 56. Smith, K. M.; Unsworth, J. F., <u>Tetrahetron</u>, **1975**, <u>31</u>, 367.
- 57. Janson, T. R.; Katz, J. J., Porphyrins, 1979, vol. 4, 1-54.
- 58. Fischer, H.; Gebhardt, H.; Rathhass, A., <u>Justus liebigs Ann. Chem.</u>, 1930, 482, 1.
- 59. Fischer, H., Pfeiffer, H., <u>Justus Liebigs Ann. Chem.</u>, **1944**, <u>556</u>, 131.
- 60. Chang, C. K., <u>Biochemistry</u>, **1980**, <u>19</u>, 1971.
- 61. Collins, C. J., Q. Rev. Chem. Soc., 1960, 14, 357.
- 62. Fischer, H.; Eckoldt, H., <u>Justus Liebigs Ann. Chem.</u>, **1940**, <u>554</u>, 138.
- 63. Chang, C.K.; Sotiriou, C., <u>J. Org. Chem.</u>, **1985**, <u>50</u>, 4989.
- 64. Sotiriou, C.; Chang, C. K., J. Am. Chem. Soc., 1988, 110, 2264.
- 65. Sotiriou, C., Ph. D. Dissertation, Michigan State University, 1987.

- 66. Oster, M. Y., Ph., D. issertation, University of Wisconsin, 1971.
- 67. Fischer, H.; Zischler, H. Z., <u>Physiol. Chem., (Hoppe-Segler's)</u> 1937, 245, 123.
- 68. McDonald, S. F.; Stedman, R. J., Cana. J. Chem., 1954, 32, 896.
- 69. Chang, C. K.; Sotiriou, C., <u>J. Hetercycl. Chem.</u>, 1985, <u>22</u>, 1379.
- 70. Agius, L.; Ballan, J. A.; Ferrito, V.; Jaccarini, V.; Murray-Rust, P.; Peltera, A.; Psaila, A.F.; Schember, P. J., Pure Appl. Chem., 1979, 51, 1847.
- 71. Scott, A. I.; Irwin, A. J.; Siegel, L. M.; Shoolery, J. N., <u>J. Am. Chem. Soc.</u>, **1978**, <u>100</u>, 7987.
- 72. Battersby, A. B.; McDonald, E., <u>Bioorg. Chem.</u>, **1978**, <u>7</u>, 161.
- 73. Witlock Jr. H. W.; Hanauar, R.; Oster, M. I.; Bowry, B. K., <u>J. Am. Chem. Soc.</u>, **1969**, <u>91</u>, 7485.
- 74. Smith, K. M.; Goff, D. A.; <u>J. Am. Chem. Soc.</u>, 1985, 107, 4954.
- 75. Griffiths, G. F.; Kenmer, G. W.; McCombie, S. W., Smith, K. M.; Sutton, M. J., <u>Tetrahetron</u>, **1976**, <u>32</u>, 275.
- 76. Fischer, H.; Orth, H., "Die Chemie des Pyrrols", Vol. III, PP290.
- 77. Sparatore, F.; Manzerall, D., <u>I. Org. Chem.</u>, **1960**, <u>25</u>, 1073.
- 78. Smith, K. M.; Goff, D. A., J. Org. Chem., 1985 50, 2073.
- 79. Inhoffen, H. H.; Jaeger, P.; Mahlhop, P., <u>Justus Liebigs Ann. Chem.</u>, 1971, 749, 109.
- 80. Harrison, P. J.; Fookes, C. J. R.; Battersby, A. R., <u>J. Chem. Soc. Chem. Commun.</u>, **1981**, **797**.
- 81. Battersby, A. R.; Reiter, L. A., <u>I. Chem. Soc. Perkin. Trans. I</u>, 1984, 2743.
- 82. Paine, J. R.; Chang, C. K.; Dolphin, D., <u>Heterocycles</u>, **1977**, <u>7</u>, 831.
- 83. Smith, K. M.; Parish, D. W.; Inouge, W. S., <u>I. Org. Chem.</u>, **1985**, <u>51</u>, 666.
- 84. Battersby, A. R.; Hamilton, A. D.; Mcdonald, E.; Mombelli, L.; Wong, O. H., J. Chem. Soc. Perkin. Trans. I, 1980, 1283.
- 85. Kenner, G. W.; McCombie, S. W.; Smith, K. M., <u>J. Chem. Soc. Chem. Commun.</u>, **1972**, 1347.
- 86. Mancuso, A. J.; Brownfain, D. S.; Swern, D. J., <u>J. Org. Chem.</u>, 1979, <u>23</u>, 4148.

- 87. Corey, E. J.; Gilman, N. W.; Ganem, B. G., <u>J. Am. Chem. Soc.</u>, **1968**, 90, 5616.
- 88. Corey, E. J.; Schmidt, G., <u>Tetrahetra Lett.</u>, **1979**, 399.
- 89. Fischer, H.; Ecoldt, H., <u>Justus Libigs Ann. Chem.</u> **1940**, <u>544</u>, 159.
- 90. Dar'eva and Miklukhin, J. Gen. Chem. USSR, 1959, 29, 620.
- 91. Sievers, R. E., Ed., "Nuclear Magnetic Resonance Shift Reagents", Academic, New York, 1973.
- 92. Battersby, A. R., <u>I. Chem. Soc. Chem. Commun.</u>, 1979, 539.
- 93. Storzenberg, A.M.; Laliberte, M. A., <u>I. Org. Chem.</u>, **1987**, <u>52</u>, 1022.
- 94. Mason, S. F., <u>I. Chem. Soc. Chem.</u>, **1958**, 976.
- 95. Matthew, J. M.; Lewis, M. S.; Heery, K., J., Biol. Chem., 1973, 248, 2801.
- 96. Bellamy, L. J., "The Infrared Spectra of Complex Molecules", 3rd Edition, 1975, Chapan and Hall, London.
- 97. Ching, Y.; Ondrias, M. R.; Rousseau, D. L.; Muhoberac, B. B.; Whaton, D. C., <u>FEBS Lett.</u>, **1982**, <u>138</u>, 239.
- 98. Boktos, G., 1981, Master Thesis, Michigan State University.
- 99. Cotton, T. M.; Timkovich, R.; Cork, M. S., FEBS Lett., 1981, 133, 39.
- 100. Ondrias, M. R.; Carson, S. D.; Hirasawa, M.; Knaff, D. B., <u>Biochem.</u> <u>Biophys. Acta</u>, **1985**, <u>830</u>, 159.
- 101. Lutz, M.; Hoff, A. J.; Brehamet, L., <u>Biochem. Biophys. Acta</u>, **1982**, <u>679</u>, 331.
- 102. Cotton, T. M.; Van Duyan, R. P., FEBS Lett., 1982, 147, 81.
- 103. Anderson, L. A.; Loehr, T. M.; Sotiriou, C.; Chang, C. K., <u>I. Am. Chem. Soc.</u>, **1987**, 109, 258.
- 104. Chang, C. K.; Barkigia, K. M.; Hanso, L. K.; Fajer, J., <u>J. Am. Chem. Soc.</u>, 1986, 108, 1352.
- 105. Suh, M. P.; Pwepston, P. N.; Ibers, J. A., <u>I. Am. Chem. Soc.</u>, 1984, <u>106</u>, 5164.
- 106. Barkigia, J.; Fajer, J.; Chang, C. K.; Willams, G. J. B., <u>J. Am. Chem. Soc.</u>, 1982, 104, 315.
- 107. Chang, C. K.; Hanson, L. K.; Richardson, P. R.; Young, R.; Fajer, J., Proc. Natl. Acad. Sci., U. S. A., 1981, 78, 2652.

- 108. Stortzenberg, A. M.; Strauss, S. H.; Holm, R. H., <u>I. Am. Chem. Soc.</u>, **1981**, <u>103</u>, 4763.
- 109. Storztenberg, A. M.; Glazer, P. A.; Foxman, B. M., Inorg. Chem., 1986, 25, 983.
- 110. Yamanaka, T.; Okunuki, K., <u>Biochem. Z.</u>, **1963**, <u>338</u>, 62.
- 111. Hill, K. E.; Whaton, D. C., J. Biol. Chem., 1978, 253, 489.
- 112. Weeg-Aerssens, E.; Tiedje, J. M.; Hausinger, R. P.; Averill, B. A., <u>I. Bacteriol.</u>, **1988**, (in press).
- 113. Smith, P. K.; Krohn, R. I.; Hermanson, G. T.; Mallia, A. K., <u>Anal.</u> <u>Biochem.</u>, **1985**, <u>150</u>, 76.
- 114. Walsh, T. A.; Johnson, M. K.; Barber, D.; Thomson, A. T.; Greenwood, C., <u>I. Inorg. Biochem.</u>, 1980, 14, 15.
- 115. Yamanaka, T.; Okunuki, K., <u>Biochem. Biopyhs. Acta</u> 1963, <u>67</u>, 407.
- 116. Yamanaka, T.; Okunuki, K., <u>Biochem. Biopyhs. Acta</u> 1963, <u>67</u>, 379 and 406.
- 117. Kadama, T., Plant Cell Physiol., 1970, 11, 231.
- 118. Weeg-Aerssens, E.; Tiedje, J. M.; Averill, B. A., <u>J. Am. Chem. Soc.</u> 1988, (in press).
- 119. Barkigia, K.; Wu, W.; Fajer, J.; Chang, C. K., unpublished results.
- 120. Mayo, S. L.; Ellis, W. R.; Crutchley, R. J.; Gray, H. B., <u>Science</u>, **1986**, <u>233</u>, 948.

